Process Development for Fine Chemicals (acetaldehyde dimethylacetal) Synthesis

A Dissertation Presented to the

UNIVERSIDADE DO PORTO

For the Degree of Doctor in Chemical Engineering

By

Ganesh Kumar Gandi

Supervisor
Prof. Alírio E. Rodrigues

Co-Supervisor
Dr. Viviana M. T. M. Silva

LSRE – Laboratory of Separation and Reaction Engineering
Department of Chemical Engineering
Faculty of Engineering, University of Porto
Rua Dr. Roberto Frias, Porto 4200-465
PORTUGAL

January, 2006

ACKNOWLEDGEMENTS

There are many people who supported me on my journey leading to this work, and I would like to express my sincere gratitude to all of them, especially to those whom I cannot mention explicitly in the following. I am quite aware that I wouldn't have reached this point without them and I hope that I can return this help – to them or to other people who need it.

First of all, it is difficult to overstate my gratitude to my Ph.D. supervisor, Prof. Alírio Rodrigues. With his enthusiasm, his inspiration, and his great efforts to explain things clear and simple. Throughout my thesis-writing period, he provided encouragement, sound advice, and lots of good ideas. I would have been lost without him.

I would like to mention thankfulness to my co-supervisor Dr.Viviana Silva for her continuous readiness to assist me when ever I was in need.

I am grateful to Mr. Mike for his help in starting the SMB equipment without which I would have not completed my Thesis.

I was little bit depressed and lonely when I joined this LSRE as a Ph.D student as I left back my great days at SOCL, UDCT and AUEC, so I am very unfortunate to miss Mr.TRSrinivas, Mr.GRamesh Mr.BSChakravarthy, Mr.PRamesh, Mr.KVSMurthy, Mr.Mishra, Mr.RShinde, Dr.SMukhopadhyaya, Dr.KChandanani, Mr.Jamwal, Mr.Sujeet, Dr.AKSingh, Mr.Deshmukh, Mr.Kesrwani, MrGaikward, Mr.Mandal. But thanks to Dr.Carlos Grande, Mr.Danial, Dr.Eduardo Silva, Mr.Mike, Dr.PurnaKala, Dr.Sooraj, Dr.Nagendra for giving me a friendly atmosphere during my whole stay at LSRE.

I would like to mention thankfulness to all my colleagues Mr.Eduardo, Dr.Kishore, Dr.Simone, Dr.Martha, Mr.Migule, Ms.Miriam, Dr.Miriana, Mr.Nabil, Dr.Paula, Mr.Pedro, Mr.Philip, Ms.PingLi, Dr.Prakash, Dr.Rodrigo, Ms.Sofia, Ms.Thirja, Dr.Vera, Dr.Xiu from AER group for their kind cooperation during my work. I should also be thankful to other colleagues, Mr.Ertugrul, Mr.Paulo, Dr.Ricardo and all members and Professors of LSRE.

I am grateful to the secretary Ms.Susana for her assistance in the administrational work. I am also thankful to the other secretaries and technical assistants of the Chemical Engineering Department.

I would like to mention thankfulness to Ms.Andreia, Mr.Fred, Mr.Ricardo, Mr.Reinaldo, for making me feel that I am with a joint family at Students Residence (Paranhos Hostel) during my stay.

I should also express my humble thanks to CEMUP (Portugal), Novasep (France), Rohm and Haas (France), Smoptech (Finland) for giving me the assistance when ever I was in need.

I have to thank my parents (Mr.Sankara Rao & Mrs.Parvathi) in many respects, but in this context especially for supporting all my various and frequently changing interests. I should be grateful to my wife Gayathri and to my son Ravi Teja for putting up with my late hours, my spoiled weekends, my bad temper, but above all for putting up with me and surviving the ordeal.

I deeply express my thanks to my sisters (Hari Priya & Aruna), brother-in-laws (Mr.Suresh & Mr.Sudhakar) and brother (Mr.Chinna Babu) for taking care of my parents during my absence.

I also express my thanks to my father-in-laws Mr.&Mrs.Madupalli Ramana, Mr.&Mrs.Marupalli Satya Rao, Mr.&Mrs.NagaMalleswara Rao. I am thankful to all members of Gandi and Matha Families.

At last but not the least I must be grateful to *Fundação para a Ciência e a Tecnologia* (FCT-Portugal) for the financial support provided as my Ph.D Grant.

Ganesh Gandi

ABSTRACT

Dimethylacetal also named as acetal or 1,1-dimethoxyethane (DME) is an important raw material used at commercial scale and in laboratory research. Importantly, DME is used for the manufacture of fragrances and pharmaceutical products. It is not only used as the raw material, but also as an important intermediate for the synthesis of various industrial chemicals, organic solvent, in the design of synthetic perfumes and for the production of polyacetals, and as an oxygenated fuel additive.

Acetalization reaction for DME ynthesis was performed by reversible liquid-phase reaction with methanol and acetaldehyde reaction, catalyzed by acid ion exchange resin, Amberlyst 15

Experiments were performed in a laboratory-scale jacketed glass reactor in the temperature range of 20-60 ^{o}C, in order to determine kinetics and thermodynamics for the dimethylacetal sysnhesis with Amberlyst-15 resin as catalyst. The effect of particle size, effect of agitation, amount of catalyst, initial reactants molar ratio, temperature and pressure on the reaction rate were studied. A two-parameter model based on a Langmuir-Hinshelwood rate expression, using activity coefficients from the UNIFAC method is proposed. This model was extended in order to include external and internal mass transfer resistances and to be able to predict the experimental kinetic results obtained in a batch reactor.

Secondly, experiments were performed in a laboratory-scale jacketed glass column (26mm ID, 120mm length) packed with Amberlyst-15 resin. Reaction experiments were performed at 20 ^{o}C and atmospheric pressure. To obtain model parameters, binary adsorption experiments were organised in absence of reaction. The multicomponent equilibrium adsorption relationship was assumed to follow the modified Langmuir type. The model for the adsorptive reactor includes axial dispersion, external and internal mass-transfer resistances, constant temperature and multicomponent Langmuir Isotherms, and model equations were solved by orthogonal collocation in finit elements method, which was implemented in the PDECOL package, using the measured model parameters.

With the above results from the Batch Reactor and Fixed Bed Adsorptive Reactor experiments, it is now possible to design and to optimize an efficient process in a integrated unit, which unit is a combination of reaction and separation units, so-called Simulated Moving Bed Reactor (SMBR). The Simulated Moving Bed Reactor (SMBR) for the synthesis of dimethylacetal was studied experimentally and with simulations. The experimental results are compared with the TMBR modeling strategy. The mathematical model assumes axial dispersion flow for the bulk fluid phase, plug flow for the solid phase, linear driving force (LDF) for the particle mass transfer rate and multicomponent adsorption equilibria. The stationary steady-state predicted from the TMBR model is in agreement with the experimental SMBR cyclic steady-state at the middle of the switching time behaviour, in terms of internal concentration profiles.

DME synthesis with Smopex 101 fibres catalyst was also studied in batch and fixed bed reactor.

Resumo

Dimetilacetal, também denominado acetal ou 1,1-dimetoxietano (DME), é uma importante matéria-prima usada à escala comercial e em investigação laboratorial. DME é principalmente usado para manufactura de fragrâncias e produtos farmacêuticos. Este composto não é somente usado como matéria-prima, mas também como um importante intermediário para a síntese de vários produtos químicos industriais, solventes orgânicos, no projeto de perfumes sintéticos e para a produção de poliacetais, e como um aditivo combustível oxigenado.

A reacção de acetização para a síntese de DME foi realizada através da reacção reversível em fase líquida de metanol e acetaldeído, sendo catalisada pela resina de troca iônica ácida, Amberlyst 15.

As experiências foram realizadas num reactor de vidro encamisado de escala laboratorial numa gma de temperatura de 20 a 60 ºC, a fim de determinar dados cinéticos e termodinâmicos para a síntese do dimetilacetal com a resina Amberlyst-15 como catalisador. O efeito do tamanho da partícula, agitação, quantidade de catalisador, razão molar dos reagentes iniciais, temperatura e pressão sobre a velocidade de reação foram estudados. Um modelo a dois parâmetros baseado numa equação de velocidade do tipo Langmuir-Hinshelwood, usando coeficientes de actividade do método UNIFAC, é proposto. Este modelo foi estendido para incluir as resistências à transferência de massa externa e interna e para prever os resultados cinéticos experimentais obtidos num reactor fechado.

A seguir experiências foram realizadas numa coluna de vidro encamisada de escala laboratorial (diâmetro de 26mm; comprimento de 120mm) empacotada com resina Amberlyst-15. Estas experiências de reacção foram efectuadas a 20ºC e á pressão atmosférica. Para obter os parâmetros do modelo, experiências de adsorção binária foram realizadas sem a presença de reacção. A relação de adsorção de equilíbrio multicomponente foi assumida conforme o tipo Langmuir modificado. O modelo para o reactor adsorptivo inclui dispersão axial, resistências à transferência de massa externa e interna, temperatura constante e isotermas de Langmuir multicomponente. As equações do modelo foram resolvidas pelo método da colocação ortogonal em elementos finitos, o qual foi implementado no software PDECOL, usando os parâmetros do modelo medidos.

Com os resultados das experiências efectuadas no reactor fechado e no reactor adsorptivo de leito fixo, é possível projectar e optimizar um processo eficiente num sistema integrado, que é uma combinação de unidades de reacção e de separação, chamado Reactor de Leito Móvel Simulado (RLMS). O Reactor de Leito Móvel Simulado (RLMS) para a síntese de dimetilacetal foi estudado experimentalmente e com simulação. Os resultados experimentais são comparados com aqueles obtidos pela estratégia de modelização de um equivalente TMBR. O modelo matemático assume escoamento com dispersão axial para a fase fluida, escoamento pistão para a fase sólida, força motriz linear (FML) para a taxa de transferência de massa na partícula e equilíbrio de adsorção multicomponente. O estado estacionário predito pelo modelo de equivalente TMBR está em acordo com o estado cíclico estacionário obtido experimentalmente no SMBR considerando os perfis de concentração interna na metade do tempo de permutação.

A síntese de DME com o catalisador de fibras Smopex 101 foi também estudada em reator fechado e de leito fixo.

Résumé

Le diméthylacétal, aussi appelé acétal ou 1,1-diméthoxyéthane (DME) est utilisé de manière importante en tant que matière première à l'échelle commerciale ainsi que pour la recherche en laboratoire. Le DME est principalement utilisé pour la production de fragrances et de produits pharmaceutiques. Outre son utilisation comme matière première, le DME est un important intermédiaire pour la synthèse de différents produits chimiques industriels, les solvants organiques, pour la conception de parfums synthétiques, pour la synthèse de polyacétals et comme additif pour le fuel oxygéné.

La réaction d'acétalisation pour la synthèse de DME a été réalisée par réaction réversible en phase liquide du méthanol et d'acétaldéhyde, catalysée par Amberlyst 15.

Les expérimentations ont été réalisées dans un réacteur de laboratoire en verre à double enveloppe,à des températures entre 20 et 60°C, de manière à déterminer les paramètres cinétiques et thermodynamiques pour la synthèse du diméthyacétal en présence de catalyseur résine Amberlist 15. Les effets de la taille des particules, de l'agitation, de la quantité de catalyseur, de la composition initiale des réactifs, de la température et de la pression sur le taux de réaction ont été étudiés. Le modèle proposé est un modèle à deux paramètres basé sur l'expression de Langmuir-Hinshelwood, et utilisant des coefficients d'activité de la méthode UNIFAC. Ce modèle a été étendu pour inclure les transferts de masse interne et externe et permet de prédire les résultats d'une étude cinétique dans un réacteur batch.

Ensuite, les expérimentations ont été conduites dans une colonne de laboratoire à double enveloppe en verre (26mm Di, 120mm L) remplie de résine Amberlist 15. Les réactions ont été réalisées à 20°C à pression atmosphérique. Pour obtenir les paramètres du modèle, des expériences d'adsorption binaire sans réaction ont été conduites. L'équilibre d'adsorption multicomposant est choisi comme étant du type Langmuir modifié. Le modèle pour le réacteur d'adsorption suppose dispersion axiale, résistances de transfert interne et externe, température constante, isothermes du type Langmuir, et les équations du modèle ont été traitées par collocation orthogonale par la méthode des éléments finis, qui a été mise en application dans le PECDOL package, en utilisant les paramètres du modèle mesurés.

Les résultats des expériences menées dans le réacteur batch et dans le réacteur d'adsorption à lit fixe, permettent de concevoir et d'optimiser un procédé efficace dans une unité intégrée , qui serait combinaison d'une unité de séparation et d'une unité de séparation, appelée Réacteur à Lit Mobile Simulé (SMBR). Le SMBR pour la synthèse du diméthyacétal a été étudié expérimentalement et par simulation. Les résultats expérimentaux obtenus ont été comparés à la stratégie de modélisation TMBR. Le modèle mathématique suppose : écoulement à dispersion axiale pour la phase fluide, écoulement piston pour la phase solide, théorie de la LDF pour le taux de transfert intra particulaire et équilibre d'adsorption multicomposant. L'état d'équilibre prévu par le modèle TMBR est en accord avec l'état d'équilibre cyclique expérimental du SMBR à la moitié d'une période de permutation, en termes de profiles de concentration internes.

La synthèse du DME avec catalyseur fibres Smopex 101 a aussi été étudiée en réacteur batch ainsi qu'en réacteur à lit fixe.

Table of Contents

List of Figures

Chapter 2:

Chapter 3:

Chapter 4

Chapter 5

Chapter 6

List of Tables

Chapter 5

Chapter 6

1. Introduction

1.1 Relevance and Motivation

The central idea of this thesis is to study the synthesis of dimethylacetal (1,1-dimethoxyethane), concentrating both on reaction and separation unit processes. Process development requires the evaluation of thermodynamic and kinetics of reaction along with adsorption parameters for the design of a new integrated reaction-separation unit Simulated Moving Bed Reactor (SMBR).

Dimethylacetal, ($CH_3OCH(CH_3)OCH_3$) also named as 1,1-dimethoxyethane (DME), acetaldehyde dimethylacetal herein referred as acetal, is an important raw material used both at commercial scale and in laboratory research. Importantly, dimethylacetal is used for the manufacture of fragrances (Bauer et al., 1990) and pharmaceutical products (Merck Index, 1996). It is not only used as a raw material, but also as an important intermediate for the synthesis of various industrial chemicals, such as higher acetal like 1-hydroxy-2-lower alkoxy benzene (Gupta, 1987), for the design of synthetic perfumes to increase the resistance to oxidation and therefore the lifespan of the perfumes and for the production of polyacetal resins (Aizawa et al., 1994).

During the last decade the development for eco-friendly processes for manufacturing gasoline and fuels has taken the major efforts of shares for allotment of research funds to Research and Development Field through out the Chemical Industry world. Obviously, high-octane quality of gasoline can be achieved by the addition of oxygenated compounds to fuel. MTBE commonly is been using as the octane enhancer (Shikata et al., 1997), however, the environmental concern with the contamination of ground water by this toxic chemical (Hatzinger et al., 2001), surely open a new idea to investigate some other environment friendly additives. This is the case of lower and higher acetals that are used as cetane enhancers for diesel. A high cetane number indicates the ability of a diesel engine fuel to ignite quickly after being injected into the combustion cylinder. Seemingly, acetals can also be blended with diesel fuels and many recent patents have been claimed that these acetals could be used as an effective additive, which would boost the cetane number of a diesel fuel is roughly analogous to the octane number of gasoline to decrease the auto ignition temperature which nonetheless, helps in the combustion of the resulting mixture.

Any acetals can be produced by a reversible liquid phase reaction between aldehydes and alcohol, in an acidic medium (Morrison and Boyd, 1983; Guinot, 1932). Above reaction process is named as acetalization reaction, and this acetalization reversible reactions are of particular interest to the Latin American countries, because bio-ethanol and acetaldehyde are the by-products of the cane sugar industry and have been studied in the frame work of a CYTED Project IV.9, "Production of Oxygenated Additives to Diesel from Ethanol" (Laborde, 1997) to obtain high-added value products from ethanol. The synthesis of diethylacetal was previously studied at LSRE (Laboratory of Separation and Reaction Engineering, FEUP, Porto) by Silva, 2003.

Here the considered acetalization reversible liquid phase reaction between acetaldehyde and methanol.

In relevancy of the reversible reactions which are limited to the chemical equilibrium where more than one product is formed, conversion can be intensified in a well designed apparatus where the products are separated as they are formed. So it is necessary, that the catalyst used for the above type of reactions, should have the capability to adsorb one or more of the products formed. As the resin is one of the materials which can be used as both catalyst and as well as adsorbent in this kind of integrated reaction-separation unit (Chopade & Sharma, 1997), naturally it is a feasible process for performing above process and in particular the chromatographic reactor-separator like the Simulated Moving Bed Reactor (SMBR) can be used (Mazzotti et al., 1996; Silva and Rodrigues, 2005 a, b).

1.2 Objective and Outline

The main objective of this present thesis is to perform and determine the thermodynamic, reaction kinetics and adsorption parameters data in order to evaluate the information to design a Simulated Moving Bed Reactor for the synthesis of dimethylacetal using acetaldehyde and methanol as raw-material.

The thesis presented here includes 7 Chapters dealing with different aspects of dimethylacetal synthesis:

In Chapter 1 brief introductory part is included as a motivation and objective of this thesis. Chapter 2 contains a detailed literature review on acetalization reactions of aldehydes or ketones and alcohols in presence of acidic medium. The type of catalysts used, their activities, selectivity and other important characters and aspects have been discussed. A general review of acetalization of aldehydes with alcohols in presence of

mineral acid or heterogeneous acidic catalyst has been presented. Comparison of different processes for the reaction and separation units during the production of acetals has been included. A brief survey on dimethylacetal applications, mainly in perfumery and flavoring, pharmaceuticals, and as additive to diesel fuel has been discussed.

In Chapter 3 the performance of the experiments for determining the thermodynamic and reaction kinetics data, the experimental laboratory scale set-up has been described. A detailed study of the synthesis of dimethylacetal has been presented in a batch reactor using acetaldehyde and methanol as raw-material in the liquid phase reaction, and the acidic resin Amberlyst-15 as catalyst. Acetal synthesis was also performed with Y-type zeolite in order to compare the results for both catalysts. The reaction equilibrium constant was determined experimentally. The standard molar reaction properties were obtained. A two-parameter model based on Langmuir-Hinshelwood rate expression was considered, using activity coefficients from UNIFAC method, which can describe the experimental kinetic results.

Chapter 4 deals with the synthesis of dimethylacetal using acetaldehyde and methanol as raw-material on a fixed bed adsorptive reactor packed with Amberlyst-15 resin. Performance of dynamic binary adsorption experiments in absence of reaction in a laboratory scale column was studied. The parameters of the multicomponent adsorption isotherms, Langmuir type were determined. The mathematical model to describe the adsorptive reactor dynamic behavior includes axial dispersion, mass transfer resistances, constant temperature, and multicomponent Langmuir adsorption isotherms was studied. The mass transport phenomena through the external film and particle pores were discussed. Evaluation of proposed mathematical model for the

reaction and regeneration experiments in fixed bed adsorptive reactor with different lengths of bed was performed.

Description of the Smopex-101 Fibers is presented in Chapter 5. In this chapter, preliminary batch reactor experimental results to determine the kinetics and thermodynamics of the reaction for the synthesis of dimethyalacetal are presented. Binary adsorptive experiments in absence of reaction performed are discussed and adsorptive parameters of the components involved in the acetalization reaction mixture are also determined. Synthesis of dimethylacetal on fixed bed reactor packed with Smopex-101 Fibers and the regeneration experiment performed after reaction experiments are also presented here.

The detailed description of True Moving Bed (TMB) and Simulated Moving Bed (SMB) were presented in this Chapter 6 as an introduction to integrated reaction-separation unit. Dimethylacetal synthesis performed on this Simulated Moving Bed Reactor was discussed in detail. The simulated results compared with the experimental results were also discussed here in this chapter. Different aspects like effect of switching time, feed concentration studied were presented here. The conditions for operating Simulated Moving Bed Reactor were determined in order to perform experiments with desired productivity were discussed.

In this Chapter 7, general conclusions of this work along with the future proposals for the research are presented.

1.3 References

1. Aizawa, T.; Nakamura, H.; Wakabayashi, K.; Kudo, T.; Hasegawa, H. *Process for producing acetaldehyde dimethylacetal*. U.S. Patent 5,362,918, **1994**.

2. Bauer, K.; Garbe, D.; Surburg, H. *Common Fragrance and Flavor Materials*; Wiley-VCH: Weinheim, **1990**.
3. Chopade, S. P.; Sharma, M. M. Reaction of ethanol and formaldehyde: use of versatile cation-exchange resins as catalyst in batch reactors and reactive distillation columns. *React. Funct. Polym.* **1997**, 32, 53.
4. Guinot, H.M. *Process for the Manufacture of Acetal*. U.S. Patent 1,850,836 **1932**.
5. Gupta, B. B.G. *Alkoxyalkylation of phenol*. U.S. Patent 4,694,111, **1987**.
6. Laborde, M. CYTED Project IV.9: *Production of oxygenated additives to diesel from ethanol*. **1997**.
7. Mazzotti, M.; Kruglov, A.; Neri, B.; Gelosa, D.; Morbidelli, M. A continuous chromatography reactor: SMBR. *Chem. Eng. Sci.* **1996**, 51, 1827.
8. Merck Index; Merck & Co., Inc.: RAHWAY, USA, 1983.
9. Morrison, R.; Boyd, R. *Organic Chemistry*. 4th Edition, Allyn and Bacon: London, 1983.
10. Silva, V. M. T. M. "Diethylacetal synthesis in simulated moving bed reactor". *Ph.D Thesis*, Faculty of Engineering, University of Porto, Porto, Portugal, **2003**.
11. Silva, V. M. T. M.; Rodrigues, A. E. Processo industrial de produção de acetais num reactor adsorptivo de leito móvel simulado", *Portuguese Patent No. 103,123* (Patent Pending) **2004**.
12. Silva, V. M. T. M.; Rodrigues, A. E. "Novel process for dimethylacetal synthesis" *AIChE. J.* **2005**, *51*, 2752.

2. Literature Review on Dimethylacetal: Synthesis And Applications

In this chapter, a brief review for the applications of dimethoxyethane (acetaldehyde dimethyl acetal) and processes for the production of the same is presented.

2.1 Process for Producing Dimethylacetal

The basic process reaction for producing acetals is given by the following reversible reaction (Morrison and Boyd, 1996; Yadav and Pujari, 1999; Yadav and Krishnan, 1999) between alcohol and aldehydes in order to form acetal and water:

Acetals have the structure of ethers and, like ethers, are cleaved by acids and are stable towards bases. The acetals differ from ethers, however, in the extreme ease with which they undergo acidic cleavage; they are rapidly converted even at room temperature into the aldehydes and alcohol by dilute mineral acids. Allowing the aldehydes to stand with excess of the alcohol and a little anhydrous acid, usually hydrogen chloride, carries out the mechanism for the acetal formation (Guinot, 1932). There is good evidence that in alcoholic solution an aldehyde exists in equilibrium with a compound called hemiacetal:

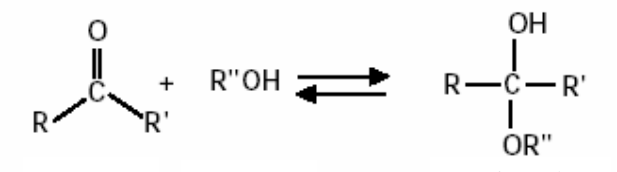

Aldehyde Alcohol Hemiacetal

In presence of the acidic medium, the hemiacetal formed, acting as an aldehyde, reacts with more of the alcohol to form the acetal and water as shown in the below mentioned reaction:

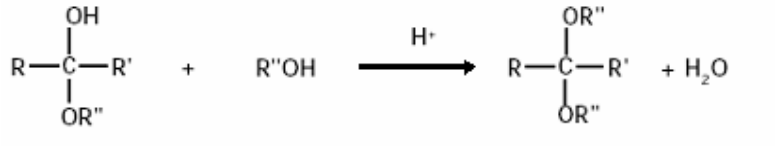

Hemiacetal Alcohol Acetal Water

The extension of the mechanism to heterogeneous catalytic reactions has been proposed for the reaction between aldehydes with alkanols over solid catalysts (Yadav and Pujari, 1999; Yadav and Krishnan, 1999)

Various acetals with lower and higher molecular weights formed with the reaction of different aldehydes and alcohols are given in Table 2.1. Physical properties of all given acetals are also presented in the same Table 2.1.

As far as the literature is concerned to the production of dimethylacetal, most known acetalization reactions reported involve the reaction of acetaldehyde and methanol in presence of acidic medium (Iwasaki et al., 1998; Zinke-Allmang et al., 1979; Hsu et al., 1988; Guinot, 1932). Generally this reaction is carried out in presence of anhydrous acid medium like hydrochloric acid, sulphuric acid, p-toluene sulhonic

acid or acetic acid as catalyst (Kohlpaintner et al., 1999). While using these soluble acidic catalysts in acetalization reactions, there exists number of disadvantages.

Table 2.1. Different Acetals and their Physical Properties (Kohlpaintner et al., 2002)

Acetal Name	Molecular Formula	MW	Density	BP (^{o}C)	RI
Formaldehyde dimethylacetal	$CH_2(OCH_3)_2$	76	0.8593	41.6	1.3589
Formaldehyde diethylacetal	$CH_2(OCH_2CH_3)_2$	104	0.832	88.0	-
Acetaldehyde dimethylacetal	$CH_3CH(OCH_3)_2$	90	0.8516	64.5	1.3665
Acetaldehyde diethylacetal	$CH_3CH(OCH_2CH_3)_2$	118.18	0.8254	102.7	1.3819
Acetaldehyde dipropylacetal	$CH_3CH(O\ CH_2CH_2CH_3)_2$	146	-	-	-
Acetaldehyde dibutylacetal	$CH_3CH(OCH_2CH_2CH_2CH_3)_2$	174	-	-	-
Propionaldehyde dimethyl acetal	$CH_3CH_2CH(OCH_3)_2$	101.15	0.8649	84 – 86	-
Propionaldehyde diethyl acetal	$CH_3CH_2CH(OCH_2CH_3)_2$	132.21	0.8232	124	1.3924
Butyraldehyde dimethyl acetal	$CH_3CH_2CH_2CH(OCH_3)_2$	118.18	-	112 – 113	1.3888
Butyraldehyde diethyl acetal	$CH_3CH_2CH_2CH(OC_2H5)_2$	146.22	0.8320	145 – 45.5	1.3970
Pentanal diethyl acetal	$CH_3(CH_2)_3CH(OCH_2CH_3)_2$	160.25	0.8304	162.5 – 163.5	1.4021
Hexanal diethyl acetal	$CH_3(CH_2)_4CH(OCH_2CH_3)_2$	174.28	-	155 – 158	-

Disadvantages can be the solubility of catalyst in the reaction mixture which needs to be neutralized after reaction. As being soluble in the reaction mixture, it is even difficult to separate from the reaction mixture. Obviously, using solid catalyst for this type of reaction in order to separate the catalyst from the reaction mixture will be the advantage of the process. Therefore, the heterogeneous catalysts like ion-exchange resin (acidic) or zeolite can be used in these acetalization reactions which have the advantage of separating from the reaction mixture easily and can be reused for several times. Resins are of particular interest due to their character of catalyzing the acetalization reactions and they can be used as selective adsorbent to the species involved in the process (Mazzotti et al., 1996; Yadav and Pujari, 1999; Silva and Rodrigues, 2001)

The synthesis of acetals is a reversible reaction; in order to obtain reasonable acetal yields during the acetalization reaction of any alcohol and aldehydes, the equilibrium must be displaced in the direction of the acetal formation. Several methods can be adopted to displace this equilibrium towards the acetal formation, such as:

1) to use excess of one of the reactants, in general the alcohol which then requires elimination of the excess alcohol in the purification step for the desired product;
2) to eliminate water by the azeotropic distillation between a solvent and water, the solvent and water must be partially miscible and the boiling points of the different constituents in the reaction medium must be compatible with that azeotrope formed.
3) To use reactive separation (as reactive distillation, simulated moving bed reactor, pervaporation reactor, etc.) in order to remove the products from the reaction mixture.

At present, the process for producing acetals (diethylacetal, dimethylacetal or other acetals) consists of a reaction followed by separation, usually consecutive distillations to separate the mixture (Chopade and Sharma, 1997a; Chopade and Sharma, 1997b; Mahajani et al., 1995)

2.1.1 Patents Review for Acetals Synthesis

There are great number of patents related to acetal production, any of the technologies were performed at industrial scale. A brief description of few patents is shown below in Table 2.2.

2.1.2 Catalyst Review

Catalysts are extremely important materials of commerce. Most of the industrial reactions pertaining to the chemical, petrochemical, and pharmaceutical sector and almost ass biological reactions are catalytic in nature. Products like food, clothing, drugs, fuels, etc. which drive today's economy involve catalysts in some way or the other. Catalysts also form an integral part of environmental protection and emission control strategies. Catalysts have been used commercially for more than century dealing from the Deacon and Contact process for sulfuric acid, used in the late 1800s to the latest FCC process for petrochemical cracking.

Majority of chemical reactions use catalysts to enhance the reaction rates in order to obtain the desired products in an economical way. Catalysts in general are classified into two types, depending on the phase in which the catalyst is presented. Homogeneous catalysis, in which reactants, products as well as catalyst are presented in a single phase, and where as, in heterogeneous catalysis, the catalyst is presented in a different phase than

Table 2.2. Review of Patents

Distilleries Des Deux-Sevres Henri Martin Guiton, 1932	Alcohol and aldehydes are placed together, the reaction being produced by means of a certain quantity of a catalyst, such as hydrochloric acid, sulphuric acid, p-toluene sulphonic acid, or acetic acid, hydrogen phosphide, calcium chloride, various other metallic salts, or the like. Acetal is formed, and the production stops at the state of equilibrium, where the reaction medium contains the four components. Due to the difficulty of separating acetal from the reaction mixture, two principal methods have been proposed. One of these consists in the use of certain salts, such as calcium chloride, to adsorb the water which is formed. And the other proposed method consists in adding to the mixture in the reaction, liquid which is insoluble in water, such as gasoline.
Celanese Corporation of America. Robenson et al., 1950	The production of formals, acetals and ketals were studied in order to improve the process for the production of the same in increase yields. For removing water from the reaction mixture, an entraining agent was adapted in a continuously operated azeotropic distillation
Union Rheinische Braunkohlen Kraftstoff Aktiengesellschaft. Korff et al., 1981	The improved process for the production of acetaldehyde dimethylacetal by reacting methanol with carbon monoxide and hydrogen in the presence of a cobalt-containing catalyst, halogen or halide as promoter and a 3-valent phosphorus compound as ligand using a nickel compound as a co-catalyst was presented.
Union Carbide Corporation Wegman et al., 1984	Process for selective production of acetaldehyde and dimethylacetal by the reaction of methanol and carbon monoxide in contact with a catalyst containing cobalt atom, halide atom and a mixture of a trivalent phosphorus compound and a trivalent nitrogen compound. The amount of trivalent nitrogen compound in its mixture varies from 5 mole percent to 50 mole percent of such mixture.
Kuraray Co. Ltd. Iwasaki et al., 1998	Description of producing acetals comprising reacting an aldehyde or a ketone with an alcohol in presence of a titanium compound having an acetylacetone as a ligand, or in the presence of a compound selected from the group consisting of stannous chloride dihydrate, cerium chloride hexahydrate and bismuth chloride. The process can be used in the synthesis of unstable acetals or when water exists in the reaction mixture.
Catalytic Distillation Technologies Smith, Jr., et al., 2000	Acetals are produced from the reaction of aldehydes and alcohols, e.g. methylal is produced by the reaction of formaldehyde and excess methanol. By the reaction in a reactive distillation column, the products acetal and water formed through the reaction in presence of catalyst were separated through the fractional distillation of the reaction mixture.
BASF Aktiengesellschaft Worms et al., 2003	The preparation of acetals relates to a continuous process for the preparation of unsaturated acetals by reacting olefinically unsaturated aliphatic compounds with allyl alcohol in a reaction column, the resulting acetal is concentrated in at least two successive evaporation stages, and the recovered reactants are returned to the reaction column.
DSM IP Assets B.V. Paisley et al., 2004	This process for the preparation of acetals and ketals by reacting an aldehydes or ketone with excess alcohol in the presence of an acidic catalyst and removing water formed by pervaporation. Manufacturing equipment for the preparation of acetals and ketals is also provided.

that of the reactants. The main drawback of homogeneous catalysts is in the difficulty of catalyst separation from the reaction mixture.

Heterogeneous catalysts are preferred over the soluble acid catalyst due to easier separation of the products without contamination, ease of handling, higher rates of reactions, high selectivity, and reusability of the catalyst and minimum corrosion of equipment. Heterogeneous catalysts, by virtue of their surface properties, accelerate gas-phase, liquid phase, or multi-phase reactions.

2.1.2.1 Ion Exchange Resins

The processes using ion exchange resin as catalysts represent important examples of solid acid catalysts. In heterogeneous catalysis, the forces active at a solid surface can distort or even dissociate an absorbed reactant molecule and affect the rate of reaction. The use of ion-exchange catalysis should now be regarded not merely as an elegant preparative technique but also as a potential method in modern chemical technology, combining simplicity in the design and operation of the plant with high yield of valuable products. Strong acid cation exchange resins have been used commercially as solid acid catalysts in many areas. For example, (1) etherification of olefins with alcohols, (2) dehydration of alcohols to olefins or ethers. There is evidence that resins can be used as a catalyst for the acetalization reactions.

2.1.2.2 Zeolites

The use of zeolites as catalysts in the chemical and petroleum industries is based on their acidity (both Bronsted and Lewis), pore size and adsorption properties. The characterization of zeolites with respect to its pore size and adsorption properties is usually carried out gravimetrically using a quarty spring McBain-Balar, or an electronic balance. Zeolites are also used as catalyst for acetalization reactions.

2.1.2.3 Smopex-101 Fibers

Smopex 101 (Smoptech Ltd. Finland) is a fibrous polymer supported by sulphonic acid which fibers are grouped as if the fibers are tied together. These polymer fibers can be manufactured by supporting sulphonic acid on poly (ethylene-graft-polystyrene). Grafted co-polymers were prepared by using irradiation grafting technique (Llilja et al., 2002; Aumo et al., 2002). These fibers can be used as a catalyst for esterification, etherification, and acetalization type of reversible reactions. The polyethylene-based fiber catalysts can be modified by grafting with different functional groups, such as pyridine, carboxylic acid, sulphonic acid or a combination of them. In this way the homogeneous catalysts can be replaced by heterogeneous fiber catalysts.

2.1.3 Equilibrium of Reversible Reactions

As one or more products forms during reversible reactions like etherification, esterification, acetalization and etc., a limited conversion of reactants exists by the nature of the equilibrium in the reaction. In order to increase the yield of one of the products in the reversible reactions, it would be necessary to take some manipulations as discussed in the section 2.1. During the acetalization reaction, in order to increase the yield of the product acetal, the by-product water formed should be removed as it formed and then the reaction advances. To eliminate the water in the reaction mixture, distillation of an azeotrope between a solvent and water, and water, the solvent and water must be at the least partially miscible and boiling points of the different constituents in the reaction medium must be compatible with that azeotrope. Or the water can be eliminated by adsorption on a dehydrating solid which may be a molecular sieve or any other material which can adsorb water without interfering in the reaction of

the acetal formation. This operation can be performed through different types of methods.

2.1.4 Integrated Reaction and Separation Unit

In almost all chemical processes, it is natural to have a reaction and then comes separation unit operation step in any chemical industry even today. Integration of any unit operation with chemical reaction into one single apparatus may allow for significant improvement in process performance and has therefore been studied in different forms for last years (Freeport and Lake Jackson, 1958; Agar, 1999). Examples for such multifunctional reactors are reactive distillation process, integrating chemical conversion and separation, or reverse-flow reactors to combine chemical reaction and heat transfer. In the former case, the major advantage is given by the possibility to tune the concentration profiles within the unit in order to either overcome a chemical equilibrium limitation or to optimize process selectivity. On the other hand, this process intensification also reduces the degrees of freedom in the design of this process, potentially limiting their performance. Nevertheless, the general concept has proved its potential, and for example, reactive distillation has become the process of choice for number of industrial applications. Apart from this reactive distillation process, there exist other types of integrated unit operations like pervaporation, simulated moving bed reactor for the reactive-separation operation.

2.1.4.1 Reaction and Separation in Reactive Distillation Column

Reactive distillation column is a multifunctional reactor, filled with catalytically active packing. In this column, chemicals are converted on the catalyst while products formed are continuously separated by fractionation. There is reported literature concern to the process operated in reactive distillation integrated unit which involves

simultaneous chemical reaction and distillation as shown in Figure 2.1. (Hsu and Ellis, 1986; Chopade and Sharma, 1997).

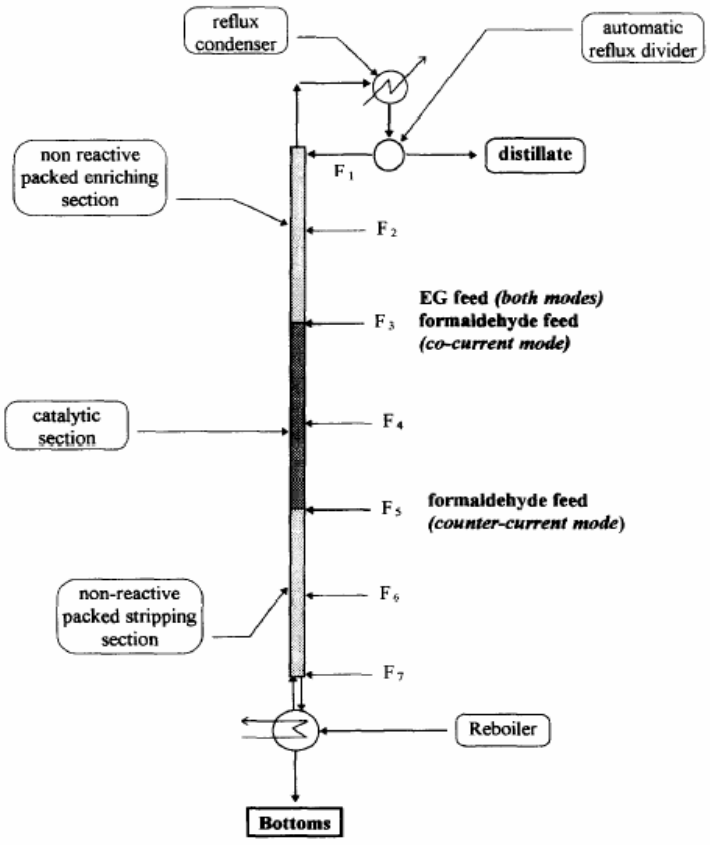

Figure 2.1 Schematic diagram for reaction of aqueous formaldehyde and ethylene glycol in RDC (Chopade and Sharma, 1997).

The chemical reaction usually takes place in the liquid phase or at the surface of a solid catalyst in contact with the liquid phase. General application of reactive distillation described, is the separation of a close-boiling or azeotropic mixture of components, where a reactive entrainer is introduced into the distillation column (Seader and Henley, 1998).

In this patent a continuous process for the production of dimethylformamide was studied comprising the steps: (a) reacting methyl formate and dimethylamine in a

reactive distillation column under conditions to form dimethylformamide and by-product methanol; (b) vaporizing the by-product methanol and generating a liquid dimethylformamide while in said reactive distillation column; (c) removing at least a major portion of the by-product methanol as an overhead from said reactive distillation column; (d) removing a crude liquid dimethylformamide containing residual by-product methanol as a bottoms fraction from said reactive distillation column; (e) introducing said bottoms fraction containing dimethylformamide and residual by-product methanol to a purification column wherein the by-product methanol is removed from said dimethylformamide as an overhead and purified dimethylformamide is removed as a bottoms fraction; and, optionally, (f) recycling the by-product methanol removed as an overhead from the purification column to the reactive distillation column (Maliszewskyj et al., 2004).

High yields can be obtained in the equilibrium limited reactions by achieving removal of one of the products from the reaction mixtures, either in a semi-batch mode or in a continuous mode (Astle et al., 1954, Chopade and Sharma, 1997) was discussed in detail. It was successfully demonstrated the efficiency of continuous reactive distillation column for acetalization reactions, higher that 99% conversion of the limiting reactant was achieved in the reactive distillation column.

This reactive-distillation unit is also used in esterification reactions for producing methyl acetate from acetic acid and methanol (Wei Song, 1998), ethyl acetate from acetic acid and ethanol (Kirbaslar et al., 2001; Xu and Chuang, 1997).

2.1.4.2 Simulated Moving Bed Reactor and True Moving Bed Reactor

As an alternative for the reaction-separation unit, there is evidence that the chromatographic reactor (Broughton et al., 1961) which utilizes the difference in

adsorptivity of the different components involved rather than difference in their volatility. It is especially attractive as an alternative to reactive distillation when the species involved are either non-volatile or sensitive to temperatures, as is the case, for example, in some fine chemicals or pharmaceutical applications, or exhibit small volatility difference. The general representation of the Simulated Moving Bed Reactor is shown in Figure 2.2.

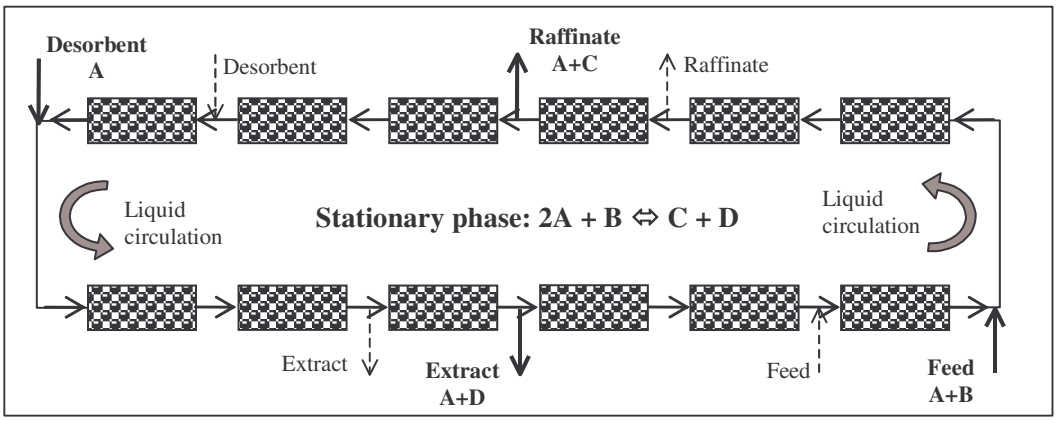

Figure 2.2 Typical Simulated Moving Bed Reactor (Silva and Rodrigues, 2004, 2005)

There is also evidence of using the apparatus simulated moving bed reactor with high efficiency at the industrial scale. This simulated moving bed separation system is designed, in which a fluid circulation flow path can be washed for a short time. This system is provided with two or more packed bed connected in series in a closed loop. It is also provided with desorbing-charging inlet, extract draw-out port, feed stock introducing port and raffinate draw-out port arranged in this order in the direction of circulation liquid flow, which ports are allowed to intermittently shift in the circulation liquid flow direction. System is provided with packed bed-washing pipes, valves and pumps (Ikeda, 2003; Fricke and Schmidt-Traub, 2003).

The simultaneous reaction and separation process using a simulated moving bed apparatus was studied by researchers previously in esterification reactions for producing β-phenethylacetate (Kawase et al., 1996), ethylacetate (Mazzotti et al., 1996), hydrogenation of 1,3,5-trimethylbenzene (Ray et al., 1994), acetalization reaction for producing diethylacetal (Silva and Rodrigues, 2005). So, obviously this integrated reactive-separation unit simulated moving bed reactor is worthful apparatus to work with the liquids which are to be separated after reaction.

2.1.4.3 Pervaporation Process of Separation

Along with the above explained integrated reaction-separation units, reactive distillation multifunctional reactor and simulated moving bed reactor, there exists another process for the separation called pervaporation membrane separation process. This pervaporation process can one of the alternative process candidate for separation of desired products and as well as saving energy

Pervaporation process was studied in the separation of acetic acid-water mixture during the production of acetic acid itself, vinyl acetate, acetic anhydrate (Ray et al., 1998; Işiklam and Şanli, 2005; Netke et al., 1995). The typical process apparatus for the pervaporation study for the acetic acid-water mixture separation is shown in Figure 2.3.

2.2 Uses of Dimethylacetal

Dialkoxyalkanes are generally called as acetals, which are produced by the reaction of an alcohol and an aldehydes in presence of acid medium. The above said reaction is also named as acetalization reaction. The acetals produced from the acetalization reactions are in the form of R^2-CH(-O-R^1)$_2$, where R^1 and R^2 are alkyl groups from alcohol and aldehydes respectively (Morrison and Boyd, 1998). During this

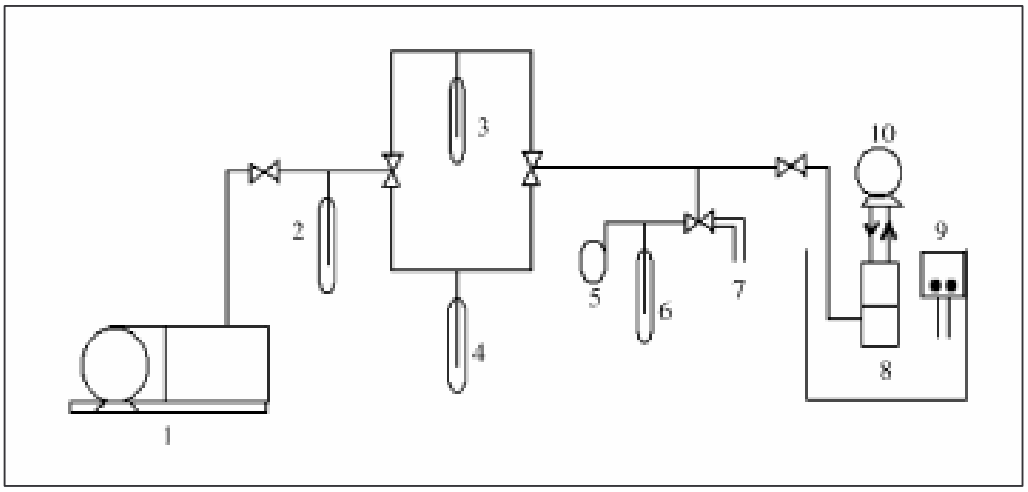

Figure 2.3. Schematic diagram of pervaporation apparatus (Işiklam and Şanli, 2005).

1. Vacuum pump; 2,3. Trap; 4,6. Cold traps for collecting samples;
5. Vacuum monometer; 7. Vent to atmosphere; 8. Permeation cell;
9. Water bath with temperature indicator; 10. Peristaltic pump.

reaction of alcohol and aldehydes in presence of acidic medium, initially hemiacetal is formed from the reaction of one molecule of alcohol with one molecule of aldehydes, and then the hemiacetal formed reacts with another molecule of alcohol to form stable acetal.

Acetalization reaction is sometimes a necessary requirement to protect carbonyl groups in the presence of other functional groups during the manipulation of multifunctional organic molecules. Acetals are generally stable to bases, Grignard reagents, hydrogenation reagents, metal hydrides, oxidants, bromination and esterification reagents. Besides the interest of acetals as protecting groups, many of them have found direct application as fragrance (Curtis and Williams, 1994), in cosmetics, food and beverages additives (Kelly et al., 1999), pharmaceuticals, in detergents and in lacquer industries (Bauer et al., 1990). Sometimes several acetals

named as 'potential fragrances' (which exhibits little or no odor) are introduced together into the different formulations and, at the contact with the skin the products are hydrolyzed and the odorous molecules are released (Suffis et al., 1997). Acetals also used in perfumes to imparting fruity odor (Kohlpaintener et al., 1999). Acetals are also used as starting material for agriculture chemicals manufacture and as an intermediate for pharmaceutical chemicals (Godefroi and Heeres, 1971; Gupta, 1987).

During last few years the eco-friendly process for gasoline and fuels manufacturing allotted major shares of research funds. The development of gasoline and fuels are more environmentally acceptable has been studied exclusively. The composition generally comprises one or more compounds selected from dialkoxyalkane chemical family. In a preferred embodiment of the present research, the diesel fuel composition consists of moderate amounts of dimethoxypropane and dimethoxyethane blended into a conventional diesel fuel (Waller et al., 1999; Ancillotti and Fattore, 1998; Taylor, 1988).

An electrolyte solvent system for use in a electrochemical cells in which the electrolyte solvent system consists essentially of a diaxolane-based solvent and a dimethoxyethane-based solvent in a weight ratio of about 1:3. In this present research, it was also disclosed electrolyte solutions and electrochemical cells comprising such a solvent system (Webber et al., 2001).

In this patent, it was described that dimethoxyethane can be used in a lithium rechargeable cells. It was presented that, a rechargeable lithium cell is provided comprising a lithium anode, a lithium intercalating cathode, and an electrolyte comprising a solution of a lithium salt such as $LiAsF_6$ or $LiAlCl_4$ in 24.4 mass percent 4-butyrolactone (4-BL) in dimethoxyethane (DME). The cell exhibits improved low

temperature (-40 ^{o}C. $\leq t \leq 0$ ^{o}C) performance and rate capability (Salomon et al., 1985; Gupta, 1987).

2.3 Conclusions

In this present chapter, brief description of the processes for the production of acetals and the uses of dimethylacetal as raw-material for fragrances, in pharmaceutical industries, as intermediate in fine chemical industries and as an fuel oxygenate to enhance cetane number are presented. Integration of reaction and separation units was discussed to overcome the thermodynamic equilibrium conversion. Remaining part of the thesis is focused on the synthesis of dimethylacetal using different catalysts (Amberlyst 15 Resin, Smopex 101 fibres and USY-Type Zeolite) from acetaldehyde and methanol as reactants. Synthesis of dimethylacetal in a Simulated Moving Bed Reactor is also addressed in order to study the separation process for separating dimethylacetal from the reaction mixture at equilibrium position.

2.4 References

1. Agar, D.W. Multifunctional reactors: Old preconceptions and new dimensions. *Chem. Eng. Sci.*, **1999**, 56, 1299-1305.
2. Ancillotti, F. and Fattore, V. Oxygenate fuels: Market expansion and catalytic aspect of synthesis. *Fuel Proc. Tech.,* **1998**, 57, 163-194.
3. Astle, M.J.; Zaslowsky, J.A. and Lafyatis, P.G. Catalysis with Cation-Exchange Resins. *Ind. Eng. Chem.*, **1954**, 46, 787-791.
4. Aumo, J.;, Lilja, J.;, Maki-Arvela, P.; Salmi, T.; Sundell, M.; Vainio, H.; Murzin, D. Yu. Hydrogenation of citral over a polymer fiber catalyst. *Catal. Lett.* **2002**, 84, 219-224.

5. Bauer, K.; Garbe, D. and Surburg, H. *Common Fragrances and Flavors Material*, 2nd Edition, VCH, New York, 1998.
6. Broughton, D.B. and Gerhold, C.G. *Continuous sorption process employing fixed bed sorbent and moving inlets and outlets*. U.S. Patent 2,985,589, **1961**.
7. Chitnis, S.R. and Sharma, M. M. "Alkylation of aniline with α-methylstyrene and separation of close boiling aromatic amines through reaction with α-methylstyrene, using acid-treated clay catalysts". *React. Funct. Polym.* **1997**, 33, 1-12.
8. Chopade, S. P. and Sharma, M. M. Acetalization of ethylene glycol with formaldehyde using cation-exchange resins as catalysts: batch versus reactive distillation. *React. Funct. Polym.* **1997**, 34, 37-45.
9. Chopade, S. P. and Sharma, M. M. Reaction of ethanol and formaldehyde: use of versatile cation-exchange resins as catalyst in batch reactors and reactive distillation columns. *React. Funct. Polym.* **1997**, 32, 53-65.
10. Curtis, T. and Williams, D., *Introduction to Perfumery*, ELLIS HORWOOR Limited, New York, 1994.
11. Freeport, G.C.B. and Lake Jackson, L.A.K. *Separation of ketals*. U.S. Patent 2,827,495, **1958**.
12. Fricke, J. and Schmidt-Traub, H. A new method supporting the design of simulated moving bed chromatographic reactors. *Chem. Eng. Proc.*, **2003**, 42, 237-248.
13. Godefroi, E.F. and Heeres, J. *Ketal Derivatives of Imidazole*. U.S. Patent 3,575,999, **1971**.

14. Guinot, H. M. *Process for the Manufacture of Acetal*. U.S. Patent No. 1,850,836, **1932**.
15. Gupta, B. B. G. *Alkoxyalkylation of Phenol*. U.S. Patent 4,694,111, **1987**.
16. Hsu, Chao-Yang and Ellis Jr., Paul E. *Process for the production of 2,2-dimethoxypropane.* U.S. Patent 4,775,447, **1988**.
17. Hsu; Chao-Yang; Ellis, Jr.; Paul, E. *Process for the production and purification of diethoxymethane by azeotropic distillation*. U.S. Patent No. 4,613,411, **1986**.
18. Ikeda, H. *Simulated moving bed separation system.* U.S. Patent No. 6,652,755, **2003**.
19. Işıklan, N. and Şanlı, O. Separation characteristics of acetic acid–water mixtures by pervaporation using poly (vinyl alcohol) membranes modified with malic acid. *Chem. Eng. Proc.*, **2005**, 44, 1019-1027.
20. Iwasaki, H.; Kitayama, M.; Onishi, T. *Process for producing acetals*. U.S. Patent 5,792,876, **1998**.
21. Kawase, M.; Suzuki, T.B.; Inoue, K.; Yoshimoto, K. and Hashimoto, K. Increased esterification conversion by application of the simulated moving-bed reactor. *Chem. Eng. Sci.*, **1996**, 51, 2971-2976.
22. Kelly, J.; Chapman, S.; Brereton, P.; Bertrand, A.; Guillou, C. and Wittkowski, R. "Gas Chromatographic Determination of Volatile Congeners in Spirit Drinks: Interlaboratory Study". *J. AOAC Int.*, **1999**, 82, 1375.
23. Kirbaslar, S.I.; Baykal, Z.B and Dramur, U. Esterification of acetic acid with ethanol catalyzed by an acidic ion-exchange resin. *Turk. J. Eng. Environ. Sci.* **2001**, 25, 569-577.

24. Kohlpaintner, C.; Schulte, M.; Falbe, J.; Lappe, P. and Weber, J. "Aldehydes, aliphatic and araliphatic", *Ullmann´s Encyclopedia of Industrial Chemistry*, 6th Edition, 1999.

25. Lilja, J.; Aumo, J.; Salmi, T.; Murzin, D. Yu.; Mäki-Arvela, P.; Sundell, M.; Ekman, K.; Peltonen, R. and Vainio, H. Kinetics of esterification of propanoic acid with methanol over a fibrous polymer-supported sulphonic acid catalyst. *Appl. Catal.* A, **2002**, 228, 253-267.

26. Mahajani, S.M.; Kolah, A.K. and Sharma, M. M. Extractive reactions with cationic exchange resins as catalysts (acetalization of aldehydes with alcohols). *React. Funct. Polym.* **1995**, 28, 29-38.

27. Maliszewskyj, R.J.; Turcotte, M.G. and Mitchell, J.W. *Dimethylformamide synthesis via reactive distillation of methyl formate and dimethylamine.* U.S. Patent 6,723,877, **2004**.

28. Mazzotti, M.; Kruglov, A.; Neri, B.; Gelosa, D. and Morbidelli, M. A continuous chromatographic reactor: SMBR. *Chem. Eng. Sci.*, **1996**, 51, 1827-1836.

29. Morrison, R.; Boyd, R. *Organic Chemistry*, 4th Edition, Allyn and Bacon, London, 1983.

30. Netke, S.A.; Sawant, S.B.; Joshi, J.B., and Pangarkar, V.G. Sorption and permeation of acetic acid through zeolite filled membrane. *J. Membr. Sci.*, **1995**, 107, 23-33.

31. Ray, A.K.; Carr, R.W. and Aris, R. The simulated countercurrent moving bed chromatographic reactor: a novel reactor-separator. *Chem. Eng. Sci.*, **1994**, 49, 469-480.

32. Ray, S.K.; Sawant, S.B.; Joshi, J.B., and Pangarkar, V.G. Dehydration of acetic acid by pervaporation. *J. Membr. Sci.*, **1998**, 138, 1-17.

33. Saha, B. and Sharma, M. M. Esterification of formic acid, acrylic acid and methacrylic acid with cyclohexene in batch and distillation column reactors: ion-exchange resins as catalysts. *React. Funct. Polym.* **1996**, 28, 263-278.

34. Salomon, M.; Plichta, E. J. *Rechargeable lithium cell having an electrolyte comprising 4-butyrolactone in dimethoxyethane*. U.S. Patent 4,560,630, **1985**.

35. Seader, J.D. and Henley, E.J. *Separation Process Principles*, John Wiley & Sons, New York 1998.

36. Silva, V. M. T. M. and Rodrigues, A. E. Synthesis of diethyl acetal: thermodynamic and kinetic studies. *Chem. Eng. Sci.*, **2001**, 56, 1255-1263.

37. Silva, V. M. T. M.; Rodrigues, A. E. "Novel process for diethylacetal synthesis" *AIChE. J.* **2005**, *51*, 2752.

38. Silva, V. M. T. M.; Rodrigues, A. E. "Processo industrial de produção de acetais num reactor adsorptivo de leito móvel simulado", Portuguese Patent 103,123 (Patent Pending) **2004**.

39. Song, W.; Venimadhavan, G.; Manning, J.M.; Malone, M.F. and Doherty, M.F. Measurement of Residue Curve Maps and Heterogeneous Kinetics in Methyl Acetate Synthesis. *Ind. Eng. Chem. Res.*, **1998**, 37, 1917-1928.

40. Suffis, R.; Barr, M.L.; Ishida, K.; Sawano, K.; van Loveren, A. G.; Nakatsu, T.; Green, C.B.; Reitz, G.A.; Kang, R. K. L. and Sato deceased, T. *Composition containing body activated fragrance for contacting the skin and method of use.* U.S. Patent 5,626,852 **1997**.

41. Taylor, W. F. *Fuel having improved cetane.* U.S. Patent 4,723,963, **1988**.

42. Waller; F. J.; Weist, Jr., E. L.; Brown, D. M. and Tijm, P. J. A. *Diesel fuel composition comprising dialkoxy alkanes for increased cetane number.* U.S. Patent 5,858,030, **1999**.

43. Webber, A. *Dioxolane and dimethoxyethane electrolyte solvent system.* U.S. Patent 6,218,054, **2001**.

44. Xu, Z.P and Chuang, K.T. "Effect of internal diffusion on heterogeneous catalytic esterification of acetic acid". *Chem. Eng. Sci.* **1997**, 52, 3011-3017.

45. Yadav, G. D. and Krishnan, M. S. Solid acid catalysed acylation of 2-methoxy-naphthalene: role of intraparticle diffusional resistance. *Chem. Eng. Sci.* **1999**, 54, 4189-4197.

46. Yadav, G. D. and Pujari, A. A. "Kinetics of acetalization of perfumery aldehydes with alkanols over solid acid catalysts". *Canadian Journal of Chemical Engineering*, *77*, **1999**, 489-496.

47. Zinke-Allmang, H. and Scheidmeir, W. *Manufacture of dialkyl-ketals.* U.S. Patent 4,136,124, **1979**.

3. Thermodynamic and Reaction Kinetics for the Synthesis of Dimethoxyethane in Batch Reactor

The synthesis of dimethylacetal using acetaldehyde and methanol as raw-material in presence of Amberlyst-15 resin as acid catalyst is studied. The description of the Laboratory scale experimental set-up for the determination of thermodynamic and reaction kinetics data is presented. The catalyst used Amberlyst-15 resin is a sulphonic acid resin; acidic zeolite was also considered as catalyst in order to compare the results of the reaction experiments for the synthesis of dimethylacetal. Initially the reaction equilibrium constant was determined, the activity coefficients calculated from the UNIFAC method was used to determine the equilibrium constant. A two-parameter model based on a Langmuir-Hinshelwood rate expression using activities was proposed to describe the experimental kinetic results and it was compared with the kinetic rate law expressed with molar fractions. A mathematical model including film and pore diffusion was developed in order to verify the existence of limitations to mass transfer and to obtain the true kinetic constants. The dependence of the effectiveness factor with the Thiele modulus and temperature was studied.

3.1 Introduction

The basic process reaction for producing acetals is given by the following reversible reaction between alcohol and aldehydes in order to form acetal and water:

$$2\ \text{Alcohol} + \text{Aldehyde} \longleftrightarrow \text{Acetal} + \text{Water}$$

The simple mechanism of the above reaction for the synthesis of dimethylacetal for homogeneous is given by three steps (Morrison and Boyd, 1983; Chopade and Sharma, 1996), the reaction between acetaldehyde molecule and methanol molecule typically leads to the formation of intermediate hemiacetal which is not stable. The hemiacetal is then reacted with second methanol molecule to form the final product acetal. The various steps takes place during this reaction are shown below:

$$A + B \overset{H^+}{\longleftrightarrow} I_1$$

$$I_1 + H^+ \longleftrightarrow I_2 + D$$

$$I_2 + A \longleftrightarrow C + H^+$$

where I_1 and I_2 are intermediate species.

The main drawback of these reversible reactions is that, the conversion of reactants is limited to some extent. Once the reaction reaches the equilibrium stage, thereafter the reactants will not convert to products any more. In order to make the displacement of the equilibrium, one of the products from the reaction mixture should be removed. So, unless the water from the above reaction is removed continuously, or a large excess of methanol is taken initially, the reaction does not go to completion. As the hemi-acetal formed in the acetalization is reported to be quit fast in comparison with the acetal formation. Therefore, the reaction of water formation is the limiting step.

Several mineral acids have been employed as homogeneous catalysts in the acetal synthesis: sulhponic acid, nitric acid and hydrochloric acid were in common use

for the acetalization reactions. Instead of highly polluting and corrosive mineral acids, the use of solid acids, such as sulfated zirconia, clays, ion exchange resins, zeolites and zeotypes in alkylation, isomerization, esterification, etherification, acylation and nitration of organic compounds is reported in detail for last few years (Thorat and Yadav, 1992). Solid acid catalyzed epoxidation of C_8, C_{10}, C_{12} α-olefins and the isomerization of the corresponding epoxides to aldehydes have been studied. Additionally, clay based acidic catalyst are cheap and versatile. Particularly relevant applications based in reactions between olefins and alcohols catalyzed by acid resins, are those that involve the production of oxygenated compounds. It is thus appeared, that there exists a scope for conducting acetalization reactions on solid catalysts. Along with the acetalization reaction, the detailed investigation of acetalization of aldehydes and alcohols by using heterogeneous catalysts were reported earlier. Acetalization of n-octanal with methanol (Yadav and Pujari, 1999), acetalization reaction of acetaldehyde and ethanol (Silva and Rodrigues, 2001; Fedriani et al., 2000), acetalization of ethylene glycol with formaldehyde using cation-exchange resins as catalysts (Chopade and Sharma, 1997) was studied in detail. The reported literature for the production of oxygenated compounds is listed in the Table 3.1 (Silva, 2003).

The extension of acetalization mechanism to heterogeneous catalytic reactions has been proposed for reaction between n-octanal and methanol (Yadav and Pujari, 1999). It was also considered a three step reaction mechanism for this acetalization reaction: Following are the steps considered,

- the reaction between the adsorbed aldehydes and methanol to produce hemi-acetal.
- the reaction for the water formation, which was considered as the limiting step.

- the reaction for the acetal formation.

Considering the above mentioned acetalization reactions of different aldehydes and alcohols, here in this chapter the acetalization of acetaldehyde and methanol was considered. Here Amberlyst-15 resin used as catalyst to study the acetalization reaction of acetaldehyde and methanol in order to produce dimethylacetal in a batch reactor in the temperature range 293.15 – 333.15 K at 0.6 MPa was studied. In order to determine thermodynamic and kinetic data, laboratory scale experimental set-up was prepared. The experimental set-up is as shown in Figure 3.1. Experiments were performed in the below mentioned points of view in a batch reactor (Figure 3.1.):

- to obtain thermodynamic data for the synthesis of dimethylacetal;
- to study the effect of temperature, initial molar ratio of reactants and pressure on the reaction kinetics;
- reaction mechanism and a rate equation with experimentally measured kinetic parameters;

to study the internal mass transfer effects on reaction kinetics.

3.2 Experimental

3.2.1 Experimental Set-up

Experiments were carried out in a glass-jacketed 1 dm^3 capacity autoclave (Buchi, Switzerland), with batch mode operations. The reactor provided with mechanically agitated stirrer with the range of 0 – 2900 rpm (revolutions per minute). Reactor equipped with pressure sensor (pressure transducer Lucas P1231-0005-15 BAR A and manometer), and a temperature sensor (thermocouple K type, Omega, TJ36-CAIN-116(G)-12) along with safety blow-off valve as shown in Figure 3.1.

Table 3.1. Experimental investigation literature for oxygenate production (Silva, 2003).

Source	Experimental Apparatus	Product	Catalyst	Kinetic Model	Expression of the Components	Activation Energy (kJ/mol)
Ali and Bhatia, 1990	Fixed Bed Catalytic Reactor	MTBE	A15	Langmuir-Hinshelwod-Hougen-Watson	Concentrations	68.9
Rehfinger and Hoffmann, 1990	CSTR	MTBE	A15	Langmuir-Hinshelwod	Activities	92.4
Caetano et al., 1994	CSTR	MTBE	A18	Langmuir-Hinshelwod	Concentrations	85.1
Fite at al., 1994	Differential Tube Reactor	ETBE	Lewatit K2631	Eley-Rideal	Activities	79.3
Zhang and Datta, 1995	Upflow Integral Reactor, continuous	MTBE	A15	Langmuir-Hinshelwod	Molar Fractions	85.4
Oost and Hoffmann, 1996	Continuous Flow Recycle Reactor	TAME	Liwatit SPC 118	Adsorption based kinetic model	Activities	89.5
Mazzoti et al., 1997	CSTR	Ethyl Acetate	A15	Equilibrium between liquid and resin using Flory-Huggins Theory	Activities	15.8
Fite et al., 1998	Continuous upflow packed-bed reactor	MTBE	Bayer K2631	Introduction of empirical correction	Activities	79.5
Pöpken et al., 2000	CSTR	Methyl Acetate	A15	Adsorption based kinetic model	Activities	60.5
Silva and Rodrigues, 2001	CSTR	Diethyl Acetal	A18	Langmuir-Hinshelwod	Activities	65.0

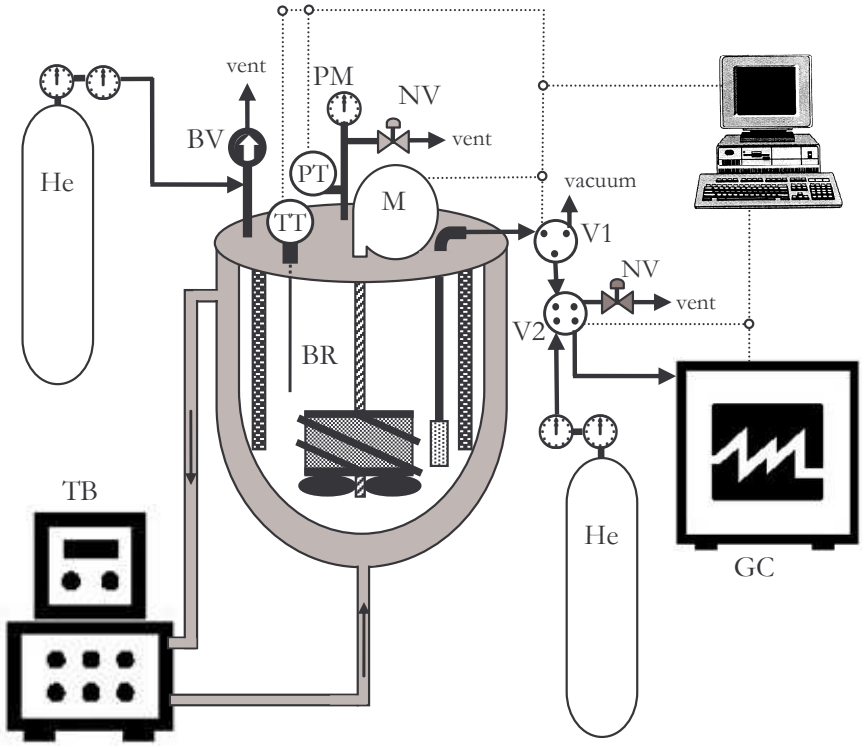

Figure 3.1. Laboratory-Scale Experimental Set-up: **BR-batch reactor; M-motor; TT-temperature sensor; PT-pressure sensor; PM-manometer; BV-blow-off valve; V1-sampling valve; V2-injection valve; NV-needle valve; GC-gas chromatograph; TB-thermostatic bath.**

The temperature in the reactor was controlled by a thermostatic water pump, model RE104 (Lauda, Germany) with 4 liters capacity and temperature range from -10 ^{o}C to 120 ^{o}C can be operated, which water flows through the glass-jacketed autoclave in order to maintain the desired reaction temperature.

In order to maintain the reaction mixture in the liquid phase over the whole temperature range, the pressure was set at 6 atm to 10 atm with the helium gas. Stainless steel meshed (10 μm mesh) basket is arranged to place the catalyst, the basket was initially placed at the top of the agitator with the help of agitator's shaft support. The

catalyst basket is introduced to the reactant's mixture at the beginning of the agitation (time zero) and after attaining the desired reaction conditions. One of the outlets of the reactor was connected directly to the liquid sampling valve (Valco, USA), which injects 0.1 μL of pressurized liquid in the reactor to the Gas Chromatograph (GC).

3.2.2 Sampling and Analysis

The sampling line is connected directly to a three-way valve, which valve was connected to a sampling valve (Valco, USA) controls the sampling, analysis and cleaning of lines which filled with earlier sample as shown in the Figure 3.2. During the experiment, there are periodic cycles for sampling and the cleaning of the sample lines. The sampling and cleaning cycle constituted of two steps, which are given below:

***First Step*:** At initial position (time zero), the reactor line is open and the pressurized liquid from the reactor flows in the tube (1/16") until it fills the loop. This step takes 1 minute, in order to ensure that the loop is completely full. At the end of the tube there is a needle valve to guarantee that full line is pressurized, avoiding vaporization of liquid inside. The total amount of liquid that leaves the reactor is about 1 mL.

***Second Step*:** At this position, the reactor line is closed and the loop inside the sampling line switches on the position, the liquid sample is then carried with helium to the injector where it is vaporized and then is separated in the column; simultaneously, the sample line is cleaned by means of vacuum. The line is completely cleaned after 7.5 minutes from the beginning and at this position the gas chromatograph is ready to start a new sample analysis.

Position 1- Sampling 0 <t (min) < 1

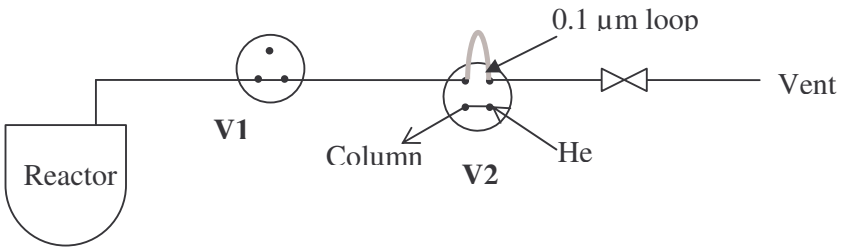

Position 2- Sample injection, analysis and line cleaning 1 <t (min) < 8.5

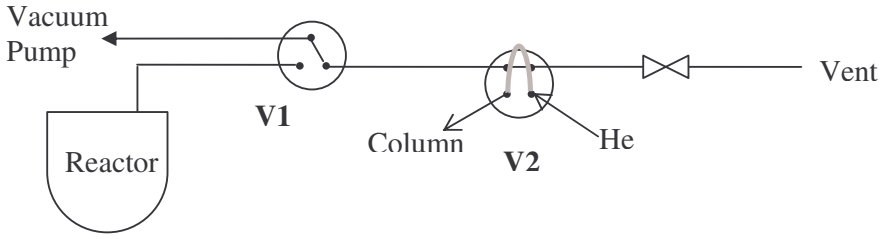

Figure 3.2. Valves scheme for sampling, analysis and line cleaning: V1-Three-way Valve; V2- Sampling Valve; He-Helium gas

3.2.3 Data Acquisition Section

The computer used was a Pentium II, 233 MHz, 64 Mb of RAM and 6 Gb of hard disk connected to a data acquisition board Advantech, model PCL-818HG. This board has the following features: 16 single-ended and 8 differential analog inputs, switch selectable; 12-bit A/D, up to 100 KHz sampling rate with MA transfer and different gain for each channel; one 12-bit analog output channel; 16 digital inputs and 16 digital outputs, TTL/DTL compatible. The PCL-818 HG package includes a special wiring board (PCLD-8115) with a DB-37 connector and CJC circuits, which allows directed reading from thermocouple. The signals measured (pressure, temperature and the thermal conductivity detector) are saved in a file.

The computer is also connected to the PCLD-885 Power Relay Output Board (Advantech), which is equipped with 16 electromechanical SPST relay outputs, driven via a 16 bit digital output port. These relays can be used for general purpose switching control applications, such as setting up test configurations or power ON/OFF switching. This board is used to send the signal to the motor in the beginning of the experiment, to the gas chromatograph to start the samples analysis and to command the valves V1 and V2 as show in Figure 3.2.

3.2.4 Method of Analysis

The analysis of reactants and products was carried out using Gas chromatography. The Gas Chromatography used for analysis was from Chrompack model Chrompack 9100 (Netherlands). The compounds were separated in a fused silica capillary column (Chrompack CP-wax 57 CB), 25 m X 0.53 mm ID, df = 2.0 using a thermal conductivity detector (TCD 903 A) for detection of peak separation of reactants and products. The conditions used for the sample analysis are presented in Table 3.2. The column temperature was programmed with a 2 min initial hold-up at 50 ^{o}C, followed by 40 ^{o}C/min increase in temperature up to 100 ^{o}C and then hold again for 1 min. The carrier gas used was helium. At these conditions the retention time for acetaldehyde, acetal, methanol and water are 1.0, 1.6, 2.4 and 3.4 minutes respectively.

The calibration curves were obtained for each component by injecting several volumes of pure component, at certain temperature. The response factor, (f_i) as defined as:

$$n_i = f_i A_i \tag{3.1}$$

where n_i is the number of moles of component i (μmol) and A_i is the peak area of component i (u.a.).The values obtained are presented in Table 3.3 (See Appendix A).

Table 3.2 Operating conditions used in Gas Chromatography

Injector temperature	150 °C
Detector temperature	250 °C
Column pressure drop	80 kPa
Column flow rate at 50 °C	10.7 mL/min
Make up flow rate	9.3 mL/min
Reference flow rate	20.0 mL/min

Table 3.3 Retention time and response factors for each component.

Component	Retention time (min)	Response Factor (µmol/u.a.)
Acetaldehyde	1.00	6.8293
Acetal	1.55	3.3027
Methanol	2.40	8.1185
Water	3.40	11.652

The points for the calibration curves were obtained by calculating the average area of at least 3 analyses for each sample (See Appendix A). The criteria of reproducibility, based on peak area were:

$$R.C.(\%) = \frac{\sigma_A}{A} \times 100 \leq 5\% \tag{3.2}$$

For determination of species concentration in mixtures, the molar fraction of each species was first calculated, according to:

$$x_i = \frac{f_i A_i}{\sum_n f_n A_n} \tag{3.3}$$

The concentration was then evaluated using the liquid molar volumes:

$$C_i = \frac{x_i}{\sum_n x_n V_{ml,n}} \tag{3.4}$$

With this procedure, the results were not affected if any changes in operating conditions occur (different injection volume, change in helium flow rate) of gas chromatography since all peak areas would be affected in the same way. The calibration curves were determined every time that some changes occurred (change of helium cylinder, maintenance, flow rate adjustments, etc.) and verified at the beginning of the each set of experiments by analyzing a standard sample. It was also verified the good agreement between manual and automated injection.

3.2.5 Chemicals used

The chemicals used were methanol (>99.9 % pure), acetaldehyde (>99.5 % pure) and acetal (>97.0 %) from Sigma-Aldrich, UK. The water used for calibration was deionized. The use of these chemicals, mainly acetaldehyde and acetal requires extra precautions (See Appendix B).

3.2.5.1 Physical and Thermodynamic properties

In the below mentioned Table 3.4, the physical and thermodynamic properties of acetal, acetaldehyde, methanol and water, available from literature are listed here in (Reid et al., 1987; Dear, 1999; Perry et al., 1997):

3.2.6 Catalyst

3.2.6.1 Amberlyst 15 resin

A commercial sulfonic acidic ion exchange resin (Amberlyst 15, Rohm and Haas, France) was used as a catalyst. The resin is in a bead-form macro reticula polymer of styrene and divinylbenzene with particle diameter varying from 300 to 1200 µm. The

Table 3.4 Physical and Thermodynamic properties

Properties	Acetaldehyde	Methanol	Acetal	Water
Molecular weight – M (g/mol)	44.054	32.04	90.12	18.015
Melting temperature – T_f (K)	150.2	175.5	163.8	273.2
Normal boiling temperature – T_b (K)	294.0	337.7	337.5	373.2
Critical temperature – T_c (K)	461.0	512.6	507.8[a]	647.3
Critical pressure –P_c (bar)	55.7	80.9	37.7[a]	221.2
Critical volume –V_c (cm^3/mol)	154.0	118.0	289.5[a]	57.1
Acentric factor – ω	0.303	0.556	0.403[a]	0.344

[a] calculated for this work.

ion exchange capacity and other properties of the resin used in this work are presented in Table 3.5.

Table 3.5 Physical and Chemical properties of Amberlyst 15 resin.

Properties	Amberlyst 15
Moisture content	52-57 %
Shipping weight	770 g/L
Particle size	300 – 1200 µm
Concentration of acid sites	1.7 meq/mL
Surface area	45 m^2/g
Porosity	0.36
Average pore diameter	24 nm

3.2.6.1.1 Resin conditioning

The catalyst should be conditioned before use in order to guarantee the anhydrous resin. It may be convenient to rinse off water from the resin by another solvent (can be ethanol). By placing water-wet Amberlyst 15 resin in a column and allowing 2.5 bed volumes of ethanol to percolate through the resin over a period of one hour, most of the water can be removed with this method to maximum extent. Finally, the resin should be dried at 105 ^{o}C for 2 to 4 hours in order to dry the traces of water present in the resin. This procedure of drying the catalyst was adopted, as water adsorbed on the surface of catalyst decreases the reaction kinetics as water itself is one of the products in the acetalization reactions.

3.2.6.2 Zeolite

Zeolites are members of a family of minerals called tectosilicates, which includes dense-phase materials such as the feldspars and various forms of silica. Zeolites are micro porous, with high internal surface area crystalline materials with an open three-dimensional framework consisting of tetrahedral AlO_4^{-5} and SiO_4^{-4} units linked through shared oxygen. The USY-type zeolite (UOP, USA) properties are mentioned above in the Table 3.6

Table 3.6 Properties of USY-type Zeolite (UOP, USA)

Properties	Zeolite
LOI @ 1000°C	3.4 wt %
Surface Area	656 m^2/g
Crush Strength	7.12 kg
Bulk Density	637.5 kg/m^3
Diameter	0.17 cm
Unit Cell Size	24.5 A^o
Na_2O	0.1 wt%

3.2.6.2.1 Zeolite conditioning

The zeolite was dried by heating to approximately 350 ^{o}C while passing inert gas stream (Helium) through the bed in which zeolite was packed for drying. The column temperature was programmed to heat from 30 ^{o}C to 120 ^{o}C during 45 minutes, followed by a 2 ^{o}C/min increase rate in temperature up to 350 ^{o}C and held for 20 hours. The zeolite packed bed was allowed to cool to room temperature for overnight in presence of inert gas helium stream. The amount of water adsorbed in the zeolite can be minimized by the above followed procedure of drying, which makes the equilibrium displacement towards the products formation during acetalization reaction.

3.3 Thermodynamic Results

Thermodynamic quantities in process design such as the enthalpy change of the reaction and equilibrium constant are important. As well for the dimethylacetal synthesis, these thermodynamic and equilibrium constant were not reported in the literature. As above parameters are necessary for designing and scale-up of any manufacturing plants, here the experiments to measure the equilibrium constant for the acetalization reversible reaction were carried out. The temperature dependency of equilibrium constant was determined from the Van't Hoff equation:

$$\ln K_{eq} = \frac{\Delta S^{o}}{R} - \frac{\Delta H^{o}}{R}\frac{1}{T} \qquad (3.5)$$

Therefore, this work was undertaken to determine the experimental values of equilibrium constant at several temperatures. Then the standard enthalpy change of acetal synthesis could be determined and compared with the estimated theoretically. It is also possible to calculate the standard enthalpy of acetal formation in liquid phase in order to compare with the value -420.2 kJ/mol calculated from the heat of combustion (Dean, J.A, 1999).

Table 3.7 Standard thermochemistry data

Chemical Component	ΔH_f^o (kJ/mol)	ΔG_f^o (kJ/mol)	S_f^o (J/mol/K)
Methanol [a]	- 239.10	- 166.60	126.80
Acetaldehyde [a]	- 192.11	- 127.60	160.40
Water [a]	- 285.83	- 237.13	69.95
Dimethylacetal [a]	- 420.2	-	-

[a] Lange's Handbook of Chemistry (1979)

All the experiments to measure the equilibrium constant for this reversible reaction were performed in a temperature range of 293.15 to 333.15 K at 0.6 MPa with Amberlyst-15 Resin. The reactants mixture volume is about 600 mL and the reactants initial molar ratio is the stoichiometric: $r_{A/B} = 2.0$. All experiments lasted long enough for the reaction to reach equilibrium. Table 3.8 shows the experimental conditions and average equilibrium compositions at each temperature.

Table 3.8 Experimental Equilibrium compositions expressed in molar fractions.

T(K)	293.15	303.15	313.15	323.15	333.15
x_{A_e}	0.3167	0.3268	0.3272	0.3564	0.3682
x_{B_e}	0.1383	0.1556	0.1558	0.1586	0.1604
x_{C_e}	0.2725	0.2588	0.2585	0.2425	0.2357
x_{D_e}	0.2725	0.2588	0.2585	0.2425	0.2357

The thermodynamic equilibrium constant for the liquid phase reaction was considered here as a non-ideal system and is given by,

$$K_{eq} = \frac{a_{C_e} \times a_{D_e}}{a_{A_e}^2 \times a_{B_e}} = \frac{x_{C_e} \times x_{D_e}}{x_{A_e}^2 \times x_{B_e}} \times \frac{\gamma_C \times \gamma_D}{\gamma_A^2 \times \gamma_B} = K_x \times K_\gamma \tag{3.6}$$

The equilibrium constant can also be evaluated in terms of molar fractions, if the mixture has an ideal behavior and is given in the following Equation 3.7:

$$K_x = \frac{x_{C_e} \times x_{D_e}}{x_{A_e}^2 \times x_{B_e}} \tag{3.7}$$

This equilibrium constant expressed in terms of the molar concentration was also reported and it is given as shown in Equation 3.8:

$$K_C = \frac{C_{C_e} \times C_{D_e}}{C_{A_e}^2 \times C_{B_e}} \tag{3.8}$$

The concentrations were determined from the liquid molar volumes, estimated with Gunn-Yamada method (Reid et al., 1987) and are given according to:

$$C_i = \frac{x_i}{\sum_j x_j V_{ml,j}} \tag{3.9}$$

The numbers of moles of the species at equilibrium in the reaction mixture for different temperatures obtained are shown in Table 3.9

Table 3.9 Number of moles of species at Equilibrium.

T(K)	293.15	303.15	313.15	323.15	333.15
n_A	3.2724	3.4140	3.4162	3.7718	3.9158
n_B	1.4300	1.6260	1.6272	1.6797	1.7054
n_C	2.8159	2.7033	2.6989	2.5662	2.5063
n_D	2.8159	2.7033	2.6989	2.5662	2.5063

The activity coefficients of compounds, γ, were computed by UNIFAC method (Fredeslund et al., 1977). The UNIFAC parameters of pure species, shown in Tables 3.10 and 3.11, are the relative group volume (R_k) and surface area (Q_k) parameters and the group-group interaction parameters ($a_{m,n}$). The activity coefficients of all species in

the reaction mixture at equilibrium are given in the Table 3.12 at different temperatures. Chromatograms of a typical experiment (Run No. 2) at 0, 51, 120 and 180 minutes of the reaction are given in Figures A.5, A.6, A.7 and A.8 respectively of Appendix A.

*Table 3.10 Relative molecular volume and surface area of pure species parameters (*Reid *et al., 1987)*

(i)	Molecule	Group identification			$v_k^{(i)}$	R_k	Q_k
		Name	No. Main	No. Sec			
1	Methanol	CH_3OH	6	16	1	1.4311	1.432
2	Acetaldehyde	CH_3	1	1	1	0.9011	0.848
		CHO	10	21	1	0.9980	0.948
3	Acetal	CH_3	1	1	1	0.9011	0.848
		CH	1	3	1	0.4469	0.228
		CH_3O	13	25	2	1.1450	1.088
4	Water	H_2O	7	17	1	0.9200	1.400

*Table 3.11 Interaction parameters (*Reid *et al., 1987)*

$a_{m,n}$ (K)	1	6	7	10	13
1	0.0	697.2	1318.0	677.0	251.5
6	16.510	0.0	-181.0	306.4	-128.6
7	300.0	289.6	0.0	-257.3	540.5
10	505.7	-340.2	232.7	0.0	304.1
13	83.36	238.4	-314.7	-7.838	0.0

Table 3.12 Activity coefficients of species at equilibrium for different temperatures.

T(K)	293.15	303.15	313.15	323.15	333.15
γ_A	0.8653	0.8600	0.8747	0.8917	0.8976
γ_B	0.5109	0.5466	0.5668	0.5714	0.5918
γ_C	1.1895	1.2018	1.2051	1.2143	1.2200
γ_D	1.3177	1.3444	1.3693	1.3928	1.4139

The equilibrium constants in terms of molar fraction, molar concentrations and activity coefficients are given the Table 3.13.

Table 3.13 Equilibrium Constants at different temperatures

T(K)	293.15	303.15	313.15	323.15	333.15
K_x	5.3532	4.0305	4.0062	2.9191	2.5547
K_γ	4.0974	3.9689	3.8052	3.7225	3.6177
K_C	0.5178	0.3856	0.3836	0.2756	0.2402
K_{eq}	21.9344	15.9965	15.2441	10.8663	8.9092

The dependence of equilibrium constant on temperature can be estimated by fitting experimental values of $\ln K_{eq}$ vs. $1/T$ to:

$$\ln K_{eq} = \frac{\Delta S^o}{R} - \frac{\Delta H^o}{R}\frac{1}{T} \tag{3.10}$$

The fitting of experimental data by Eq. (3.10), where the equilibrium constant was calculated with respect to activity coefficients as shown in Figure 3.3 and is given as follows,

$$\ln K_{eq} = \frac{2142.5}{T(K)} - 4.2475 \tag{3.11}$$

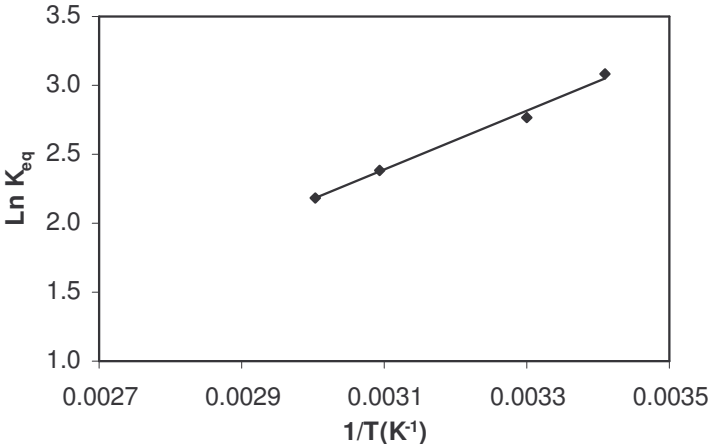

Figure 3.3 Experimental and theoretical values plot for $\ln K_{eq}$ *vs* $1/T(K^{-1})$.

Therefore, it is obtained $\Delta H^o = -17.81$ kJ mol^{-1} and $\Delta S^o = -35.34$ J mol^{-1} K^{-1} from the slope and the intercept, respectively. The standard free energy change for the liquid-phase reaction can be related to the standard enthalpy and entropy changes by,

$$\Delta G^o = \Delta H^o - T \times \Delta S^o \tag{3.12}$$

Leading to $\Delta G^o = -7.28$ kJ mol^{-1}.

The standard molar properties for formation of acetal in the liquid phase at 298.15 K were estimated: $\Delta H_f^o = -402.29$ kJ mol^{-1}, $\Delta G_f^o = -230.95$ kJ mol^{-1} and $S_f^o = 308.71$ Jmol^{-1} K^{-1} and are given in the Table 3.7.

The pressure influence in the value of K_{eq} was estimated by correction factor K_P (Smith and Van Ness, 1987):

$$K_P = \exp\left[\frac{(P-1)}{RT} \times \sum \nu_i V_{ml,i}\right] \tag{3.13}$$

Where P is the pressure, v_i is the stoichiometric coefficient of component 'i' and $V_{ml,i}$ is the molar volume of component 'i'. By using liquid molar volumes in Table 3.14 and the experimental conditions of the present work done, it can be seen that, neglecting K_P in the calculation of K_{eq} as the negligible error was observed. Therefore, we can confirm that, K_{eq} is only a function of temperature.

Table 3.14 Liquid molar volumes (mL/mol) calculated with the Hankinson-Brobst-Thomson (HBT) method (Reid et al., 1988) and K_P values.

T(K)	V_A	V_B	V_C	V_D	K_P
293.15	40.52	56.21	105.80	17.96	0.9972
303.15	41.11	57.16	107.16	18.14	0.9972
313.15	41.73	58.18	108.57	18.32	0.9971
323.15	42.38	59.26	110.04	18.51	0.9971
333.15	43.06	60.42	111.56	18.70	0.9970

The influence of temperature dependence of the heat capacities ($C_{P,i}$) in the liquid phase for all components on the equilibrium constant (K_{eq}) were checked along the temperature range of 273.15 – 373.15K considering the Van't Hoff equation. The variation of heat capacities with temperature has a negligible effect on the equilibrium constant for the above mentioned temperature range. Heat capacities of reactants and products at different temperatures were calculated using the constants presented in Table 3.15 and heat capacities of reactants and products were plotted against temperature (See Appendix C).

Table 3.15 Constants for estimation C_p value ($C_P = a + bT + cT^2 + dT^3, T(K)$), J/(mol.K).

Component	a_i	b_i	c_i	d_i
Mehanol [c]	21.15	7.092×10^{-2}	2.587×10^{-5}	-2.852×10^{-8}
Acetaldehyde [c]	7.716	1.823×10^{-1}	-1.007×10^{-4}	2.380×10^{-8}
Water[c]	32.24	1.924×10^{-3}	1.055×10^{-5}	-3.596×10^{-8}
Dimethyl Acetal[d]	222.19	-3.538×10^{-1}	1.040×10^{-3}	6.661×10^{-16}

[c] Properties of Gases and Liquids (Reid *et al.*, 1987).

[d] Estimated with the Missenard Group Contribution Method (Reid *et al.*, 1987) (See Appendix C).

3.4 Kinetic Results

Summary of the Experiments performed for the synthesis of dimethoxyethane from acetaldehyde and methanol by changing different parameters is given in the Table 3.16.

3.4.1 Effect of type of catalyst

Reactions were carried out with Amberlyst-15 resin and USY-type Zeolite (hydrogen form) to synthesize dimethylacetal. The conversion of acetaldehyde as a function of time is shown in Figure 3.4. The reaction rate and conversion of the limiting reactant

(acetaldehyde) is higher for the reaction performed with Amberlyst-15 resin. This could be explained from the difference in the number of acid sites between the two catalysts and its accessibility. For the Amberlyst 15 wet, the concentration of acid sites is 1.7 meq/mL; for the zeolite, none information was available.

All further experiments were performed with Amberlyst-15 resin in order to study effects of different parameters on the rate of reaction for the synthesis of dimethylacetal.

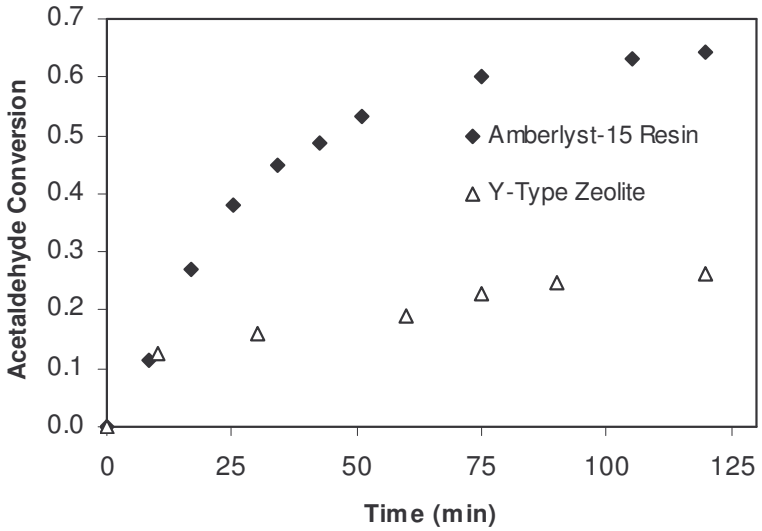

Figure 3.4 Effect of type of catalyst on conversion of acetaldehyde as function of time: $T = 293.15\,K$, $P = 6\,atm$, $V = 600$ *mL,* $w_{cat} = 1.5\,g$, $d_p = 500\,\mu m$, $r_{A/B} = 2.0$.

3.4.2 Effect of Speed of Agitation (soa)

To ascertain the influence of external resistance to mass transfer of the reactants to the catalyst surface, the speed of agitation of the reaction mixture was studied over a range of 400 to 800 rpm (revolutions per minute) maintaining other parameters of the reaction with same conditions. It was observed that, the speed of agitation had no appreciable effect on the conversion of limiting reactant acetaldehyde to products and hence, on the

Table 3.16 Summary of the acetaldehyde and methanol system experiments for DME synthesis.

Run No.	Pellet Diameter (μm)	Catalyst Loading (g)	Speed of Agitation (rpm)	Reaction Temp. (°C)	Reaction Pressure (atm)	Methanol Conc. (mol/L)	Aldehyde Conc. (mol/L)	Initial Molar Ratio
1	567.5	1.505	600	10.0	6.0	14.65	7.26	2.023
2	567.5	1.501	400	20.0	6.0	14.65	7.26	2.019
3	567.5	1.500	800	20.0	6.0	14.64	7.25	2.021
4	335	0.792	600	20.0	6.0	14.67	7.25	2.024
5	510	0.786	600	20.0	6.0	14.70	7.25	2.028
6	800	0.794	600	20.0	6.0	14.62	7.25	2.017
7	567.5	1.506	600	20.0	6.0	14.67	7.25	2.025
8	567.5	1.504	600	30.0	6.0	14.67	7.24	2.026
9	567.5	1.504	600	40.0	6.0	14.65	7.24	2.024
10	567.5	1.508	600	60.0	6.0	14.65	7.25	2.022
11	567.5	1.502	600	20.0	6.0	12.82	8.55	1.499
12	567.5	1.507	600	20.0	6.0	16.88	5.63	2.996
13	567.5	1.502	600	20.0	6.0	18.32	4.59	3.995
14	567.5	0.751	600	20.0	6.0	14.59	7.26	2.009
15	567.5	2.252	600	20.0	6.0	14.61	7.25	2.015
16	335	0.791	600	20.0	6.0	13.05	8.43	1.55
17	335	0.797	600	20.0	6.0	17.88	5.13	3.485
18	335	0.768	600	30.0	6.0	14.68	7.23	2.030
19	335	0.792	600	30.0	6.0	17.70	4.98	3.554
20	335	0.793	600	30.0	6.0	12.90	8.58	1.500
21	510	0.785	600	30.0	6.0	14.62	7.30	2.003
22	800	0.790	600	30.0	6.0	14.76	7.18	2.056

rate of reaction beyond 600 rpm. Thus, there was no limitation of external mass transfer beyond this speed of agitation. Further experiments were conducted with the above-mentioned speed of agitation of 600 rpm. The conversion rate of limited reactant acetaldehyde is as shown in the Figure 3.5 at different speeds of agitation: 400 rpm (run 2), 600 rpm (run 1) and 800 rpm (run 3).

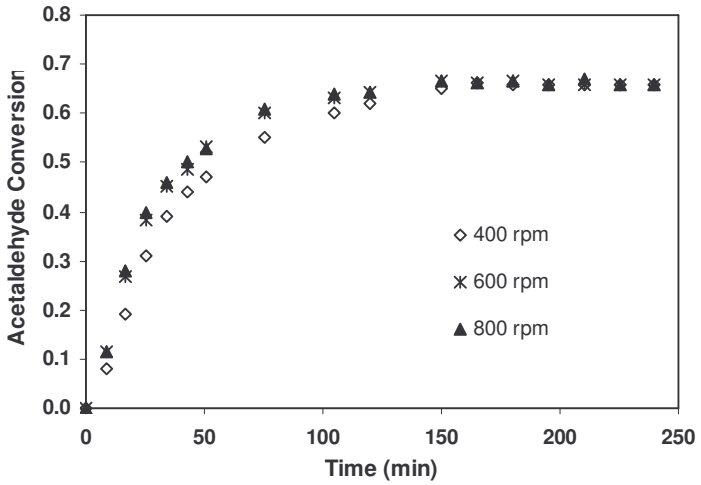

Figure 3.5 Effect of speed of agitation on conversion of acetaldehyde as function of time: $T = 293.15\,K$, $P = 6\ atm$, $V = 600$ mL, $w_{cat} = 1.5$ g, $d_p = 500$ μm, $r_{A/B} = 2.0$.

3.4.3 Effect of particle size

The catalyst was separated by particle size and three classes with different mean diameters were obtained: 335 μm, 510 μm and 800 μm. Figure 3.6 shows the conversion of acetaldehyde, X, as a function of time (runs 4, 5, and 6).

It is observed that there is internal diffusion limitation for the particle diameter equal to 510 μm and 800 μm with respect to the smallest particle size of the particle (335 μm).

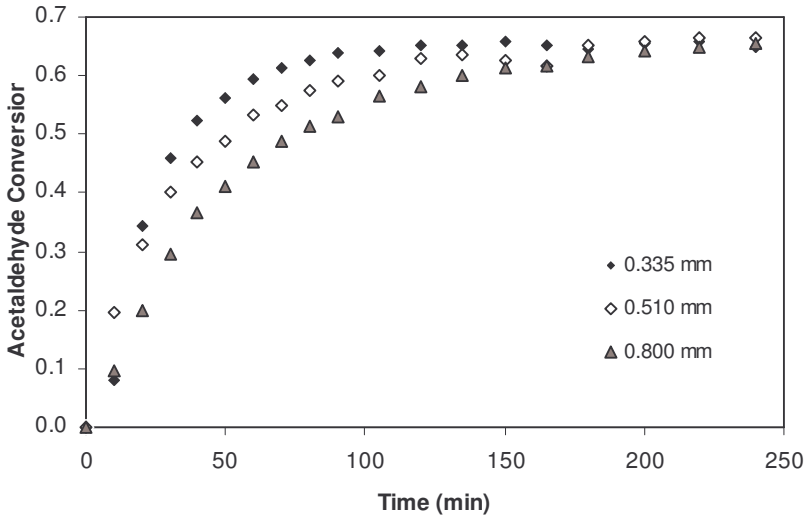

Figure 3.6: Effect of particle size on conversion of acetaldehyde as function of time: $soa = 600$ rpm, $P = 6\ atm$, $V = 600$ mL, $w_{cat} = 1.5$ g, $T = 293.15$ K, $r_{A/B} = 2.0$.

3.4.4 Effect of Temperature

All experiments were carried out at almost constant temperature. The maximum variation of 1.5 ^{o}C was noticed during the initial stage of reaction, and then decreased to desired temperature. Figure 3.7 shows four experiments performed at different temperatures: 20 ºC, 30 ºC, 40 ºC and 60 ºC, with respect to experiments 7, 8, 9 and 10, respectively as mentioned in Table 3.9. The rate of reaction increased with the increase of temperature, even though the equilibrium conversion decreased due to the exothermic nature of reaction, equilibrium conversion values for the conducted experiments were mentioned in Table 3.9.

3.4.5 Effect of Initial Reactants Molar Ratio $r_{A/B}$

As the experiments were performed without introducing any inert in the present liquid phase reaction between acetaldehyde and methanol, it was not possible to examine the influence of initial concentration effect of the each reactant individually on the rate of

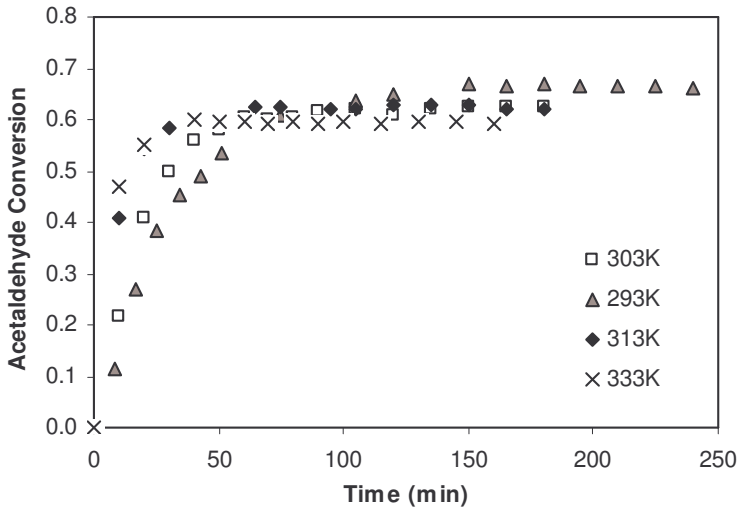

Figure 3.7: Effect of temperature on conversion of acetaldehyde as function of time: $soa = 600$ rpm, $P = 6\ atm$, $V = 600$ mL, $w_{cat} = 1.5$ g, $d_p = 500$ µm, $r_{A/B} = 2.0$.

reaction. So, the influence of the initial concentration dealt the study of initial molar ratio of reactants methanol (A) and acetaldehyde (B), $r_{A/B}$. The experiments 7, 11, 12 and 13 were performed at different initial molar ratio of reactants and its influence on the time evolution of the acetaldehyde conversion and number of moles of dimethoxyethane is shown in Figures 3.7 and Figure 3.8 respectively. The kinetics was not too affected by the initial molar ratio of reactants; but the amount of dimethylacetal produced is higher for the stoichiometric ratio $r_{A/B} = 2$.

3.4.6 Effect of Catalyst Loading

The catalyst loading was varied over a range of 0.1% w/V to 0.4% w/V on the basis of amount of total volume of reactants taken initially were studied. The effect of catalyst loading (runs 7, 14 and 15) on the conversion of acetaldehyde is shown in the Figure 3.9. The overall rate of reaction increases with the catalyst loading. This is due to the increasing of the total number of acidic sites available (Chopade and Sharma, 1997).

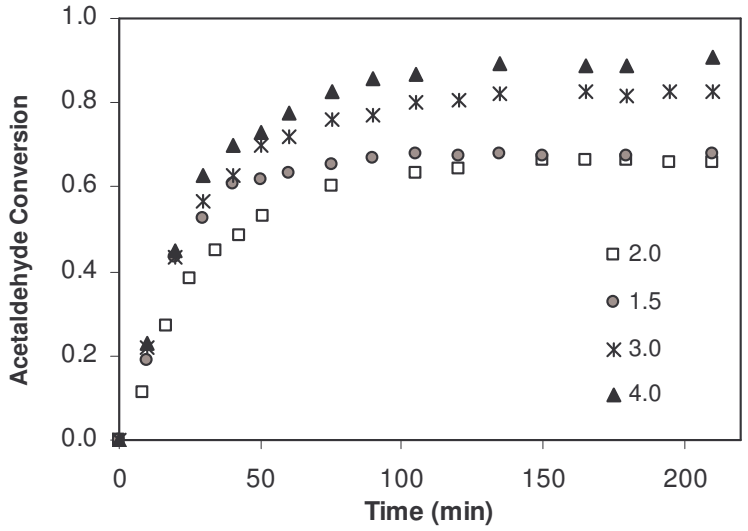

Figure 3.8(a): Effect of Initial Molar Ratio of Reactants (methanol/acetaldehyde) on acetaldehyde conversion as function of time: $T = 293.15K$, $P = 6\ atm$, $V = 600$ mL, $w_{cat} = 1.5$ g, $d_p = 500$ μm, $soa = 600$ rpm.

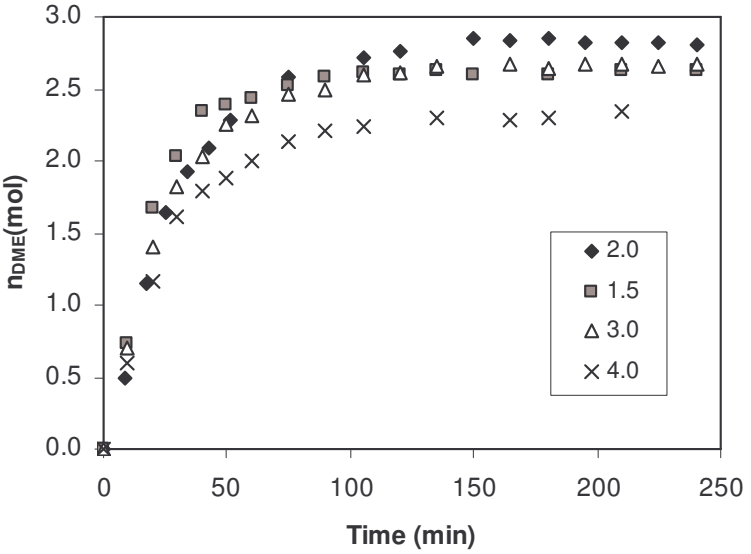

Figure 3.8(b) Effect of Initial Molar Ratio of Reactants (methanol/acetaldehyde) on number of moles of DME (n_{DME}) produced as function of time: $T = 293.15K$, $P = 6\ atm$, $V = 600$ mL, $w_{cat} = 1.5$ g, $d_p = 500$ μm, $soa = 600$ rpm

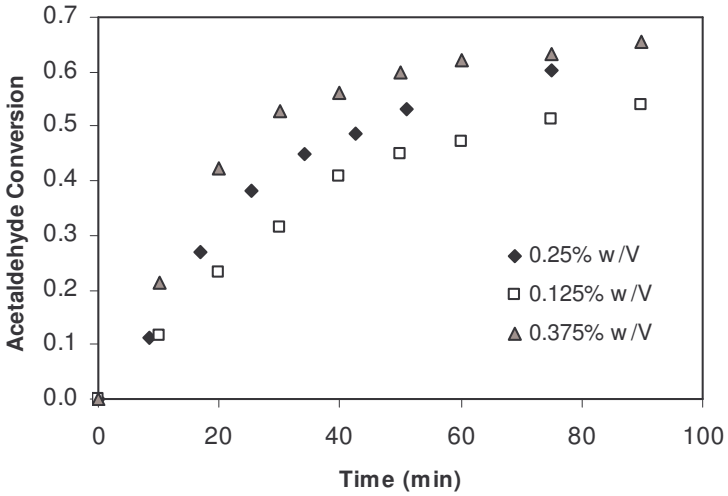

Figure 3.9: Effect of Catalyst Loading on acetaldehyde conversion as function of time: $T = 293.15\,K$, $P = 6\,atm$, $V = 600$ mL, $d_p = 500$ μm, $soa = 600$ rpm.

3.4.7 Effect of Pressure

In order to ensure that all species are in the liquid phase, the reactor was pressurized with Helium.

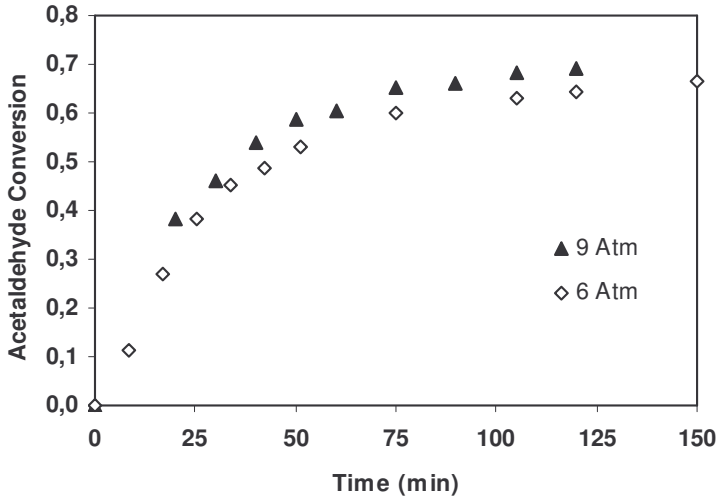

Figure 3.10: Effect of Pressure Catalyst Loading on acetaldehyde conversion as function of time: $T = 293.15\,K$, $P = 6\,atm$, $V = 600$ mL, $w_{cat} = 1.5$ g, $d_p = 500$ μm, $soa = 600$ rpm.

Two experiments were performed with total pressures of 6 atm and 9 atm, respectively. It was observed that the reaction rate was not simply affected as shown in the Figure 3.10.

3.5 Kinetic Model

The kinetic model for the production of acetal from methanol and acetaldehyde is given on the basis of the below mentioned steps. Once the species methanol and acetaldehyde diffuse into the catalyst pore space, various different mechanisms can be considered, like adsorption, surface reaction, desorption. Typically Langmuir-Hinshelwood-Hougen-Watson (LHWW), Eley-Rideal or Power Model is used. In the present work, the Langmuir model was tested with experimental data, considering the following steps in the model,

a) Adsorption of Methanol (A),

b) Adsorption of Acetaldehyde (B),

c) Surface reaction of adsorbed acetaldehyde and adsorbed methanol to give adsorbed hemi-acetal,

d) Surface reaction to obtain adsorbed water (rate controlling step),

e) Surface reaction of formation of adsorbed acetal,

f) Desorption of acetal (C),

g) Desorption of water (D).

Silva and Rodrigues [2001] proposed a rate expression for the reaction of alcohol and aldehyde on a catalyst surface and the expression is given as follows:

$$\Re = k_c \frac{a_A a_B - \dfrac{a_C a_D}{K_{eq} a_A}}{\left(1 + \sum_{i=A}^{D} K_{S,i} a_i + K_{I_1} a_A a_B + K_{I_2} \dfrac{a_C}{a_A}\right)^2} \tag{3.14}$$

In order to reduce the number of optimization parameters, several rate equations derived from Eq. (3.10) were tested. The best fitting was obtained by considering that the water

is more adsorbed than other species, which is actually true due to the acidic property of Amberlyst 15 resin. The simplified reaction rate equation is then given by:

$$\Re = k_c \frac{a_A a_B - \frac{a_C a_D}{K_{eq} a_A}}{\left(1 + K_{s,D} a_D\right)^2} \tag{3.15}$$

The kinetic model contains two parameters k_C and $K_{s,D}$ which are obtained by the optimization.

3.6 The Batch Reactor Model

As mentioned in the section 3.5.3, it is not possible to conclude that the experiments performed with the catalyst particles of lower fraction of average diameter of 335 μm were conducted in absence of internal mass transfer mechanisms. Therefore the model of the batch reactor considers internal pore diffusion of the species inside the resin. The fitting between the experimental kinetic data and the model of the batch reactor leads to the true kinetics parameters.

3.6.1 Mathematical Model

The macroreticular ion exchange resins show bidisperse pore distribution. The heterogeneous catalysis processes are regulated by transport phenomena, the adsorption and the reaction at the solid surface. The mass transfer effects are due to three main mechanisms: the mass transfer of species between the bulk fluid phase and the external surface of the stationary phase particles (external mass transfer); the diffusive migration through the pores inside the particles (internal pore diffusion); and the surface diffusion. The internal pore diffusion may occur by molecular diffusion and Knudsen diffusion; for liquid systems, the Knudsen diffusion is negligible and, therefore, the proposed model just considers molecular diffusion as the only mechanisms of internal pore diffusion. The macro and micropore diffusion resistances should be taken into

consideration; however, a monodisperse pore structure approximation can be made for Amberlyst 15 since the micropore diffusion had insignificant contribution in the total diffusion flux into a macroreticular resin catalyst (Dogu, et al., 2003). The transport phenomena through the micropores and the surface diffusion on the gel microspheres were not taken into account; but, they could be lumped in the tortuosity factor (Sundmacher, et al., 1995).

Therefore, the mathematical model for the isothermally operated batch reactor considers the diffusion of species, initially at the bulk external film and secondly molecular diffusion through the macropores of the particle until the species reach the surface of the solid, where the reaction occurs (Silva and Rodrigues, 2005):

a) Mass balance in the bulk fluid,

$$\frac{dC_{b,j}}{dt} = -\frac{A_p}{V_{liq}} D_j \left.\frac{\partial C_{p,j}}{\partial r}\right|_{r=r_p} \qquad (j = 1,2,3 \;\&\; 4) \tag{3.16}$$

$$A_p = \frac{3}{r_p} V_p \tag{3.17}$$

where $C_{b,j}$ is the bulk concentration for species j, $C_{p,j}$ is the concentration of species j inside the particle pores, A_p is the external area between the bulk fluid and the particle, V_{liq} is the total volume of reactant mixture, D_j is the effective diffusivity of species j inside the catalyst pores, r_p is particle radius, V_p is the total volume of the particles, r is the particle radial position and t is the time coordinate.

b) Mass balance in the particle,

$$\varepsilon_P \frac{\partial C_{p,j}}{\partial t} = \frac{1}{r^2}\frac{\partial}{\partial r}\left[D_j r^2 \frac{\partial C_{p,j}}{\partial r} \right] + (1-\varepsilon_p) v_j \rho_{solid} \Re \qquad (j = 1,2,3 \;\&\; 4) \tag{3.18}$$

Initial conditions:

$$t = 0 \qquad C_{b,j} = C_{b0,j} \; ; \quad C_{p,j} = C_{p0,j} \tag{3.19}$$

Boundary conditions:

$$r = 0 \qquad \frac{\partial C_{p,j}}{\partial r} = 0 \tag{3.20}$$

$$r = r_p \qquad C_{b,j} = C_{p,j}\Big|_{r=r_p} \tag{3.21}$$

It is important to observe that for $r = 0$ the Eq. (3.18) is not defined and should be substituted by a limiting expression that using the L' Hopital's rule it is transformed in[26]:

$$\varepsilon_p \frac{\partial C_{p,j}}{\partial t} = 3\frac{D_j}{r_p^2}\frac{\partial^2 C_{p,j}}{\partial \rho^2} + \left(1-\varepsilon_p\right)\nu_j \rho_{solid} \Re^p \tag{3.22}$$

where $\rho = r/r_p$ is the normalized radial variable.

The effective diffusivity of the compound j ($D_j = \varepsilon_p D^o_{j,m}/\tau$) was evaluated for the multi-component liquid mixture; the diffusion coefficient for a dilute solute j into a mixture of n components diffusivities ($D^o_{j,m}$) was determined by using the Wilke-Chang equation (Reid, et al., 1987):

$$D^o_{j,m} = 7.4X10^{-8}\frac{(\phi M)^{1/2}T}{\eta_m V^{0.6}_{ml,j}} \qquad \phi M = \sum_{\substack{k=1 \\ k\neq j}}^{n} x_k \phi_k M_k \tag{3.23}$$

where ϕ_k is the association factor of component k (ϕ_k is chosen as 2.6 for water, 1.9 for methanol, and 1.0 for unassociated compounds[24]), M_k is molecular weight of component k, T is the temperature, η_m is the mixture viscosity and was predicted by the generalized corresponding states method, $V_{ml,j}$ is the molar volume of solute j and x_k is the molar fraction for component k.

3.6.2 Optimization of the kinetic constant

In order to determine the true kinetic parameters; the optimization of the kinetic data was performed. The kinetic parameters were estimated with a non-linear regression subroutine, which uses the Levenberg –Marquardt method to minimize the sum of residual squares (SRS) between experimental and calculated molar fraction of all components.

$$SRS = \sum \sum_{i=1}^{4} (x_{i,\exp} - x_{i,theo})^2 \tag{3.24}$$

The theoretical molar fraction value ($x_{i,theo}$) were calculated by the proposed model. The values of true kinetic parameters in Eq. (3.15) are presented in the Table3.17. The average standard error between the experimental and simulated molar fractions of all species is 1.5 %. The temperature dependence of the true kinetic constants was fitted with the Arrhenius equation (Figure 3.11).

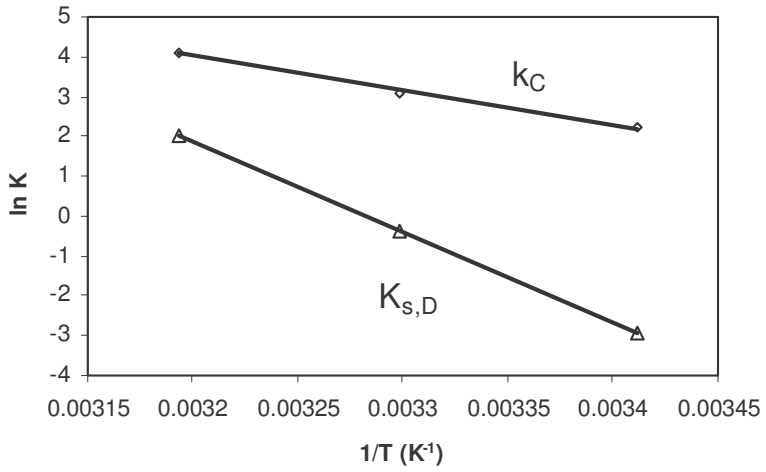

Figure 3.11 Experimental representation of ln k as function of 1/T along with linear fitting with respect to true kinetics.

Table 3.17 The true kinetic parameters

Temperature (K)	k_C (mol/g/min)	$K_{s,D}$ (dimensionless)
293.15	9.13	0.0535
303.15	22.1	0.678
313.15	60.9	7.54

The activation energy determined from the Arrhenius plot for the temperature range 293.15-313.15 K is 72.4 kJ/mol. For the synthesis of acetaldehyde diethylacetal from ethanol and acetaldehyde on Amberlyst 18, which the activation energy was 65.1 kJ/mol.[26]

The kinetic model is accurate in the range of initial molar ratio of reactants (methanol/acetaldehyde) from 1.5 to 3.5 and at the temperature range 293.15-313.15 K. The comparison of experimental and theoretical data plots for different initial molar ratio of reactants at 293.15 K (runs 4, 16 and 17) and at 303.15 K (runs 18, 19 and 20) are shown in Figures 3.12 and 3.13, respectively.

3.7 Mass transfer effect inside the catalyst pores

As the effect of catalyst particle size was studied at 293.15 K (Figure 3.6), the experimental values of molar fractions of methanol, acetaldehyde and products (acetal and water) are compared with simulated results at different catalyst particle sizes of 335, 510 and 800 μm diameter (see Figure 3.14). The agreement between the experimental and simulated results with respect to the pore diffusion model leads us to conclude that mass transfer parameters are well predicted with the above-mentioned correlations. This was also confirmed for the results obtained at 303.15 K, for pellets diameter of 335, 510 and 800 μm (runs 18, 21 and 22, respectively), as shown in Figure 3.15.

Analyzing the internal concentration profiles as shown in Figure 3.16, it is possible to conclude that the pore diffusion is the controlling mechanism. The effectiveness factor could be evaluated at each time by knowing the concentration inside the particle.

Defining the effectiveness factor as:

$$\eta = \frac{\langle \Re \rangle}{\Re_s} \tag{3.25}$$

where $\Re_s$ is the kinetic rate at the surface condition and $\langle \Re \rangle$ is the average kinetic rate defined as follows,

$$\langle \Re \rangle = \frac{\int_0^{r_p} r^2 \Re dr}{\int_0^{r_p} r^2 dr} \tag{3.26}$$

The effectiveness factors for different sizes of particle are given in Table 3.18.

Table 3.18 Effectiveness Factors (η) for different size of catalyst particles.

dp (μm)	**η**
335	0.415
510	0.286
800	0.193

For better understanding of the controlling mechanism, a dimensionless parameter, Thiele Modulus, ϕ_T, was defined as,

$$\phi_T = \frac{r_p}{3}\sqrt{\frac{\rho_p k_c}{D_{A_s} C_{A_s}}} \tag{3.27}$$

where r_p is the radius of the catalyst particle, ρ_p is the catalyst particle density, k_c is the kinetic constant for the dimethylacetal synthesis reaction, D_{A_s} is the methanol

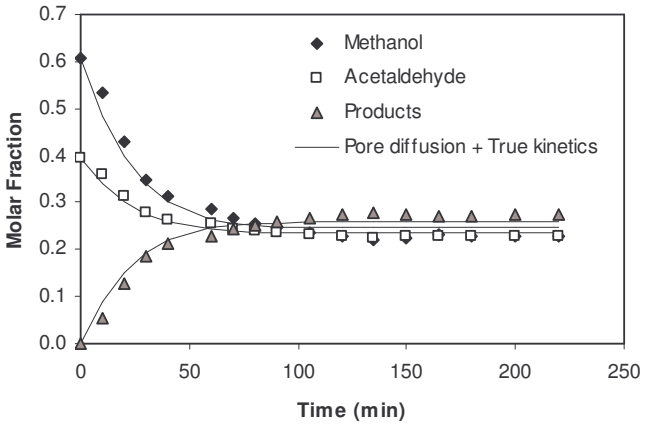

(a)

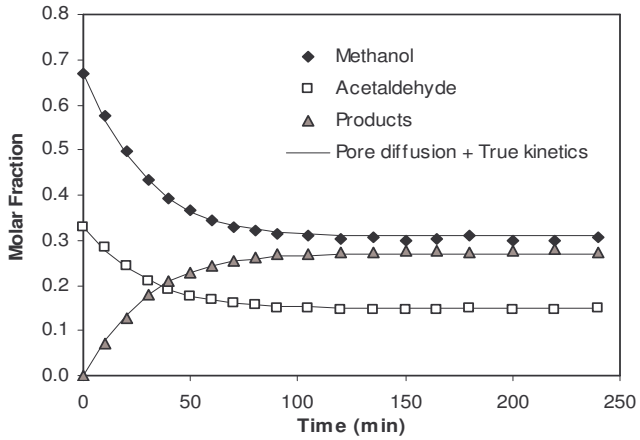

(b)

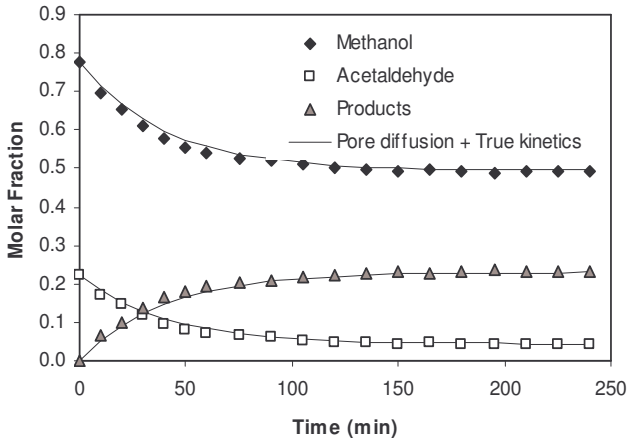

(c)

Figure3.12 Comparison between experimental and optimized kinetic curves: T = 293.15 K $P = 6\ atm$, $V = 600$ mL, $w_{cat} = 0.79$ g, $d_p = 335$ μm, $soa = 600$ rpm. (a) $r_{A/B} = 1.55$; (b) $r_{A/B} = 2.03$; (c) $r_{A/B} = 3.48$.

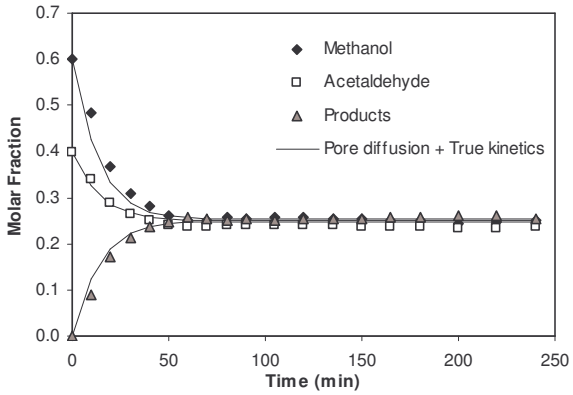

(a)

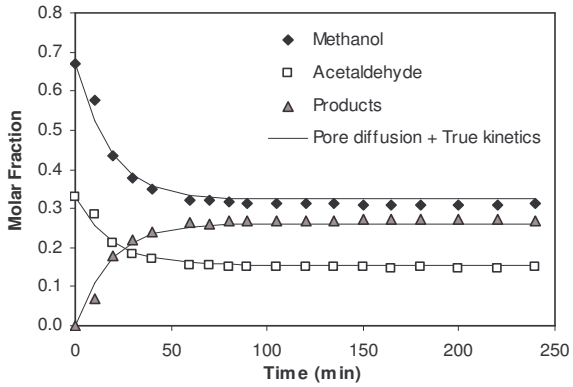

(b)

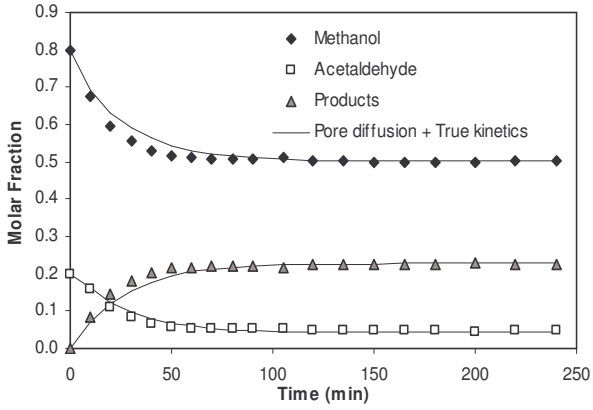

(c)

Figure 3.13: Comparison between experimental and optimized kinetic curves: T = 303.15 K $P = 6\ atm$, $V = 600$ mL, $w_{cat} = 0.79$ g, $d_p = 335\,\mu$m, $soa = 600$ rpm. (a) $r_{A/B} = 1.50$; (b) $r_{A/B} = 2.03$; (c) $r_{A/B} = 3.55$.

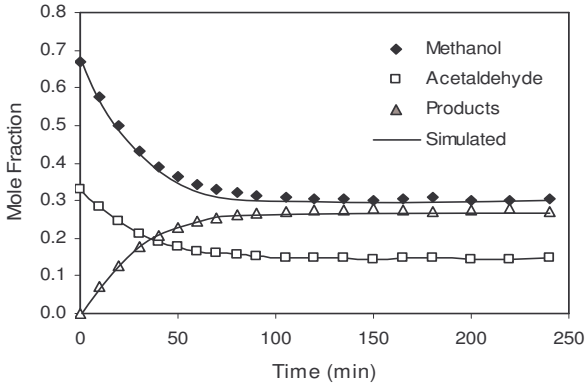

(a)

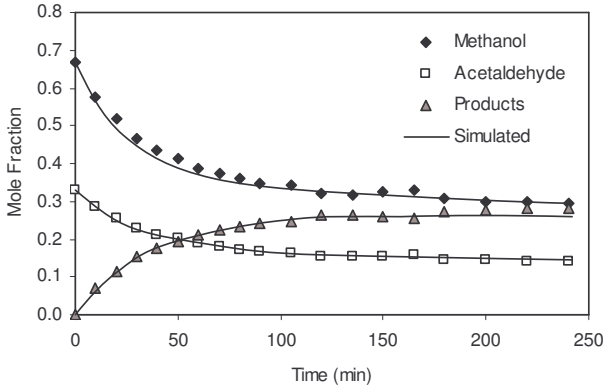

(b)

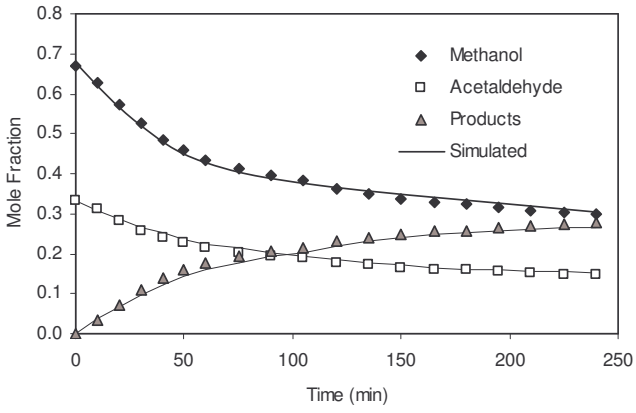

(c)

Figure 3.14: Effect of catalyst particle diameter on the molar fraction of methanol, acetaldehyde and products (acetal and water) as a function of time: T = 293.15 K, $P = 6\ atm$, $V = 600$ mL, $w_{cat} = 0.79$ g, $d_p = 335$ µm, $soa = 600$ rpm, $r_{A/B} = 2.03$. (a) $d_p = 335\mu m$; (b) $d_p = 510\mu m$; (c) $d_p = 800\mu m$.

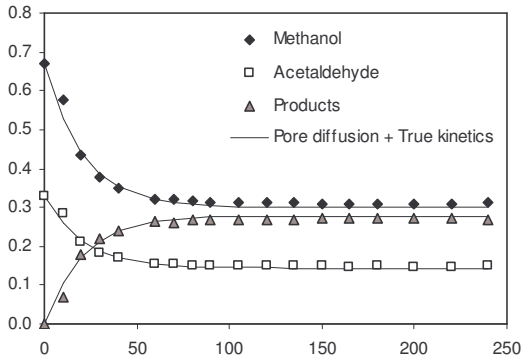

(a)

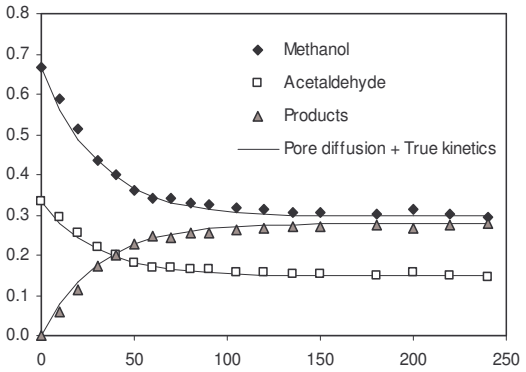

(b)

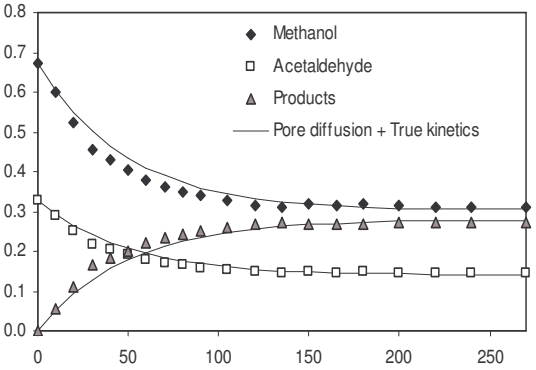

(c)

Figure3.15: Effect of catalyst particle diameter on the molar fraction of methanol, acetaldehyde and products (acetal and water) as a function of time:
T = 303.15 K, $P = 6\ atm$, $V = 600$ mL, $w_{cat} = 0.79$ g, $d_p = 335\ \mu$m, $soa = 600$ rpm, $r_{A/B} = 2.03$.
(a) $d_p = 335\mu m$; (b) $d_p = 510\mu m$; (c) $d_p = 800\mu m$.

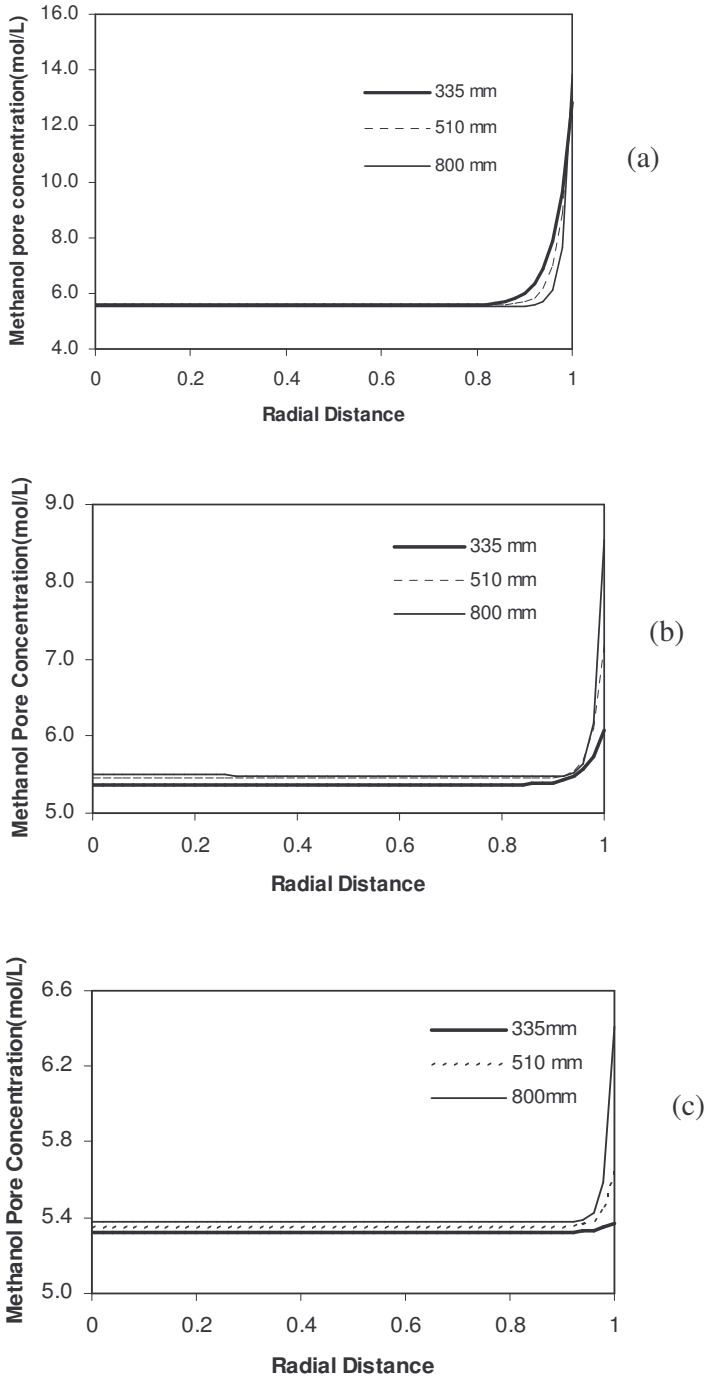

Figure 3.16: Effect of catalyst particle diameter on the internal concentration profile of methanol along the radial distance of the particle:
T = 293.15 K $P = 6\ atm$, $V = 600$ mL, $w_{cat} = 0.79$ g, $soa = 600$ rpm, $r_{A/B} = 2.03$. (a) t= 5 min, (b) t= 60 min, (c) t=120min.

effective diffusivity at the surface of the catalyst particle and C_{A_s} is the methanol concentration at the catalyst surface. The variation of the effectiveness factor with the Thiele Modulus was evaluated. For determining Thiele modulus for different particle sizes of catalyst, the values used are given in the Table 3.19. The graphical representation of the effectiveness factor against the Thiele modulus is shown in Figure 3.17. For internal diffusion controlling mechanism, corresponding to the linear region

Table 3.19 Parameters used for determining the Thiele modulus for different particle sizes.

Particle Density ρ_p *(g/L)*	**Molecular Diffusivities** D_i *(cm²/min)*			
1205	*Methanol*	*Acetaldehyde*	*Acetal*	*Water*
	1.5×10^{-3}	1.25×10^{-3}	0.85×10^{-3}	2.45×10^{-3}
Kinetic Constant k_c *(mol/g.min)*	**Surface Concentration** $C_{S,i}$ *(mol/L)*			
14.405	*Methanol*	*Acetaldehyde*	*Acetal*	*Water*
	14.703	7.247	0.0	0.0

($\phi_T \geq 10$), the relation between the effectiveness factor and the Thiele modulus is given by the following equation:

$$\text{T} = 20\ ^{o}\text{C} \qquad \ln\eta = -1.048\ln\phi_T + 1.706 \qquad R^2 = 0.9978$$

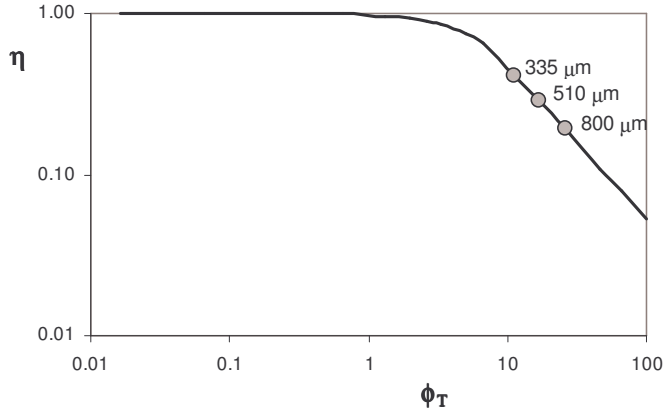

Figure 3.17: Variation of the effectiveness factor with the Thiele modulus.

3.8 Conclusions

Thermodynamic and kinetic experimental studies for acetal synthesis in a liquid phase reaction and catalyzed by Amberlyst-15 resin were performed in a Laboratory-scale experimental set-up. The thermodynamic equilibrium constant was measured in the temperature range of 293.15 – 333.15 K and given as $K_{eq} = 0.0143\exp[2142.5/T(K)]$.

The standard molar reaction properties were obtained at 298.15 K: ΔS^o = -35.34 J mol^{-1} K^{-1}, ΔH^o = -17.81 kJ mol^{-1} and ΔG^o = -7.28 kJ mol^{-1}. The standard molar properties for the formation of acetal in the liquid phase at 298.15 K were estimated from experiments:

$\Delta H_f^o = -402.29$ kJ mol^{-1}, $\Delta G_f^o = -230.95$ kJ mol^{-1} and $S_f^o = 308.71$ Jmol^{-1} K^{-1}.

As the strong non-ideality of the liquid reaction mixture, the reaction model was formulated in terms of liquid activities. The measured reaction rates were in good agreement with the proposed rate expression and the model constants dependence on temperature was found by Arrhenius equation. The rate equation can be used in the modeling simulations of the continuous reactor for the dimethylacetal synthesis. The proposed kinetic law expressed in activities is as shown below:

$$\Re = k_c \frac{a_A a_B - \frac{a_C a_D}{K_{eq} a_A}}{\left(1 + K_{s,D} a_D\right)^2}$$

and the parameters are,

$$k_c = 6.91\times10^{13} \exp\left[\frac{-8702.6}{T(K)}\right] (\text{ mol g}^{-1}\text{ min}^{-1})$$

$$K_{s,D} = 2.37 * 10^{32} \exp\left[\frac{-22713}{T(K)}\right] (\text{dimensionless})$$

The activation energy of the reaction is 72.4 kJ mol^{-1}.

The relation between the effectiveness factor and Thiele modulus was determined at 20 ^{o}C for the linear region ($\phi_A \geq 10$) and is given by: $\ln \eta = -1.048 \ln \phi_T + 1.706$.

3.9 Nomenclature

a liquid-phase activity

A_p external exchange area between the bulk fluid and the particles, cm^2

C_i concentration of component i, mol L^{-1}

C_{A_s} methanol concentration at the catalyst surface, mol L^{-1}

C_b bulk concentration, mol L^{-1}

$C_{p,j}$ concentration inside the particle, mol L^{-1}

C_p molar heat capacity at 298 K, J mol^{-1} K^{-1}

d_p mean pellet diameter, m

$D^o_{j,m}$ diffusion coefficient for a dilute solute j in mixture of n components, cm^2 min^{-1}

D_{A_s} effective diffusivity of methanol at catalyst particle surface, cm^2 min^{-1}

$E_{a,C}$ reaction activation energy, J mol^{-1}

ΔG reaction Gibbs free energy, J mol^{-1}

ΔG^o_f standard free energy of formation, J mol^{-1}

ΔH reaction enthalpy, J mol^{-1}

ΔH^o_f standard enthalpy of formation, J mol^{-1}

ΔH_s enthalpy of adsorption, J mol^{-1}

k_c kinetic constant, mol kg^{-1} min^{-1}

K_{eq} equilibrium reaction constant

K_p correction factor

K_s equilibrium adsorption constant

K_x constant based on molar fractions

K_γ constant based on activity coefficients

m mass, kg

M molecular weight, mol g^{-1}

n number of moles in the liquid phase, mol

P pressure, atm

r particle radial distance, cm

R gas constant, J mol^{-1} K^{-1}

r_p particle radius, μm

$\Re$ rate of reaction, mol kg^{-1} min^{-1}

$r_{A/B}$ initial molar ratio of reactants

ΔS reaction entropy, J mol^{-1} K^{-1}

ΔS_f^o standard entropy of formation, J mol^{-1} K^{-1}

T temperature, K

t time, s

V solution volume, m^3

V_{ml} molar volume of component i, m^3 mol^{-1}

w_{cat} mass of catalyst, kg

x molar fraction

X conversion of the limiting reactant

Greek letters

ν stoichiometric coefficient

γ activity coefficient

ρ normalized radial variable, dimensionless

ρ_p particle density, g L^{-1}

ρ_{solid} true solid density of catalyst, g L^{-1}

ϕ association factor in Eq. 3.23

ϕ_T Thiele modulus

ε porosity

ε_p particle porosity

σ_A standard deviation

τ tortuosity

Subscripts

0 initial value

A methanol

B acetaldehyde

C acetal (DME)

D water

eq equilibrium

exp experimental data

gas vapor phase

i relative to component *i*

l relative to limiting reactant

liq liquid phase

s surface condition

theo theoretical data

Superscripts

o standard state

3.10 References

(1) Aizawa, T.; Nakamura, H.; Wakabayashi, K.; Kudo, T.; Hasegawa, H. *Process for producing acetaldehyde dimethylacetal*. U.S. Patent 5,362,918, **1994**.

(2) Caetano, N. S.; Loureiro, J. M.; Rodrigues, A. E. MTBE synthesis catalysed by acid ion exchange resins: Kinetic studies and modelling of multiphase batch reactors. *Chem. Eng. Sci.* **1994,** *49* (24A), 4589. See also, Caetano, N. S. "Synthesis of MTBE". Ph.D. Thesis, University of Porto, **1995**, pp 150.

(3) Chopade, S. P.; Sharma, M. M. "Reaction of ethanol and formaldehyde: use of versatile cation-exchange resins as catalyst in batch reactors and reactive distillation column". *React. Funct. Polym.* **1997,** 32, 53-64.

(4) Chopade, S.P and Sharma, M.M. "Alkylation of methyl salicylate with isoamylene and isobutylene: ion-exchange resins versus acid-treated clay catalysts". *React. Funct. Polym.* **1996,** 28, 253-261.

(5) Dean, J.A., *Lange's Hand Book Chemistry*, 15th Edition, McGraw-Hill: New York, **1999**.

(6) Distillers Company Limited. *Manufacture of Diethylacetal*. U.S. Patent 2,519,540, **1950**.

(7) Dogu, T.; Aydin, E.; Boz, N.; Murtezaoglu, K.; Dogu, G. Diffusion Resistances and Contribution of Surface Diffusion in TAME and TAEE Production using Amberlyst-15. *Int. J. Chem. Reac. Eng.* **2003**, 1, A6.

(8) Fedriani, A.; Gonzalez-Velasco, J. R.; Lopez-Fonseca, R.; Gutierrez-Ortiz, M. A. Kinetics of 1,1-diethoxyethane synthesis catalysed by USY zeolites. *CHISA 2000, A7.7 12.30 Presentation* **2000**.

(9) Ferreira, M. V.; Loureiro, J. M. Number of active sites in TAME synthesis: Mechanism and kinetic modeling. *Ind. Eng. Chem. Res.* **2004,** 43, 5156.

(10) Fredeslund, A.; Gmehling, J.; Rasmussen, P. *Vapor-liquid Equilibrium Using UNIFAC*; Elsevier: Amsterdam, 1977.

(11) Gupta, B. B.G. *Alkoxyalkylation of phenol*. U.S. Patent 4,694,111, **1987**.

(12) Kiviranta-Paakkonen, P.; Struckmann, L.; Linnekoski, J.; Krause, A. Dehydration of the alcohol in the etherification of isoamylenes with methanol and ethanol. *Ind. Eng. Chem. Res.* **1998,** 37, 18.

(13) Kohlpaintner, C.; Schulte, M.; Falbe, J.; Lappe, P.; Weber, J. Aldehydes, aliphatic and araliphatic. *Ullmann's Encyclopedia of Industrial Chemistry,* 6th Edition, 1999.

(14) Korff, J.; Fremery, M.; Zimmermann, J. *Process for the production of acetaldehyde dimethyl acetal*. U.S. Patent 4,278,819, **1981**.

(15) Merck Index, 12th Edition 1996.

(16) Morrison, R.; Boyd, R. *Organic Chemistry*. 4th Edition. Allyn and Bacon: London, 1983.

(17) Oudshoorn, O. L.; Janissen, M.; van Kooten, W. E. J.; Jansen, J. C.; van Bekkum, H., van den Bleek, C. M.; Calis, H. P. A. Novel structured catalyst packing for catalytic distillation of ETBE. *Chem. Eng. Sci.* **1999,** *54*, 1413 -1418.

(18) Perry, R.H.; Green, D.W.; Maloney, J.O. *Perry's Chemical Engineers Handbook.* 7th Edition, McGraw-Hill: New York, 1997

(19) Reid, C. R.; Prausnitz, J. M.; Poling, B. E. *The Properties of Gases & Liquids*. 4th Edition, McGraw-Hill: New York, 1988.

(20) Silva, V. M. T. M. "Diethylacetal synthesis in simulated moving bed reactor". *Ph.D Thesis*, University of Porto, **2003**.

(21) Silva, V. M. T. M.; Rodrigues, A. E. Processo industrial de produção de acetais num reactor adsorptivo de leito móvel simulado*"*, *Portuguese Patent No. 103,123* (Patent Pending) **2004**.

(22) Silva, V. M. T. M.; Rodrigues, A. E. Synthesis of diethyl acetal: thermodynamic and kinetic studies. *Chem. Eng. Sci.*, **2001,** 56 1255-1263.

(23) Silva, V.M.T.M.; Rodrigues, A.E.; Kinetic Studies in a Batch Reactor using Ion-Exchange Resin Catalysts for Oxygenates Production: the Role of Mass Transfer Mechanisms. *Chem. Eng. Sci.* **2005**, accepted.

(24) Smith, J. M.; Van Ness, H. C. *Introduction to chemical engineering thermodynamics.* 4th Edition, McGraw-Hill: New York, 1987.

(25) Smith, Jr. L. A.; Arganbright, R. P. *Process for making Acetals*. U.S. Patent 6,015,875, **2000**.

(26) Sundmacher, K.; Zhang, R.S.; Hoffmann, U. Mass-Transfer Effects on Kinetics of Nonideal Liquid-Phase Ethyl Tert-Butyl Ether Formation. *Chem. Eng. Techn.* **1995**, 18, 269-277.

(27) Therre, J.; Kaibel, G.; Aquila, W.; Wegner, G.; Fuchs, H. *Continuous process for the preparation of acetals*. U.S. Patent 6,518,464 B2, **2003**.

(28) Thorat, T. S.; Yadav, V.M. and Yadav, G.D. Esterification of phthalic anhydride with 2-ethylhexanol by solid superacidic catalysts. *Appl. Catal. A General* **1992**, 90, 73-92.

(29) Waller, F. J.; Weist, Jr. E. L.; Brown, D. M.; Tijm, P. J. A. *Diesel fuel composition comprising dialkoxy alkanes for increased centane number.* U.S. Patent 5,858,030*,* **1999**.

(30) Wegman, R. W. *Hydroformylation Process*. U. S. Patent 4,429,165, **1984.**

(31) Yadav, G. D.; Krishnan, M. S. Solid acid catalysed acylation of 2-methoxy-naphthalene: role of intraparticle diffusional resistance. *Chem. Eng. Sci.* **1999,** 54, 4189-4197.

(32) Yadav, G. D.; Pujari, A. A. Kinetics of acetalization of perfumery aldehydes with alkanols over solid acid catalysts. *Canadian Journal of Chemical Engineering*, **1999,** *77*, 489-496.

4. Dimethylacetal Synthesis on Fixed Bed Adsorptive Reactor

The synthesis of dimethoxyethane using acetaldehyde and methanol as raw-material on a fixed bed adsorptive reactor packed with Amberlyst-15 resin was studied. Dynamic binary adsorption experiments were carried out in absence of reaction at 293.15 K in a laboratory scale column. The experimental results of the adsorption of binary non-reactive mixtures are reported and used to obtain multicomponent adsorption equilibrium isotherms of Langmuir type. The multicomponent adsorption isotherms of Langmuir type were determined, by minimizing the difference between the experimental and calculated stoichiometric times of breakthrough curves. The mathematical model used to describe the adsorptive reactor dynamic behaviour includes axial dispersion, mass transfer resistances, reaction kinetics, and multicomponent Langmuir adsorption isotherms. The mass transport phenomena through the external film and particle pores were not taken into account explicitly; however, they were lumped in the global mass transfer coefficient. The experimental results obtained for the reaction and regeneration experiments were represented in terms of effluent molar concentration of the species from the column. Model equations were solved by orthogonal collocation on finite elements (OCFE) implemented by the PDECOL package, using the measured model parameters and was validated for both reaction and regeneration steps.

4.1 Introduction

The main process for the manufacture of acetals is the reaction of an aldehyde with excess alcohol. The general acetalization reaction is given according to the below mentioned reaction (Smith Jr. and Arganbright, 2000; Hindeheru et al., 1997):

$$2\ Alcohol(A) \quad + \quad Aldehyde(B) \quad \Leftrightarrow \quad Acetal(C) \quad + \quad Water(D) \qquad (4.1)$$

Acetalization reactions of alcohol and aldehyde basically take place in presence of acidic medium (Merck Index, 1996; Morrison and Boyd, 1983; Yadav and Pujari, 1999). Generally this reaction is carried out in presence of anhydrous acid like hydrochloric acid, sulphuric acid, *p*-toluene sulphonic acid or acetic acid as catalyst; these are equilibrium-controlled reactions (Guinot, 1932). Obviously, using solid catalyst for these types of reactions in order to separate the catalyst from the reaction mixture will be the advantage of the process. Apart from the catalyst separation, separation of desired product from the reaction mixture is one of the important unit operations in these kinds of reaction processes. Several methods have been considered for the separation of acetal from reaction mixture. Few researchers have studied the acetalization reaction with simultaneous removal of either water or dialkoxyalkane in order to shift the equilibrium and to achieve higher conversion during the reaction of aldehyde with excess of alkanol in presence of acidic medium. Ethanol-DEM (diethoxymethane) azeotrope from the reaction mixture of ethanol-formaldehyde reaction have been removed, which was further purified separately by introducing cyclohexane and subsequently removing cyclohexane-ethanol azeotrope to get pure DEM. DEM was prepared in higher than 98% purity by using dichloromethane as solvent, removing the water produced as water-dichloromethane azeotrope and then

distilling out dichloromethane followed by the DEM (Chopade and Sharma, 1996; Hsu et al., 1986).

The use of ion-exchange resins as heterogeneous catalysts offers many advantages over homogeneous acidic catalysts as mentioned earlier, such as ease of separation, mild reaction conditions, better selectivity, and elimination of waste disposal problems. Amberlyst-15 resin can be used as an adsorbent (Mazzotti et al., 1996, 1997) as well as catalyst for acetalization reactions (Silva, 2003; Lode et al., 2001). It is known that the reaction of acetaldehyde with excess methanol to form dimethylacetal and water is an equilibrium controlled reaction, it is necessary to introduce a unit operation to separate the product dimethylacetal from the unreacted acetaldehyde, methanol and the co-product water.

With ordinary distillation unit operation, dimethylacetal cannot be separated from the reaction mixture due to the close boiling temperatures of methanol and acetal (64.5 and 64.3 ^{o}C, respectively) (Dean, 1999; Perry, 1984). Here adsorptive/chromatographic reaction process for the production of acetal can be considered of its feasible and economical solution. The above-mentioned application of adsorptive/chromatographic reactors to equilibrium controlled reactions leads to conversion higher than the equilibrium position. Moving bed reactors (MBR) or Simulated moving bed reactors (SMBR) can be considered for the above mentioned application on commercial scale (Wankat, 1994; Do, 1998). Simulated moving bed reactor was used for the reversible reactions (Lode et al., 2001; Silva, 2003). Until now very few applications of SMBR concept have been reported. Rigorous study is necessary in order to understand the behavior of the adsorptive reactor to validate kinetic and adsorption data to the simulated moving bed reactor (Lode et al., 2001).

This application of chromatographic reactors to equilibrium controlled reaction (Sardin et al., 1993) leads to conversion higher than the equilibrium since one of the products is being removed from the reaction zone. Perhaps one of the most interesting chromatographic reactors is the simulated moving bed reactor (SMBR). This technology has been applied to reversible reactions catalyzed by acid resins (Mazzotti et al., 1996) and also to biochemical reactions (Azevedo and Rodrigues, 2001; Barker et al., 1992). However some researchers first studied the dynamic behavior of the fixed bed adsorptive reactor to validate kinetic and adsorption data and to provide a better understanding of the performance of chromatographic reactor (Kawase et al., 1999; Lode et al., 2001; Mazzotti et al., 1997; Silva and Rodrigues, 2002). A number of mathematical models have been developed to explain the kinetic behavior of the fixed bed adsorptive reactor and to estimate the breakthrough curves. The mechanism of adsorption and reaction on a catalyst includes external diffusion, internal diffusion, the adsorption and reaction at the solid surface. The intraparticle diffusion may occur by molecular diffusion, and the surface diffusion, depending on the pore size, the adsorbate concentrations and other conditions. There exists the mass transfer mechanism that may occur in a fixed bed adsorptive reactor. The mass transfer effects are due to four main mechanisms: axial mixing in the bulk mobile phase percolating between the stationary phase particles in the column (axial dispersion); the mass transfer of molecules between the bulk mobile phase and the external surface of the stationary phase particles (external mass transfer); the diffusion migration through the pores inside the particles (internal diffusion); and the surface diffusion.

The present work addresses the detailed study for the dimethylacetal synthesis in an adsorptive reactor (Fixed bed reactor) on laboratory setup in order to validate the

results to the simulated moving bed reactor (SMBR). Adsorption and reaction experiments were carried out at 293.15 K with atmospheric pressure. The binary adsorption experiments in absence of reaction were carried out on a fixed bed of Amberlyst-15 resin in order to determine the multi-component adsorption parameters. Necessary reaction kinetic parameters for the dimethylacetal synthesis were used from the batch reactor experiments.

4.2 Materials and Methods

4.2.1 Chemicals

The chemicals methanol (>99.9% pure) acetaldehyde (> 99.5% pure) and acetaldehyde dimethylacetal (>97% pure) from Sigma-Aldrich, UK, were used in this present work.

4.2.2 Adsorbent

An Amberlyst-15 Resin (Rohm and Haas, France) with various particle sizes was used as an adsorbent and as well as a catalyst in the experiments performed.

4.2.3 Analytical method

The samples were analyzed with the help of Gas Chromatography (Chrompack 9100, Netherlands), and the compounds were separated in a fused silica capillary column of 25m-length and 0.5mm diameter (Chrompack CP-Wax 57 CB) using a thermal conductivity detector (TCD) for peak detection. The column temperature was programmed by a 40^{o}C/min ramp up to 100^{o}C and held for one minute. The detailed procedure of analytical method was explained in the section 3.2.2 of Chapter 3.

4.3 Experimental Setup

Experimental setup consists of jacketed glass column in which the Amberlyst-15 resin bed was made for known length with the support of the adjustable filter ended

stoppers in the column. Two ends of the column are arranged with tubing for inlet and outlet streams of reactants and products. Here the stream flow rates are controlled with the help of a pump, which is provided with a capacity of 1.7 x 10^{-7} m^3/s (9.99 ml/min). The outlet tubing is arranged with a three-way valve so as to with draw samples at regular intervals for analyzing. The thermostatic bath was provided externally in order to maintain the column's bed at desired temperature by circulating the liquid through the jacket of the column and also it was used to maintain the desired feed solution temperature. The experimental setup is as shown in the Figure 4.1 and characteristics of the bed in the column are given in Table 4.1.

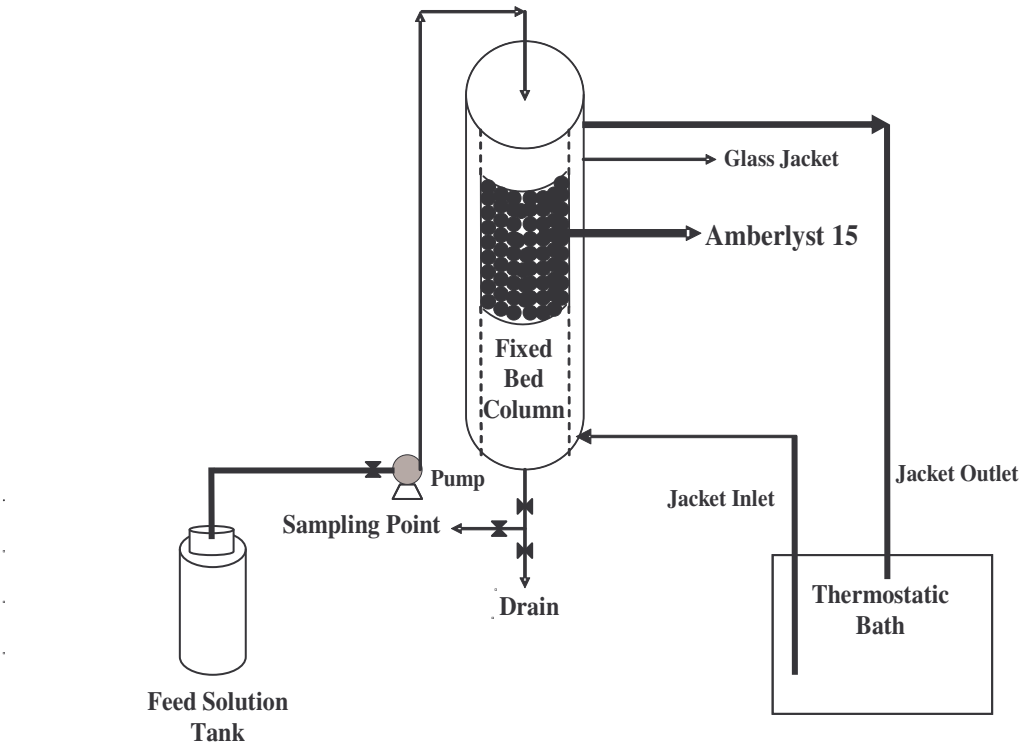

Figure 4.1: Experimental Set-up

The column was packed with sulfonic acid ion exchange resin Amberlyst-15, the ion exchange capacity is 4.7 eq $H^{\oplus}$/Kg of dry resin and the surface area of 45 m^2 /g. Contact of dry resin with fluid results in swelling of the resin and the swelling ratio varies with fluid composition.

Table 4.1 Characteristics of Fixed Bed

Solid Weight(Amberlyst 15 Resin)	47.0 X 10^{-3} Kg
Length of Bed(L)	11.0 X 10^{-2} m
Internal diameter(D_i)	2.6 X 10^{-2} m
Average radius of Resin Beads(r_p)	[300-400] μm
Bulk Density of Resin Beads(ρ_b)	792 Kg/m^3
Bed Porosity(ε)	0.40
Resin Particle Porosity(ε_p)	0.36
Surface Area of Resin(S_A)	45 m^2/g
Peclet Number	270

In order to conduct experiments with methanol and acetaldehyde so as to produce acetal (dimethoxyethane (DME) or acetaldehyde dimethylacetal) on a fixed bed, following procedure has been adopted as mentioned below. Fixed bed was made in a glass column using Amberlyst-15 resin; this resin acts as both catalyst and adsorbent for formation and separation of acetal, respectively. The adsorption/chromatographic reaction process on the resin for the production of acetal was optioned to proceed further due to the closer boiling temperatures of methanol and acetal, 64.55 and 64.30 ^oC respectively, which cannot be separated with simple reactive distillation. As adsorption parameters of the reactants and products on the Amberlyst-15 resin are not known and even reported literature is not available with this particular resin, giving

importance to the adsorption parameters, here binary adsorption experiments in absence of reaction with different combinations of pure acetal (DME), methanol and water were performed. Even though the acetaldehyde was one of the reactants, with combination of acetaldehyde, binary adsorption experiments were not conducted due to its property of polymerization in presence of acidic catalysts like resins or zeolites. Reaction experiments were also conducted with different combinations of parameters.

4.4 Fixed-Bed Adsorptive Reactor

Integration of any unit operation with chemical reaction into one single apparatus may allow for significant importance in process performance and has therefore been studied in different forms for many years (Agar, 1999; Falk, 1999; Chopade and Sharma, 1997). Examples for such multifunctional reactors are reactive distillation process, integrating chemical reaction and separation, or reversed-flow reactors to chemical reaction and heat transfer. In the former case, the major advantage is given by the possibility to make the concentration profiles within the unit in order to either overcome a chemical equilibrium limitation or to optimize the process selectivity. On the other hand, this process intensification also reduces the degree of freedom in the design of the process, potentially limiting their performance. Nevertheless, the general concept has proved its potential, and, for example, reactive distillation has become the process of choice for a number of industrial applications.

An alternative reaction-separation unit is the chromatographic reactor (Mazzotti et al., 1996) which utilizes the differences in adsorptivity of the different components involved rather than differences in their volatility, which is the case with reactive-distillation unit. It is, especially, an attractive process as an alternative to reactive-distillation when the species involved are either non-volatile or sensitive to temperature,

as in the case, for example, in some fine chemical or pharmaceutical applications, or exhibit small volatility differences.

This chromatographic technique is essentially the same as the method used in laboratory analysis. By having the targeted composite substance adsorbed into the adsorbent, the chromatographic divides the mixed substance into its parts. Now let us suppose that adsorption affinities of substance A, B, C are as follows, A< B< C. A column shown in Figure 4.1 packed with adsorbent, and then fluid with liquid desorbent. In this state, a fixed amount of sample liquid (a mixture of A, C) is fed in at one end of the column. Next, if we continuously feed in liquid desorbent, each component of sample (A and C) will move in the adsorbent layers at the migration rates U_A and U_C, each determined according to their individual adsorption affinity. Thus, if there is difference between the migration velocities U_A and U_C, as component A and component C move through the adsorbent layers they will separate from each other. In this way, by collecting the liquids as they successively drip out of the column, the mixture can be separated into fractions each abundant with one of the component materials.

Since the types and densities of the desorbents can easily be changed, fixed-bed chromatography can be applied to the separation of many types of useful substances. However, in cases where a more precise separation is required, the fact that the fixed-bed chromatographic process results in a material with low concentration means that higher costs are entailed in once again raising the material's concentration. Thus, although it is difficult to use this method in cases where the final product is not very expensive, the process is still one, which can easily be used to separate many

components. However, there are some additional drawbacks which surface when this method is used on large scale:

1. The entire adsorbent bed is not effectively utilized.
2. A large quantity of desorbent is consumed, and the separated components are obtained in a diluted state.
3. In order to obtain a successful separation, a sufficiently large difference in the adsorption affinities of the adsorbates is required.
4. The operation is not continuous.

Due to the above deficiencies, there have been many innovative attempts to improve the fixed-bed mode of operation so that it can be used as an industrial device.

4.4.1 Modeling of Fixed Bed

Here it was considered an isothermal fixed bed packed with Amberlyst-15 resin. The bed was subjected to axial (longitudinal) dispersion, external and internal mass transfer resistances in adsorbing species were considered in order to determine the model parameters using experimental data collected for the synthesis of acetal (dimethoxyethane, DME) on fixed bed, methanol and acetaldehyde as the raw-material.

4.4.2 Adsorption Isotherms

The adsorption isotherm is the equilibrium relationship between the concentration in the fluid and the concentration in the adsorbent particles at a given temperature and pressure. Particularly for liquid adsorption, role of pressure is not that effective as in the case of gas adsorption. For liquid adsorption is often expressed in mass concentrations, such as parts per million or moles per unit volume or mass per unit volume. The concentration of adsorbent on the solid is given as moles or mass adsorbed per unit mass or unit volume of original adsorbent (solid phase). Considering the Extended

Langmuir Isotherm model for multi component adsorption, it can be expressed as follows,

$$q_i = \frac{Q_i K_i C_i}{1 + \sum_{j=1}^{n} K_j C_j} \tag{4.2}$$

where q_i -fluid concentration at equilibrium of species 'i' inside the solid bed (mol/m^3)

Q_i - Adsorption capacity of species i (mol/m^3)

K_i - Adsorption constant of species i (m^3/mol)

C_i - Liquid phase concentration of species i (mol/m^3)

i = methanol, acetaldehyde, acetal (DME), & water

Langmuir isotherm is derived assuming a uniform surface of the solid.

The mathematical model can be used to describe the dynamic behavior of the fixed bed reactor (adsorber), considering the following assumptions,

1. The flow pattern is described by the axial dispersion plug flow model.
2. External and internal mass-transfer for adsorbable species is combined in a global resistance.
3. Isothermal process of adsorption.
4. Constant column length and packing porosity of bed were assumed.

The model equations consists of the following system of four second order partial differential equations in the bulk concentration of the i^{th} component, C_i, and four ordinary differential equations in the average concentration of i^{th} component into the particle pores, $\overline{C}_{P,i}$ are as follows,

Bulk fluid mass balance to component *i*

$$\varepsilon \frac{\partial C_i}{\partial t} + u \frac{\partial C_i}{\partial z} + (1-\varepsilon)\frac{3}{r_p} K_L (C_i - \overline{C}_{P,i}) = \varepsilon D_{ax} \frac{\partial}{\partial z}(C_T \frac{\partial x_i}{\partial z}) \tag{4.3}$$

Pellet mass balance to component *i*

$$\frac{3}{r_P} K_L (C_i - \overline{C}_{P,i}) = \varepsilon_P \frac{\partial \overline{C}_{P,i}}{\partial t} + (1-\varepsilon_P)\frac{\partial q_i}{\partial t} - v_i \frac{\rho_b}{1-\varepsilon} \eta \Re \tag{4.4}$$

For the above mass balance is associated with the initial and boundary conditions,

at $t = 0$, $C_i = \overline{C}_{P,i} = C_{i,0}$ (4.5)

$z = 0$ $uC_i - \varepsilon D_{ax} \left.\frac{\partial C_i}{\partial z}\right|_{z=0} = uC_{i,F}$ (4.6)

$z = L$ $\left.\frac{\partial C_i}{\partial z}\right|_{z=L} = 0$ (4.7)

Where F and 0 refers to the feed and initial states, respectively.

The balance Eq. (4.3) contains the axial dispersion coefficient D_{ax} of the fixed bed, in a fixed-bed adsorber as the flow assumed is plug flow. Deviation from this flow is described by the axial dispersion coefficient D_{ax} or a dimensionless number *Pe* of the fixed bed.

Reaction rate $\Re$ mentioned in the Eq. (4.4) can be determined based on activities of species, and the rate equation is given as shown below,

$$\Re = k_c \frac{a_A a_B - a_C a_D / K_{eq} a_A}{(1 + K_{s,D} a_D)^2} \tag{4.8}$$

$$a_i = x_i \gamma_i \qquad i = A, B, C, D \tag{4.8a}$$

activity coefficients γ_i necessary were calculated using UNIFAC method (Smith and Van Ness, 1987; Gmehling et al., 2002; Lohmann et al., 2003) corresponding relative molecular volume and surface area of pure species parameters and interaction

parameters are given in Table 3.10 and Table 3.11 respectively. The non-ideality of the system is observed by analyzing the activity coefficients calculated by UNIFAC method. Adsorption constant K_D in Equation 4.8, Equilibrium constant K_{eq}, kinetic constant k_c, in the Eq. (4.8) are given in the Table 4.2.

Table 4.2: Reaction equilibrium constant and kinetic parameters to acetal synthesis catalyzed by Amberlyst-15.

$T(K)$	K_{eq}	$k_c(mol/g.\min)$	K_D
293.15	21.9344	9.13	0.0535
303.15	15.9965	22.10	0.6780
313.15	15.2441	60.90	7.5400

Introducing the dimensionless variables for space $\zeta = \frac{z}{L}$ and time $\theta = \frac{t}{\varepsilon L/\ u}$

and the parameters:

$$Pe = \frac{uL}{\varepsilon D_{ax}} \quad \text{(Peclet number)} \tag{4.9}$$

$$Da = \frac{\rho_b \eta k_c \varepsilon L}{(1-\varepsilon)u} \quad \text{(Damköehler number)} \tag{4.10}$$

$$K_L^* = \frac{\varepsilon L}{u}\frac{3}{r_P}K_L \quad \text{(Number of mass transfer units)} \tag{4.11}$$

The above model equations, Eq. (4.3) & Eq. (4.4) can be written as follows:

$$\frac{\partial C_i}{\partial \theta} + \frac{\partial C_i}{\partial \zeta} + K_L^* \frac{1-\varepsilon}{\varepsilon}(C_i - \overline{C}_{P,i}) = \frac{1}{Pe}\frac{\partial^2 C_i}{\partial \zeta^2} \tag{4.12}$$

$$K_L(C_i - \overline{C}_{P,i}) = \varepsilon_P \frac{\partial \overline{C}_{P,i}}{\partial \theta} + (1-\varepsilon_P)\frac{\partial q_i}{\partial \theta} + v_i Daf(\overline{C}_{P,i}) \tag{4.13}$$

with initial and boundary conditions:

$$\theta = 0 \qquad C_i = \overline{C}_{P,i} = C_{i,0} \tag{4.14}$$

$$\zeta = 0 \qquad C_i - \frac{1}{Pe}\frac{\partial C_i}{\partial \zeta}\bigg|_{\zeta=0} = C_{i,F} \tag{4.15}$$

$$\zeta = L \qquad \frac{\partial C_i}{\partial \zeta}\bigg|_{\zeta=L} = 0 \tag{4.16}$$

The proposed model considers a global mass-transfer coefficient (K_L) defined as:

$$\frac{1}{K_L} = \frac{1}{k_e} + \frac{1}{\varepsilon_P k_i} \tag{4.17}$$

where, k_e and k_i are external and internal mass-transfer coefficients respectively to the liquid phase.

For calculations of parameters, requires the complete model equations inside the particles. As an approximation, the mean values of external and internal mass-transfer coefficients can be estimated with the help of below given relations.

$$k_i = \frac{5D_m/\tau}{r_P} \tag{4.18}$$

The external mass transfer coefficient can be estimated with the Wilson and Geankoplis correlation:

$$Sh_P = \frac{1.09}{\varepsilon}(\mathrm{Re}_P\, Sc)^{0.33} \qquad 0.0015 < \mathrm{Re}_P < 55 \tag{4.19}$$

where $\mathbf{S}h_P$ and Re_P are, the Sherwood and Reynolds numbers respectively relative to particle

$$Sh_P = \frac{k_e d_P}{D_m} \tag{4.20}$$

$$\mathrm{Re}_P = \frac{\rho d_P u}{\mu} \tag{4.21}$$

and Sc is the Schmidt number.

$$Sc = \frac{\mu}{\rho D_m} \tag{4.22}$$

The diffusivities in the multicomponent liquid mixture can be estimated by the modified Wilke-Chang equation (Reid et al., 1987) and it was given as follows,

$$D_{A^\circ m} = 7.4\times10^{-8}\frac{(\phi M)^{\frac{1}{2}}T}{\mu V_{ml,A}^{0.6}} \tag{4.23}$$

$$\phi M = \sum_{\substack{j=1 \\ j\neq A}}^{n} x\phi_j M_j \tag{4.24}$$

where $D_{A^\circ m}$ is the diffusion coefficient for a dilute solute A into a mixture of n components, T is the temperature, $V_{ml,A}$ is the molar volume of the solute A, x_j is the molar fraction for component *j*, ϕ_j is the associated factor for component *j*, and it is given as 2.26 for water, 1.9 for methanol and 1.0 for unassociated components[29]. The mixture viscosity μ can be predicted by the generalized corresponding states method (Teja and Rice, 1981).

The system of partial differential equations represented by Eq. (4.12) to Eq. (4.16) are solved by the method of lines (MOL) using orthogonal collocation in finite elements, with B-splines as base functions through numerical package PDECOL. Fifty subintervals for spatial discretization along the z-axis were used, with two internal collocation points in each subinterval, resulting in 200/400 time dependent ordinary differential equations for adsorption/reaction simulations. For all simulations was fixed a tolerance value EPS equal to 10^{-7}.

4.5 Experimental Results and Discussions

4.5.1 Binary Adsorption Experiments

The breakthrough curves of methanol, acetal (dimethoxyethane, DME) and water were measured in the absence of reaction. The adsorbent was saturated with a certain component A, and then the feed with pure component B was fed to the adsorbent on stepwise concentration of the feed solution. Minimizing the difference between the experimental and simulated stoichiometric times of breakthrough curves, the adsorption parameters were optimised and shown in Table 4.3. The stoichiometric time can be determined from the mass balance over the adsorbent bed in the column as shown below (Ruthven, 1984),

$$t_{st} = \frac{L}{u}\left[\varepsilon + (1-\varepsilon)\varepsilon_p + (1-\varepsilon)(1-\varepsilon_p)\frac{\Delta q}{\Delta C}\right] \tag{4.25}$$

where $$\frac{\Delta q}{\Delta C} = \frac{q(C_F) - q(C_0)}{C_F - C_0} \tag{4.26}$$

Experimental stoichiometric times were calculated from the plot of effluent concentration of column as a function of time for effluent samples analysed. In the breakthrough experiments, where component A displaces the component B, the total amount of A necessary to saturate the column is given by the product between the volumetric flow rate and the area over the breakthrough curve limited by the feed concentration. The product between the flow rate and the area under the elution curve gives the total amount of component B that was initially saturating the column. In the Figures 4.2(a) and 4.2(b), the concentration graphs of methanol and acetal are shown.

In the breakthrough of acetal, Figure 4.2(a), the errors between the experimental and theoretical amounts of acetal adsorbed and methanol displaced are 4.4 and 8.4 %,

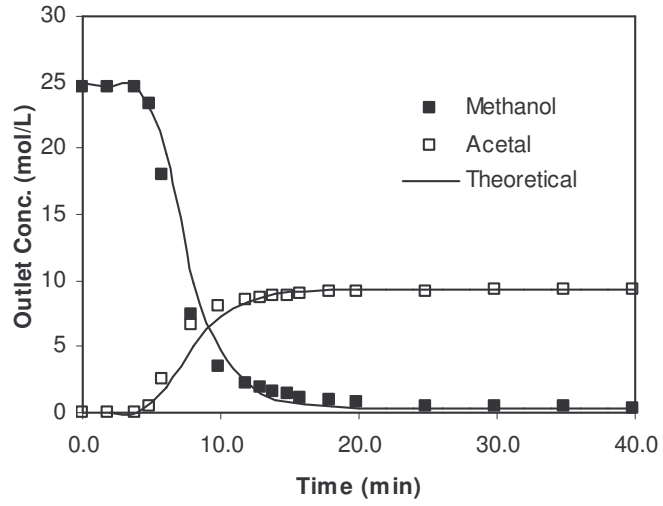

(a)

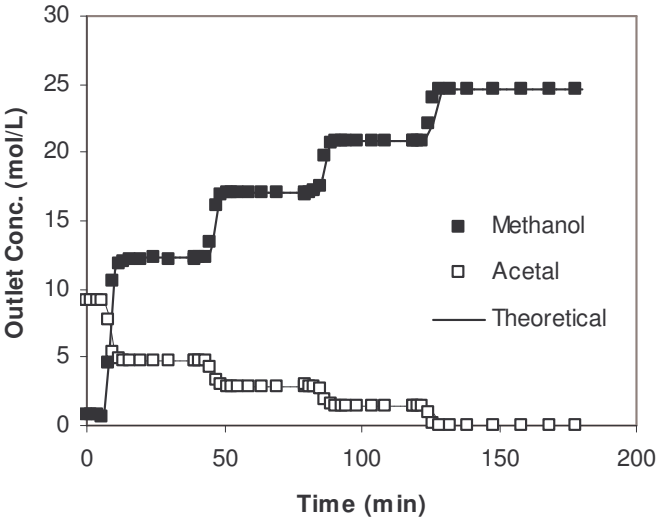

(b)

Figure 4.2: Breakthrough experiment, outlet concentration of acetal and methanol as a function of time.
(a) acetal displacing methanol; Q = 6.0 mL/min(10 X 10^{-8} m^3/s); bottom-up flow direction.
(b) methanol displacing acetal; Q = 6.0 mL/min(10 X 10^{-8} m^3/s); top-down flow direction.
Experimental data: (■)methanol; (□) acetal. (—) theoretical results.

respectively. Comparing the experimental amount of methanol adsorbed in the experiment of Figure 4.2(b) with the experimental amount of methanol desorbed in the

experiment of Figure 4.2(a), the error obtained is 2.8 %. For acetal, the error between the amount adsorbed, Figure 4.2(a), and the amount eluted, Figure 4.2(b), is 0.8 %. In the binary experiments of methanol and water, see Figure 4.3, the experimental results are well predict by the theoretical model.

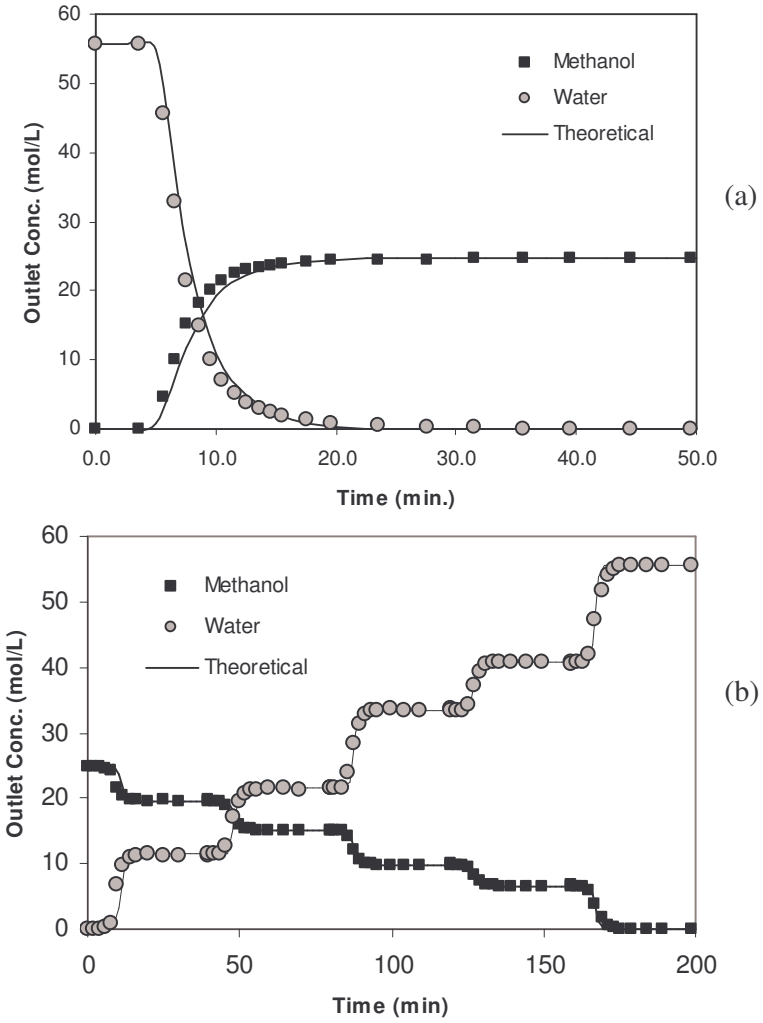

Figure 4.3: Breakthrough experiment, outlet concentration of methanol and water as a function of time.
(a) Water displacing methanol; Q = 6.0 mL/min (10 X 10^{-8} m^3/s); top–down flow direction.
(b) Methanol displacing Water; Q = 6.0 mL/min (10 X 10^{-8} m^3/s); bottom-up flow direction.
Experimental data: (■) methanol; ( ) water. (—) theoretical results.

Similarly, experiments were conducted for the combination of methanol and water breakthroughs and the breakthrough plots for methanol and water are shown in the above Figure 4.3(a) and 4.3(b). It was not possible to perform the breakthrough experiment with acetaldehyde as acetaldehyde itself polymerizes to give acetaldehyde trimer (paraldehyde). So the adsorption parameters were determined by optimizing the reaction experimental data.

Using the available information from experimental data and theoretical parameters, adsorption of acetal (DME), methanol and water on the adsorbent were calculated at different steps of feed solutions so as to determine the adsorption isotherms. From the breakthrough experiments with acetaldehyde it was not possible to obtain the adsorption parameters, since it was observed experimentally the formation of acetaldehyde trimer (paraldehyde). Therefore the adsorption parameters were determined by optimizing the reaction experimental data. The determined adsorption parameters for all components are shown in Table 4.3.

Table 4.3 Adsorption equilibrium isotherms and component densities at 293 K

Component	Q (mol / $m^3_{real\ solid}$)	K (m^3/mol)	Density (kg/m^3)
Methanol (A)	14.52×10^3	0.60×10^{-3}	791
Acetaldehyde (B)	18.65×10^3	0.38×10^{-3}	785
Acetal (C)	7.67×10^3	0.02×10^{-3}	852
Water (D)	28.49×10^3	1.15×10^{-3}	1003

Simulated plots of component A displacing component B were made with the help of adsorption parameters calculated using experimental data, and these plots were in agreement with the experimental data obtained for acetal, methanol and water.

4.5.2 Reaction Experimental Procedure

Reaction experiments were performed, by feeding continuously the mixture of methanol and acetaldehyde to the fixed bed chromatographic reactor that was initially saturated with methanol. As the feed mixture is less dense than the pure methanol, the flow direction was operated in top-down. However, it was noticed hydrodynamic effects due to axial back mixing driven by natural convection of water. The concentration fronts moving within the column are hydrodynamically stable if the component in the component above the front is less dense than the component below the front. Since the products are denser then the reactants, the reaction mixture is denser than methanol (initially saturating the column); therefore the reactants mixture should be fed from the bottom. The reactants mixture methanol and acetaldehyde at the stoichiometric ratio was fed to the column with 6 mL/min flow rate as shown in Figure 4.4, wherein the outlet concentration of the reaction mixture was indicated as the function of time. As the reaction mixture enters the column, acetaldehyde in the reactants mixture is adsorbed and reacts with adsorbed methanol in the adsorbent phase (resin). Acetal (DME) and water are formed in the stoichiometric amounts, but the resin adsorbs preferentially water, whereas acetal is soon desorbed from the resin phase and carried out by the fluid stream along the column. As water is removed from the reaction medium, the acetalization reaction last long until consumption of acetaldehyde. This process of reaction in the fixed bed will continue until the resin in the column is completely saturated with acetaldehyde and water. Once the equilibrium is reached in the resin (solid phase), the selective separation of acetal and water is not possible anymore. The concentration of the reaction mixture in the column remains constant as the steady state

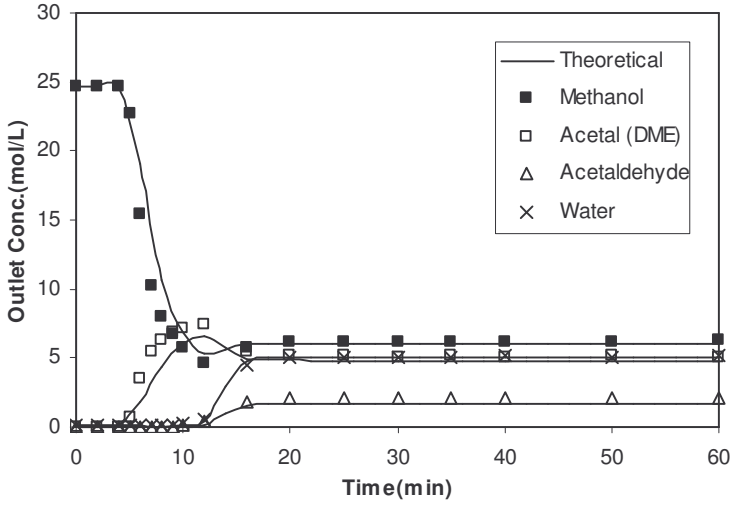

Figure 4.4: Concentration profiles in a fixed bed adsorptive reactor initially saturated with methanol and then fed with methanol and acetaldehyde mixture.
Experimental conditions: Q = 6.0 mL/min (10 X 10^{-8} m^3/s), $C_{A,F}$ = 16.03 mol/L and $C_{B,F}$ = 6.29 mol/L; Bed Length: 11.0 Cm; Bed Diameter: 2.6 Cm; Bed Temperature: 20 ^oC;
Experimental data: (■) methanol, (△) acetaldehyde, (□) acetal and (×) water; Simulated results: continuous line.

is achieved, and the reaction mixture at the equilibrium position consists of the concentrations in the outlet stream. The difference under the outlet concentration curves of the two products is relative to the difference in the adsorbed amount of acetal and water in the resin, once both products are formed at the same stoichiometric amounts. In this case, the model predictions are in agreement with the experimental data.

Here in this reaction experiment, it is observed that there are two concentration fronts. The first one is an adsorptive front where DME displaces methanol, which comes out between 5 and 15 minutes as shown in Figure 4.4. The other is a reactive front, where the acetalization and separation of the products occurs and it comes at 16 minutes. These phenomena are better understood with the analysis of propagation of these composition fronts inside the column. This is possible only by considering the simulated internal profiles for the same experimental operating conditions of Figure 4.4. Figure 4.5(a-d) shows the internal concentration profiles for all species at 2, 4, 6 and 8 minutes. Near the feed port of the reactor, there is a reaction zone where the

reactants are fast consumed till the equilibrium composition ($C_{methanol}$=6.3 x 10^3 mol/m^3, $C_{acetaldehyde}$ = 2.1 x 10^3 mol/m^3). This reaction zone is in steady state. The second reaction zone corresponds to the reactive/separative front, where reaction occurs until complete consumption of acetaldehyde. This happens since the methanol is in excess compared with the acetaldehyde and the water displaces acetal from the stationary phase. In this reaction front, the concentration fronts of acetaldehyde and water exhibit constant pattern behaviours, since it propagate along the column at constant velocities without changing their shapes. Since the resin is preferentially adsorbing water while it is produced, the velocity of water (at about 1.28×10^{-4} m/s, in Figure 4.5(d) is lower than that of the acetaldehyde front (at about 1.38×10^{-4} m/s, in Figure 4.5(b). The acetal produced is immediately desorbed, increasing the acetal fluid concentration. After the reactive front zone, there are only acetal and methanol in the separative front where acetal is displacing the methanol that initially saturates the resin (Figure 4.5(a) and Figure 4.5(c))

In order to quantify the mass transfer resistances and their relative importance, the values of the external, internal and global mass transfer coefficients are shown in Table 4.4. It is concluded that the internal diffusion is the controlling mechanism. Chromatograms of a typical experiment (Figure 4.4) at 2, 5, 10, 12, 20 and 40 minutes of the reaction are given in Figures A.9, A.10, A.11, A.12, A.13, and A.14 respectively of Appendix A.

Table 4.4 Mass transfer coefficients estimated at 293 K, at the inlet of the column to the reaction experiment.

Component	k_e (m/s)	k_i (m/s)	K_L (m/s)
Methanol	5.41×10^{-5}	1.78×10^{-5}	0.573×10^{-5}
Acetaldehyde	4.74×10^{-5}	1.47×10^{-5}	0.476×10^{-5}
Acetal (DME)	3.68×10^{-5}	1.00×10^{-5}	0.328×10^{-5}
Water	7.48×10^{-5}	2.90×10^{-5}	0.916×10^{-5}

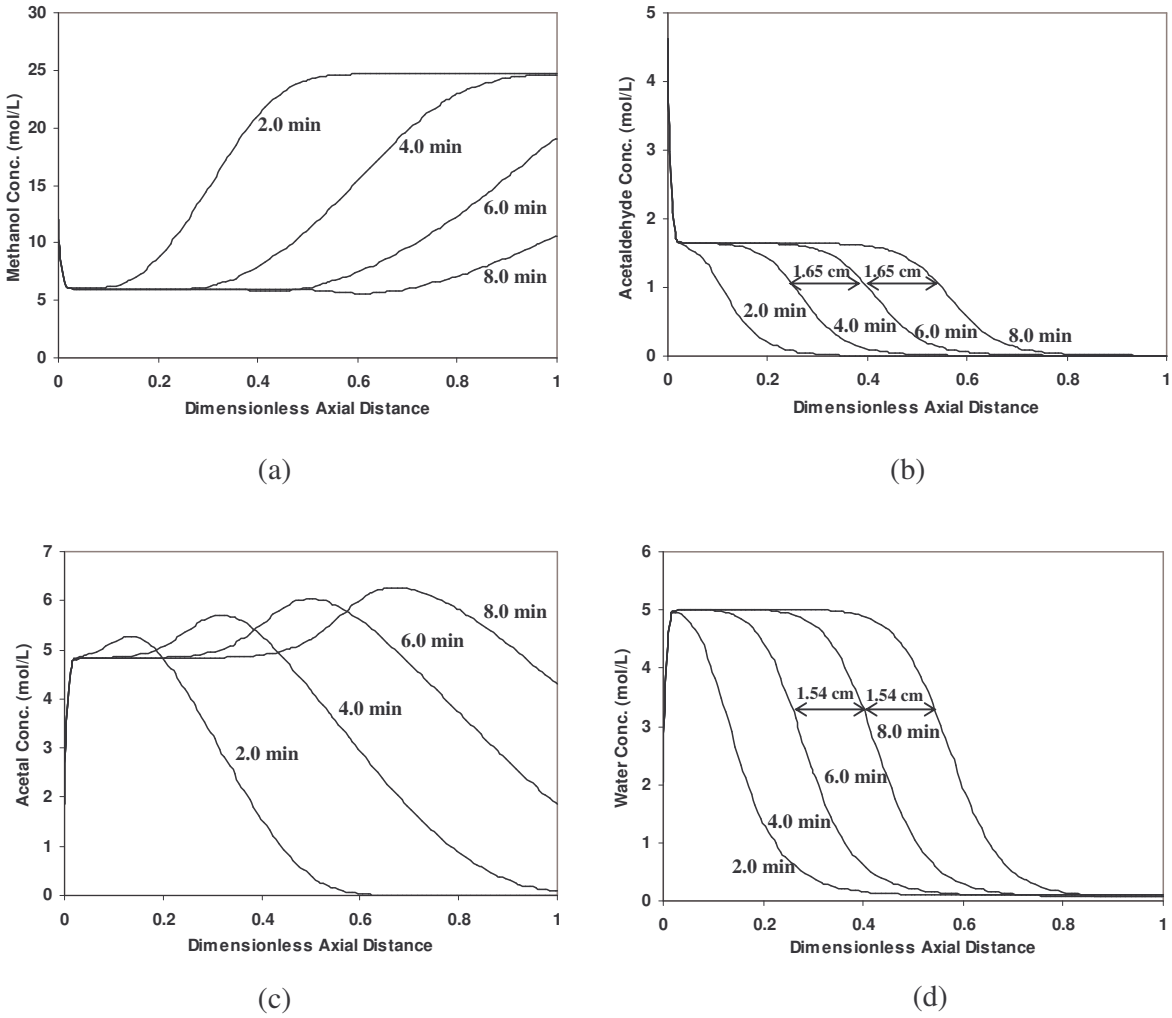

Figure 4.5: Internal concentration profiles of each species in fluid phase inside the column, at different times, during the reaction experiment of Figure 4.4; (a) methanol, (b) acetaldehyde, (c) acetal and (d) water.

After the reaction experiment, which was indicated by the attainment of steady-state, the resin should be regenerated with the desorbent before starting the new experiment in order to reuse the resin repeatedly. Loaded adsorbent can be regenerated by temperature-swing or pressure-swing adsorption process and by displacement method. In some cases, the adsorbate can be extracted from adsorbent. During regeneration of fixed bed adsorber by displacement method, the adsorbate is removed from the adsorbent by displacement from active sites, which is due to adsorption of third material (the displacing agent). The choice of a suitable displacement agent depends both on the equilibrium of the system and on the kinetics of the adsorption and desorption. Here methanol was used as a desorbent for regeneration of the bed, as acetal and acetaldehyde are the weakly adsorbed species and are the first to be desorbed.

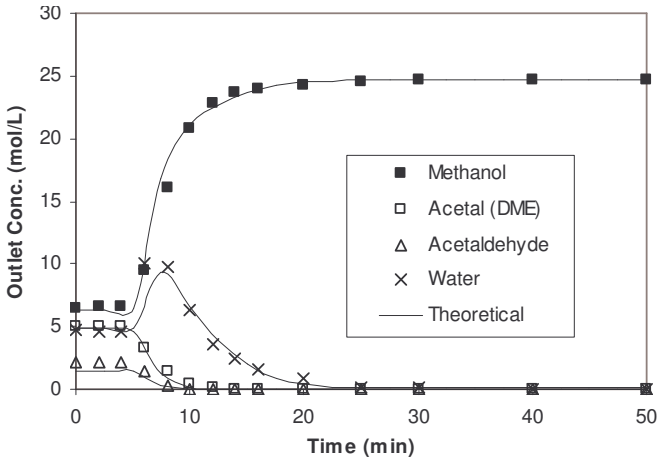

Figure 4.6: Concentration profiles in the regeneration step of a fixed bed adsorptive reactor. The initial profiles in the bed are those at the final steady state of the run in Figure 4.4.
Experimental conditions: Q = 6.0 mL/min (10 X 10^{-8} m^3/s),
$C_{A,F}$ = 24.683 mol/L and $C_{B,F}$ = 0.0 mol/L.
Experimental data: (■) methanol, (Δ) acetaldehyde, (□) acetal and (×) water.
Simulated results: continuous line.

Methanol was fed to the column in the top-down direction, as the reaction mixture present within the column is heavier than pure methanol. The outlet concentration of the column as the function of time is as shown in the Figure 4.6.

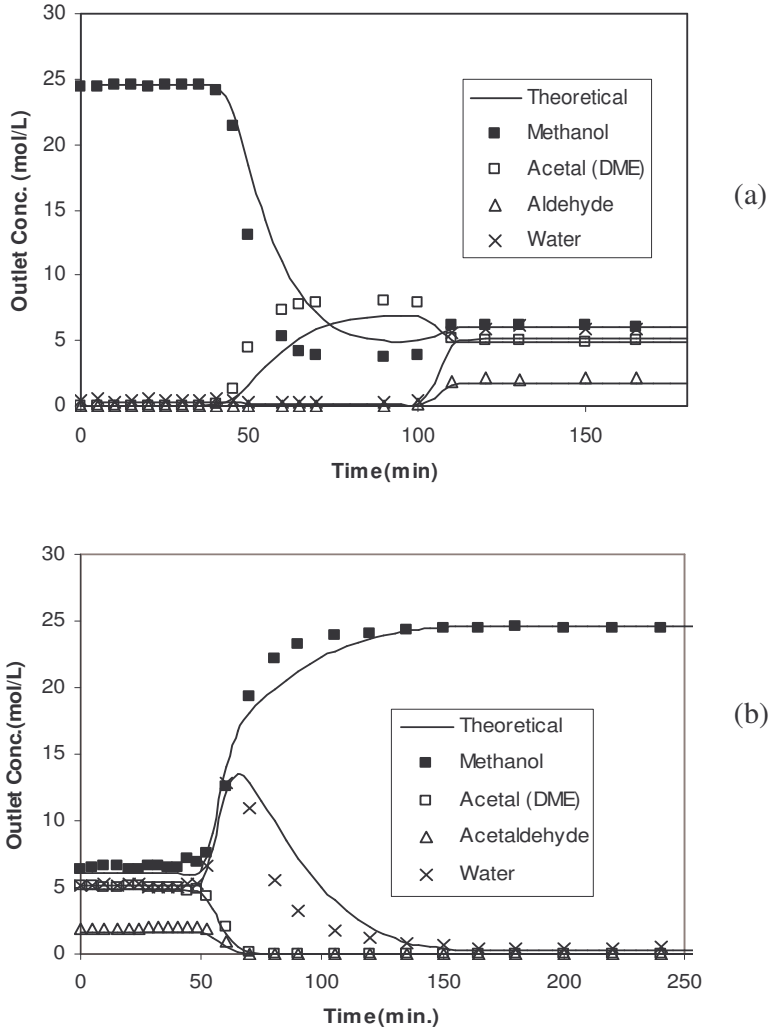

Figure 4.7: Concentration profiles in a fixed bed adsorptive reactor.
(a) Reaction Experimental conditions: Q = 6.0 mL/min (10 X 10^{-8} m^3/s), $C_{A,F}$ = 15.64 mol/L and $C_{B,F}$ = 6.48 mol/L; Bed Length: 86.0 Cm; Bed Diameter: 2.6 Cm; Bed Temperature: 20 ^oC;
Experimental data: (■) methanol, (△) acetaldehyde, (□) acetal and (×) water.
Simulated results: continuous line.
(b) Regeneration Experimental conditions: Q = 6.0 mL/min (10 X 10^{-8} m^3/s), $C_{A,F}$ = 24.683 mol/L and $C_{B,F}$ = 0.0 mol/L; Bed Length: 86.0 Cm; Bed Diameter: 2.6 Cm; Bed Temperature: 20 ^oC;
Experimental data: (■) methanol, (△) acetaldehyde, (□) acetal and (×) water.
Simulated results: continuous line.

In order to evaluate the effect of length of the reactor bed onto the behaviour of the fixed bed reactor/adsorptive reactor, another reaction and regeneration experiments were also performed with the longer bed in the column. From the results of the former reaction and regeneration experiments (shown in Figure 4.4 and Figure 4.6 respectively), it is expected that for a longer bed reactor, that the same qualitative behaviour will be found. The behaviour of the longer fixed bed reactor is shown in the Figure 4.7. The experimental outlet concentrations of the reactor along the time are in agreement with the simulated results.

4.6 Conclusions

The synthesis of acetal using acetaldehyde and methanol as raw-material on a Amberlyst-15 resin fixed bed adsorber/reactor was studied to determine the dynamic behaviour of acidic resin bed. The primary experiments conducted to collect the desired adsorption data by performing dynamic binary adsorption experiments in absence of reaction at 293.15 K, in a laboratory scale column. Minimizing the difference between the experimental and calculated stoichiometric times of breakthrough curves optimised the adsorption parameters. The mathematical model for the adsorptive reactor was developed, in which axial dispersion, external and internal mass-transfer resistances, constant temperature, and multicomponent Langmuir adsorption isotherms were measured on laboratory scale experimental set-up. The model was compared with the experimental results obtained for reaction and regeneration experiments.

4.7 Nomenclature

a – liquid phase activity

C – liquid phase concentration (mol/m^3)

C_i – bulk concentration of the i^{th} component (mol/m^3)

$\overline{C}_{P,i}$ – average concentration of i^{th} component into the particle (mol/m^3)

C_T – total liquid phase concentration (mol/m^3)

d_p – particle diameter (m)

Da – Damköehler number

D_{ax} – axial dispersion coefficient (m^2/s)

D_m – molecular diffusivity (m^2/s)

$D_{\underset{Am}{o}}$ – diffusion coefficient for a dilute solute A into a mixture (m^2/s)

k_c – kinetic constant (mol/g$_{res}$.s)

k_e – external mass transfer coefficient (m/s)

k_i – internal mass transfer coefficient (m/s)

K – Langmuir equilibrium parameter (m^3/mol)

K_{eq} – equilibrium constant

K_D – adsorption constant in equation 8

K_L – global mass transfer coefficient (m/s)

K_L^* – number of mass transfer units

L – bed length (m)

M – Molecular mass (g/mol)

Pe – Peclet number

q – solid phase concentration in equilibrium with the fluid concentration inside the particle (mol/m$^3_{res}$)

Q – adsorption capacity (mol/m$^3_{res}$)

r_P – average radius of particle

$\Re$ – rate of reaction relative to the surface concentration (mol/m^3_{res})

Re_P – Reynolds number relative to particle

Sh_P – Sherwood number relative to particle

Sc – Schmidt number

T – temperature (K)

t – time variable (s)

t_{st} – stoichiometric time defined in equation 22 (s)

u – superficial velocity of fluid in the column (m/s)

V_{ml} – molar volume in liquid phase (m^3/mol)

x_i – liquid phase molar fraction

z – axial coordinate (m)

Greek letters

γ – activity coefficient

ε – bed porosity

ρ_b – bulk density (kg_{res} /m^3)

ζ – dimensionless axial coordinate

θ – dimensionless time coordinate

η – effectiveness factor

μ – fluid viscocity (kg/m.s)

ρ – liquid density (kg/m^3)

ε_P – particle porosity

ν – stoichiometric coefficient

τ – tortuosity

Subscripts

$i-$ relative to component i $(i = A, B, C, D)$

$F-$ relative to feed

$0-$ relative to initial conditions

$p-$ relative to the surface of the particle

4.8 References

1. Agar, D. W. Multifunctional reactors: Old preconceptions and new dimensions. *Chem. Engg. Sci.* **1999**, 54 1299.
2. Bauer, K.; Garbe, D.; Surburg, H. *Common Fragrance and Flavor Materials*. 2nd Edition, Weinheim: VCH; 1990.
3. Chopade, S. P.; Sharma, M. M. Esterification of formic acid, acrylic acid and methacrylic acid with cyclohexene in batch and distillation column reactors: ion-exchange resins as catalysts. *React. Funct. Polym.* **1996,** 28, 263.
4. Chopade, S. P.; Sharma, M. M. Reaction of ethanol and formaldehyde: use of versatile cation-exchange resins as catalyst in batch reactors and reactive distillation columns. *React. Funct. Polym.* **1997,** 32, 53.
5. Dean, J.A., Lange's Hand Book Chemistry, 15th Edition, McGraw-Hill: New York, 1999.
6. Do, D. D. Adsorption Analysis: Equilibria and Kinetics. Imperial College Press, London, 1998.
7. Erik, F. G.; Jan, H. *Ketal derivatives of Imidazole*. U.S. Patent No. 3,575,999, **1971**.
8. Falk, T. Seidel-Morgenstern, A. Comparison between a fixed-bed reactor and a chromatography reactor. *Chem. Eng. Sci.* **1999,** 54, 1479.

9. Gmehling, J.; Wittig, R.; Lohmann, J.; Joh, R. A modified UNIFAC (Dortmund) Model. 4. Revision and Extension. *Ind. Eng. Chem. Res.* **2002,** 41, 1678.
10. Guinot, H.M. *Process for the Manufacture of Acetal*. U.S. Patent No. 1,850,836, **1932.**
11. Hideharu, I.; Masahiko, K.; Takash, O. *Process for producing acetals*. EP Patent No. 0771779, **1997**.
12. Hsu; Chao-Yang; Ellis, Jr.; Paul, E. *Process for the production and purification of diethoxymethane by azeotropic distillation*. U.S. Patent No. 4,613,411, **1986**.
13. Kawase, M.; Inoue, Y.; Araki, T.; Hashimoto, K. The simulated moving-bed reactor for production of bisphenol A. *Catal. Today,* **1999,** 48, 1-4.
14. Keith, A. M. W. *1-(Naphthylethyl)imidazole derivatives*. U.S. Patent No. 4,150,153, **1979**.
15. Kohlpaintner, C.; Schulte, M.; Falbe, J.; Lappe, P.; Weber, J. Aldehydes, aliphatic and araliphatic. *Ullmann's Encyclopedia of Industrial Chemistry,* 6th Edition, wiley-VCH, Verlag GmbH & Co. KGaA, **1999**.
16. Lode, F.; Houmard, M.; Migliorini, C.; Mazzotti, M.; Morbidelli, M. Continuous Reactive Chromatography *Chem. Eng. Sci.*, **2001,** 56, 269.
17. Lode, F.; Mazzotti, M.; Morbidelli, M. A New reaction-separation unit: The Simulated Moving Bed Reactor. *Chimia* **2001,** 55, 883.
18. Lohmann, J.; Wittig, R.; Gmehling, J. Vapor-Liquid Equilibrium by UNIFAC Group Contribution. 6. Revision and Extension. *Ind. Eng. Chem. Res.* **2003**, 42, 183.
19. Mazzotti, M.; Kruglov, A.; Neri, B.; Gelosa, D.; Morbidelli, M. A continuous chromatography reactor:SMBR. *Chem. Eng. Sci.* **1996**, 51, 1827.

20. Mazzotti, M.; Neri, B.; Gelosa, D.; Morbidelli, M. Dynamics of a Chromatographic Reactor: Esterification Catalyzed by Acidic Resins. *Ind. Eng. Chem. Res.*, **1997**, 36, 3163-3172.
21. Merck Index, 12th Edition, 1996.
22. Morrison, R.; Boyd, R. *Organic Chemistry*. 4th Edition, Allyn and Bacon: London, 1983.
23. Perry's Chemical Engineers Handbook, 6th Edition, McGraw-Hill, New York 1984.
24. Reid, R. C.; Prausnitz, J. M.; Poling, B. E. *The properties of gases and liquids.* 4th Edition, McGraw-Hill, New York, 1987.
25. Ruthven, D. M. *Principles of Adsorption and Adsorption Processes*. John Wiley & Sons, New York, 1984.
26. Sardin, M.; Schweich, D.; Villermaux, J. Preparative fixed-bed Chromatographic Reactor, in *Preparative and production scale Chromatography* , Marcel Dekker, New York, 1993.
27. Silva, V. M. T. M. *Diethylacetal Synthesis in Simulated Moving Bed Reactor.* PhD Thesis, Faculty of Engineering, University of Porto, Porto, Portugal, 2003.
28. Silva, V. M. T. M.; Rodrigues, A. E. Dynamics of Fixed-Bed Adsorptive Reactor for the Synthesis of Diethylacetal. *AIChE J.* **2002,** 48, 625.
29. Smith, J. M.; Van Ness, H. C. *Introduction to chemical engineering thermodynamics.* 4th Edition, McGraw-Hill, New York, 1987.
30. Smith, Jr. L. A.; Arganbright, R. P. *Process for making Acetals*. U.S. Patent 6,015,875, **2000**.

31. Teja, A. S.; Rice, P. Generalized corresponding states method for the viscosities of liquid mixtures. *Ind. Eng. Chem. Fundam.* **1981**, 20, 77.

32. Waller, F. J.; Weist, Jr. E. L.; Brown, D. M; Tijm, P. J. A. *Diesel fuel composition comprising dialkoxy alkanes for increased cetane number*. U.S. Patent 5,858,030, **1999**.

33. Wankat, P. C. Rate-Controlled Separation. Blackie Academic & Professional, London 1994.

34. Yadav, G. D.; Pujari, A. A. Kinetics of acetalization of perfumery aldehydes with alkanols over solid acid catalysts. *Canadian Journal of Chemical Engineering*, **1999**, 77, 489.

5. Dimethylacetal Synthesis with Smopex Fibres as Catalyst and Adsorbent

The synthesis of dimethylacetal using acetaldehyde and methanol as raw-material in presence of Smopex 101 fibres as catalyst and adsorbent in batch reactor and in a fixed bed adsorptive reactor, respectively, is studied. In the batch reactor the determination of thermodynamic and reaction kinetics data is presented in order to compare the results with those obtained for Amberlyst 15 resin as catalyst. A kinetic model based on a Langmuir-Hinshelwood rate expression using activities was proposed to describe the experimental kinetic results. The dynamic binary adsorption experiments were carried out in absence of reaction at 293.15 K in a laboratory scale column. The experimental results of the adsorption of binary non-reactive mixtures are reported and used to obtain multicomponent adsorption equilibrium isotherms of Langmuir type. The mathematical model was proposed to describe the adsorptive reactor dynamic behaviour. The experimental results obtained for the reaction and regeneration experiments were compared with the model proposed. Model equations were solved by orthogonal collocation on finite elements (OCFE) implemented by the PDECOL package, using the measured model parameters and was validated for both reaction and regeneration steps.

5.1 Introduction

The reaction between an alcohol and aldehydes to form an acetal and water is of considerable industrial interest. Acetals are important class of chemicals having applications in a variety of areas in the chemical industry such as perfumes, flavors, pharmaceuticals, plasticizer, solvents and intermediates (Aizawa et al., 1994; Bauer et al., 1990; Gupta, 1987).

Catalysts are extremely important materials of commerce. Most of the industrial reactions pertaining to the chemical, petrochemical, and pharmaceutical sector and almost all-biological reactions are catalytic in nature. Products like food, clothing, drugs, fuels etc., which drive today's economy involve catalysis in some way or the other. Catalysts also form an integral part of environmental protection and emission control strategies. Majority of chemical reactions use catalysts to enhance the reaction rates in order to obtain the desired products in an economical way. Catalysts in general are classified in two types, depending on the phase in which the catalyst is present. Homogeneous catalysts, in which reactants, products as well as catalyst are present in a single phase, and heterogeneous catalysis in which, the catalyst is present in a different phase than that of the reactants. Typical homogeneous catalysts are mineral acids, such as H_2SO_4, HCl, HI and $ClSO_3OH$. The use of homogeneous catalysts leads to several problems such as corrosion of equipment, hazardous of handling the corrosive acids, which are not reused, neutralization of the resulting reaction mass, and generation of large quantities of dilute dissolved salts, including loss of conversion, yield and selectivity. The biological oxygen demand (BOD), chemical oxygen demand (COD) and total dissolved solids (TDS) loads on effluent treatment plants become enormous. Ultimately the disadvantage of using homogeneous catalyst is their miscibility with the

reaction mixture, which causes separation problems; therefore, heterogeneous catalyst provides an attractive alternative to homogeneous catalysts.

Several reviews have recently been published dealing with the use of solid acids as heterogeneous catalysts for the preparation of specialty and fine chemicals. Heterogeneous catalysts have been developed in order to avoid separation problems; a catalyst-free product can be easily obtained by filtration (Kekre and Gopal Rao, 1969). There exists many solid catalysts; such as Iodine (Ramalinga, 2002), Zeolite-T membrane (Tanaka, 2001), ZSM-5 (Yadav & Krishnan, 1998; Ma et al., 1996), HY Zeolite (Ma et al., 1996), Zeolite beta (Silva-Machado et al., 2000), acid treated clays (Yadav and Krishnan, 1998), heteropolyacids (Yadav and Krishnan, 1998; Schvegher and van Bekkum, 1991; Lacage-Dufaure and Moulougui, 2000; Dupont et al., 2002). Ion exchange resins however, are the most commonly used solid catalysts and they have been proved to be effective in liquid phase acetalization (Gandi et al, 2005; Silva and Rodrigues, 2001; Fedriani et al, 2000; Yadav and Pujari, 1999; Chopade and Sharma, 1996, 1997; Roy and Bhatia, 1987). Typical resin catalysts are sulphonic acids fixed to polymer carriers, such as polystyrene cross-linked with divinylbenzene (DVB). Solid ion-exchange resins as catalyst have several advantages; the catalyst can be removed from the reaction mixture, continuous operation in column reactors is enabled, the product purity is high (Chopade and Sharma, 1996).

The complication in heterogeneous catalyst compared with homogeneous catalysis arises from the complex nature of the heterogeneous process, which includes adsorption, desorption and as well as several surface reaction steps (Doraiswamy and Sharma, 1987). However, application of adsorption, desorption and surface reaction relationships to heterogeneous catalyzed reactions is of particular interest, since it is

possible to obtain information on the reactivity of molecules in a specific reaction. Particularly analysis of kinetic and thermodynamic results can improve the knowledge of the reaction mechanisms on solid catalysts as well as the nature of the active sites of the solid catalysts.

Specific advantage of fibre catalyst is due to negligible diffusional paths, which provide high catalyst efficiency and excellent separation abilities. The novel polymer-supported fibre catalyst (Smopex-101, Smoptech Ltd., Finland) can be used in various industrially relevant heterogeneous reactions, such as esterification (Maki-Arvela et al., 1990; Lilija et al., 2002a, 2002b), etherfication (Kriner and Krause, 2001), aldolisation and hydrogenation (Aumo, 2002). The polyethylene-based fibre catalyst can be modified by grafting different functional groups, such as pyridine, carboxylic acid, and sulphonic acid or a combination of them. In this way homogeneous catalysts can be replaced by fibre catalysts

The conversion in acetalization reaction is limited by the chemical equilibrium; therefore the technology for the industrial preparation of acetals involves two consecutive steps in order to increase the capacity of the product formation. The first step is the reaction itself, which stagnates as the equilibrium is approached. The second one is the separation of products from the reaction mixture at equilibrium containing both products and reactants. The disadvantage of this two-steps procedure for operating equilibrium reactions is in its economics, because of the high energy costs and the use of different reactors and separators.

The objective of this present work to demonstrate the application of polymer supported sulphonic acid catalyst, Smopex 101 (Smoptech Ltd., Finland) in acetalization reaction of methanol and acetaldehyde to study the acetalization kinetics

and thermodynamics and thereafter to study the dynamic behavior of acetalization reaction in a fixed bed chromatographic reactor packed with Smopex 101 fibres.

5.2 Chemicals used

Acetaldehyde and acetaldehyde from Sigma-Aldrich were used in this work in order to produce acetal (DME). The authentic sample of acetal (DME) was also used for calibration of Gas Chromatography from Sigma-Aldrich. While using acetaldehyde and acetal, precautions to be taken as per the instructions given in the Appendix A.

5.3 Catalyst and Adsorbent

Smopex 101 was used in this present work. Smopex-101 was obtained from Smoptech Ltd (Johnson Matthey Company) Finland, Smopex-101 is a poly (ethylene) based fibre that is grafted with styrene, which is sulphonated with chloro-sulfonic acid. This Smopex-101 fibres is used as catalyst and as well as an adsorbent in this present work. The physical properties of Smopex-101 fibres are given in the Table 5.1 which are reported by Smoptech, Finland. The fibrous polymer-supported sulphonic acid catalyst (Smopex-101) was investigated with SEM (Scanning Electron Microscopy); typical SEM images are shown in Figure 5.1 (a-c), 5.2 and 5.3. The figures reveal the mean fibre diameter and average length of the Smopex-101 and their physical appearance. From Figures 5.2 and 5.3, it is clear that there exists no pores in the fibres; naturally diffusional resistances can be negligible which can improve the catalyst efficiency.

Table 5.1 Physical properties of Smopex-101

Property	Smopex-101
Physical state	Fibres
Color	Yellow
pH	Acidic in water
Solubility in water	Insoluble
Mean Fibre diameter	12.1 μm
Average length	0.25 mm
Bulk density (packed bed)	410 ± 10 Kg/m^3
Fibre capacity	2.9 mmol/g

Figure 5.1 a SEM Image of the Smopex-101 Fibres
Fibres Length & Diameter = 0.25mm & 12 μm

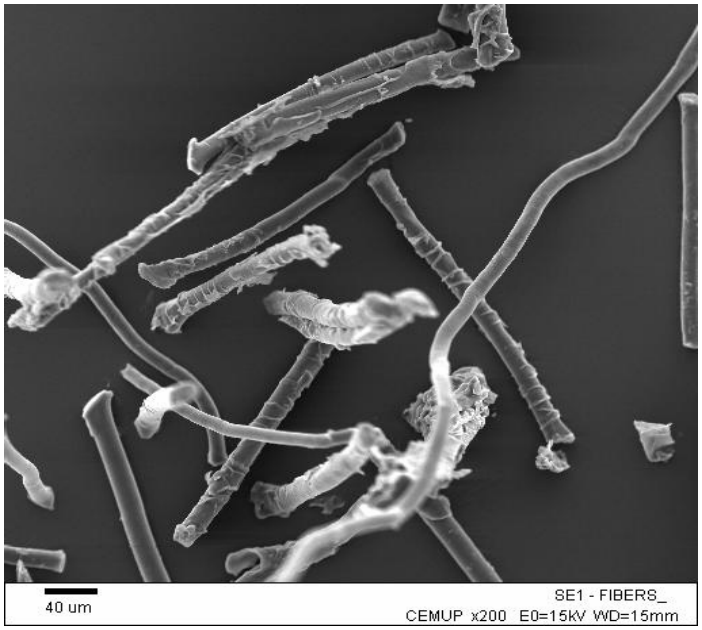

Figure 5.1b SEM Image of the Smopex-101 Fibres
Fibres Length & Diameter = 0.25mm & 12 μm

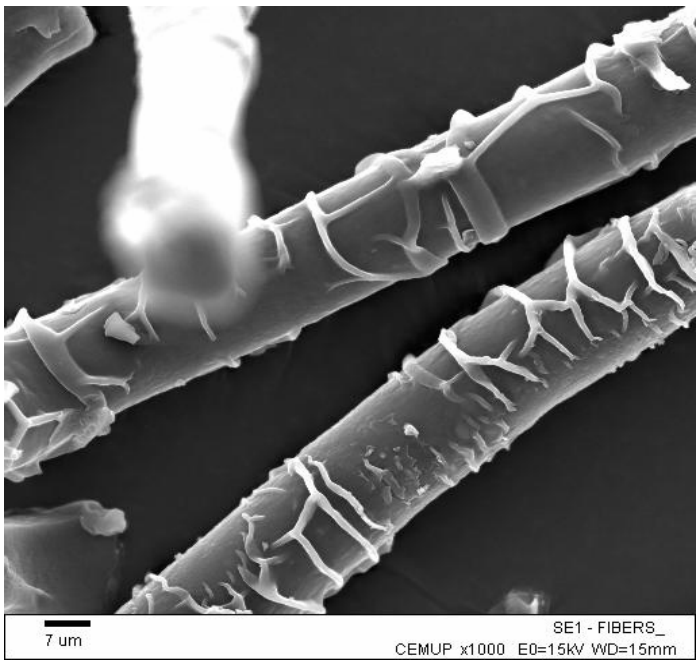

Figure 5.1 c: SEM Image of the Smopex-101 Fibres;
Fibres Length & Diameter = 0.25mm & 12 μm

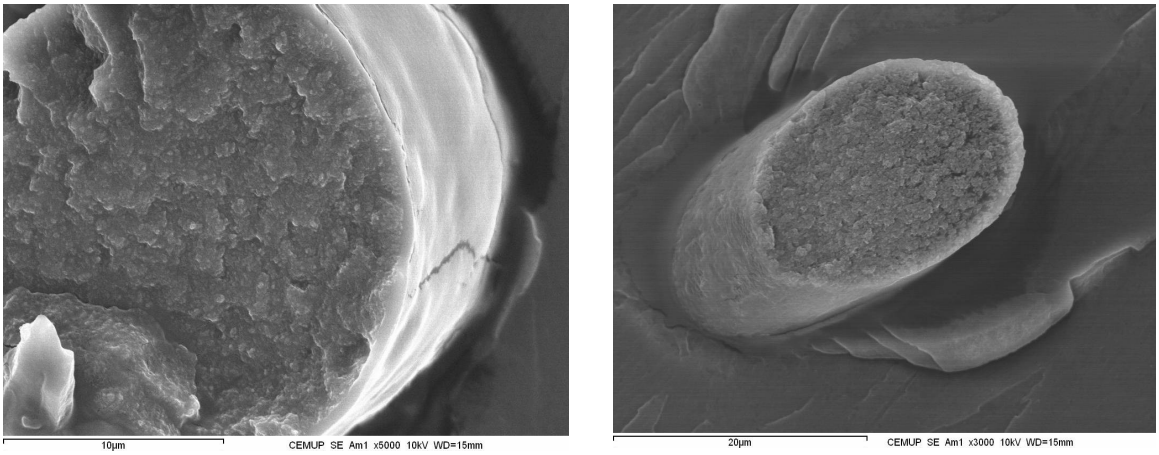

Figure 5.2: SEM Image of the Smopex-101 Fibres cross section;
Fibres Length & Diameter = 0.25mm & 12 µm

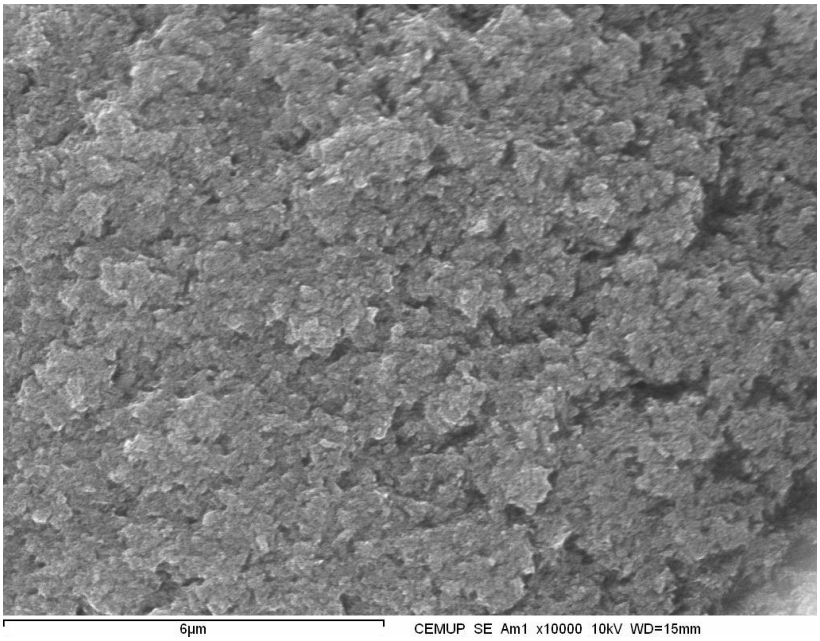

Figure 5.3: SEM Image of the Smopex-101 Fibres cross section;
Fibres Length & Diameter = 0.25mm & 12 µm

5.4 Batch Reactor

5.4.1 Experimental set-up

The experimental set-up in which acetal (DME) is produced with the acetalization reaction of acetaldehyde and methanol was shown in the below Figure 5.4. The detailed information of the experimental set-up was given in the Section 3.2.1 of Chapter 3.

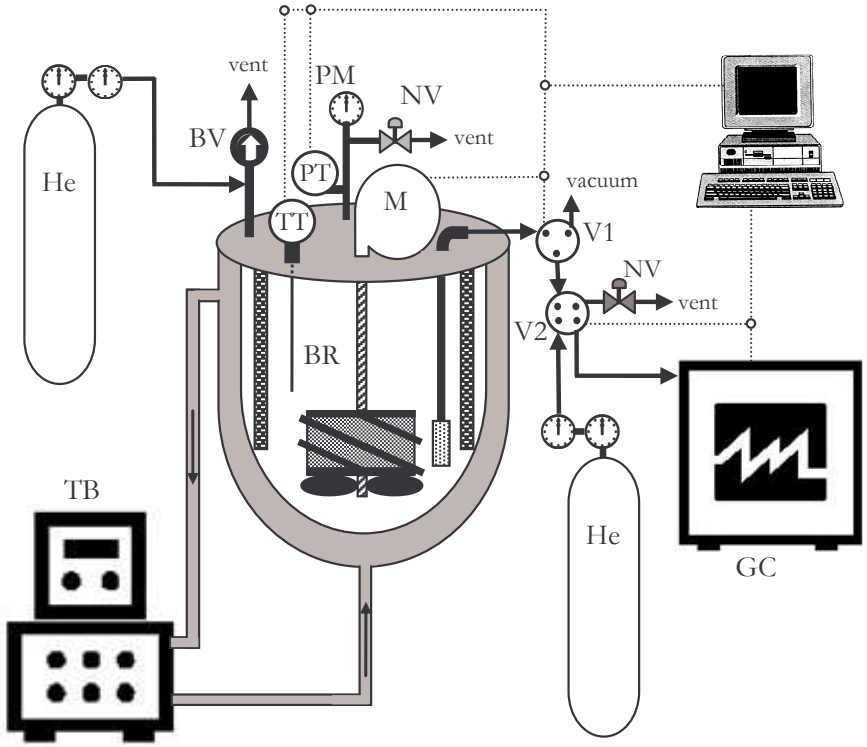

Figure 5.4: Image of the Batch Reactor Experimental Set-up

BR-batch reactor; M-motor; TT-temperature sensor; PT-pressure sensor; PM-manometer; BV-blow-off valve; V1-sampling valve; V2-injection valve; NV-needle valve; GC-gas chromatograph; TB-thermostatic bath.

5.4.2 Method of Analysis

The analysis of reactants and products was carried out using Gas chromatography. The Gas Chromatography used for analysis was from Chrompack

model Chrompack 9100 (Netherlands). The compounds were separated in a fused silica capillary column (Chrompack CP-wax 57 CB), 25 m X 0.53 mm ID, df = 2.0 using a thermal conductivity detector (TCD 903 A) for detection of peak separation of reactants and products. The conditions used for the sample analysis are presented in the below Table 3.2. The column temperature was programmed with a 2 min initial hold-up at 50 ^{o}C, followed by 40 ^{o}C/min increase in temperature up to 100 ^{o}C and then hold again for 1 min. The carrier gas used was helium at 20 ml/min.

5.4.3 Smopex-101 conditioning

The catalyst Smopex-101 should be conditioned before use in order to guarantee the anhydrous fibres. It may be convenient to rinse off water from the fibre by another solvent (can be ethanol or methanol). By placing wet Smopex-101 fibres in a column and allowing 2.5 to 3.0 bed volumes of ethanol or methanol to percolate through the fibres over a period of one hour, most of the water presented can be removed with this method to maximum extent. Finally, the fibres were dried at 90 to 100 ^{o}C for 5 hours in order to dry the traces of water present in the fibres. This procedure of drying the catalyst was adopted, as water adsorbed on the surface of catalyst decreases the reaction kinetics as water itself is one of the products in the acetalization reactions. Before performing the reaction experiments, the dried fibres were cooled in a desiccator in order to avoid moisture adsorption on the surface of the fibres catalyst.

5.4.4 Reaction Thermodynamics

As it is known that, the thermodynamic quantities play an important role in the design or scale-up of chemical reactors, it is necessary to determine enthalpy change of the reaction and equilibrium constant at different temperatures of the reaction. The

temperature dependency of equilibrium constant can be determined from the Van't Hoff equation:

$$\ln K_{eq} = \frac{\Delta S^o}{R} - \frac{\Delta H^o}{R}\frac{1}{T} \tag{5.1}$$

Hence, in this present work to determine values of equilibrium constant, experiments at several temperatures were performed. The standard enthalpy change of acetal (DME) was determined and compared with the values obtained in the Chapter 3. All the experiments to measure the equilibrium constant for this reversible acetalization liquid phase reaction were performed in a temperature range of 283 to 313 K at 0.6 MPa pressure with Smopex-101 fibres catalyst. The reactants mixture volume is about 600 mL and the initial molar ratio of reactants (methanol/acetaldehyde) is the stoichiometric; $r_{A/B}$ = 2.0. All experiments lasted long enough (3 hours) for the reaction to reach equilibrium. Average molar fractions after attaining equilibrium were represented in the Table 5.2 at different temperatures.

Table 5.2 Experimental Equilibrium compositions expressed in molar fractions.

T(K)	283.15	293.15	303.15	313.15
x_{A_e}	0.3082	0.3134	0.3159	0.3346
x_{B_e}	0.1294	0.1310	0.1521	0.1606
x_{C_e}	0.2812	0.2778	0.2660	0.2524
x_{D_e}	0.2812	0.2778	0.2660	0.2524

The non-ideal system was considered to determine the thermodynamic equilibrium constant at different temperature for liquid phase reaction of acetaldehyde and methanol and is given by the below mentioned equation:

$$K_{eq} = \frac{a_{C_e} \times a_{D_e}}{a_{A_e}^2 \times a_{B_e}} = \frac{x_{C_e} \times x_{D_e}}{x_{A_e}^2 \times x_{B_e}} \times \frac{\gamma_C \times \gamma_D}{\gamma_{A_e}^2 \times \gamma_B} = K_x \times K_\gamma \tag{5.2}$$

The number of moles of each component in the reaction mixture at equilibrium for different temperatures was determined from the liquid molar volumes estimated with Gunn-Yamada method (Reid et al., 1987) and is given in the Table 5.3.

Table 5.3: Number of moles at Equilibrium.

T (K)	283.15	293.15	303.15	313.15
n_A	3.2115	3.2230	3.2753	3.3694
n_B	1.3484	1.3472	1.5770	1.6670
n_C	2.9302	2.8569	2.7579	2.6199
n_D	2.9302	2.8569	2.7579	2.6199

The activity coefficients of compounds, γ, were computed by UNIFAC method (Fredeslund et al., 1977). The UNIFAC parameters of pure species are taken from Tables 3.10 and 3.11. The activity coefficients of all species in the reaction mixture at equilibrium are given in the Table 5.4 at different temperatures.

Table 5.4 Activity coefficients of species at equilibrium for different temperatures.

T (K)	283.15	293.15	303.15	313.15
γ_A	0.8588	0.8727	0.8625	0.8725
γ_B	0.4845	0.5042	0.5500	0.5675
γ_C	1.1792	1.1859	1.1984	1.2081
γ_D	1.2885	1.3175	1.3442	1.3692

The equilibrium constant in terms of molar fractions and activity coefficients are given in Table 5.5.

The dependency of equilibrium constant on temperature was estimated by fitting the experimental values by plotting $\ln K_{eq}$ vs. $1/T$ to Eq. (5.1), where the equilibrium

Table 5.5 Equilibrium Constants at different temperatures

T (K)	283.15	293.15	303.15	313.15
K_x	6.4283	5.9979	4.6616	3.5431
K_γ	4.2520	4.0688	3.9372	3.8289
K_{eq}	27.3332	24.4040	18.3535	13.5661
Ln K_{eq}	3.3081	3.1948	2.9098	2.6076

constant was calculated w.r.t. activity coefficient as shown in Figure 5.5 and is given by the equation and is as follows;

$$\ln K_{eq} = \frac{2103.3}{T(K)} - 4.0595 \tag{5.3}$$

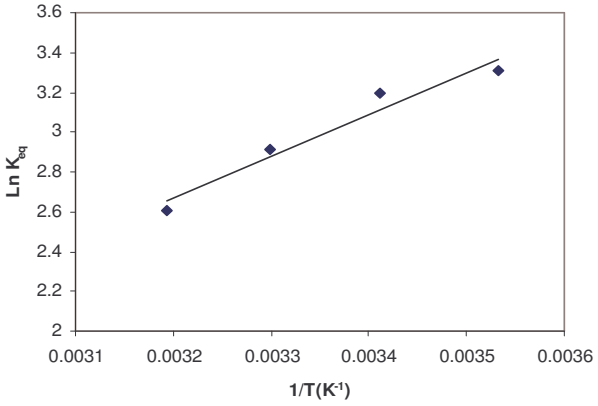

Figure 5.5 Experimental and theoretical values plot for $\ln K_{eq}$ *vs* $1/T(K^{-1})$.

From the slope and the intercept of the above Figure 5.5, it is obtained the standard entropy ($\Delta S^o = -33.75$ J mol^{-1} K^{-1}) and enthalpy of formation ($\Delta H^o = -17.49$ kJmol^{-1}). The standard free energy change for the liquid phase reaction can be related to the standard enthalpy and entropy change by:

$$\Delta G^o = \Delta H^o - T \times \Delta S^o \tag{5.4}$$

Leading to $\Delta G^o = -7.4$ kJ mol^{-1}.

The standard properties determined above are in agreement with the results obtained in the Section 3.3 of Chapter 3.

5.4.5 Reaction Kinetics

The experimental data consisting of 14 batch experiments. Some experiments were performed to test the reproducibility of the thermodynamic data. All the experiments were evaluated carefully prior to the kinetic modeling. The experimental data and experimental conditions of all experiments performed in the batch reactor are represented in the Table 5.6.

5.4.5.1 Effect of Temperature

All experiments were carried out at almost constant temperature. The maximum variation of 1.5 ^{o}C was noticed during the initial stage of reaction, and then decreased to desired temperature. Figure 5.6 shows four experiments performed at different temperatures: 10 ºC, 20 ºC, 30 ºC, and 40 ºC, with respect to experiments 1, 2, 3 and 4, respectively as mentioned in Table 5.6. The rate of reaction increased with the increase of temperature, even though the equilibrium conversion decreased due to the exothermic nature of reaction, limiting reactant acetaldehyde conversion was plotted along the time of reaction is shown in the Figure 5.6.

Table 5.6 Summary of the acetaldehyde and methanol system experiments for DME synthesis.

Run No.	Catalyst Loading (g)	Speed of Agitation (rpm)	Reaction Temp. (°C)	Reaction Pressure (atm)	Methanol Conc. (mol/L)	Aldehyde Conc. (mol/L)	Initial Molar Ratio
1	0.50753	600	10.0	6.0	14.65	7.26	2.023
2	0.50852	600	20.0	6.0	14.86	7.34	2.025
3	0.50934	600	30.0	6.0	14.64	7.25	2.021
4	0.50353	600	40.0	6.0	14.67	7.25	2.024
5	0.50431	600	20.0	6.0	16.92	5.61	3.016
6	0.50560	600	20.0	6.0	18.36	4.57	4.018
7	0.50407	600	20.0	6.0	12.84	8.54	1.504
8	0.50648	600	30.0	6.0	17.39	5.66	3.072
9	0.50531	600	30.0	6.0	18.48	4.56	4.053
10	0.50115	600	40.0	6.0	16.88	5.66	2.982
11	0.50327	600	40.0	6.0	18.35	4.57	4.015
12	0.25620	600	20.0	6.0	14.71	7.31	2.012
13	0.75734	600	20.0	6.0	14.79	7.32	2.021
14	1.01180	600	20.0	6.0	14.89	7.29	2.043

5.4.5.2 Effect of Initial Reactants Molar Ratio $r_{A/B}$

The effect of initial molar ratio of reactants methanol (A) and acetaldehyde (B), $r_{A/B}$ on acetaldehyde conversion is addressed. The experiments 2, 5, 6 and 7 were performed with different initial molar ratio of reactants methanol to acetaldehyde (2:1, 3:1, 4:1 and 1.5:1) and its influence on the time evolution of the acetaldehyde conversion and number of moles

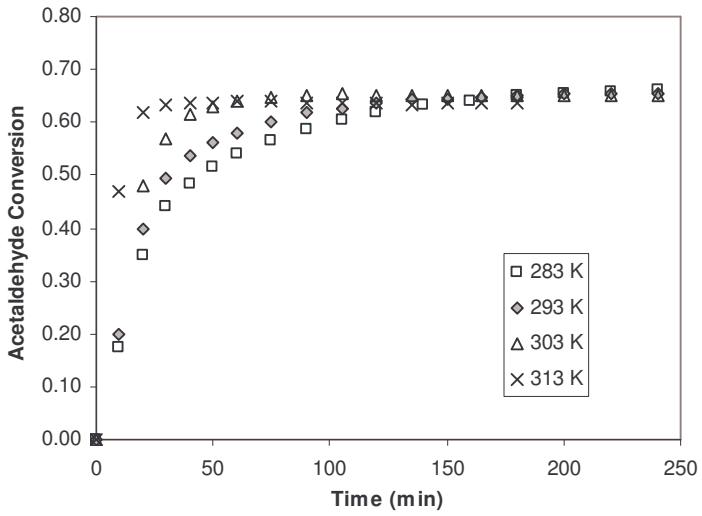

Figure 5.6: Effect of temperature on conversion of acetaldehyde as function of time: $soa = 600\,\text{rpm},\ P = 6\ atm,\ V = 600\ \text{mL},\ w_{cat} = 0.50\,\text{g},\ r_{A/B} = 2.0$.

of dimethoxyethane produced is shown in Figures 5.7 and Figure 5.8 respectively. The higher the excess of alcohol (methanol), the higher is the final conversion of the acetaldehyde. The use of excess alcohol is typical in order to shift the equilibrium towards the product formation. The kinetics was not too affected by the initial molar ratio of reactants; but the amount of dimethylacetal produced is higher for the stoichiometric ratio $r_{A/B} = 2$.

5.4.5.3 Effect of Catalyst loading

The catalyst loading was varied over a range of 0.042 % w/V to 0.167 % w/V on the basis of amount of total volume of reactants taken initially were studied maintaining all other reaction conditions constant. The effect of catalyst loading (runs 1, 12, 13 and 14) on the conversion of acetaldehyde is as shown in the Figure 5.9. As is typical for all heterogeneous reactions, the conversion is found to increase with increasing catalyst

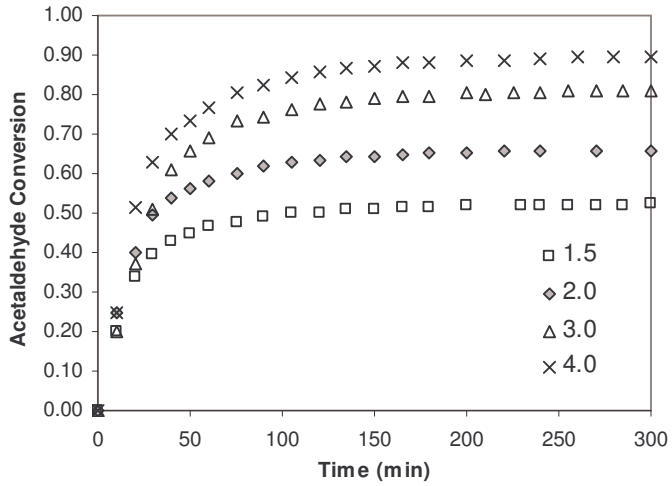

Figure 5.7: Effect of Initial Molar Ratio of Reactants $r_{A/B}$ (methanol/acetaldehyde) *on the acetaldehyde conversion as function of time:* $T = 293.15K$, $P = 6\ atm$, $V = 600$ mL, $w_{cat} = 0.5$ g, $soa = 600$ rpm.

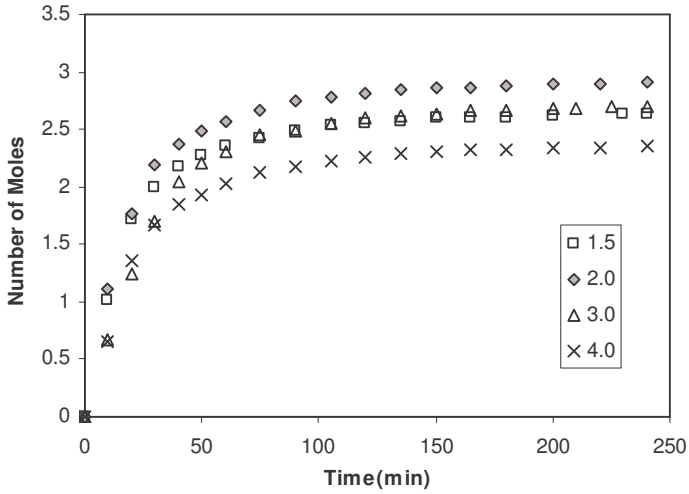

Figure 5.8 Effect of Initial Molar Ratio of Reactants $r_{A/B}$ (methanol/acetaldehyde) *on the number of moles of DME* (n_{DME}) *produced as function of time:* $T = 293.15K$, $P = 6\ atm$, $V = 600$ mL, $w_{cat} = 0.5$ g, $soa = 600$ rpm

loading but the increase is marginal; hence the overall rate of reaction increases with the catalyst loading. This is due to the increasing of the total number of acidic sites available (Chopade and Sharma, 1997).

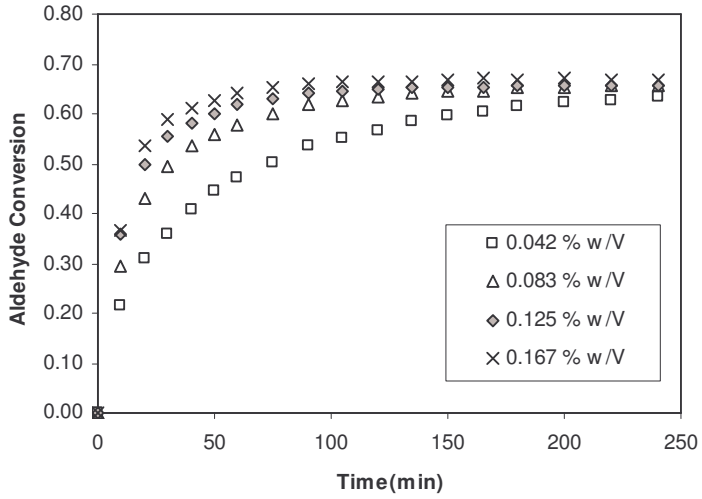

Figure 5.9: Effect of Catalyst Loading on acetaldehyde conversion as function of time:

$T = 293.15\,K$, $P = 6\ atm$, $V = 600$ mL, $soa = 600$ rpm. $r_{A/B} = 2.0$

5.4.6 Kinetic Modeling

Because of the great industrial importance of catalytic reactions, considerable effort has been spent in developing theories from which kinetic equations can rationally be developed. The kinetic model for the production of acetal from methanol and acetaldehyde is given on the basis of the below mentioned steps. The most useful for our purposes suppose that the reaction takes place on an active site on the surface of the catalyst. Here with this Smopex-101 catalyst, it can be considered that the reaction is taking place on the active sites on the surface of the catalyst due to the absence of the pores in the catalyst. Thus three steps are viewed to occur successively at the surface of the catalyst:

Step 1: A molecule is adsorbed onto the surface and is attached to an active site on the catalyst

Step 2: It then reacts either with another molecule on an adjacent site with one coming from the main stream or it simply decomposes while on the site.

Step 3: Products are desorbed from the surface, which then frees the site.

Here in this case, all species of molecules, free reactants (acetaldehyde and methanol), and free products (acetal and water) as well as site-attached reactants, intermediates and products taking part in these above three steps are assumed to be in equilibrium. Rate expressions derived from various postulated mechanisms are all of the form;

$$rate\ of\ \ reaction = \frac{(kinetic\ term)(driving\ \ force\ or\ displacement\ \ from\ equilibrium)}{resistance\ \ term} \qquad (5.5)$$

Reaction rate proposed previously in our Laboratory of separation and reaction engineering (LSRE) (Silva and Rodrigues, 2001) for the acetaldehyde and ethanol reaction on the surface of the catalyst and is given in the Eq. (5.6);

$$\Re = k_c \frac{a_A a_B - \frac{a_C a_D}{K_{eq} a_A}}{\left(1 + \sum_{i=A}^{D} K_{S,i} + K_{I_1} a_A a_B + K_{I_2} \frac{a_C}{a_A}\right)^2} \qquad (5.6)$$

Several rate equations derived from Eq. (5.6) were tested, in order to reduce the number of optimization parameters, the best fitting was obtained by considering that all the species in the reaction mixture adsorbed on the catalyst is negligible. The simplified reaction rate equation is then given by:

$$\Re = k_c\left(a_A a_B - \frac{a_C a_D}{K_{eq} a_A}\right) \tag{5.7}$$

The kinetic model contains only one parameter k_C (kinetic constant), which can be obtained by the optimization.

5.4.6.1 Parameter estimation

In order to estimate the kinetic parameter k_C of the Eq. (5.7), the mass balance in a batch reactor for acetal production, in the liquid phase, at constant temperature (isothermal process) is considered. The mass balance is given as follows:

$$\frac{dn_C}{dt} = w_{cat} r \tag{5.8}$$

Where n_C is the number of moles of acetal, *t* is the time, w_{cat} is the mass of catalyst and *r* is the reaction rate referred to the catalyst mass.

The number of moles of component *i* (n_i) as a function of the conversion *X* of the limiting reactant (*l*) is given by the Eq. (5.9);

$$n_i = n_{l,0}\left(r_{i/l} + \nu_i \frac{X}{|\nu_l|}\right), \tag{5.9}$$

where $n_{l,0}$ and ν_l are, respectively, the initial moles number and the stoichiometric coefficient of the limiting reactant and,

$$r_{i/l} = \frac{n_{i,0}}{n_{l,0}} \tag{5.10}$$

$n_{i,0}$ is the initial number of moles of component *i*.

Introducing Eq. (5.9) into Eq. (5.8) we can get the relation as follows:

$$\frac{n_{l,0}}{w_{cat}|\nu_l|}\frac{dX}{dt} = \Re(a_A, a_B, a_C, a_D, T, P), \tag{5.11}$$

where $\Re$ is given by Eq. (5.7) and the initial condition of Eq. (5.11) is $t = 0;\ X = 0$.

The suggested reaction rate was fitted, at each temperature, to the experimentally measured rates of reaction. The estimation of model parameter k_C was carried out with a non-linear regression subroutine DR8LIN (IMSL, 1991) that uses the Levenberg-Marquardt method to minimize the sum of residual squares (*SRS*) between the experimental and calculated rate of reaction:

$$SRS = \sum(\Re_{\exp} - \Re_{theo})^2 \tag{5.12}$$

The theoretical reaction rate ($\Re_{theo}$) is expressed by the r.h.s. of Eq. (5.11) and the experimental rate of reaction ($\Re_{\exp}$) is expressed by the l.h.s. Figure 5.11, Figure 5.12 and Figure 5.13 shows the comparison between experimental and simulated results for acetaldehyde, methanol and products (acetal and water) at 293.15, 303.15 and313.15 K, respectively. The average standard error between the experimental and simulated molar fractions of all species is 2.0 %. The values of the kinetic parameter k_C used in the simulations are presented in Table 5.7. The temperature dependence of the kinetic constant was fitted with the Arrhenius equation (Figure 5.10).

Table 5.7 The kinetic parameters.

Temperature (K)	k_C (mol/g/min)
293.15	1.67
303.15	2.915
313.15	5.992

The energy of the activation Arrhenius plot was calculated to be 48.67 kJ/mol (Figure 5.10). The kinetic parameter is given below:

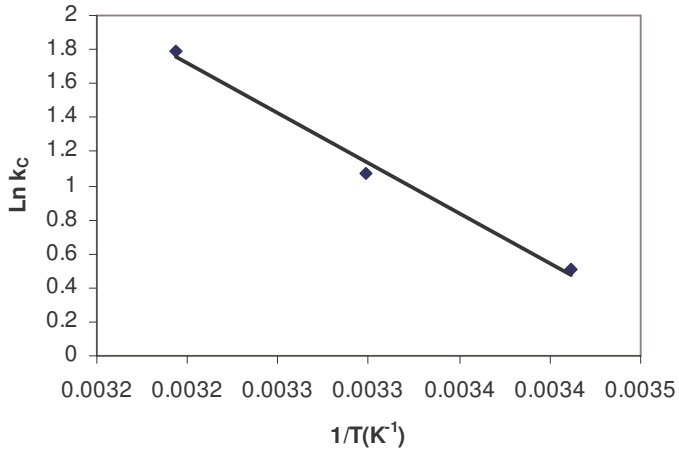

Figure 5.10 Experimental representation of ln k as function of 1/T along with linear fitting with respect to kinetics parameters.

$$k_c = 7.59\times10^{8}\exp\left[\frac{-5853.8}{T(K)}\right](\text{mol g}^{-1}\text{ min}^{-1}); \qquad R^2 = 0.9914 \tag{5.13}$$

The kinetic model is in agreement with experimental results for the range of initial molar ratio of reactants from 1.5 to 4.0 and at the temperature range 293.15-313.15 K. The comparison of experimental and theoretical (true kinetics) data plots for different initial molar ratio of reactants at 293.15 K (runs 2, 5, 6 and 7), at 303.15 K (runs 3, 8 and 9) and at 313.15 K (runs 4, 10 and 11) are shown in Figures 5.11, 5.12 and 5.13, respectively.

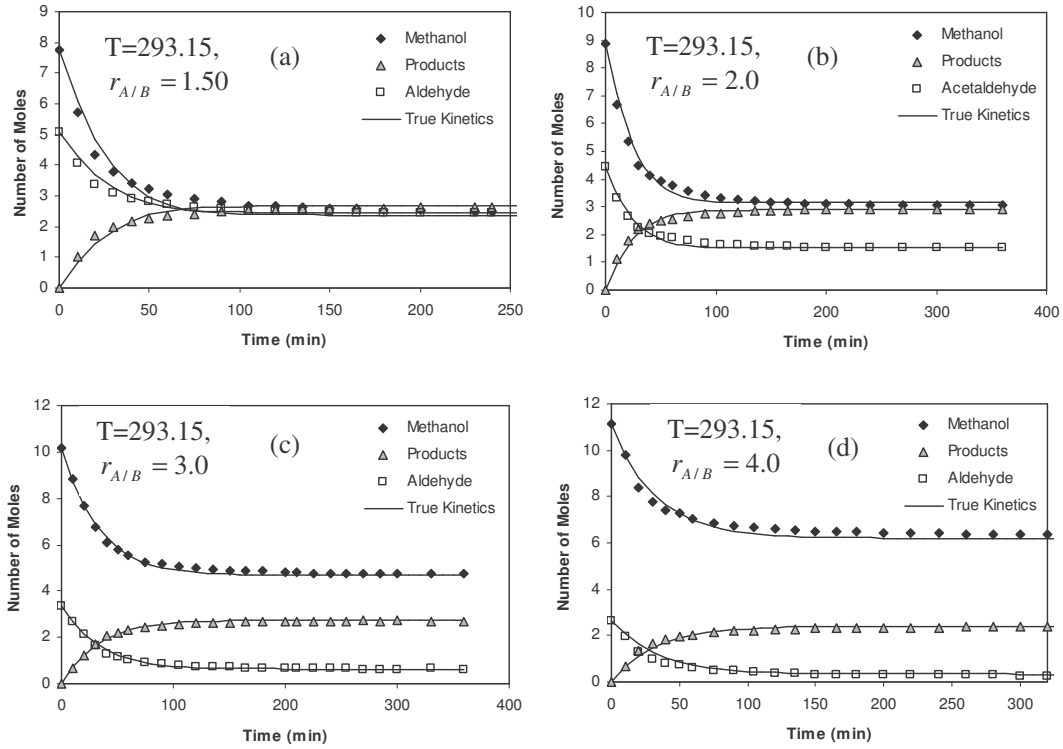

Figure 5.11: Comparison between experimental and true kinetic model curves at 293.15 K: effect of $r_{A/B}$ *(methanol/acetaldehyde)* $P = 6\ atm$, $V = 600$ mL, $w_{cat} = 0.50$ g, $soa = 600$ rpm. (a) $r_{A/B} = 1.50$; (b) $r_{A/B} = 2.0$; (c) $r_{A/B} = 3.0$; (d) $r_{A/B} = 4.0$

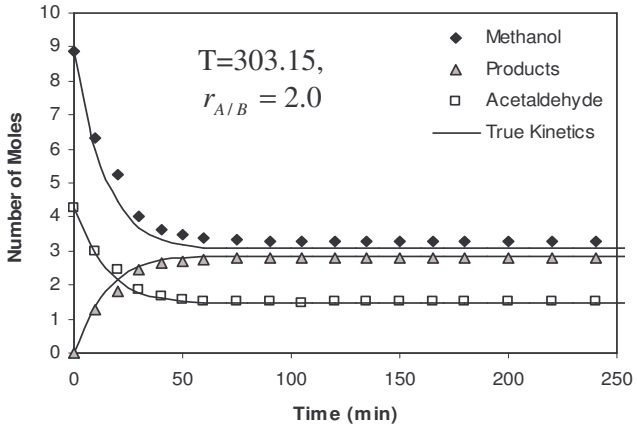

(a)

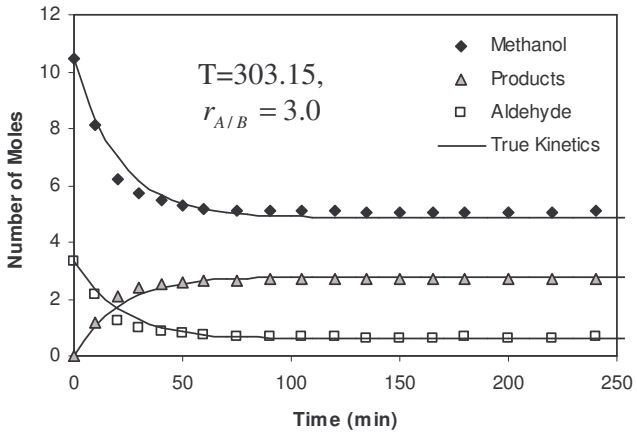

(b)

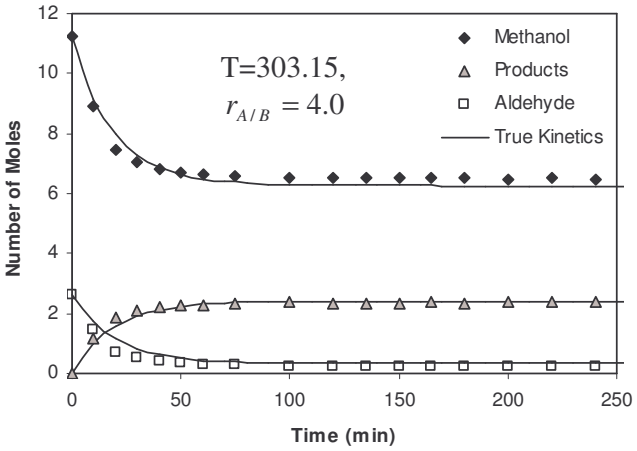

(c)

Figure 5.12: Comparison between experimental and true kinetic model curves at 303.15 K: effect of $r_{A/B}$ *(methanol/acetaldehyde)* $P = 6\ atm$, $V = 600$ mL, $w_{cat} = 0.50$ g, $soa = 600$ rpm.
(a) $r_{A/B} = 2.0$; (b) $r_{A/B} = 3.0$; (c) $r_{A/B} = 4.0$

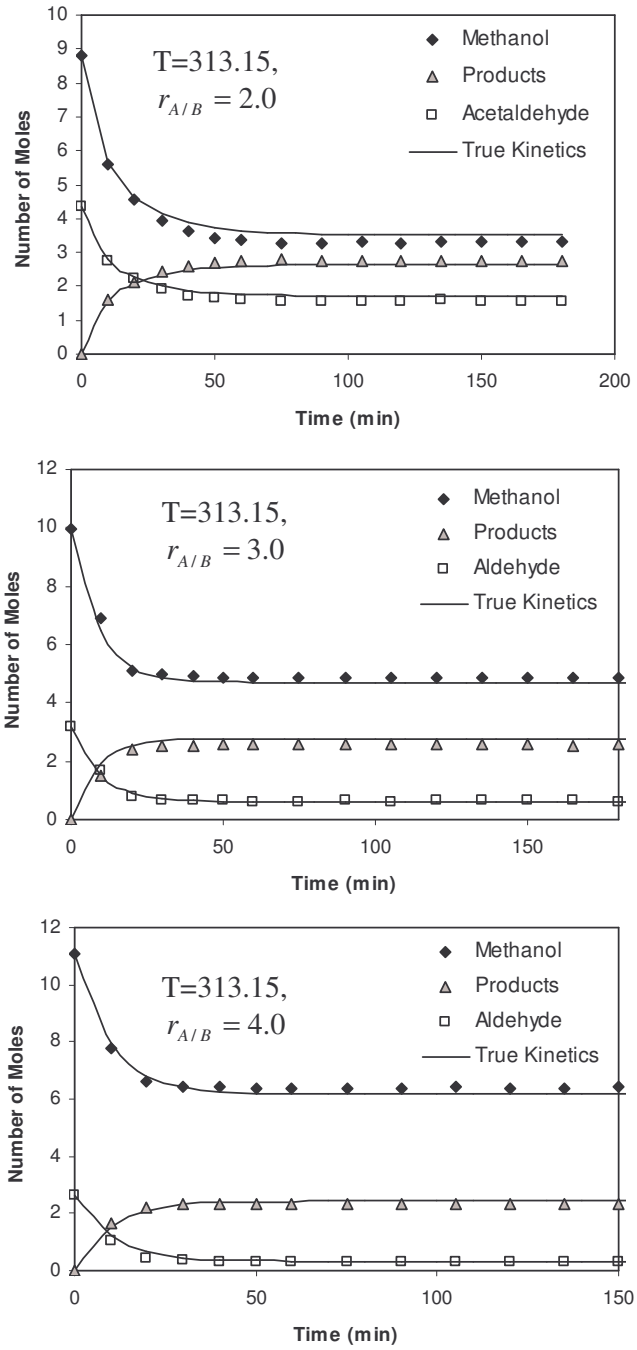

Figure 5.13: Comparison between experimental and true kinetic model curves at 313.15 K: effect of $r_{A/B}$ *(methanol/acetaldehyde)* $P = 6\ atm$, $V = 600$ mL, $w_{cat} = 0.50$ g, $soa = 600$ rpm.
(a) $r_{A/B} = 2.0$; (b) $r_{A/B} = 3.0$; (c) $r_{A/B} = 4.0$

5.5 Fixed Adsorptive Reactor

5.5.1. Experimental set-up

The laboratory-scale experimental set-up is shown in the Figure 5.14 and the characteristic of the Smopex 101 bed in the column is given Table 5.8. The Smopex 101 bed was prepared introducing glass beads in the jacketed glass column. The glass beads were introduced to the Smopex 101 bed in order to avoid building of pressure in the column due to the compression of the bed if Smopex 101 adsorbent alone is packed. Known amount of Smopex 101 slurry was prepared with the methanol; column was packed with the slurry along with the known weight and volume of glass beads. The porosity of the bed prepared with Smopex 101 adsorbent and supporting inert material glass beads was determined by tracer experiments.

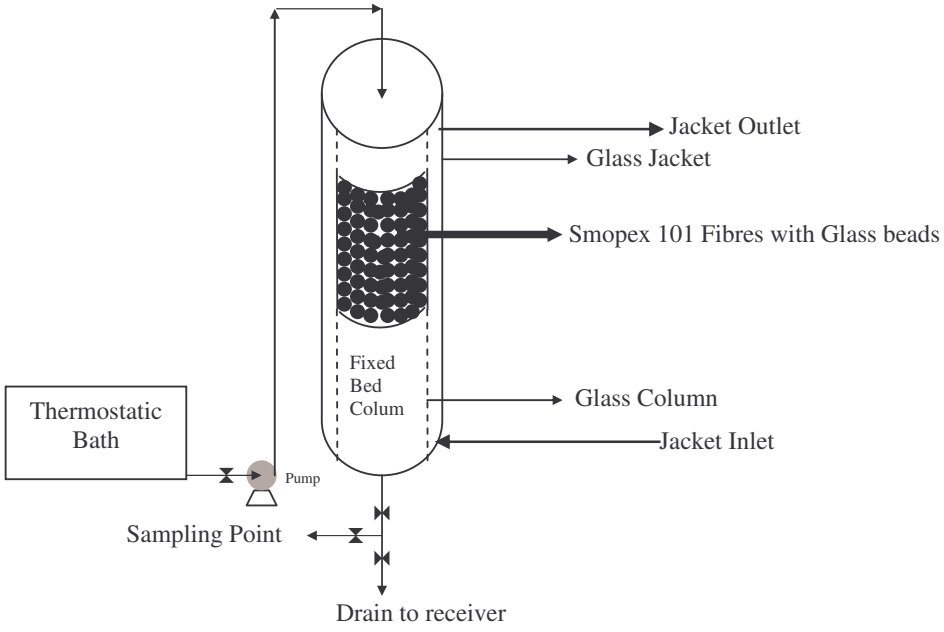

Figure 5.14 Laboratory Scale Fixed Bed Column Experimental Set-up

Table 5.8 Characteristic of bed.

Solid Weight (Smopex 101 Fibres)	3.4 X 10^{-3} Kg
Length of Bed (L)	9.5 X 10^{-2} m
Internal diameter (D_i)	2.6 X 10^{-2} m
Average diameter of fibres (r_p)	12.1 X10^{-6} m
Average length of fibres	250 X10^{-6} m
Bulk Density of Smopex fibres(ρ_b)	410 Kg/m^3
Apparent Density of Smopex fibres (ρ_f)	567 Kg/m^3
Fibres capacity	2.9 mmol/g
Mass of Glass Beads	0.076 Kg
Diameter of Glass Bead	0.003 m
Volume occupied by Glass Beads	31.0 ml

To determine the Peclet number and the bed porosity, pulse experiments of tracer were performed, a nonreactive substance blue dextran solution with low concentrations (5 kg/m^3) was used to perform tracer experiments. Samples of 0.2 cm^3 were injected at the inlet of the column under different flow rates, and the column response was monitored at the end of the column using a UV-VIS detector at 300 nm. The bed porosity was calculated from the stoichiometric time of the experimental response curves. Calculating the second moment of the experimental curves, an average Peclet number can be determined for the range of flow rates to be used in the column. In Figure 5.15, different tracer experiments were plotted and the corresponding values of bed porosity and the Peclet number are given in Table 5.9.

Table 5.9 Bed porosity and Peclet number in the column

	Q (ml/min)	τ (min)	ε	σ^2	Pe
Run 1	2	6.912	0.274	13.74	198
Run 2	3	4.429	0.264	7.87	308
Run 3	4	3.481	0.276	3.15	410
Run 4	5	2.578	0.256	1.53	530
Run 5	6	2.358	0.269	0.86	605

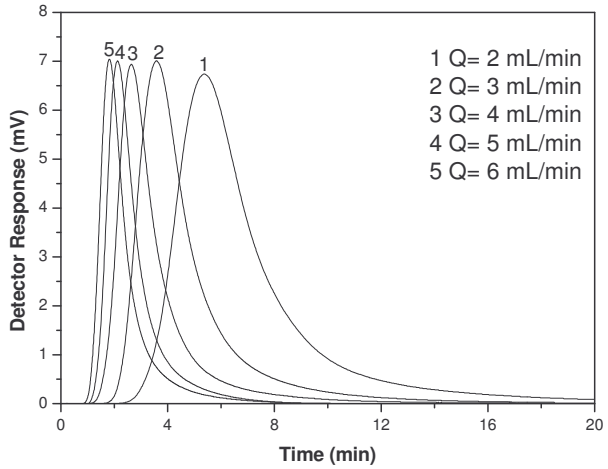

Figure 5.15 Tracer experiment using Blue Dextran solution.

5.5.2. Adsorption Isotherms

The adsorption isotherm is the equilibrium relationship between the concentration in the fluid and the concentration in the adsorbent particles at a given temperature and pressure. Particularly for liquid adsorption, role of pressure is not that effective as in the case of gas adsorption. Liquid adsorption is often expressed in mass concentrations, such as parts per million or moles per unit volume or mass per unit

volume. The concentration of adsorbent on the solid is given as moles or mass adsorbed per unit mass or unit volume of original adsorbent. The multicomponent adsorption equilibrium was described by the extended Langmuir model related to the fibres surface concentration:

$$q_i^s = \frac{Q_i K_i C_{s,i}}{1 + \sum_{j=1}^{n} K_j C_{s,j}} \tag{5.14}$$

Where q_i-fluid concentration at equilibrium of species '*i*' inside the solid bed, Q_i- Adsorption capacity of species *i*, K_i- Adsorption constant of species *i*, C_i- Liquid phase concentration of species *i*, i = methanol, acetaldehyde, acetal (DME), & water.

5.5.3 Fixed Bed Reactor Model

The mathematical model used to describe the dynamic behavior of the fixed bed reactor, considering the following assumptions:

1. The flow pattern is described by the axial dispersed plug flow model;
2. External mass-transfer resistance is considered;
3. The reaction and adsorption of species occur at the fibres surface;
4. Thermal effects are not taken into account;
5. Constant column length and packing porosity are assumed;
6. The fibres are non-porous and the geometry is approximated to infinite cylinders.

The model equations consists of the following system of four second order partial differential equations in the bulk concentration of the i^{th} component, C_i, and four ordinary differential equations in the average concentration of i^{th} component into the particle pores, $\overline{C}_{P,i}$ are as follows;

Bulk fluid mass balance to component *i*

$$\varepsilon \frac{\partial C_i}{\partial t} + u\frac{\partial C_i}{\partial z} + f(1-\varepsilon)\frac{2}{r_p}K_{f,i}\left(C_i - C_{s,i}\right) = \varepsilon D_{ax}\frac{\partial}{\partial z}\left(C_T \frac{\partial x_i}{\partial z}\right) \tag{5.15}$$

Fibres surface mass balance to component *i*

$$\frac{2}{r_p}K_{f,i}\left(C_i - C_{s,i}\right) = \rho_f \left(\frac{\partial q_i^s}{\partial t} - \nu_i \Re\right) \tag{5.16}$$

The above mass balance equations are associated with the initial and Danckwerts boundary conditions:

At $t = 0$, $C_i = C_{s,i} = C_{i,0}$ (5.17)

$z = 0$ $uC_i - \varepsilon D_{ax}\left.\frac{\partial C_i}{\partial z}\right|_{z=0} = uC_{i,F}$

(5.18a)

$z = L$ $\left.\frac{\partial C_i}{\partial z}\right|_{z=L} = 0$

(5.18b)

Where subscripts F and 0 refers to the feed and initial states, respectively. respectively, subscript f representing for fibres, f is fraction of solid volume due to fibres, u is the superficial velocity, K_f is the external film mass transfer coefficient, D_{ax} is the axial dispersion coefficient, t is the time variable, z is the axial coordinate, ν_i is the stoichiometric coefficient of component i, ρ_f represents the apparent density of fibres and $\Re$ is the rate of the chemical reaction expressed in terms of the liquid activities at the surface of the fibres expressed in terms of moles per mass of fibres and per time:

$$\Re = k_c\left(a_A a_B - \frac{a_C a_D}{K_{eq} a_A}\right) \text{ (mols/ kg}_{\text{fibres}}\text{.min)} \tag{5.7}$$

where the activities of the components are relative to the liquid phase on the catalyst surface. The activity coefficients were evaluated using the UNIFAC method (Fredenslund et al., 1977).

The multicomponent adsorption equilibrium was described by the extended Langmuir model related to the fibres surface concentration:

$$q_i^s = \frac{Q_i K_i C_{s,i}}{1 + \sum_{j=1}^{n} K_j C_{s,j}} \tag{5.14}$$

where Q_i and k_i represent the total molar capacity per unit mass of fibres and the equilibrium constant for component *i*, respectively.

Introducing the parameter space time $\tau = \varepsilon L / u$ and the dimensionless variables for space $\zeta = \frac{z}{L}$ and time $\theta = t/\tau$, $\tilde{C} = C / C_{F,T}$, $\tilde{q} = q / q_{F,T}$ and the parameters:

Where $C_{F,T} = \sum_{i=1}^{n} C_{F,i}$ and $q_{F,T} = \sum_{i=1}^{n} q_i\left(C_{F,1}, C_{F,2}, ..., C_{F,n}\right)$

$$Pe = \frac{uL}{\varepsilon D_{ax}} \qquad \text{(Peclet number)} \tag{5.19}$$

$$Da = \frac{k_c \tau}{q_{F,T}} \qquad \text{(Damköehler number)} \tag{5.20}$$

$$N_{f,i} = \frac{1-\varepsilon}{\varepsilon} f \frac{2}{r_p} K_{f,i} \tau \qquad \text{(Number of film mass transfer units)} \tag{5.21}$$

$$\xi = \frac{(1-\varepsilon) f \rho_f q_{F,T}}{\varepsilon C_{F,T}} \qquad \text{(Mass capacity related to the feed)} \tag{5.22}$$

The above model Equations 5.15 and 5.16 respectively becomes as follows:

$$\frac{\partial \tilde{C}_i}{\partial \theta} + \frac{\partial \tilde{C}_i}{\partial \zeta} + N_{f,i}\left(\tilde{C}_i - \tilde{C}_{s,i}\right) = \frac{1}{Pe} \frac{\partial}{\partial \zeta}\left(\tilde{C}_T \frac{\partial^2 x_i}{\partial \zeta^2}\right) \tag{5.23}$$

$$N_{f,i}\left(\tilde{C}_i - \tilde{C}_{s,i}\right) = \xi \frac{\partial \tilde{q}_i^s}{\partial \theta} - \nu_i \xi Da \left(a_{s,A}\, a_{s,B} - a_{s,C}\, a_{s,D} / (K_{eq}\, a_{s,A})\right) \tag{5.24}$$

with initial and boundary conditions:

$$\theta = 0 \qquad C_i = C_{s,i} = C_{0,i} \tag{5.25}$$

$$\zeta = 0 \qquad C_i - \frac{1}{Pe} \left.\frac{\partial C_i}{\partial \zeta}\right|_{\zeta=0} = C_{i,F} \tag{5.26a}$$

$$\zeta = 1 \qquad \left.\frac{\partial C_i}{\partial \zeta}\right|_{\zeta=1} = 0 \tag{5.26b}$$

The external mass transfer coefficient was estimated by the Wilson and Geankoplis correlation (Ruthven, 1984):

$$Sh_p = \frac{1.09}{\varepsilon}\left(Re_p\, Sc\right)^{0.33} \qquad 0.0015 < Re_p < 55 \tag{5.27}$$

where Sh_p and Re_p are, respectively, the Sherwood and Reynolds numbers, relative to particle:

$$Sh_p = \frac{k_e\, d_p}{D_m} \tag{5.28}$$

$$Re_p = \frac{\rho\, d_p\, u}{\mu} \tag{5.29}$$

and Sc is the Schmidt number:

$$Sc = \frac{\mu}{\rho\, D_m} \tag{5.30}$$

The diffusivities in multicomponent liquid mixture were estimated by the modified Wilke-Chang equation, proposed by Perkins and Geankoplis (Reid et al., 1987):

$$D_{Am}^{o} = 7.4\times10^{-8}\frac{(\phi M)^{1/2}T}{\mu V_{ml,A}^{0.6}} \tag{5.31}$$

$$\phi M = \sum_{\substack{j=1 \\ j\neq A}}^{n} x_j \phi_j M_j \tag{5.32}$$

where D_{Am}^{o} is the diffusion coefficient for a dilute solute A into a mixture of n components, T is the temperature, $V_{ml,A}$ is the molar volume of the solute A, x_j is the molar fraction for component j, ϕ_j is the association factor for component j, that is equal to 2.6 for water, 1.9 for methanol and 1.0 for unassociated components. The mixture viscosity, μ was predicted by the generalized corresponding states method purposed by Teja and Rice (Teja and Rice, 1981).

The system of partial differential equations represented by Eq. (5.23) to Eq. (5.26) are solved by the method of lines (MOL) using orthogonal collocation in finite elements to discretize the axial coordinate, with B-splines as base functions through numerical package PDECOL. Fifty subintervals for spatial discretization along the z-axis were used, with two internal collocation points in each subinterval, resulting in 200/400 time dependent ordinary differential equations for adsorption/reaction simulations. For all simulations was fixed a tolerance value EPS equal to 10^{-7}.

5.5.4 Experimental Results and Discussions

5.5.4.1 Binary Adsorption Experiments

The breakthrough curves of methanol, acetal (DME) and water were measured in the absence of reaction. The adsorbent was saturated with a certain component A, and then the feed with pure component B was fed to the adsorbent on stepwise concentration of the Feed Solution. The adsorption parameters were optimised by minimizing the difference between the experimental and simulated stoichiometric times of

breakthrough curves. The stoichiometric time can be determined from the mass balance over the adsorbent bed in the column as shown below,

$$t_f = \frac{L}{u}\left(\varepsilon + \rho_f^* \frac{\Delta q}{\Delta C}\right) \tag{5.33}$$

where the parameter ρ_f^* is defined as:

$$\rho_f^* = \frac{m_f}{V_b} \tag{5.34}$$

and m_f is the mass of fibres and V_b is the bed volume in the column. The adsorption amount q is expressed in number of moles adsorbed per mass of fibres (mol/kg_{fibre}).

The apparent density of the fibres can be calculated by:

$$\rho_f = \frac{\rho_f^*}{f(1-\varepsilon)} = \frac{m_f}{V_f} \tag{5.35}$$

where $$\frac{\Delta q}{\Delta C} = \frac{q(C_F) - q(C_0)}{C_F - C_0} \tag{5.36}$$

Experimental stoichiometric times of the experiments were calculated from the plot of outlet concentration of column and time of outlet samples analysed. In the breakthrough experiments, where component A displaces the component B, the total amount of A necessary to saturate the column is given by the product of volumetric flow rate and the area over the breakthrough curve limited by the feed concentration. The product between the flow rate and the area under the effluent curve gives the total amount of component B that was initially saturating the column.

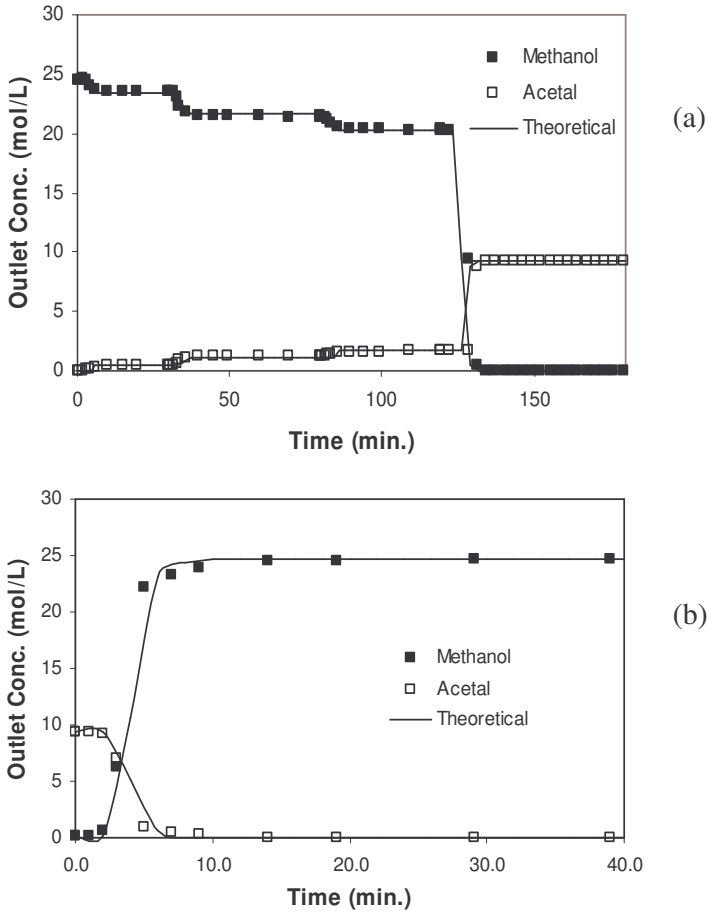

Figure 5.16: Breakthrough experiments, outlet concentration of acetal and methanol as a function of time. (a) Acetal displacing methanol; Q = 4.0 mL/min, bottom-up flow direction; (b) methanol displacing acetal; Q = 4.0 mL/min, top-down flow direction. Experimental data: (■) methanol; (□) acetal. (—) Theoretical results.

In the Figures 5.16(a) and 5.16(b), the concentration graphs of methanol and acetal are shown. In the breakthrough of acetal, Figure 5.16(a), the errors between the experimental and theoretical amounts of acetal adsorbed and methanol displaced are 3.7 and 6.4 %, respectively. Comparing the experimental amount of methanol adsorbed in the experiment of Figure 5.16(b) with the experimental amount of methanol desorbed in the experiment of Figure 5.16(a), the error obtained is 4.9 %. For acetal, the error

between the amount adsorbed, Figure 5.16(a), and the amount eluted, Figure 5.16(b) is 3.8 %.

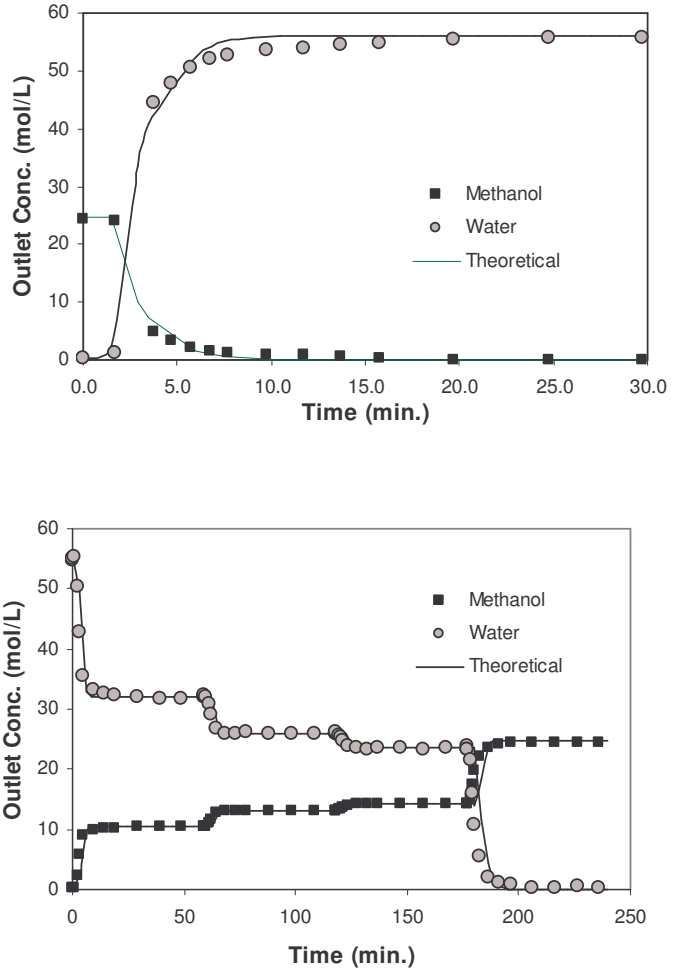

Figure 5.17: Breakthrough experiments, outlet concentration of methanol and water as a function of time. (a) Water displacing methanol; Q = 4.0 mL/min, bottom-up flow direction; (b) Methanol displacing water; Q = 4.0 mL/min, top-down flow direction. Experimental data: (■) methanol; (●) Water. (—) Theoretical results.

Similarly, experiments were conducted for the combination of methanol and water breakthroughs and the breakthrough plots for methanol and water are shown in the above Figure 5.17(a) and 5.17(b), the experimental results are in agreement with the model predictions.

Using the experimental data and theoretical parameters, adsorption of methanol, acetal (DME) and water on the adsorbent (Smopex 101) were calculated at different steps of feed solutions so as to determine the adsorption isotherms. Adsorption parameters for methanol, acetal and water were calculated with the data obtained from the stepwise and binary experiments of both Methanol-Water and Acetal-Methanol systems. The adsorption parameters for acetaldehyde were determined by optimization of reaction experimental data. The adsorption parameters for acetal, acetaldehyde, methanol and water are given in Table 5.10.

Table 5.10 Adsorption isotherms.

Component	Q (mol / $m^3_{real\ solid}$)	K (m^3/mol)
Methanol (A)	7.0	0.93×10^{-3}
Acetaldehyde (B)	7.0	0.38×10^{-3}
Acetal (C)	7.0	0.84×10^{-3}
Water (D)	7.0	0.93×10^{-3}

5.5.4.2 Reaction Experimental Procedure

Reaction experiments were performed, by feeding continuously the mixture of methanol and acetaldehyde to the fixed bed chromatographic reactor that was initially saturated with methanol. As the feed mixture is less dense than the pure methanol, the flow direction was operated in top-down. However, it was noticed hydrodynamic effects due to axial backmixing driven by natural convection of water. The concentration fronts moving within the column are hydrodynamically stable if the component above the front is less dense than the component below the front. Since the products are denser than the reactants, the reaction mixture is denser than methanol (initially saturating the column); therefore the reactants mixture should be fed from the bottom. The reactants

mixture methanol and acetaldehyde at the stoichiometric ratio was fed to the column with 3 ml/min flow rate as shown in Figure 5.18 and Figure 5.19 respectively for 20 ^{o}C and 10 ^{o}C reaction temperature, wherein the outlet concentration of the reaction mixture was represented as the function of time. Typical chromatograms for the experiment shown in Figure 5.18 at 2, 3, 5, 8,10 16, 25 and 30 minutes are given in Figure A.15, A.16, A.17, A.18, A.19, A20, A.21 and A.22 respectively of Appendix A.

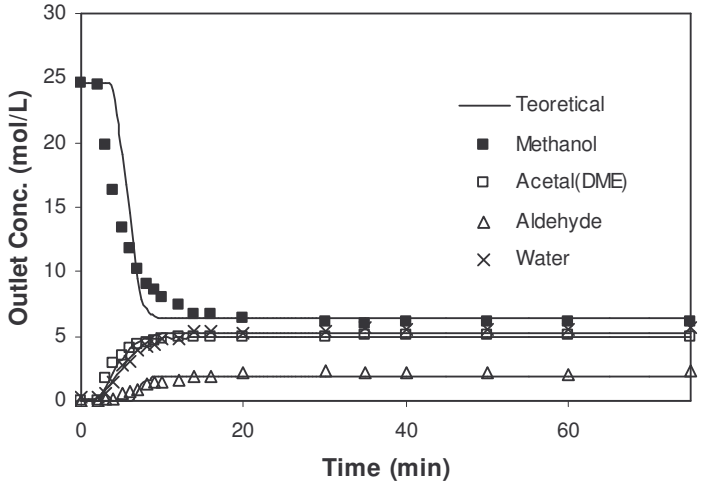

Figure 5.18: Concentration profiles in a fixed bed adsorptive reactor initially saturated with methanol and then fed with methanol and acetaldehyde mixture.
Experimental conditions: Q = 3.0 mL/min, $C_{A,F}$ = 16.03 mol/L and $C_{B,F}$ = 6.29 mol/L; Bed Length: 9.5 cm; Bed Diameter: 2.6 cm;
Bed Temperature: 20 ^{o}C;
Experimental data: (■) methanol, (Δ) acetaldehyde, (□) acetal and (×) water.
Simulated results: continuous line.

As the reactants mixture enters the column, acetaldehyde in the reactants mixture is adsorbed and reacts with adsorbed methanol on the adsorbent surface (Smopex 101 fibres). Acetal (DME) and water are formed in the stoichiometric amounts. The acetalization reaction continues until the surface of fibres saturated with the reaction mixture. The concentration of the reaction mixture in the column remains constant as the steady state is achieved, and the reaction mixture at the steady state position consists of the concentrations in the outlet stream. In this reaction, the model predictions are in

agreement with the experimental data. Here in this reaction experiment, it is observed the concentration front of reaction only. The reactive front of acetalization occurs in between 2 and 8 minutes. These phenomena are better understood with the analysis of propagation of these composition fronts inside the column.

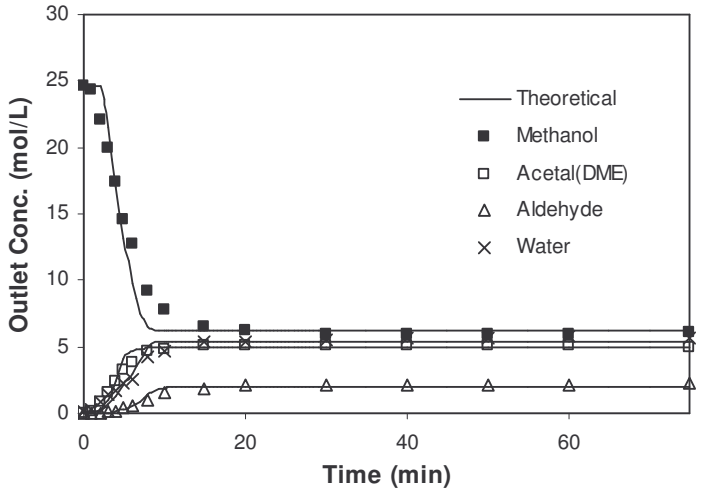

Figure 5.19: Concentration profiles in a fixed bed adsorptive reactor initially saturated with methanol and then fed with methanol and acetaldehyde mixture.
Experimental conditions: Q = 3.0 mL/min, $C_{A,F}$ = 16.03 mol/L and $C_{B,F}$ = 6.29 mol/L; Bed Length: 9.5 cm; Bed Diameter: 2.6 cm;
Bed Temperature: 10 ^{o}C;
Experimental data: (■) methanol, (Δ) acetaldehyde, (□) acetal and (×) water.
Simulated results: continuous line.

This is possible only by considering the simulated internal profiles for the same experimental operating conditions of Figure 5.18. Figure 5.20 (a-d) shows the internal concentration profiles for all species at 2, 4, 5 and 6 minutes near the feed port of the reactor, there is a reaction zone where the reactants are fast consumed till the equilibrium composition ($C_{methanol}$ = 5.9 x 10^3 mol/m^3, $C_{acetaldehyde}$ = 2.0 x 10^3 mol/m^3). This reaction zone is in steady state. In this reaction front, the concentration fronts of acetal, acetaldehyde, methanol and water exhibit constant pattern behaviours, since it

propagate along the column at constant velocities without changing their shapes as shown in Figure 5.20 (a-d).

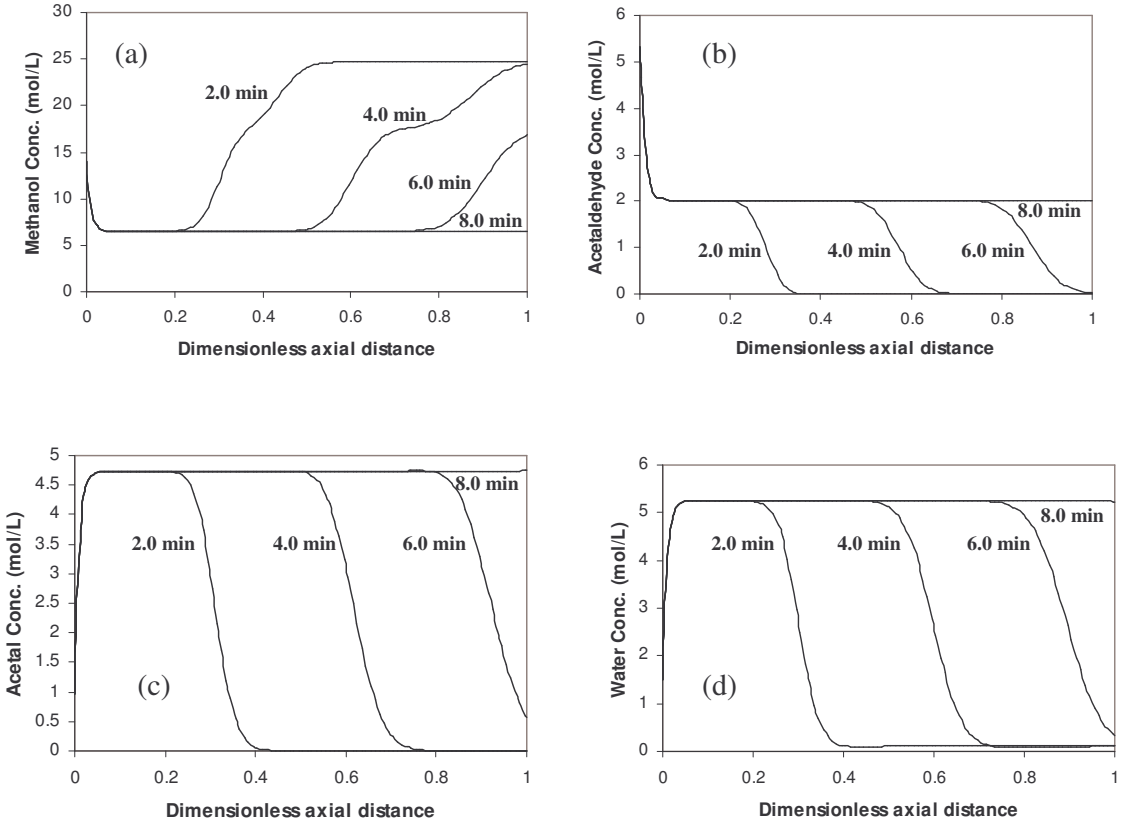

Figure 5.20: Internal concentration profiles of each species in fluid phase inside the column, at different times, during the reaction experiment of Figure 5.18; (a) methanol, (b) acetaldehyde, (c) acetal and (d) water.

5.5.4.3 Regeneration of Fixed bed Adsorber/Reactor

After the reaction experiment, which was indicated by the attainment of steady-state, the fibres (Smopex 101) should be regenerated with the desorbent in order to reuse the fibres repeatedly before starting the new experiment. Loaded adsorbents can be regenerated by temperature-swing or pressure-swing adsorption process and by displacement method. In some cases, the adsorptive can be extracted from adsorbent.

During regeneration of fixed bed adsorber by displacement method, the adsorbate is removed from the adsorbent by displacement from active sites which is due to adsorption of third material (the displacing agent). The choice of a suitable displacement agent depends both on the equilibrium of the system and on the kinetics of the adsorption and desorption. Here methanol was used as a desorbent for regeneration of the bed. Methanol was fed to the column in the bottom-up direction. The outlet concentration for the regeneration of the column as the function of time is shown in the Figure 5.21 with respect to the reaction performed in Figure 5.18.

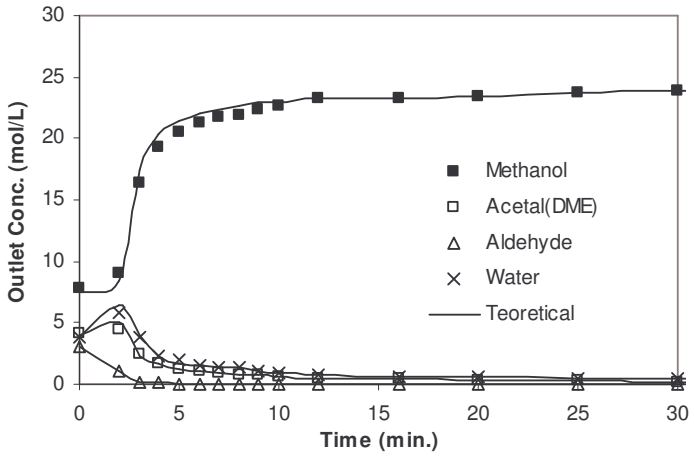

Figure 5.21: Concentration profiles in the regeneration step of a fixed bed adsorptive reactor. The initial profiles in the bed are those at the final steady state of the run in Figure 5.18.
Experimental conditions: Q = 3.0 mL/min, $C_{A,F}$ = 24.683 mol/L and $C_{B,F}$ = 0.0 mol/L; Bed Length: 9.5 cm; Bed Diameter: 2.6 cm;
Bed Temperature: 10 °C; Top-Down flow direction
Experimental data: (■) methanol, (Δ) acetaldehyde, (□) acetal and (×) water.
Simulated results: continuous line.

5.6 Conclusions

The synthesis of acetal (1,1-dimetoxyethane) using acetaldehyde and methanol as raw-material on a Smopex 101 fibres both in batch reactor and in fixed bed adsorber/reactor. The thermodynamic equilibrium constant was measured in the

temperature range of 293.15 – 333.15 K and given as $K_{eq} = 0.0173\exp[2103.3/T(K)]$.

The kinetic law was proposed which expressed in activities is shown below:

$$\Re = k_c\left(a_A a_B - \frac{a_C a_D}{K_{eq} a_A}\right)$$

and the parameter k_c is given as follows;

$$k_c = 7.59\times10^8 \exp\left[\frac{-5853.8}{T(K)}\right] (\text{ mol g}^{-1}\text{ min}^{-1}).$$

The activation energy of the reaction is 48.7 kJ mol^{-1}.

The dynamic behaviour of fibres bed was studied. The primary experiments conducted to collect the desired adsorption data by performing dynamic binary adsorption experiments in absence of reaction at 293.15 K, in a laboratory scale column. Minimizing the difference between the experimental and calculated stoichiometric times of breakthrough curves optimised the adsorption parameters. The mathematical model for the adsorptive reactor was developed and multicomponent Langmuir adsorption isotherms were measured on laboratory scale experimental set-up. The model was compared with the experimental results obtained for reaction and regeneration experiments.

5.7 Nomenclature

a liquid-phase activity

A_p external exchange area between the bulk fluid and the particles, cm^2

C_i concentration of component i, mol L^{-1}

C_{A_s} methanol concentration at the catalyst surface, mol L^{-1}

C_b bulk concentration, mol L^{-1}

$C_{p,j}$ concentration inside the particle, mol L^{-1}

C_p molar heat capacity at 298 K, J mol^{-1} K^{-1}

d_p mean pellet diameter, m

$D^o_{j,m}$ diffusion coefficient for a dilute solute j in mixture of n components, cm^2 min^{-1}

D_{A_s} effective diffusivity of methanol at catalyst particle surface, cm^2 min^{-1}

$E_{a,C}$ reaction activation energy, J mol^{-1}

ΔG reaction Gibbs free energy, J mol^{-1}

ΔG^o_f standard free energy of formation, J mol^{-1}

f fraction of solid volume due to fibres

ΔH reaction enthalpy, J mol^{-1}

ΔH^o_f standard enthalpy of formation, J mol^{-1}

ΔH_s enthalpy of adsorption, J mol^{-1}

k_c kinetic constant, mol kg^{-1} min^{-1}

K_{eq} equilibrium reaction constant

K_p correction factor

K_s equilibrium adsorption constant

K_x constant based on molar fractions

K_γ constant based on activity coefficients

m mass, kg

M molecular weight, mol g^{-1}

n number of moles in the liquid phase, mol

P pressure, atm

r particle radial distance, cm

R gas constant, J mol^{-1} K^{-1}

r_p particle radius, μm

$\Re$ rate of reaction, mol kg^{-1} min^{-1}

$r_{A/B}$ initial molar ratio of reactants

ΔS reaction entropy, J mol^{-1} K^{-1}

ΔS_f^o standard entropy of formation, J mol^{-1} K^{-1}

T temperature, K

t time, s

V solution volume, m^3

V_{ml} molar volume of component *i*, m^3 mol^{-1}

w_{cat} mass of catalyst, kg

x molar fraction

X conversion of the limiting reactant

Greek letters

ν stoichiometric coefficient

γ activity coefficient

ρ_p particle density, g L^{-1}

ρ_f apparent density of fibres, g L^{-1}

ϕ association factor in Eq. 3.23

ϕ_T Thiele modulus

ε porosity

ε_p particle porosity

τ tortuosity

Subscripts

0 initial value

A methanol

B acetaldehyde

C acetal (DME)

D water

eq equilibrium

exp experimental data

gas vapor phase

f fibres

i relative to component *i*

l relative to limiting reactant

liq liquid phase

s surface condition

theo theoretical data

Superscripts

o standard state

5.8 References

1. Aizawa, T.; Nakamura, H.; Wakabayashi, K.; Kudo, T.; Hasegawa, H. *Process for producing acetaldehyde dimethylacetal*. U.S. Patent 5,362,918, **1994**.

2. Aumo, J.; Lilja, J.; Maki-Arvela, P.; Salmi, T.; Sundell, M.; Vainio. H.; Murzin, D. Yu. Hydrogenation of citral over a polymer fiber catalyst. *Catal. Lett.* **2002**, 84, 219.
3. Bauer, K.; Garbe, D.; Surburg, H. *Common Fragrance and Flavor Materials*; Wiley-VCH: Weinheim, **1990**.
4. Chopade, S. P.; Sharma, M. M. Esterification of formic acid, acrylic acid and methacrylic acid with cyclohexene in batch and distillation column reactors: ion-exchange resins as catalysts. *React. Funct. Polym.* **1996,** 28, 263.
5. Chopade, S. P.; Sharma, M. M. Reaction of ethanol and formaldehyde: use of versatile cation-exchange resins as catalyst in batch reactors and reactive distillation columns. *React. Funct. Polym.* **1997,** 32, 53.
6. Doraiswamy, L. K.; Sharma, M. M. *Heterogeneous Reactions: Analysis, Examples, and Reactor Design.* Wiley-Interscience, New York, **1987**.
7. Dupont, P.; Védrine, J. C.; Paumard, E.; Hecquet, G.; Lefebvre, F. Heteropolyacids supported on activated carbon as catalysts for the esterification of acrylic acid by butanol. *Appl. Catal.* A. **1995**, 129, 217.
8. Fedriani, A.; Gonzalez-Velasco, J. R.; Lopez-Fonseca, R.; Gutierrez-Ortiz, M. A. Kinetics of 1,1-diethoxyethane synthesis catalysed by USY zeolites. *CHISA 2000, A7.7 12.30 Presentation* **2000**.
9. Fredeslund, A.; Gmehling, J.; Rasmussen, P. *Vapor-liquid Equilibrium Using UNIFAC*; Elsevier: Amsterdam, 1977.
10. Gupta, B. B.G. *Alkoxyalkylation of phenol*. U.S. Patent 4,694,111, **1987**.

11. Kekre, S. Y.; Gopala Rao, M. Kinetics of the liquid phase esterification of n-butanol and acetic acid catalyzed by cation exchange resins Indian Chem. Eng. **1969**, 4, 115.
12. Kriner, R. S.; Krause, A. O. I. Kinetic model for the etherfication of 2,4,4-trimethyl-1-pentene abd 2,4,4-trimethyl-2-pentene with methanol. *Ind. Eng. Chem. Res.* **2001**, 40, 6073.
13. Lacaze-Dufaure, C; Moulougui, Z. Catalysed or uncatalysed esterification reaction of oleic acid with 2-ethyl hexanol. *Appl. Catal.* A. **2000**, 204, 223.
14. Lilja, J.; Aumo, J.; Salmi, T.; Murzin, D. Yu; Maki-Arvela, P.; Sundell, M.; Ekman, K.; Peltonen, R.; Vainio. H. Kinetics of esterification of proponic acid with methanol over a fibrous polymer-supported sulphonic acid catalyst. *Appl. Catal.* A. **2002** (a), 228, 253.
15. Lilja, J.; Murzin, D. Yu; Salmi, T.; Aumo, J.; Maki-Arvela, P.; Sundell, M. Esterification of different acids over heterogeneous and homogeneous catalysts and correlation with the Taft equation. *J. Mol. Catal.* A. **2002** (b), 182-183, 555.
16. Ma, Y.; Wang, Q. L.; Yan, H.; Ji, X.; Qiu, Q. Zeolite-catalyzed esterification I. Synthesis of acetates, benzoates and phthalates. *Appl. Catal.* A. **1996**, 139, 51.
17. Maki-Arvela, P.; Salmi, T.; Sundell, M.; Ekman, K.; Peltonen, R.; Lehtonen, J. Comparison of polyvinylbenzene and polyolefin supported sulphonic acid catalysts in the esterification of acetic acid. *Appl. Catal.* A. **1999**, 184, 25.
18. Ramalinga, K.; Vijayalakshmi, R.; Kaimal, T. N. B. A mild and efficient method for esterification and transesterification catalyzed by iodine. *Tetrahedron Lett*. **2002**, 43, 879.

19. Reid, C. R.; Prausnitz, J. M.; Poling, B. E. *The Properties of Gases & Liquids*. 4th Edition, McGraw-Hill: New York, 1988.
20. Roy, R.; Bhatia, S. Kinetics of esterification of benzyl alcohol with acetic acid catalysed by cation-exchanged resin (Amberlyst-15). *J. Chem. Tech. Biotechnol.* **1987**, 37, 1.
21. Schwegler, M. A.; Bekkum, H. van, Heteropolyacids as catalysts for the production of phthalate diesters. *Appl. Catal.* A. **1991**, 74, 191.
22. Silva, V. M. T. M.; Rodrigues, A. E. Synthesis of diethyl acetal: thermodynamic and kinetic studies. *Chem. Eng. Sci.*, **2001,** 56 1255-1263.
23. Silva-Machado, M. da; Cardoso, D.; Pérez-Pariente, J.; Sastre, E. Esterification of lauric acid with glycerol using modified zeolite beta as catalyst. *Stud. Surf. Sci. catal.* **2000**, 130D, 3417.
24. Yadav, G. D.; Kishnan, M. S. An ecofriendly catalytic route for the preparation of perfumery grade methyl anthranilate from anthranilic acid and methanol. *Org. Pro. Res. Dev*. **1998**, 2, 86.
25. Yadav, G. D.; Pujari, A. A. Kinetics of acetalization of perfumery aldehydes with alkanols over solid acid catalysts. *Canadian Journal of Chemical Engineering*, **1999,** *77*, 489-496.

6. Dimethylacetal Synthesis on Simulated Moving Bed Reactor

Synthesis of dimethylacetal (1,1-dimethoxyethane) was performed in a SMBR (Simulated Moving Bed Reactor) pilot unit LICOSEP 12-26 (Novasep, France) with twelve columns packed with the acid resin Amberlyst 15 (Rohm and Hass, France). Mathematical model based on TMBR (True Moving Bed Reactor) strategy was used to explain the experimental results of SMBR. The effect of switching time and the configuration of SMBR in the performance of SMBR was studied. The simultaneous reaction and separation concept is used for the operation of the existing SMBR equipment in order to produce the dimethylacetal.

6.1. Introduction

The integration of reaction and separation of the desired products in one single unit allows significant improvement in process performance, particularly in the case of equilibrium limited reactions, in addition to obvious saving in the equipment cost. Typical examples include condensation, esterification, transesterification, etherification, acetalization reactions and others. By separating the reaction products, the equilibrium limitation can in fact be overcome and the conversion can be driven to the completion in a single pass in the unit. Currently, the industrial application of such multifunctional

units is substantially limited to the reactive distillation, where however is not suitable for complex molecules that are difficult to evaporate, such as those typically of interest in the fine chemical and pharmaceutical industries. An interesting alternative is the integration of chemical reaction and adsorptive separation into one single unit, i.e., reactive chromatography.

6.2. Moving Bed Reactors and Chromatographic Reactors

6.2.1. Moving Bed Reactor

In most chemical engineering unit operations, continuous counter-current flow is used since it is usually the most efficient way to operate. This is the case for equilibrium staged reaction and separation processes. Unfortunately, counter-current movement of solid and fluid is difficult to achieve without extensive mixing of solid particles. This difficulty has catalyzed considerable research in this area. Counter-current schemes have included flow in open columns, the hypersorption process where solids flow was controlled by opening and closing of holes in the sieve trays, moving belt schemes, counter-current flow of gases and solids in sieve tray columns with down-comers, pulsed operation in sieve tray columns without down-comers and magnetically stabilized moving bed systems. The idealized analysis of all these systems will be similar. In some cases counter-current movement has been abandoned and simulated counter-current flow has been used. The simulated counter-current system uses a series of packed beds and moves the location of all feed and product withdrawing ports. A close approximation to continuous counter-current movement can be obtained with simulated systems (McCabe et al., 1991; Ruthven, 1984).

6.2.2. Chromatographic Reactors

6.2.2.1 Batch Chromatographic Reactor

The simplest way to realize a chromatographic reactor is to run it in a batch mode. Figure 6.1 illustrates the operating principle of a batch chromatographic reactor for a reversible decomposition reaction (Ruthven, 1984). The reactant A is injected as a sharp pulse into the column. During its propagation along the column it reacts to build the products B and C. The different adsorption component B and C leads to different propagation velocities and the products are separated from each others.

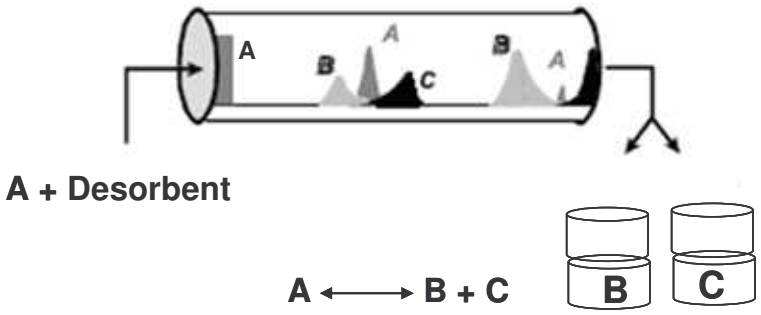

Figure 6.1 Batch chromatographic reactor operating principle.

Therefore, it is possible to totally convert the reactant A into the products although the reaction is limited by chemical equilibrium. Additionally, no separation unit following the chromatographic reactor is necessary to gain the products in high purity. It should be pointed out, that the operation conditions should be chosen in such a way to make use of one of the major advantages of chromatographic reactor, e.g. complete conversion. Otherwise additional separation unit is necessary to recycle the reactant which was not converted. After the invention of the chromatographic reactor in 1961 (Dinwiddie and Morgan, 1961), most of the experimental as well as theoretical

studies dealt with the concept described above. Recently, for running chromatographic reactors in a preparative scale, research has been mainly focused on continuous chromatographic reactors as described in section 6.2.2.2 and section 6.2.2.3.

6.2.2.2 True Moving Bed (TMB)

The underlying principle in a True Moving Bed (TMB) for the separation of mixture of two fluids is contacted with a solid adsorbent phase in a counter-current manner (Chu and Hashim, 1995; Minceva and Rodrigues, 2005), as shown for example in Figure 6.2 for the case of separating a mixture of *A+B*. Here, the solid phase is passing at a constant flow rate from top to bottom through the unit, while the carrier fluid or eluent or desorbent D is introduced to the unit at the bottom and is proceeding in the opposite direction with respect to the solid phase.

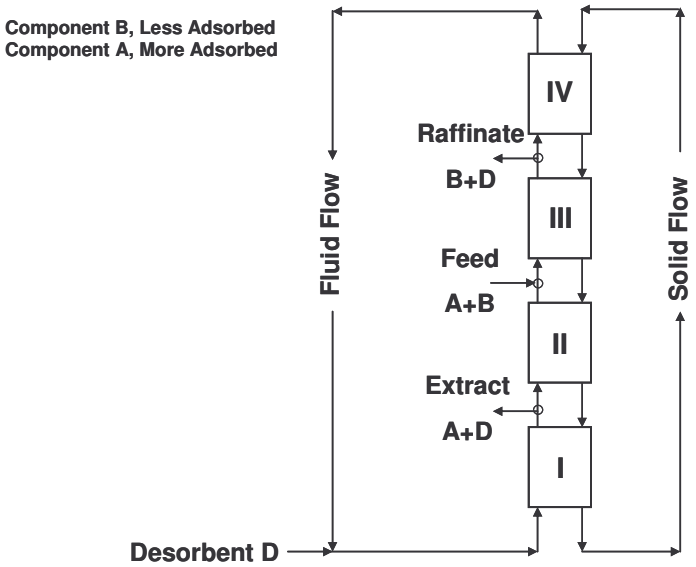

Figure 6.2 Schematic diagram of four-section True Moving Bed (TMB).

The two inlet streams, desorbent/feed and the two withdrawal streams, extract/raffinate divide the unit into four sections as indicated in the Figure 6.2. As the inlet stream A+B is fed to the central part of the unit, the chemical separation takes

place on the basis of adsorption affinity of the species to the solid. The more strongly adsorbing compound i.e. A in this example, is carried downwards by the solid phase which can be withdrawn in the extract stream, while the less retained species, B, moves in the direction of fluid towards the raffinate outlet. Before being recycled, both the solid and the fluid phases are regenerated in the section 1 and 4, respectively. If the solid and fluid flow rates are properly adjusted, complete separation is possible within the two central sections of the unit, where both species can be withdrawn at high purity from the extract and raffinate streams.

6.2.2.3 Simulated Moving Bed

The practical implementation of this so-called True Moving Bed (TMB) (Do, 1998; Ruthven, 1984; Wankat, 1994) unit is difficult due to the movement of the solid, while an equivalent unit can easily be realized by simply redesigning the TMB unit with reference to an observer moving with the solid phase. This leads to the Simulated Moving Bed (SMB) Unit (Giovanni et al., 2001; Juza et al., 1998, Migliorini et al, 2001), This continuous chromatographic counter-current process developed during 1960's by Universal Oil Products (UOP), USA (Broughton and Gerhold, 1961). The process was first patented for the SORBEX process and issued for a number of large-scale separations in the petrochemical and sugar industries. In recent years, the SMB technology has shown many advantages over batch preparative chromatography and has attracted the interest of the fine chemical and pharmaceutical industries (Grill at al., 2004; Guest, 1997; Huthmann and Juza, 2005; Miller et al., 2003). The simulated moving bed is based on the principle of True Moving Bed (TMB). The true moving bed shown in Figure 6.2, the movement of the fluid phase and solid phase are in opposite direction as indicated. The inlet ports (feed and desorbent or eluent) and outlet ports

(extract and raffinate) are fixed along the equipment. According to the position of the inlet and outlet streams, four different sections could be distinguished:

Section I : Located between eluent and extract stream;

Section II : Located between extract and feed streams;

Section III : In between feed stream and raffinate stream;

Section IV : Exists in between raffinate and eluent ports.

The SMB technology can overcome the major problems connected with the solid movement in the TMB operation: like backmixing of solid which reduces the efficiency of the process, another is the abrasion of the particles caused by the movement. Hence, in practice the movement of the solid is not feasible. So, the TMB is replaced by the SMB configuration. In this SMB configuration, a certain number of fixed beds are connected in series to form a closed loop, and the counter-current movement of the solid and fluid is simulated by changing the inlet and outlet steams in the direction of the fluid flow. An example schematic diagram of the laboratory SMB is shown in Figure 6.3.

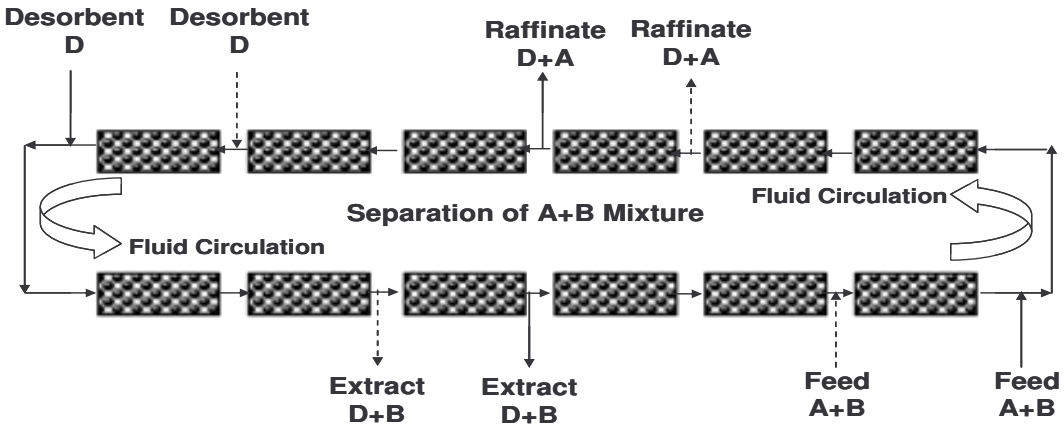

Figure 6.3 Schematic diagram of Simulated Moving Bed (SMB).

It is worth noting that the non-reactive, i.e. purely separative version of this unit has attained significant success in the industry during last few years, particularly with the separation of xylenes from aromatic fraction (Minceva, 2004; Minceva and Rodrigues, 2005), applications in the areas of biotechnology, pharmaceuticals, fine chemicals (Grill at al., 2004; Guest, 1997; Huthmann and Juza, 2005; Miller et al., 2003), fructose-glucose separation (Azevedo and Rodrigues, 2001; Klatt et al., 2002), chiral separations (Pais et al., 1997, Rodrigues et al., 1995; Rekoske, 2001). Several projects in our group contributed to the success of SMB technology: chiral separations (Pais et al., 1997), fructose-glucose separation (Azevedo and Rodrigues, 2001), xyelenes separation modeling (Minceva and Rodrigues, 2005) development of reaction and separation (Silva, 2003; Silva and Rodrigues, 2004, 2005). The continuous chromatographic reactor-separator (Simulated Moving Bed Reactor) is one interesting physical equipment. In this SMBR unit, the counter-current contact between the solid and mobile phase is achieved by periodically shifting the inlet (feed and eluent) and outlet (extract and raffinate) ports in the direction of fluid flow as in the case of SMB chromatography. In such reactor, reaction takes place either in the mobile phase (fluid phase) or in the stationary phase (solid phase). In case of reactions like esterification and transesterification (Ferreira and Loureiro, 2004; Yadav and Manjula Devi, 2004), acetalization (Chopade and Sharma, 1997; Gandi et al., 2005; Silva and Rodrigues, 2001; Yadav and Pujari, 1999), etherification (Cruz et al., 2005; Yadav and Lande, 2005), and others which are catalyzed by acid sites, the use of acid ion exchange resin, Ambelyst 15 is of interest as the resin can be used as catalyst and as well as a selective adsorbent (Silva and Rodrigues, 2001, 2002). In fact the acetalization reaction is also a chemical equilibrium controlled reaction, and therefore the removal of the reaction

products leads to reactants conversion above the equilibrium limit. Hence the dimethylacetal synthesis and separation in SMBR can be an interesting process which is considered here in this work.

A closed loop 3-3-3-3 configuration (three chromatographic columns per section of the unit) is shown in Figure 6.3, where the outlet from the Section IV is recycled directly. Due to the switching of inlet and outlet lines, each column changes the boundary conditions after the end of each switching time interval, depending on its location (section or zone). This time dependence of the boundary conditions leads to cyclic steady state for the SMB system, instead of a real steady-state present in the TMB approach; it means that, after the cyclic steady-state is achieved, the internal concentration profiles vary along the switching time interval, but they are identical at the same time for any consecutive cycles. The cyclic steady-state of the SMB is equivalent to the real steady-state of the TMB for high degree of subdivisions of the SMB adsorbent bed is used (Azevedo and Rodrigues, 2000; Pais et al., 1998; Silva and Rodrigues, 2004). Hence it is better to simulate and obtain the optimum operating conditions using the TMBR model since it requires lower computing time. The cyclic behavior of the SMB can be predicted from the steady-state model of the TMB, by considering the relation between the interstitial solid velocity U_s and the switching t^* in SMB operation:

$$U_s = \frac{L_C}{t^*} \tag{6.1}$$

where L_C is the length of the column.

The equivalence between the SMB and TMB system is made by keeping constant net-flow of the liquid relative to the solid:

$$U_j^{SMB} = U_j^{TMB} + U_s \tag{6.2}$$

where U_j is the interstitial fluid velocity in the j section of the moving bed. The ratio between the fluid and solid interstitial velocities in each section is given by:

$$\gamma_j = \frac{U_j^{TMB}}{U_s} \tag{6.3}$$

The design of SMB involves the right choice of the operating conditions like switching time period and flow rates in each section of the unit. The net flow rate has to be selected in each section in order to ensure the regeneration of the adsorbent in the Section I (Zone I), the desorption of the less adsorbed component in Section II, the adsorption of more retained component in Section III and the regeneration of the eluent in Section IV. These conditions will guarantee the separation, since the more adsorbed component, B, moves to the extract port with solid phase and the less retained component, A, moves to the raffinate port along with the liquid phase.

Since it is not adequate to search suitable SMB operating conditions by trial and error procedures, great progress should be made by using the equilibrium model applied to the equivalent TMB, where axial mixing and mass transfer resistance are neglected and linear adsorption equilibrium is assumed. The analysis of the equivalent representation of a true moving bed under an equilibrium model leads to explicit inequality relations between liquid and solid interstitial velocities in the four TMB sections (γ_j):

$$K_B < \gamma_1 < \infty \tag{6.4}$$

$$K_A < \gamma_2 < \gamma_3 < K_B \tag{6.5}$$

$$0 < \gamma_4 < K_A \tag{6.6}$$

where K_A and K_B are the adsorption equilibrium constants for the less and more retained components, respectively. With the equilibrium theory, it is possible to set the net-flows in Section I and Section IV which ensure the solid and eluent regeneration, respectively. And hence the design of the SMB consists in the determination of the set of pairs of net-flow in the Section II and Section III that accomplish the desired separation. These space-operating parameters lead to the separation region (Triangle Theory) as shown in Figure 6.4.

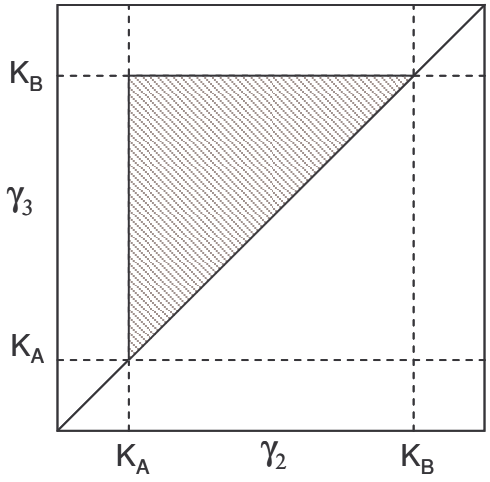

Figure 6.4 Separation region for the complete separation under the equilibrium theory.

The equilibrium models cannot be linked to the product purities with the section flowrates, zone lengths and mass transfer parameters; therefore, the resulting design can only serve as an initial for the SMB optimization. The suitable operating conditions (like flowrates, switching time, feed concentration) and geometrical parameters (like column dimensions, extra-column piping etc.) could be obtained by the use of a complete model that includes the mass transfer effects. For the SMB design, the Linear Driving Force (LDF) approximation is introduction to describe the mass transfer effects, which shows that the separation region was considerably reduced when the mass-

transfer resistances are significant (Pais et al., 1997; Silva et al, 2004, Silva and Rodrigues, 2004).

6.2.2.4. Simulated Moving Bed Reactor (SMBR)

In this present work, the application of the SMB process in which introducing a reactive mixture indicates as a Simulated Moving Bed Reactor (SMBR) is addressed. The main application is in the case of reactions limited by the chemical equilibrium. Thus coupling the reaction and separation in the same unit allows driving the reaction to completion while recovering the products one in the extract and other in the raffinate streams. Besides reactive distillation, reactive extraction or reactive adsorption, coupling of chemical and biochemical reaction with chromatographic separation is an attractive integrated process for producing high-purity products. The integration of reaction and chromatographic separation offers various advantages worth mentioning for reversible reactions, conversion can be increased beyond chemical equilibrium by continuously removing the products from the reaction zone. Obviously, the combination of two unit operations in one single apparatus leads to smaller capital investments. Several applications for the liquid reactions in SMBR are, for biochemical reactions (Anjushri et al., 2005), the isomerization of glucose by the action of glucose isomerase (Zhang et al., 2004), the inversion of sucrose by action of invertase (Azevedo and Rodrigues, 2001). For chemical reactions, major examples are reversible reactions catalyzed by ion exchange resins. Examples are the esterification of acetic acid with b-phenetyl alcohol (Kawase et al., 1996), ethyl acetate synthesis on Amberlyst 15 (Mazzotti et al., 1996; Migliorini et al., 1999), synthesis of bisphenol A from acetone and phenol (Kawase et al., 1999), esterification of acetic acid with methanol (Lode et

al., 2001), synthesis of MTBE (Zhang et al., 2001), acetalization of ethanol and acetaldehyde (Silva and Rodrigues, 2005).

The design and optimization of SMBR should be carried out simultaneously, the continuous reaction and separation are essential to define the feasibility of the process at industrial scale. The design will define geometric and operating parameters that should lead not only to the product separation but also to high reaction conversion. The recent publications are evidence for the reversible reactions catalyzed by ion exchange resins. A key aspect of this technology to be competitive is the proper design of the operating conditions; which is due to the complexity of the unit requires the development of the appropriate simulation models. Design procedures have been recently developed, starting from the so-called triangle theory developed earlier for non-reactive SMBs.

Here in this Chapter, acetalization reaction of acetaldehyde and methanol was considered to produce acetal in SMBR, which reaction is limited by chemical equilibrium. The product, acetal (dimethylacetal or 1,1-dimethoxyethane) is having large number of industrial interest in various areas such as intermediates, solvent, pharmaceuticals, flavors, fragrances, fuel additives and others. The feasibility of the process for the production of acetal in SMBR will be studied experimentally using SMBR pilot unit Licosep 12-26 (Novasep, France) with twelve columns packed with acid resin Amberlyst 15 (Rohm and Haas, France). A mathematical model for SMBR unit based on the TMBR strategy, using a suitable representation of the experimentally determined reaction kinetics in batch reactor and multicomponent adsorption equilibrium from fixed bed experiments is developed and validated. The SMBR process is investigated through numerical simulations in order to identify the governing design parameters.

6.3 SMBR Unit (LICOSEP 12-26)

6.3.1 Experimental Apparatus

The SMBR Unit is a pilot unit LICOSEP 12-26 (Novasep, France), in which all SMBR experiments were performed in this present work. The SMBR Unit is constructed with twelve columns of Superformance SP 300-26 (300 mm length of the column and internal diameter of 26 mm), by Göteo Labartechnik (Mühltal, Germany). These columns can withstand up to 60 ^{o}C and 60 Bar pressure. All the twelve columns were packed with the acid resin Amberlyst 15 (Rohm and Haas, France). Each column is jacketed to ensure the desired temperature in the column; the jackets of each column are connected to one another with the help of silicon houses through a thermostat bath (Lauda, Germany). The thermostat bath can be operated for the circulation of water through the columns jacket in order to maintain the desired temperature of the packed bed in the column. Between every two columns, there exists a four-port valve (Top-Industrie, France) actuated by the control system. According to the operating conditions of the SMBR, when required, the valves allow either pumping of the feed or eluent into the columns or withdrawal of extract or raffinate from the system. Each of the inlet streams (feed or eluent) and outlet streams (extract or raffinate) is pumped by means of HPLC pumps. The recycling pump is arranged for the SMBR unit, and this is a positive displacement three-headed membrane pump (Dosapro Milton Roy, France), which can deliver flow-rates as low as 20 mL/min up to 120 mL/min and it an withstand upto 100 Bar pressure. The calibration of the recycling pump should be performed every time when ever eluent or desorbent is changed. The procedure to perform the calibration of the recycling pump is given in Appendix D. The other flow-rates (eluent, extract, feed and raffinate) are controlled by four Merck-Hitachi pumps (Merck-Hitachi L-6000

model for extract and raffinate, where as for eluent and feed are Merck-Hitachi L-6200 model, Japan) All the pumps (eluent, extract, feed, raffinate and recycling) are controlled by a central system composed of a micro-computer ARCHE 386 SX 25 MHz with an in-built arithmetic co-processor. The flow-rates in the eluent and extract pumps can be operated up to 30 mL/min, where as in the feed and raffinate pump it is only up to 10 mL/min. In all the above pumps, the maximum allowable pressure is 60 Bar. Between the 12^{th} column and the 1^{st} column of the system, there is a six-port valve used to perform internal tests. Figure 6.5 shows a front view of the SMB pilot unit, where other six columns are fixed on the other side of the system.

Figure 6.5 SMB Pilot Unit at LSRE (Laboratory of Separation and Reaction Engineering).

The SMBR equipment is accomplished with its own process control software (Licosep), which enables to accomplish the following tasks:

1. Switching the inlet (Eluent and Feed) and outlet (Extract and Raffinate) streams at regular time intervals (as desired by user) by opening and closing on-off pneumatic valves;

2. Monitors the flow-rates in the system and keep steady and constant section flow-rates as assigned by user;
3. Monitors the pressure in all the pumps and alarms if the pressure is exceeding the limit in the system;
4. Keep suction pressure of the recycling pump ± 0.5 Bar to a set point assigned by the user.

All tubing between the columns consists of 1/16" external diameter and 1 mm internal diameter. The recycling pump introduces a dead volume and this accounts for 21 cm^3. Its adverse effects in delaying the concentrations leaving the last column (12^{th} column) and entering to the first column and this is been overcome by desynchronizing the switches of the ports which are about to or have been shifted across the pump at each cycle. In such cases, the switching time is delayed by t_d minutes, which is calculated from the following Equation 6.7:

$$t_d \text{ (min)} = \frac{21}{\overline{Q} \ (mL/\text{min})} \tag{6.7}$$

$$\text{where } \overline{Q} = \frac{\sum_{1}^{4} Q_j}{4} \tag{6.8}$$

and Q_j (j = 1 to 4) represents the recycling flow-rate set by Licosep depending on the recycling pump location (in section I, II, III, or IV). Each of the twelve columns were assumed to be homogeneously packed. The characteristics of the columns packed are used in the simulations and are presented in the Table 6.1.

6.3.2. Mathematical Model

As stated earlier, the SMBR modeling strategy is more precise than the TMBR

Table 6.1. Characteristics of the SMB Column packed with Amberlyst 15 (Silva, 2003)

Length of the Packed bed (L)	0.23 m
Internal diameter of the column	0.026 m
Radius of the particle (r_p)	400 μm
External void fraction (ε)	0.4
Internal void fraction (ε_p)	0.4
Peclet number	300
Bulk density (ρ_b)	390 kg/m^3

model since it performs as the actual physical equipment operation. It allows the visualization of the axial movement of concentration profiles and the variations in extract and raffinate concentrations within a period. However, it demands considerably higher computational effort than the TMBR strategy, especially when a large number of columns are involved. Cyclic behavior of the SMBR can be predicted from the steady-state model of the TMBR model with good accuracy. Hence, the mathematical model used to observe the SMBR performance is on the basis of TMBR strategy considering axial dispersion flow for the bulk fluid phase, plug flow for solid phase, linear driving force (LDF) for the particle mass transfer rate and multicomponent adsorption equilibria. Length of the column (packed bed length) and porosity of the packed bed are assumed to be constant.

Bulk fluid mass balance to component i and in section j :

$$\varepsilon \frac{\partial C_{ij}}{\partial t} + \varepsilon u_j \frac{\partial C_{ij}}{\partial z} + (1-\varepsilon)\frac{3}{r_p} K_{L,i}(C_{ij} - \overline{C}_{p,ij}) = \varepsilon D_{ax,j} \frac{\partial^2 C_{ij}}{\partial z^2} \qquad (6.9)$$

where C_{ij} and $\overline{C}_{p,ij}$ are the bulk and average particle concentrations in the fluid phase of species *i* in section *j* of the TMBR, respectively, $K_{L,i}$ is the global mass transfer coefficient of the component *i*, ε is the bulk porosity (bed porosity), *t* is the time variable, *z* is the axial coordinate, $D_{ax,j}$ and u_j are the axial dispersion coefficient and the interstitial velocity in section *j*, respectively, and r_p is the particle radius.

Pellet mass balance to component i and in section j :

$$U_s\left[\varepsilon_p\frac{\partial\overline{C}_{p,ij}}{\partial z}+(1-\varepsilon_p)\frac{\partial q_{ij}}{\partial z}\right]+\frac{3}{r_p}K_{L,i}(C_{ij}-\overline{C}_{p,ij})=\varepsilon_p\frac{\partial\overline{C}_{p,ij}}{\partial t}+(1-\varepsilon_p)\frac{\partial q_{ij}}{\partial z}-\nu_i\rho_p\eta\Re \quad (6.10)$$

where q_{ij} is the average adsorbed phase concentration of species *i* in section *j* in equilibrium with $\overline{C}_{p,ij}$, U_s is the solid velocity and ε_p is the particle porosity, ν_i is the stoichiometric coefficient of component *i*, ρ_p is the particle density, η is the effectiveness factor of the catalyst and $\Re$ is the chemical reaction rate relative to the bulk liquid phase which was given as (Gandi et al., 2005):

where $$\eta=\frac{R(\overline{C}_p)}{R(C_b)} \quad (6.11)$$

$$\Re=k_c\frac{a_Aa_B-\frac{a_Ca_D}{K_{eq}a_A}}{\left(1+K_{s,D}a_D\right)^2} \quad (6.12)$$

and effectivness factor, η is 0.415 at 20 ^{0}C.

Initial and Danckwerts boundary conditions:

at $t=0$ $$C_{ij}=\overline{C}_{p,ij}=C_{ij,0} \quad (6.13)$$

$z=0$ $$u_jC_{ij}-D_{ax,j}\left.\frac{\partial C_{ij}}{\partial z}\right|_{z=0}=u_jC_{ij,F} \quad (6.14)$$

$$z = L \qquad \left.\frac{\partial C_{ij}}{\partial z}\right|_{z=L} = 0 \text{ and} \qquad \overline{C}_{ij,L} = \overline{C}_{ij+1,0} \tag{6.15}$$

where *F* and 0 refer to the feed and initial states, respectively.

Multicomponent adsorption equilibrium isotherm:

$$q_{ij} = \frac{Q_{ads,i} K_i \overline{C}_{p,kj}}{1 + \sum_{k=1}^{n} K_k \overline{C}_{p,kj}} \tag{6.16}$$

where $Q_{ads,i}$ and K_i represent the total molar capacity per unit volume of resin and the equilibrium constant for component *i*, respectively.

Mass balances at the nodes of the inlet and outlet lines of the TMBR:

Eluent Node: $$C_{ij+1,0} = \frac{u_4}{u_1} C_{ij,L_j} \tag{6.17}$$

Extract Node: $$C_{ij+1,0} = C_{ij,L_j} \tag{6.18}$$

Feed Node: $$C_{ij+1,0} = \frac{u_2}{u_3} C_{ij,L_j} + \frac{u_F}{u_3} C_{i,F} \tag{6.19}$$

Raffinate Node: $$C_{ij+1,0} = C_{ij} \tag{6.19}$$

The relationships between fluid velocities in the four zones (Section I, II, III, and IV) of the TMBR:

$$u_1 = u_4 + u_D,\ u_2 = u_1 + u_X,\ u_2 = u_3 + u_F,\ u_4 = u_3 - u_R \tag{6.20}$$

where u_1, u_2, u_3, and u_4 are the fluid velocities in the Sections I, II, III and IV, respectively. The subscripts *D, F, R* and *X* refer to the desorbent, feed, raffinate and extract streams, respectively.

SMBR performance criteria

The SMBR process performance can be evaluated according to the following criteria:

Raffinate Purity (%): $$PUR = \frac{C_{C,R}}{C_{B,R} + C_{C,R} + C_{D,R}} \times 100 \quad (6.21)$$

Extract Purity (%): $$PUX = \frac{C_{D,R}}{C_{B,R} + C_{C,R} + C_{D,R}} \times 100 \quad (6.22)$$

Acetaldehyde Conversion (%): $$X = \left(1 - \frac{Q_X C_{B,X} + Q_R C_{B,R}}{Q_F C_{B,F}}\right) \times 100 \quad (6.23)$$

Raffinate Productivity (mol/min/L): $$PR = \frac{Q_R C_{C,R}}{(1-\varepsilon) V_{unit}} \quad (6.24)$$

Desorbent Consumption (L/mol): $$DC = \frac{Q_D C_{A,D} + Q_F \left(C_{A,F} - 2X\, C_{B,F}\right)}{Q_F C_{B,F}} V_{ml,A} \quad (6.25)$$

Just for the raffinate stream, the productivity is defined here as acetal (desired product) produced is coming out from the raffinate stream. Desorbent consumption is considered here is the amount of methanol consumed as a desorbent and not the methanol consumed for reaction. Above model equations were solved numerically by using the gPROMS-general PROcess Modelling System (gPROMS, 2003). gPROMS is a software package for modeling and simulation of processes with both discrete and continuous as well as lumped and distributed characteristics. The mathematical model involves a system of partial and algebraic equations (PDAEs). Third order orthogonal collocation in finite elements method (OCFEM) was used in the discretization of axial domain. Twenty equal elements per section with two collocation points in each element were used. The system of ordinary differential and algebraic equation (ODAEs) was integrated over time using the DASOLV integrator implementation in gPROMS. For all simulations was fixed a tolerance equal to 10^{-5}.

6.3.3. Effect of SMBR Switching time

Period of rotation or Switching time is the time period between two successive movements of the inlet (feed and eluent) and outlet (extract and raffinate) ports of the SMBR system. The influence of the switching time on the SMBR system performance was studied with three different switching times for a feed composition of 60 % (mole %) acetaldehyde and a twelve-column configuration (3 columns in each section) keeping the same section flow-rates. Initially all columns are completely saturated with methanol as methanol being used as desorbent. The operating conditions and simulated performances of the system are given in the Table 6.2.

Table 6.2 Operating conditions and simulated performance of the SMBR unit.

Operating Conditions and Data	Run 1	Run 2	Run 3
Switching time (t^*)	**3.0 min**	**3.2 min**	**2.8**
Desorbent flow-rate (Q_D)	40.0 mL/min	40.0 mL/min	40.0 mL/min
Temperature	293.15 K	293.15 K	293.15 K
Feed flow-rate (Q_F)	10.0 mL/min	10.0 mL/min	10.0 mL/min
Extract flow-rate (Q_X)	30.0 mL/min	30.0 mL/min	30.0 mL/min
Raffinate flow-rate (Q_R)	20.0 mL/min	20.0 mL/min	20.0 mL/min
Section IV Recycling flow-rate (Q_4)	25.0 mL/min	25.0 mL/min	25.0 mL/min
PUR	99.24 %	83.95 %	98.11 %
PUX	99.33 %	97.29 %	84.39 %
Conversion of acetaldehyde (X)	99.78 %	92.02 %	97.65 %
Desorbent consumption ($L_{methanol}$/ kg_{acetal})	3.11	3.52	3.79
Raffinate Productivity ($kg_{acetal}/L_{adsorbent}$/day)	17.63	15.97	14.57

The influence of switching time on the steady-state profiles for acetaldehyde, acetal (DME), methanol and water in the SMBR performance is shown in Figure 6.6 for the runs performed shown in Table 6.2. It can be seen that for the switching time with 3.0 min, high purities of extract, raffinate and high conversion of acetaldehyde is observed in the performance of the SMBR unit.

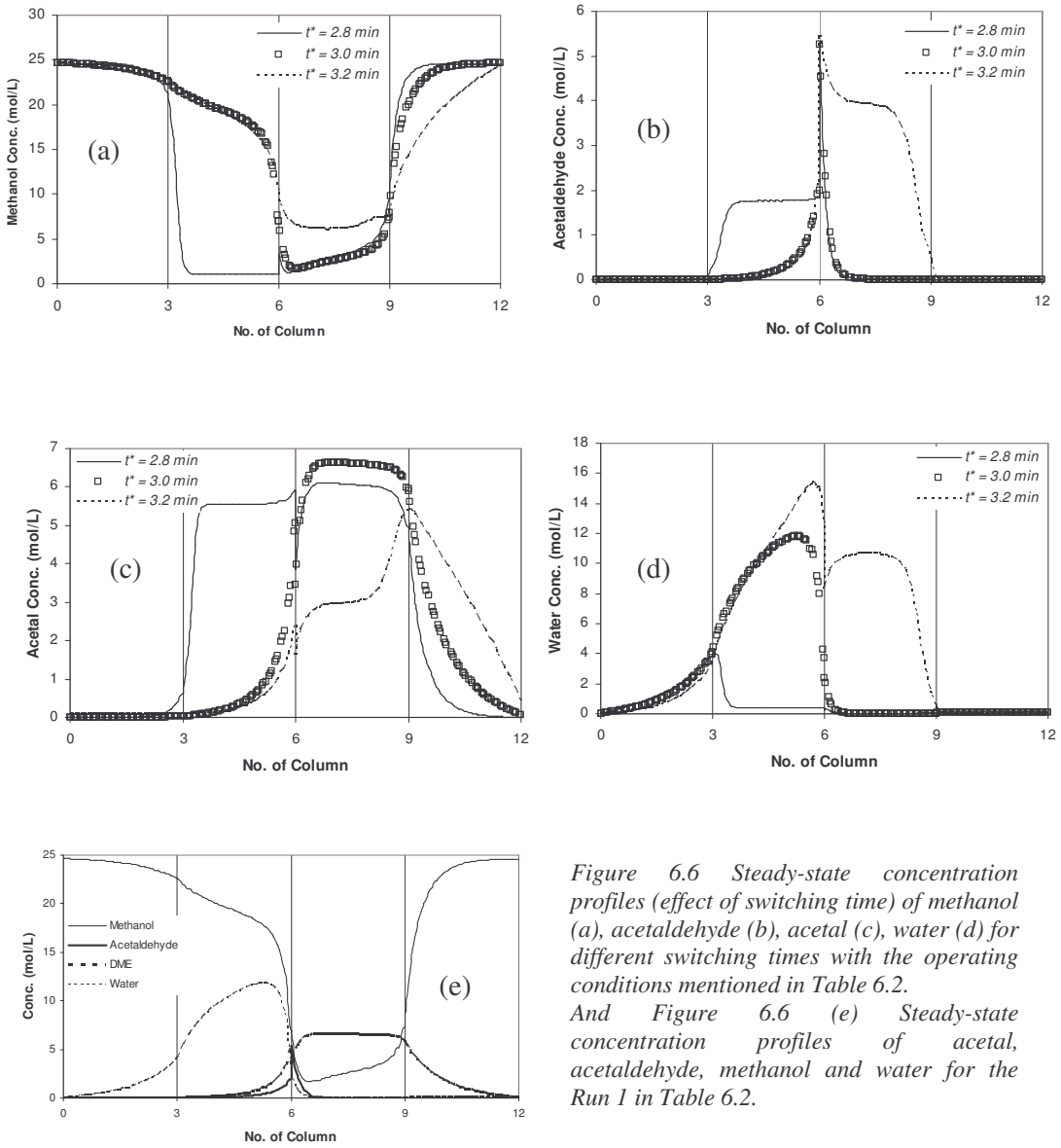

Figure 6.6 Steady-state concentration profiles (effect of switching time) of methanol (a), acetaldehyde (b), acetal (c), water (d) for different switching times with the operating conditions mentioned in Table 6.2.
And Figure 6.6 (e) Steady-state concentration profiles of acetal, acetaldehyde, methanol and water for the Run 1 in Table 6.2.

Where as it was not the same case with switching time 2.8 min and 3.2 min with respect to the extract, raffinate purities and the acetaldehyde conversion. It is clear from the Figure 6.6, that the influence of switching time plays a significant role both for the reaction and separation parts on the SMBR unit performance. If the conditions of section II and section III guarantee the acetal-water separation in the range of t^* = 2.8 and 3.2 min, the switching time will affect the acetaldehyde net-flow and acetaldehyde appears only in the section II for t^* = 2.8 min or in section III for t^* = 3.2 min or in both sections with t^* = 3.0 min, and the residence time of acetaldehyde in that sections should be enough to achieve complete conversion.

6.3.4. Effect of SMBR Configuration

The optimization at the design stage allows more flexibility as one can determine optimal values of length, number and distribution of columns in different sections in addition to the one discussed in section 6.3.3.1. Here, it was studied only the distribution of columns in each section of the SMBR unit. One case study was performed for the run 3 indicated in the Table 6.2 consisting of 3 columns in section I, 5 columns in section II and 2 columns in both section III and section IV. It can be seen that the improvement in the SMBR performance (extract, raffinate purities and acetaldehyde conversion) is not significant as given in the Table 6.3.

Table 6.3 Simulated performance of the SMBR unit.

Experiment Conditions and Data	Run 3	Run 4
Switching time (t^*)	2.8	2.8
Configuration (no. of columns in each section)	**3-3-3-3**	**3-5-2-2**
PUR	98.11 %	98.16 %
PUX	84.39 %	85.37 %
Conversion of acetaldehyde (X)	97.65 %	97.81 %
Desorbent consumption ($L_{methanol}$/ kg_{acetal})	3.79	3.73
Raffinate Productivity ($kg_{acetal}/L_{adsorbent}$/day)	14.57	14.81

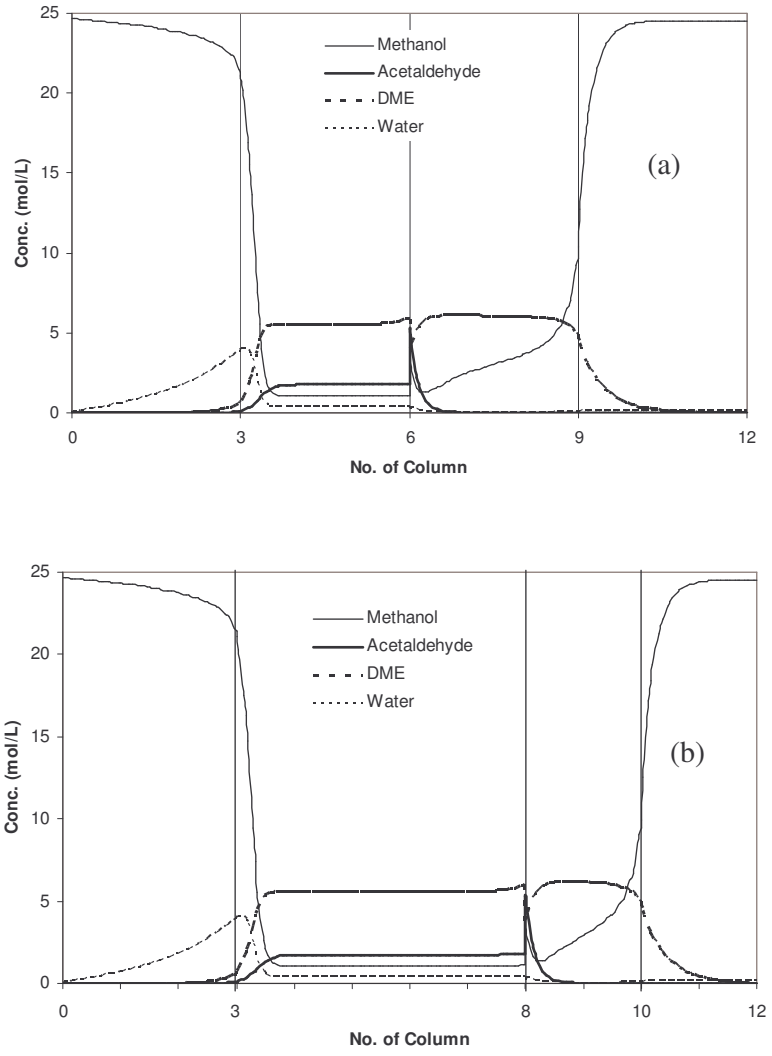

Figure 6.7 Steady-state concentration profiles: effect of configuration (a) Configuration 3-3-3-3 (b)Configuration 3-5-2-2

The performance profiles at steady-state shown in the Figure 6.7.

6.3.5. Experimental Results and Discussion

The SMBR experiments were performed under the conditions of completely adsorbent regeneration in Section I. The recycle pump was operated at the minimum flow-rate (25 mL/min). For the desorbent the maximum flow-rate of the pump (30 mL/min) was not used as the system was not stable at higher flow-rates.

One experiment of dimethylacetal synthesis was performed at 20 ^{o}C in the SMBR unit, the configuration of the SMBR unit was 3 columns per section. The mixture of acetaldehyde and methanol was fed to the system with feed composition of 40% acetaldehyde molar fraction ($C_{A,F}$ = 12.82 mol/L; $C_{B,F}$ = 8.55 mol/L). The flow-rates of feed, rafiinate and extract streams were Q_F = 3.0 mL/min, Q_R = 8.0 mL/min, Q_X = 20.0 mL/min. The other experimental conditions and the SMBR experimental and simulated (inside brackets) performance criteria are presented in Table 6.4. The steady-state concentration profiles obtained experimentally at the middle of the switching time after 8 cycles are compared with the steady-state profiles obtained from the simulated results by the TMBR model in Figure 6.8. The stationary steady-state predicted with the TMBR model are compared with the experimental results, continuous lines in the Figure 6.8 represents the concentration profiles from TMBR model and points are experimental profiles in a SMBR at the middle of a switching time at cyclic steady-state (8th Cycle)

Table 6.4 Operating conditions and experimental/simulated performance parameters of the SMBR unit.

Experiment Conditions and Data	
Switching time (t^*)	3.0 min
Desorbent flow-rate (Q_D)	25.0 mL/min
Section IV Recycling flow-rate (Q_4)	25.0 mL/min
PUR	91.41 (95.33)%
PUX	99.95 (98.74)%
Conversion of acetaldehyde (X)	97.61 (99.08)%
Productivity	8.62 (5.79)
Desorbent Consumption	4.52 (6.72)

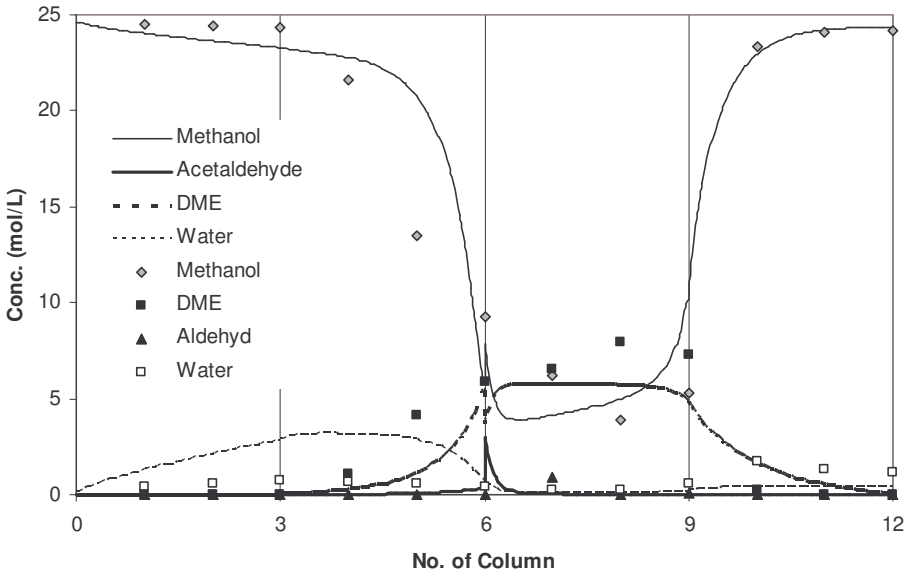

Figure 6.8 Experimental and simulated concentration profiles in a SMBR at the middle of a switching time at cyclic steady-state (8th Cycle).

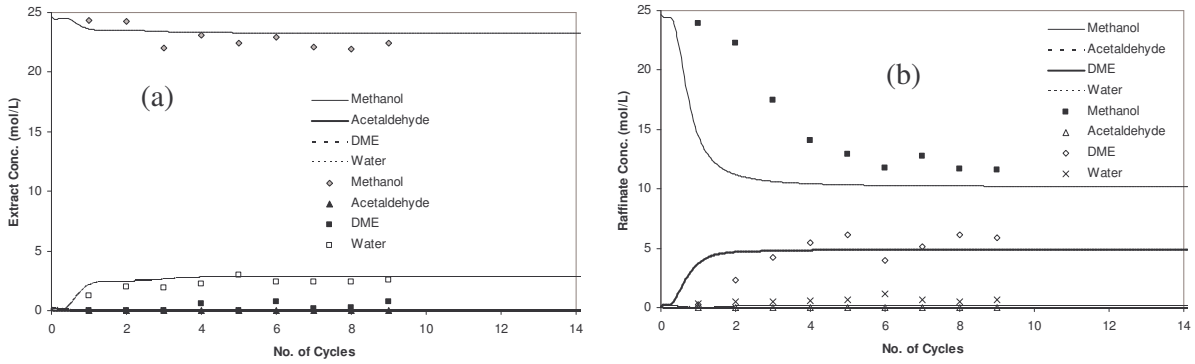

Figure 6.9Extract and Raffinate purities along the cycle. (a) Extract Purity (b) Raffinate Purity. Lines are simulated results; points are experimental

Extract and raffinate purity concentration was analyzed for all the cycles of the SMBR experiment. Concentration plots were presented in the Figure 6.9 for both extract and raffinate along with the simulated profiles. The steady-state SMBR profiles for the above experiment with the operating conditions mentioned in Table 6.4 are presented in

the Appendix E. Two other experiments with different switching time and configuration was performed in the SMBR, the experimental SMBR profiles were presented in Appendix E along with the operating conditions and initial conditions of the system.

6.4 Conclusions

Brief review was made to the True Moving Bed (TMB), Simulated Moving Bed (SMB) and Simulated Moving Bed Reactor (SMBR) concepts. The Simulated Moving Bed Reactor (SMBR) for the synthesis of dimethylacetal dimethylacetal was studied experimentally and with simulations. The experimental results are compared with the TMBR modeling strategy. The mathematical model assumes axial dispersion flow for the bulk fluid phase, plug flow for the solid phase, linear driving force (LDF) for the particle mass transfer rate and multicomponent adsorption equilibria. In the prediction of SMBR performance, the kinetic and adsorption parameters obtained from batch and fixed bed reactor experiments were considered in the TMBR modeling strategy. The stationary steady-state predicted from the TMBR model are in agreement with the experimental SMBR cyclic steady-state at the middle of the switching time behavior, in terms of internal concentration profiles.

6.5 Nomenclature

a - liquid-phase activity

C - liquid phase concentration (mol/L)

C_b - bulk liquid phase concentration (mol/L)

$\overline{C}_p$ - average liquid phase concentration inside the particle (mol/L)

d_p - particle diameter (m)

D_{ax} - axial dispersion (m^2/s)

DC - desorbent consumption (m^3/mol)

k_c - kinetic constant (mol/kg_{res}s)

K - Langmuir equilibrium parameter (m^3/mol)

K_{eq} - equilibrium reaction constant

K_L - global mass transfer coefficient (m/s)

L_c - column length (m)

Pe - Peclet number

PR - raffinate productivity (mol/min/L)

PUR - raffinate purity (%)

PUX - extract purity (%)

p - solid phase concentration (mol/m^3_{res})

Q_{ads} - adsorption capacity (mol/m^3_{res})

Q - volumetric flow-rate (m^3/s)

$\Re$ - reaction rate (mol/kg_{res}s)

r_p - particle radius (m)

t - time (s)

t^* - switching time (min)

u - interstitial fluid velocity (m/s)

U_s - interstitial solid velocity (m/s)

V_{ml} - molar volume in liquid phase (m^3/mol)

X - acetaldehyde conversion (%)

z - axial coordinate (m)

Greek letters

ε - bulk porosity

ε_p - particle porosity

ν - stoichiometric coefficient

γ - ratio between liquid and solid interstitial velocities

η - effectiveness factor

ρ_b - bulk density (kg/m^3)

ρ_p - particle density (kg/m^3)

Subscripts

D - relative to the desorbent

i - relative to component i ($i = A, B, C, D$)

j - relative to the section in SMB

p - relative to particle

R - relative to raffinate

SMB - relative to a SMB process

X - relative to extract

0 - relative to initial conditions

TMB – relative to a TMB process

6.6 References

(1) Azevedo, D. C. S.; Rodrigues, A. E. Fructose-Glucose Separation in a SMB Pilot Unit: Modeling, Simulation, Design, and Operation. *AIChE. J.*, **2001**, 47, 2042-2051.

(2) Broughton, D.B.; Gerhold, C. G. *Continuous sorption process employing fixed bed of sorbent and moving inlets and outlets*. U.S. Patent No. 2,985,589, **1961**.

(3) Chopade, S. P.; Sharma, M. M. Reaction of ethanol and formaldehyde: use of versatile cation-exchange resins as catalyst in batch reactors and reactive distillation column. *React. Funct. Polym.* **1997,** 32, 53-64.

(4) Chu, K. H.; Hashim, M. A. Simulated countercurrent adsorption processes: a comparison of modelling strategies. *Chem. Eng. J*. **1995**, 56, 59-65.

(5) Cruz, V. J.; Izquierdo, J. F.; Cunill, F.; Tejero, J.; Iborra, M.; Fité, C. Acid ion-exchange resins catalysts for the liquid-phase dimerization/etherification of isoamylenes in methanol or ethanol presence. *React. Funct. Polym.* **2005,** 65, 149-160.

(6) Dinwiddie, J. A.; Morgan, W. *Fixed bed type reactor*. U.S. Patent No. 2,976,132, **1961**.

(7) Do, D. D. Adsorption Analysis: Equilibria and Kinetics. Imperial College Press, London, 1998.

(8) Ferreira, M. V.; Loureiro, J. M. Number of active sites in TAME synthesis: Mechanism and kinetic modeling. *Ind. Eng. Chem. Res.* **2004,** 43, 5156.

(9) Gandi, G. K.; Silva, V. M. T. M.; Rodrigues, A. E. "Process development for the dimethylacetal synthesis: Thermodynamics and reaction kinetics". *Ind. Eng. Chem. Res.* **2005**, *44*, 7287-7297.

(10) Giovanni, O. Di.; Mazzotti, M.; Morbidelli, M.; Denet, F.; Hauck, W.; Nicoud, R. M. Supercritical fluid simulated moving bed chromatography II. Langmuir isotherm. *J. Chromatogr. A*. **2001**, 919, 1-12.

(11) gPROMS. gPROMS v 2.2.3. User Guide. (Process System Enterprise Ltd., London, 2003).

(12) Grill, C. M.; Miller, L. Resolution of a racemic pharmaceutical intermediate A comparison of preparative HPLC, steady state recycling and simulated moving bed. *J. Chromatogr. A*. **2004**, 1026, 101-108.

(13) Guest, D. W. Evaluation of simulated moving bed chromatography for pharmaceutical process development. *J. Chromatogr. A*. **1997**, 760, 159-162.

(14) Huthmann, E.; Juza, M. Less common applications of simulated moving bed chromatography in the pharmaceutical industry. *J. Chromatogr. A*. **2005**, 1092, 24-35.

(15) Juza, M.; Giovanni, O. Di; Biressi, G.; Schurig, V.; Mazzotti, M.; Morbidelli, M. Continuous enantiomer separation of the volatile inhalation anesthetic enflurane with a gas chromatographic simulated moving bed unit. *J. Chromatogr. A*. **1998**, 813, 333-347.

(16) Kawase, M.; Inoue, Y.; Araki, T.; Hashimoto, K. The Simulated Moving Bed reactor for production of bisphenol A. *Catal. Today* **1999**, 48, 199-209.

(17) Kawase, M.; Suzuki, T. Ben; Inoue, K.; Yoshimoto, K.; Hashimoto, K. Increased esterification conversion by application of the Simulated moving-bed reactor. *Chem. Eng. Sci*. **1996**, 51, 2971-2976.

(18) Klatt, Karsten-Ulrich; Hanisch, F.; Dünnebier, G. Model-based control of a simulated moving bed chromatographic process for the separation of fructose and glucose. *Journal of Process Control*, **2002**, 12, 203-219.

(19) Kurup, A. S.; Subramani, H. J.; Hidajat, K.; Ray, A. K. Optimal design and operation SMB bioreactor for sucrose inversion. *Chem. Eng. J*. **2005**, 108, 19-33.

(20) Lode, D.; Houmard, M.; Migliorini, C.; Mazzotti, M.; Morbidelli, M. Continuous reactive chromatography. *Chem. Eng. Sci*. **2001**, 56, 269-291.

(21) Mazzotti, M.; Kruglov, A.; Neri, B.; Gelosa, D.; Morbidelli, M. A Continuous Chromatographic Reactor: SMBR. *Chem. Eng. Sci*. **1996**, 51, 1827-1836.

(22) McCabe, W. L.; Smith, J. C.; Harriott, P. *Unit Operations of Chemical Engineering*. 5th Edition, McGraw-Hill: New York, 1991.

(23) Migliorini, C.; Fillinger, M.; Mazzotti, M.; Morbidelli, M. Analysis of Simulated Moving Bed Reactors. *Chem. Eng. Sci*. **1999**, 54, 2475-2480.

(24) Migliorini, C.; Wendlinger, M.; Mazzotti, M.; Morbidelli, M. Temperature Gradient Operation of a Simulated Moving Bed Unit. *Ind. Eng. Chem. Res*. **2001**, 40, 2606-2617.

(25) Miller, L; Grill, C.; Yan, T.; Dapremont, O.; Huthmann, E.; Juza, M. Batch and simulated moving bed chromatographic resolution of a pharmaceutical racemate. *J. Chromatogr. A*. **2003**, 1006, 267-280.

(26) Minceva, M. Separation/isomerisation of xylenes by simulated moving bed technology. *Ph.D. Thesis*, University of Porto, **2004**.

(27) Minceva, M.; Rodrigues, A. E. Modeling and simulation in chemical engineering: Tools for process innovation. *Comp. Chem. Eng*. **2005**, 29, 1167-1183.

(28) Pais, S. L.; Loureiro, J. M.; Rodrigues, A. E. Separation of 1,1'-bi-2-naphthol enantiomers by continuous chromatography in simulated moving bed. *Chem. Eng. Sci*. **1997**, 52, 245-257.

(29) Rekoske, J. E. Chiral Separation. *AIChE*. **2001**, 47, 2.

(30) Rodrigues, A.E.; Lu, Z. P.; Loureiro, J. M.; Pais, S. L. Separation of enantiomers of 1a,2,7,7a-tetrahydro-3methoxynaphtha(2,3b)-oxirane by liquid chromatography: laboratory-scale elution chromatography and modeling of simulated moving bed. *J. Chromatogr.* **1995**, 702, 223.

(31) Ruthven, D. M. *Principles of Adsorption and Adsorption Processes*. John Wiley & Sons, New York, 1984.

(32) Silva, V. M. T. M. *Diethylacetal Synthesis in Simulated Moving Bed Reactor. Ph.D. Thesis*, University of Porto, **2003**.

(33) Silva, V. M. T. M.; Minceva, M.; Rodrigues, A. E. Noval analytical solution for a Simulated Moving Bed in the presence of Mass-Transfer Resistance. *Ind. Eng. Chem. Res*. **2004**, 43, 4494-4502.

(34) Silva, V. M. T. M.; Rodrigues, A. E. "Dynamics of Fixed-Bed Adsorptive Reactor for the Synthesis of Diethylacetal". *AIChE J.* **2002**, 48, 625-634.

(35) Silva, V. M. T. M.; Rodrigues, A. E. "Novel process for dimethylacetal synthesis" *AIChE. J.* **2005**, *51*, 2752.

(36) Silva, V. M. T. M.; Rodrigues, A. E. "Processo industrial de produção de acetais num reactor adsorptivo de leito móvel simulado", Portuguese Patent No. 103,123 (Patent Pending) 2004.

(37) Silva, V. M. T. M.; Rodrigues, A. E. Synthesis of diethyl acetal: thermodynamic and kinetic studies. *Chem. Eng. Sci.*, **2001,** 56 1255-1263.

(38) Wankat, P. C. Rate-Controlled Separation. Blackie Academic & Professional, London 1994.

(39) Yadav, G. D.; Lande, S. V. Rate intensive and selective etherification of vanillin with benzyl chloride under solid–liquid phase transfer catalysis by aqueous omega phase. *J. Mol. Catal. A: Chem*. **2005**, 244, 271-277.

(40) Yadav, G. D.; Manjula Devi, K. Immobilized lipase-catalysed esterification and transesterification reactions in non-aqueous media for the synthesis of

tetrahydrofurfuryl butyrate: comparison and kinetic modeling. *Chem. Eng. Sci*. **2004**, 59, 373-383.

(41) Yadav, G. D.; Pujari, A. A. Kinetics of acetalization of perfumery aldehydes with alkanols over solid acid catalysts. *Canadian Journal of Chemical Engineering*, **1999,** *77*, 489-496.

(42) Zhang, Y.; Hidajat, K.; Ray, A. K. Application of Simulated Countercurrent Moving Bed Chromatographic Reactor for MTBE Synthesis. *Ind. Eng. Chem. Res*. **2001**, 40, 5305-5316.

(43) Zhang, Y.; Hidajat, K.; Ray, A. K. Optimal design and operation SMB bioreactor: production of high fructose syrup by isomerization of glucose. *Biochem. Eng. J*. **2004**, 21, 111-121.

7. Conclusions and Suggestions for Future Work

The aim of this thesis was to study the process development for the synthesis of dimethylacetal (1,1-dimethoxyethane) from acetaldehyde and methanol as raw-material and to catalyze the above acetalization reaction with acid ion exchange Amberlyst 15 resin. Thermodynamic and kinetic experimental studies for acetal synthesis in a liquid phase reaction and catalyzed by Amberlyst-15 resin were performed in a Laboratory-scale experimental set-up. The thermodynamic equilibrium constant was measured in the temperature range of 293 – 333 K and given as $K_{eq} = 0.0143\exp[2142.5/T(K)]$. The standard molar reaction properties were obtained at 298.15 K: ΔS^o = -35.34 J mol^{-1}K^{-1}, ΔH^o = -17.81 kJ mol^{-1} and ΔG^o = -7.28 kJ mol^{-1}. The standard molar properties for formation of acetal in the liquid phase at 298.15 K were estimated from experiments: $\Delta H_f^o = -402.29$ kJ mol^{-1}, $\Delta G_f^o = -230.95$ kJ mol^{-1} and $S_f^o = 308.71$ Jmol^{-1} K^{-1}.

As the strong non-ideality of the liquid reaction mixture, the reaction model was formulated in terms of liquid activities. Reaction experiments were performed at different particle sizes with mean diameter of 335, 510, 800 µm. The measured reaction rates were limited by diffusion inside the particle. The batch reactor mathematical model that includes pore diffusion inside the particle was proposed and used to obtain

the true kinetic rate expression and the model constants dependence on temperature was found by Arrhenius equation. The rate equation can be used in the modeling simulations of the continuous reactor for the dimethylacetal synthesis. The proposed kinetic law expressed in activities is as shown below:

$$\Re = k_c \frac{a_A a_B - \frac{a_C a_D}{K_{eq} a_A}}{\left(1 + K_{s,D} a_D\right)^2}$$

and the parameters are,

$$k_c = 6.91 \times 10^{13} \exp\left[\frac{-8702.6}{T(K)}\right] (\text{mol g}^{-1} \text{ min}^{-1})$$

$$K_D = 2.37 * 10^{32} \exp\left[\frac{-22713}{T(K)}\right] (\text{dimensionless})$$

The activation energy of the reaction is 72.4 kJ mol^{-1}.

The relation between the effectiveness factor and Thiele modulus was determined at 20 ^{o}C for the linear region ($\phi_A \geq 10$) and is given by: $\ln \eta = -1.048 \ln \phi_T + 1.706$ and the Thiele modulus was calculated for different particle sizes with respect to methanol is given below:

$$\phi_T = \frac{r_p}{3} \sqrt{\frac{\rho_p k_c}{D_{A_s} C_{A_s}}}$$

The synthesis of acetal using acetaldehyde and methanol as raw-material in an acidic Amberlyst-15 resin fixed bed adsorptive reactor was studied to determine the dynamic behaviour of acidic resin bed. The primary experiments conducted to collect the desired adsorption data by performing dynamic binary adsorption experiments in absence of reaction at 293.15 K, in a laboratory scale column. The adsorption parameters determined are in the table below:

Component	Q (mol / $m^3_{real\ solid}$)	K (m^3/mol)
Methanol (A)	14.52×10^3	0.60×10^{-3}
Acetaldehyde (B)	18.65×10^3	0.38×10^{-3}
Acetal (C)	7.67×10^3	0.02×10^{-3}
Water (D)	28.49×10^3	1.15×10^{-3}

The mathematical model for the adsorptive reactor was developed, in which axial dispersion, external and internal mass-transfer resistances, constant temperature, and multicomponent Langmuir adsorption isotherms were measured on laboratory scale experimental set-up. The model was compared with the experimental results obtained for reaction and regeneration experiments.

Brief review was made to the True Moving Bed (TMB), Simulated Moving Bed (SMB) and Simulated Moving Bed Reactor (SMBR) concepts. The Simulated Moving Bed Reactor (SMBR) for the synthesis of dimethylacetal dimethylacetal was studied experimentally and with simulations. The experimental results are compared with the TMBR modeling strategy. The mathematical model assumes axial dispersion flow for the bulk fluid phase, plug flow for the solid phase, linear driving force (LDF) for the particle mass transfer rate and multicomponent adsorption equilibria. In the prediction of SMBR performance, the kinetic and adsorption parameters obtained from batch and fixed bed reactor experiments were considered in the TMBR modeling strategy. The stationary steady-state predicted from the TMBR model is in agreement with the experimental SMBR cyclic steady-state at the middle of the switching time behavior, in terms of internal concentration profiles.

The synthesis of acetal (1,1-dimetoxyethane) using acetaldehyde and methanol as raw-material on a Smopex 101 fibres both in batch reactor and in fixed bed

adsorber/reactor. The thermodynamic equilibrium constant was measured in the temperature range of 293.15 – 333.15 K and given as $K_{eq} = 0.0173\exp[2103.3/T(K)]$. The kinetic law was proposed which expressed in activities is shown below:

$$\Re = k_c\left(a_A a_B - \frac{a_C a_D}{K_{eq} a_A}\right)$$

and the parameter k_c is given as follows;

$$k_c = 7.59\times10^8 \exp\left[\frac{-5853.8}{T(K)}\right] (\text{ mol g}^{-1}\text{ min}^{-1}).$$

The activation energy of the reaction is 48.7 kJ mol^{-1}.

The dynamic behaviour of fibres bed was studied. The primary experiments conducted to collect the desired adsorption data by performing dynamic binary adsorption experiments in absence of reaction to determine the adsorption parameters are in the table below.

Component	Q (mol / $m^3_{\text{real solid}}$)	K (m^3/mol)
Methanol (A)	7.0	0.93×10^{-3}
Acetaldehyde (B)	7.0	0.38×10^{-3}
Acetal (C)	7.0	0.84×10^{-3}
Water (D)	7.0	0.93×10^{-3}

Minimizing the difference between the experimental and calculated stoichiometric times of breakthrough curves optimised the adsorption parameters. The mathematical model for the adsorptive reactor was developed and multicomponent Langmuir adsorption isotherms were measured on laboratory scale experimental set-up. The model was

compared with the experimental results obtained for reaction and regeneration experiments.

The production of other acetals (formed form the combination of other alcohols and aldehydes) in SMBR can be an interesting research in order to update the existing process. It is also interesting to extend the research with Sompex 101 fibres in Simulated Moving Bed Reactor for esterification reactions.

Appendix A: Calibration

Pure Component

The calibration was performed by injecting different volumes of pure components at 15 ^{o}C. The volume is converted to number of moles using the molar volumes at 15 ^{o}C shown in Table A.1.

Table A.1. Molar volumes of pure components

Component	Molar Volume (ml/mol)
Acetaldehyde	55.30
Acetal	104.47
Methanol	39.94
Water	17.79

The response factor, (f_i) defined as:

$$n_i = f_i A_i \qquad \text{(A.1)}$$

Where n_i is the number of moles of component *i* (μ mol) and A_i is the area of component *i* (u.a.).

Table A.2. Acetaldehyde

V (µl)	A (u.a.)	n (µmol)
0.1	0.2958	1.7782
0.2	0.5597	3.5584
0.3	0.7857	5.3376
0.4	1.0479	7.1168
0.5	1.2732	8.8959

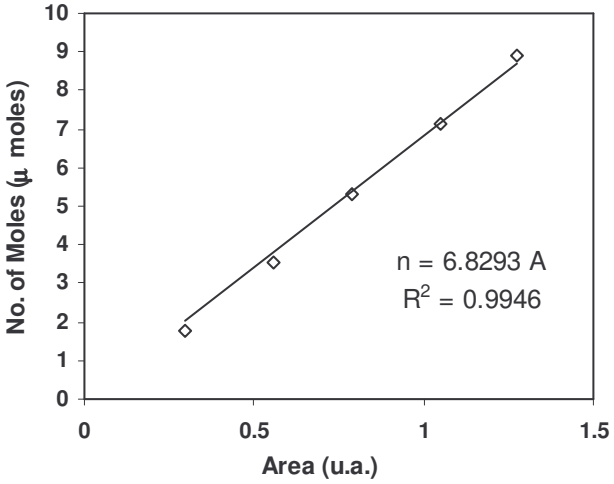

Figure A.1

Table A.3. Acetal (1,1-dimethoxyethane)

V (µl)	A (u.a.)	n (µmol)
0.1	0.2744	0.9572
0.2	0.5229	1.9144
0.3	0.7532	2.8716
0.4	0.9692	3.8289
0.5	1.1823	4.7861

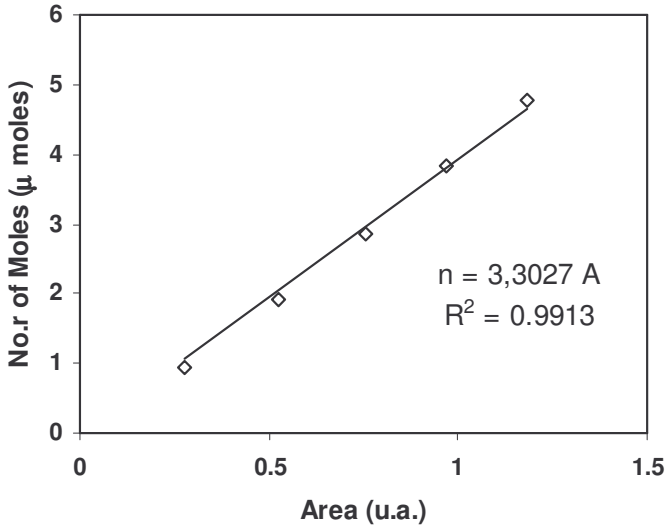

Figure A.2

Table A.4. Methanol

V (µl)	A (u.a.)	n (µmol)
0.1	0.3565	2.5038
0.2	0.6612	5.0075
0.3	0.9547	7.5113
0.4	1.2301	10.015
0.5	1.5088	12.519
0.6	1.7708	15.023

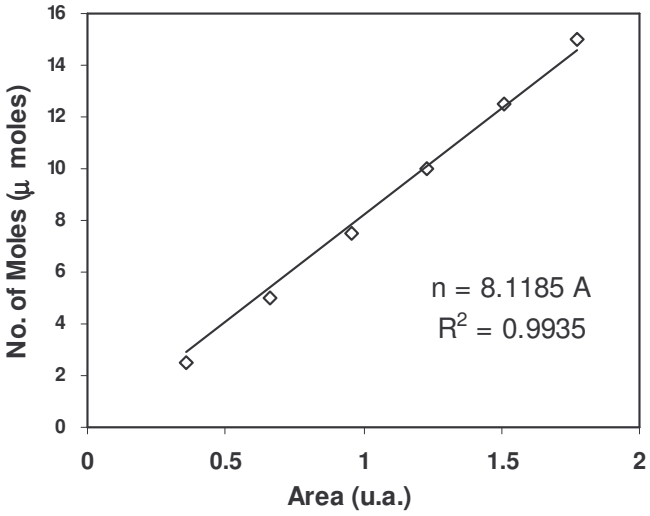

Figure A.3

Table A.5. Water

V (µl)	A (u.a.)	n (µmol)
0.1	0.5250	5.6211
0.2	1.0062	11.242
0.3	1.4814	16.863
0.4	1.9235	22.485
0.6	2.8329	33.727

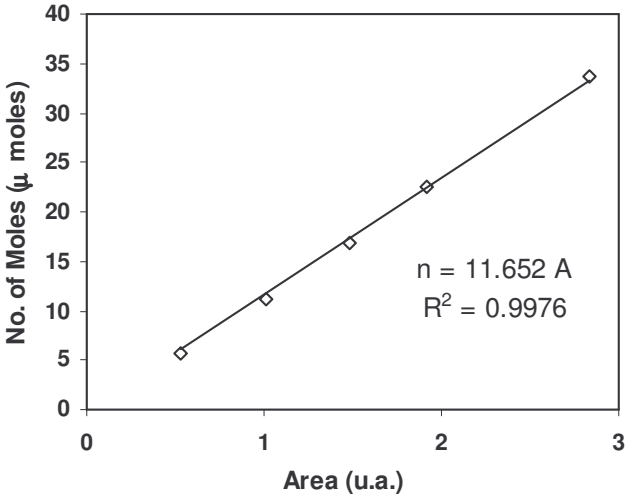

Figure A.4

Chromatograms of Typical Experiment in Batch Reactor

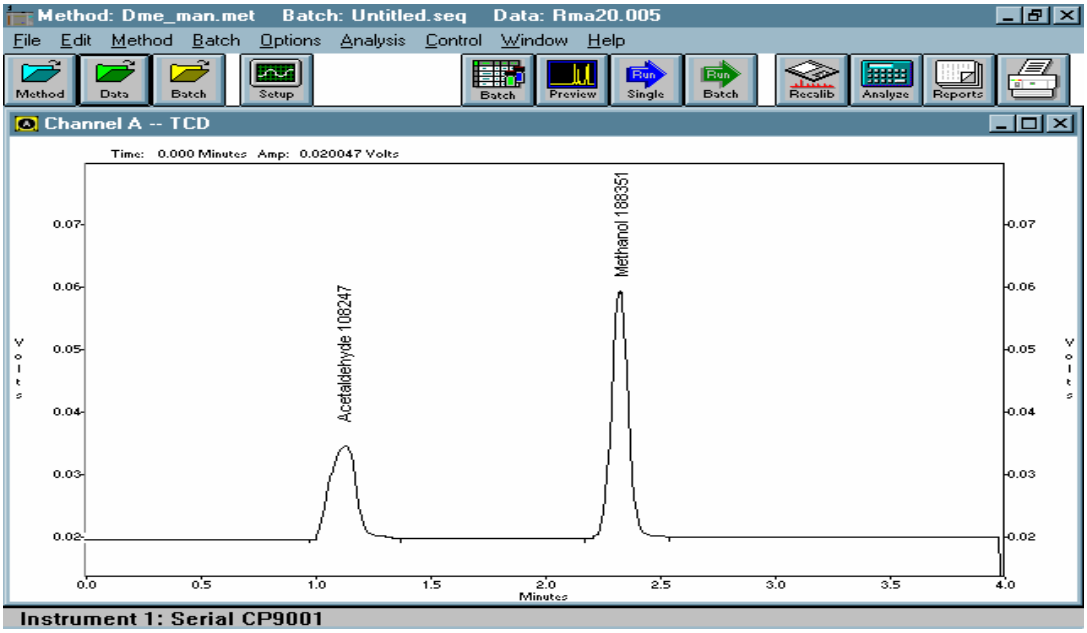

Figure A.5. Initial Time of Reaction

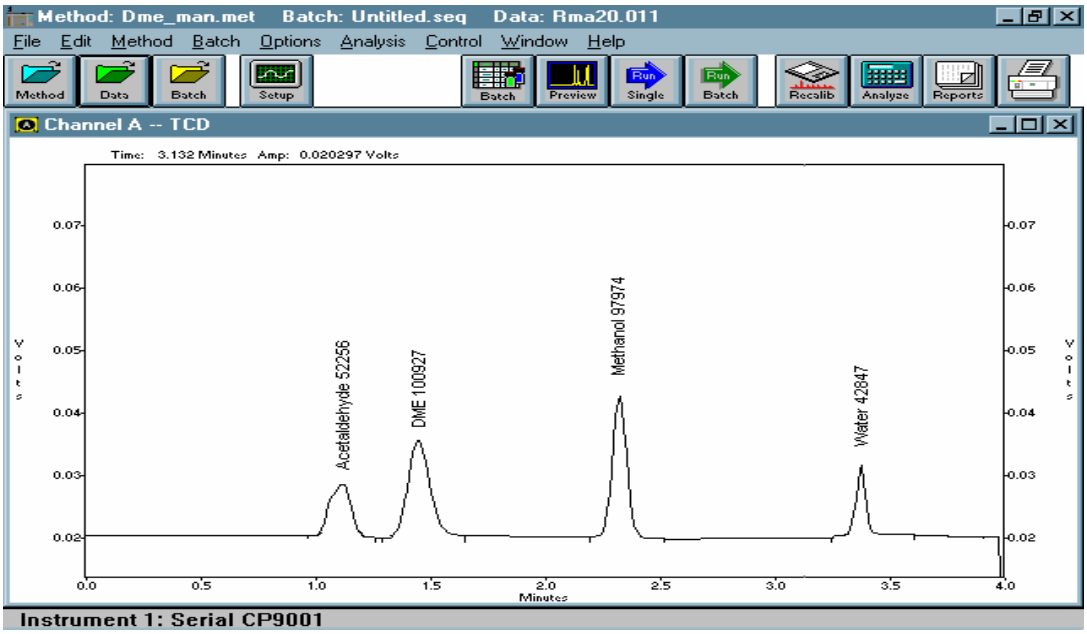

Figure A.6. Reaction Mixture Chromatogram at 51 mins

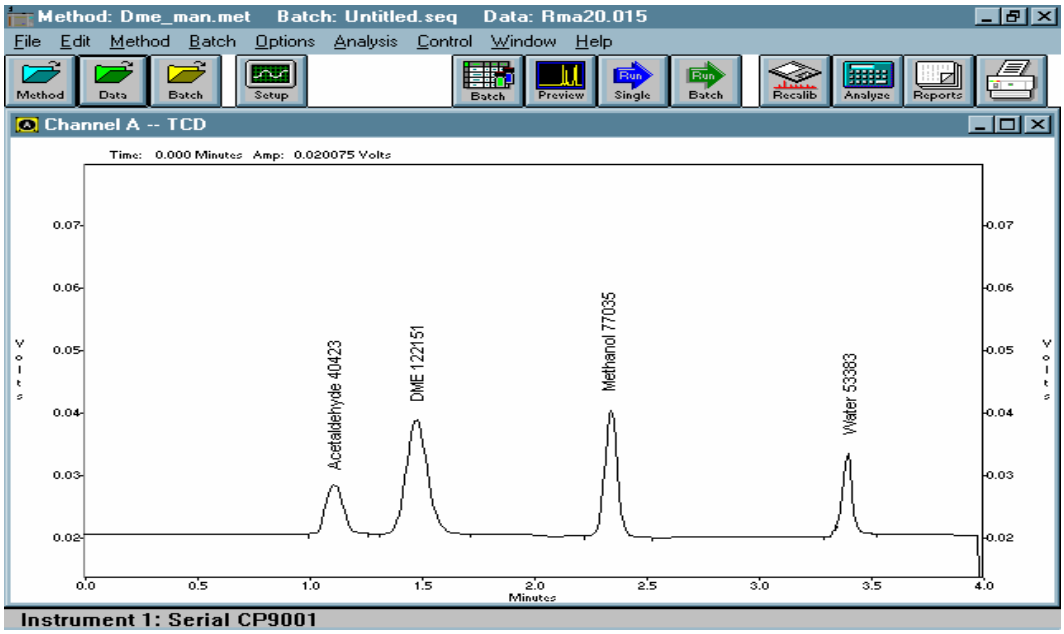

Figure A.7. Reaction Mixture Chromatogram at 120 mins

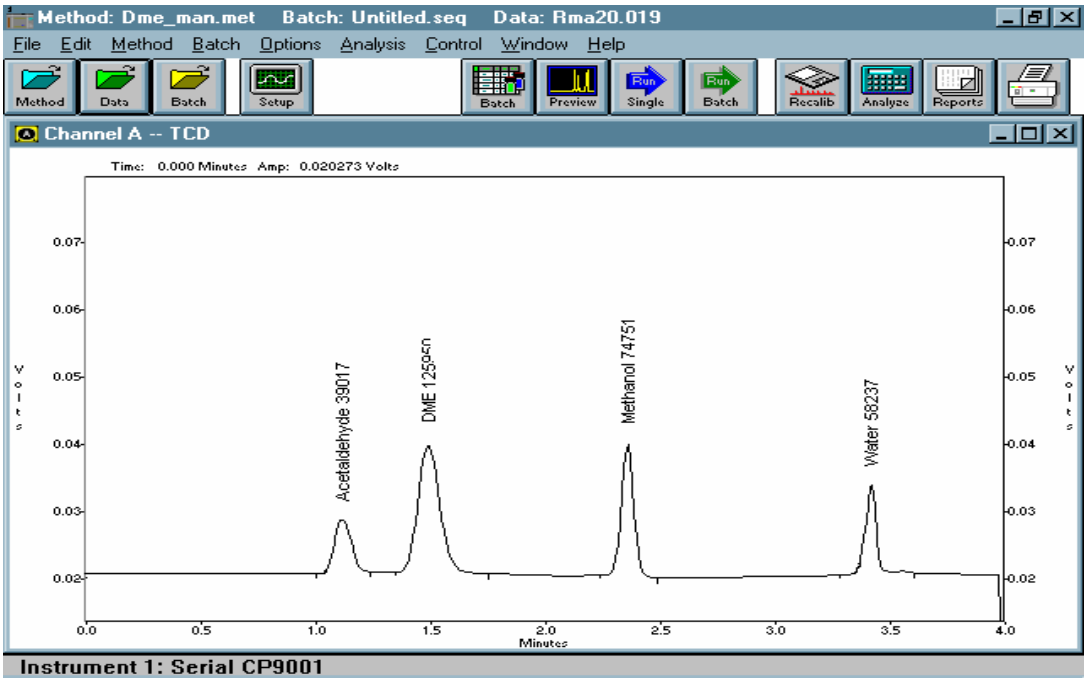

Figure A.8. Reaction Mixture Chromatogram at 180 mins

Chromatograms of Typical Experiment in Fixed Bed (Amberlyst 15) Adsorptive Reactor

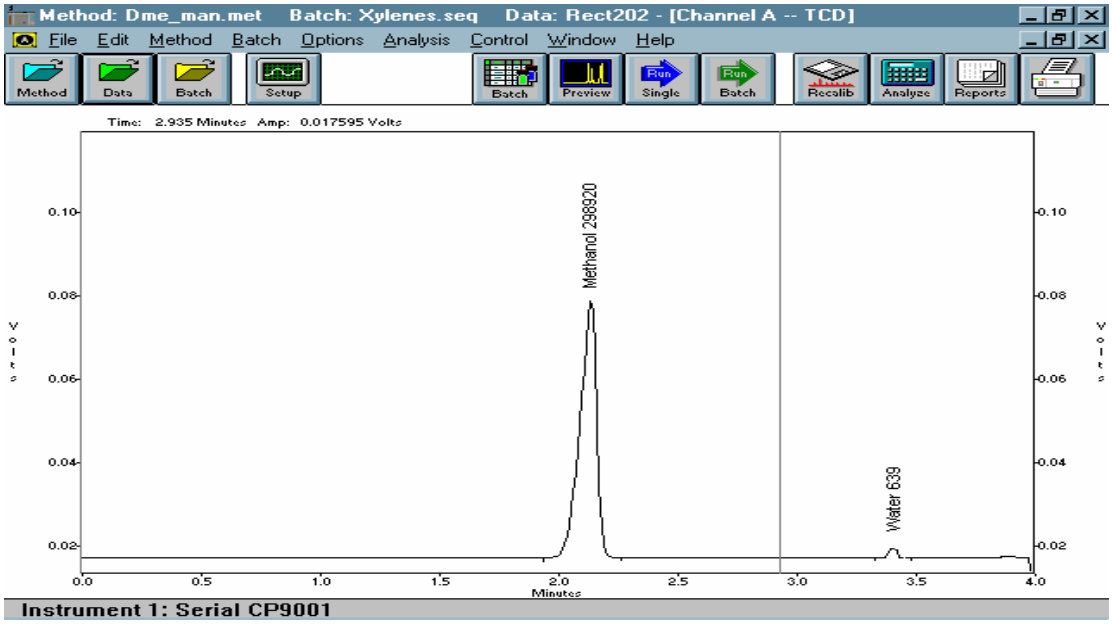

Figure A.9. Reaction Mixture Chromatogram at 2 mins

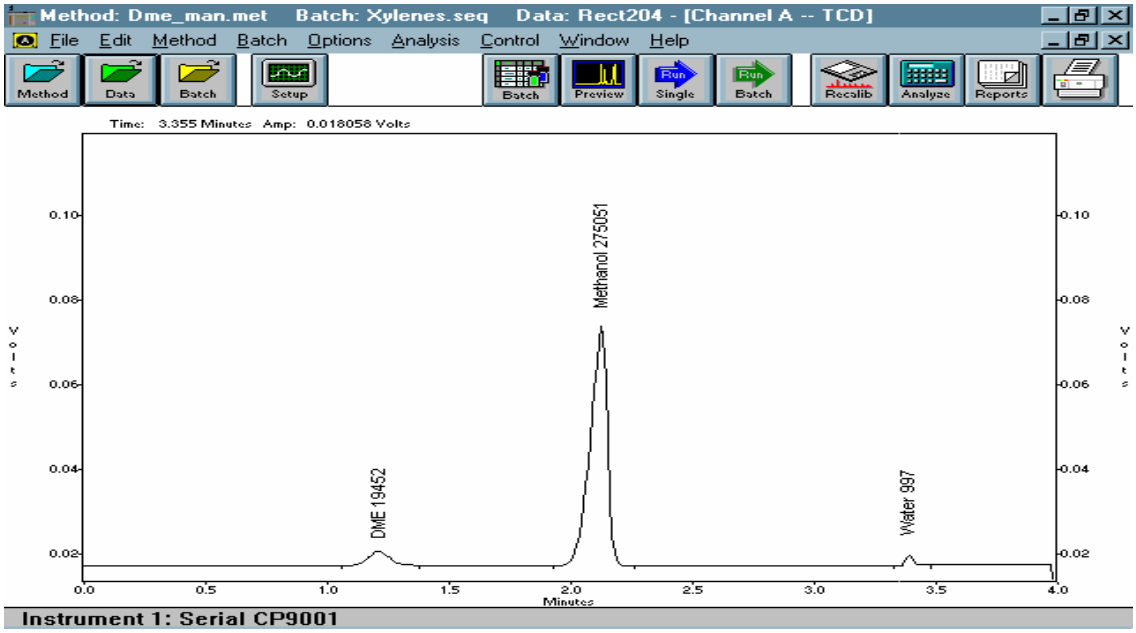

Figure A.10. Reaction Mixture Chromatogram at 5 mins

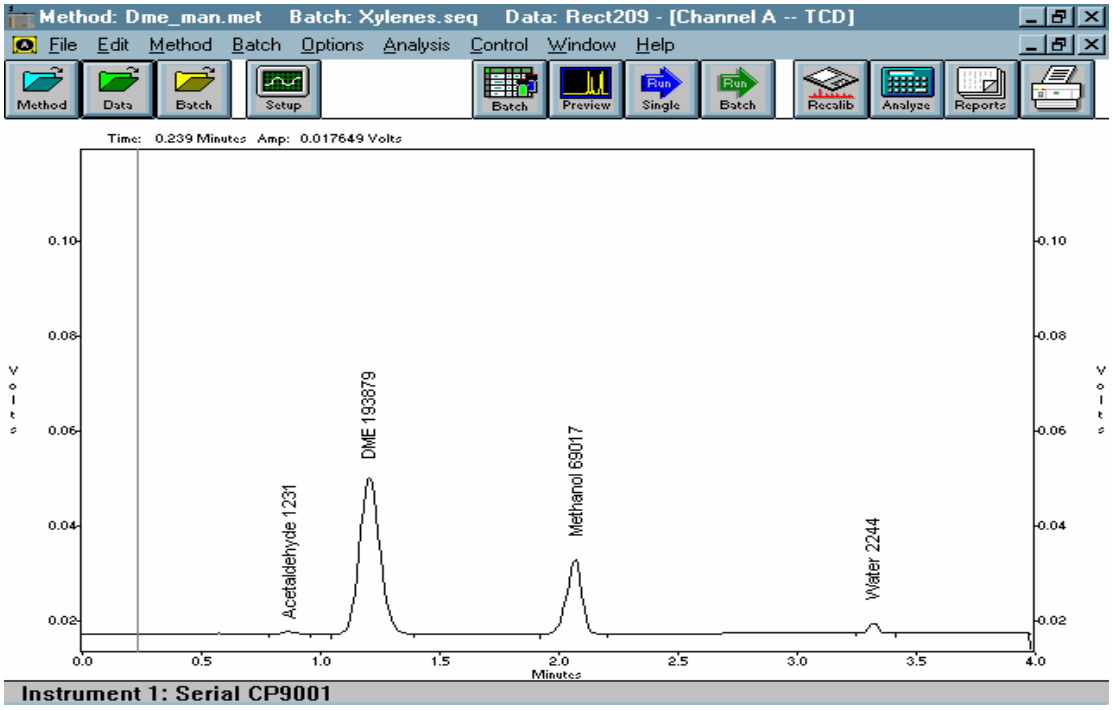

Figure A.11. Reaction Mixture Chromatogram at 10 mins

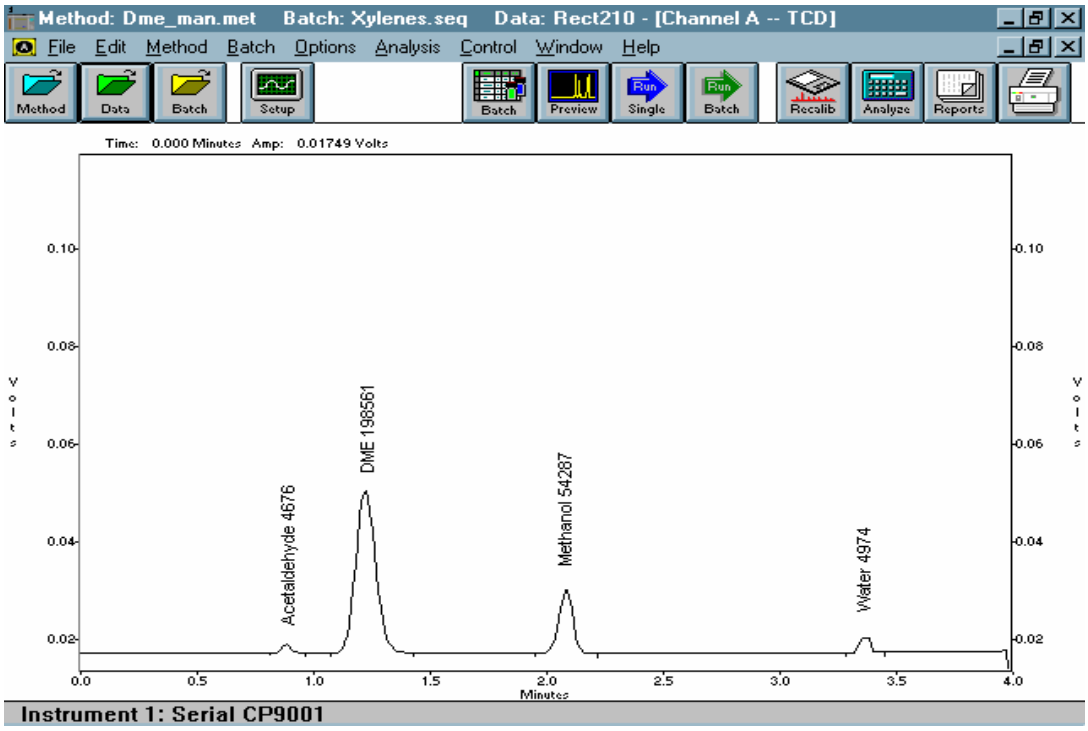

Figure A.12. Reaction Mixture Chromatogram at 12 mins

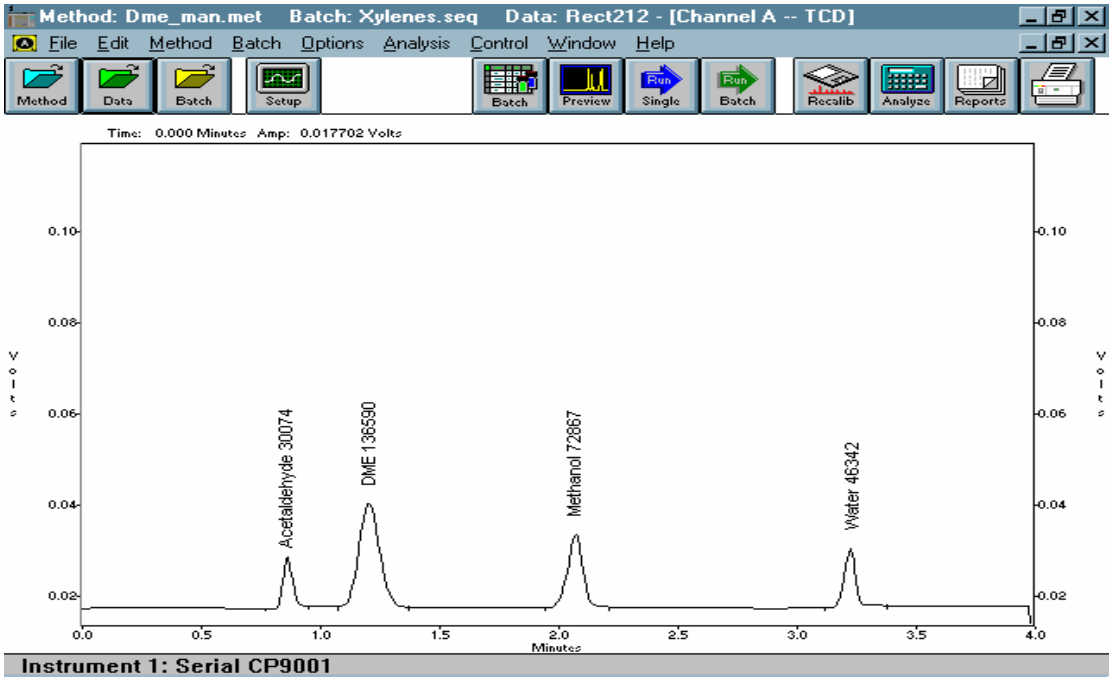

Figure A.13. Reaction Mixture Chromatogram at 20 mins

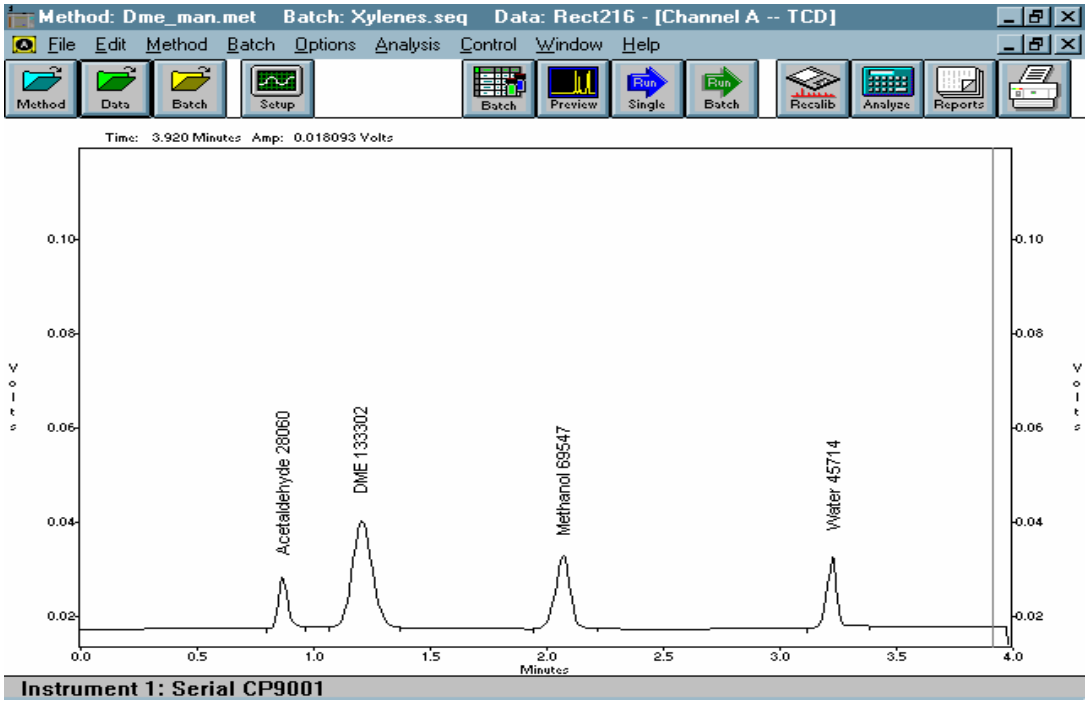

Figure A.14. Reaction Mixture Chromatogram at 40 mins.

Chromatograms of Typical Experiment in Smopex 101 Fixed Bed Adsorptive Reactor

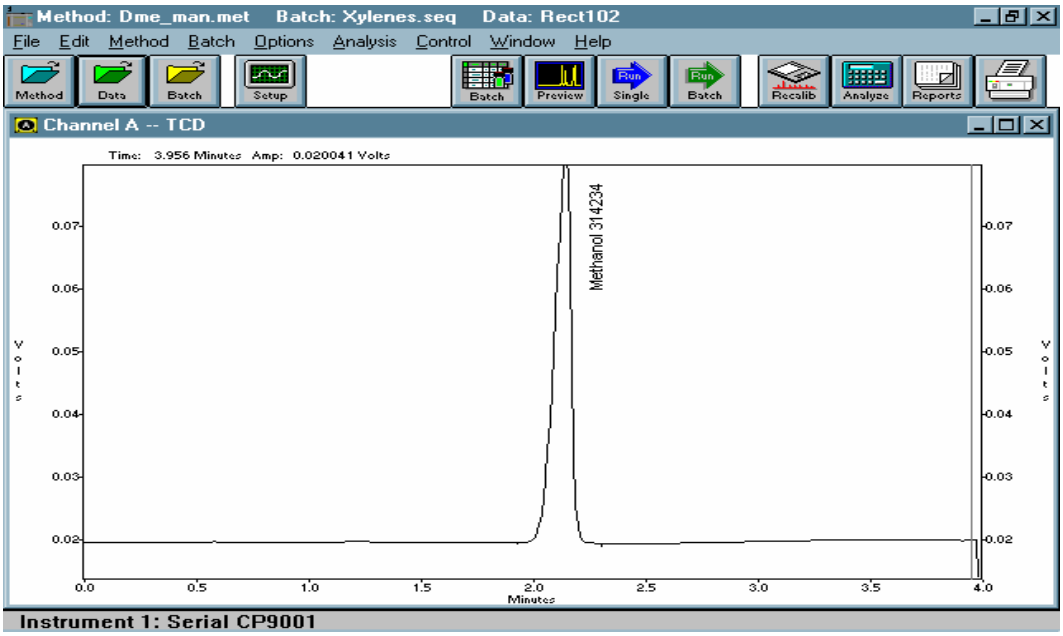

Figure A.15. Reaction Mixture Chromatogram at 2 mins.

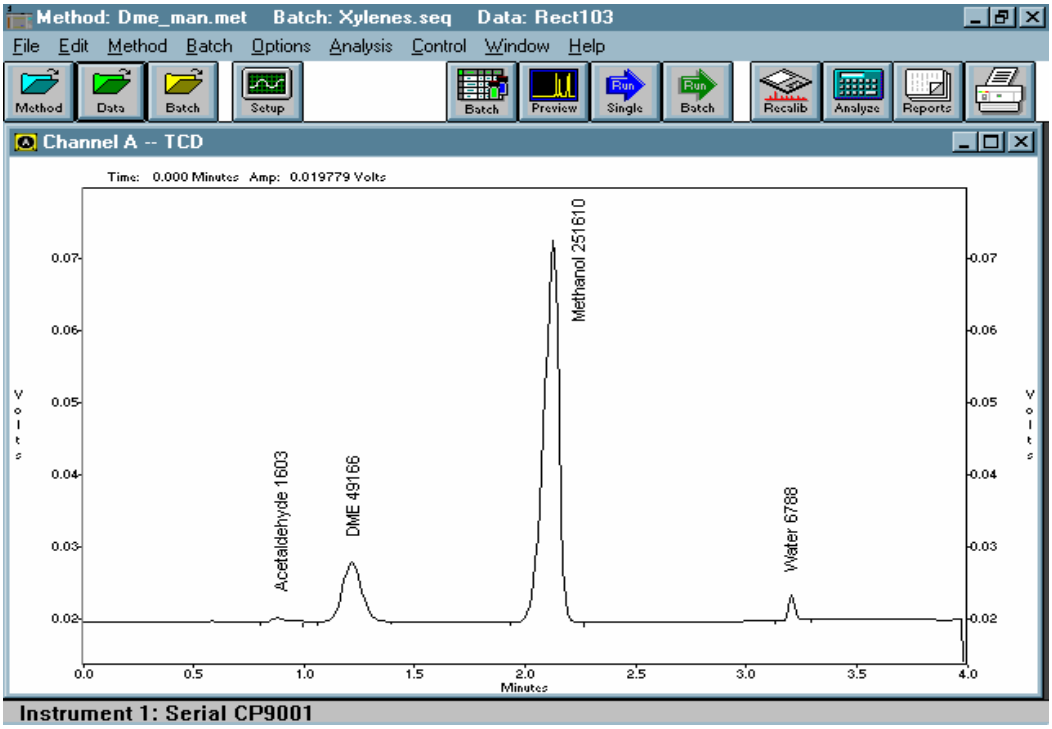

Figure A.16. Reaction Mixture Chromatogram at 3 mins.

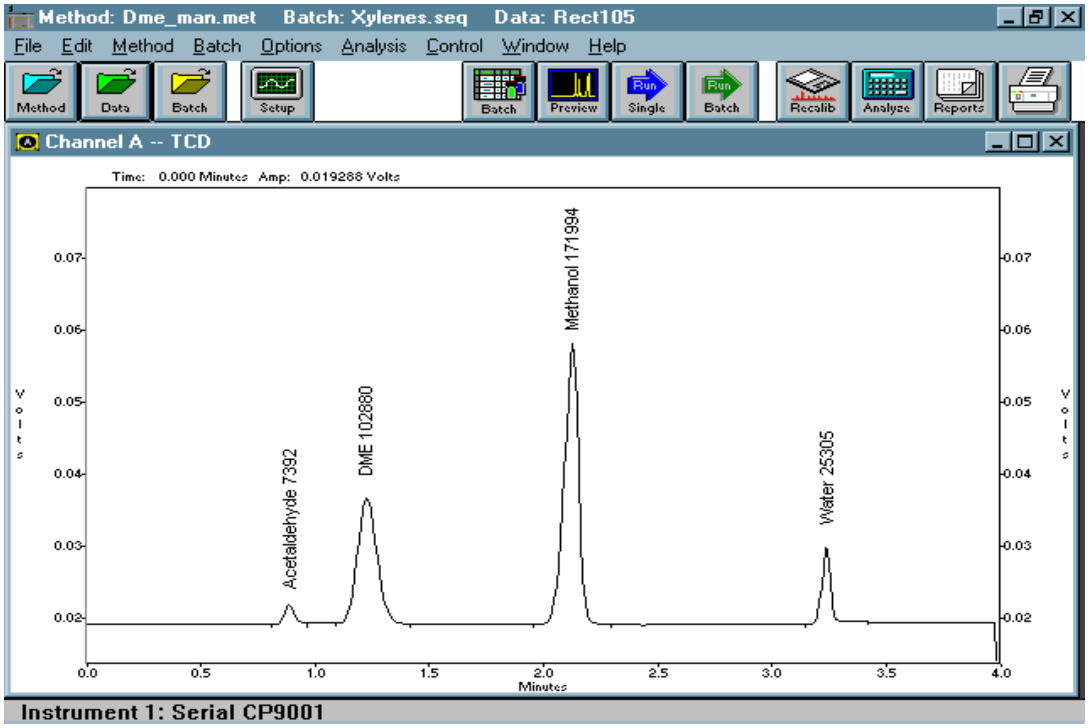

Figure A.17. Reaction Mixture Chromatogram at 5 mins.

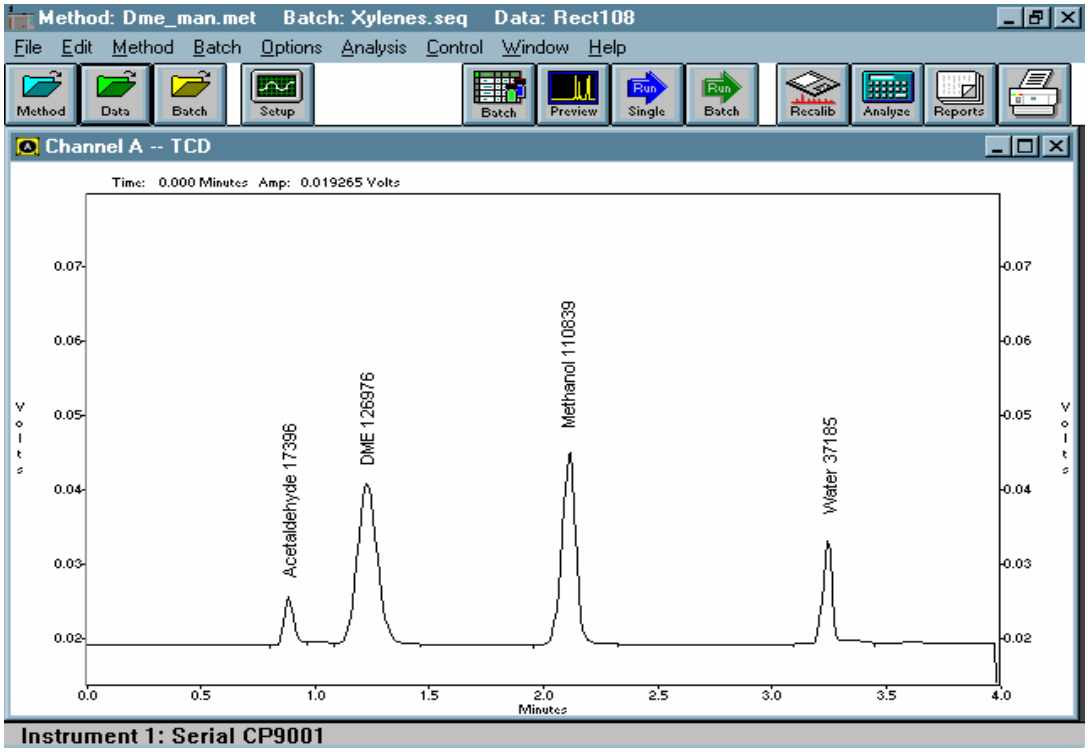

Figure A.18. Reaction Mixture Chromatogram at 8 mins.

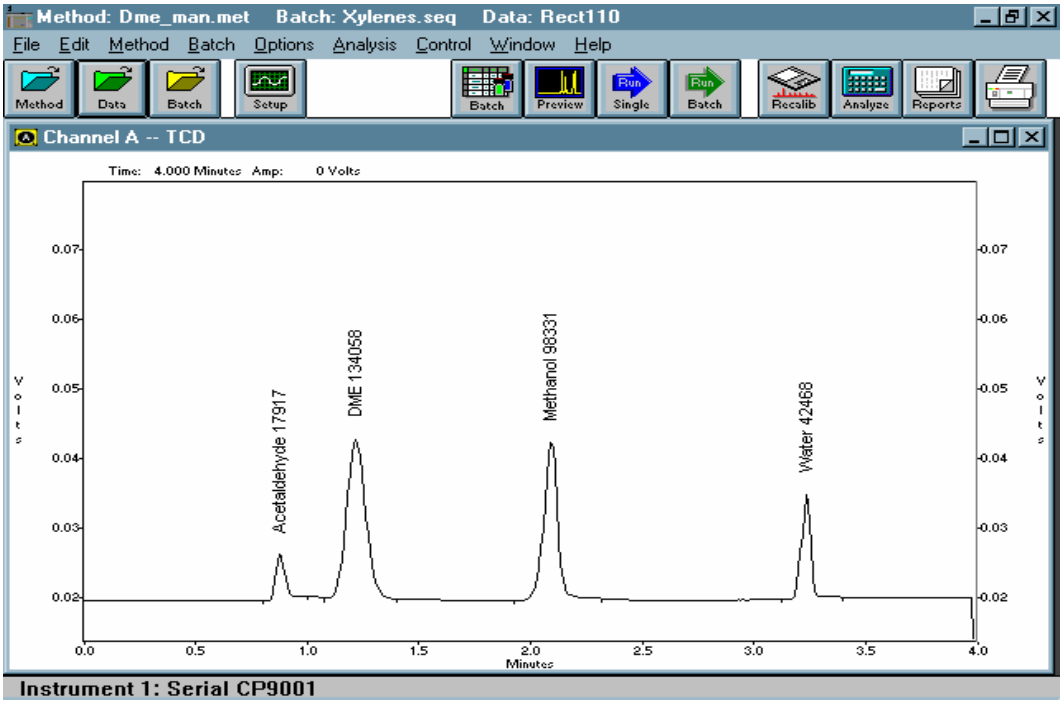

Figure A.19. Reaction Mixture Chromatogram at 10 mins.

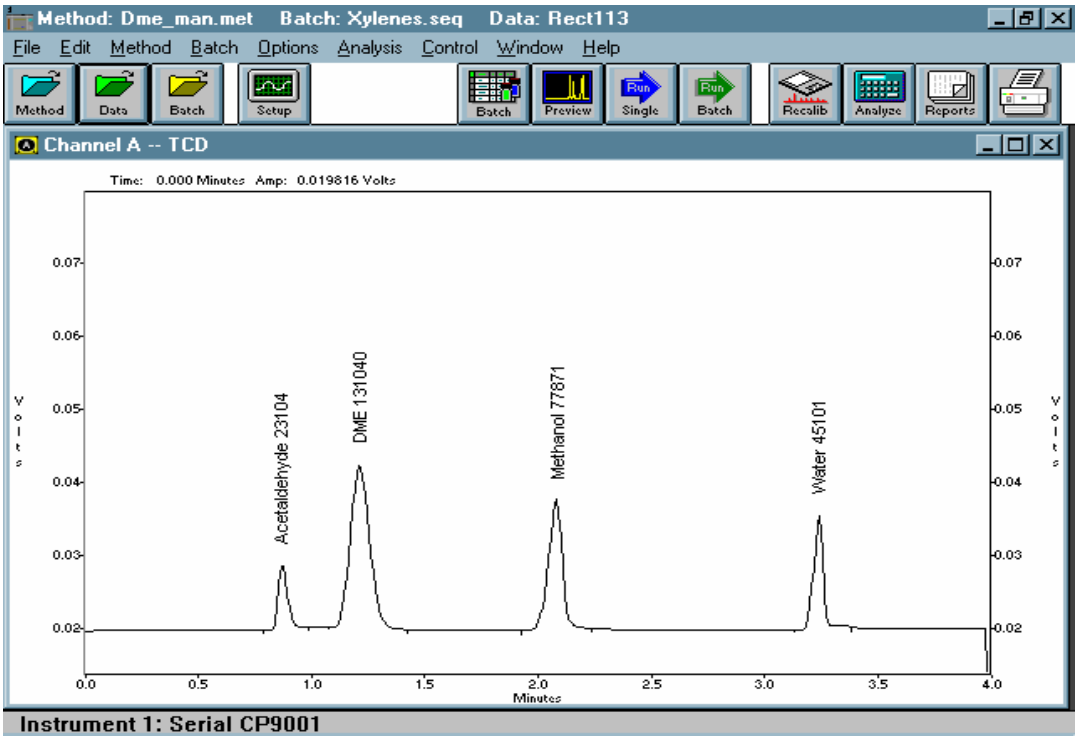

Figure A.20. Reaction Mixture Chromatogram at 16 mins.

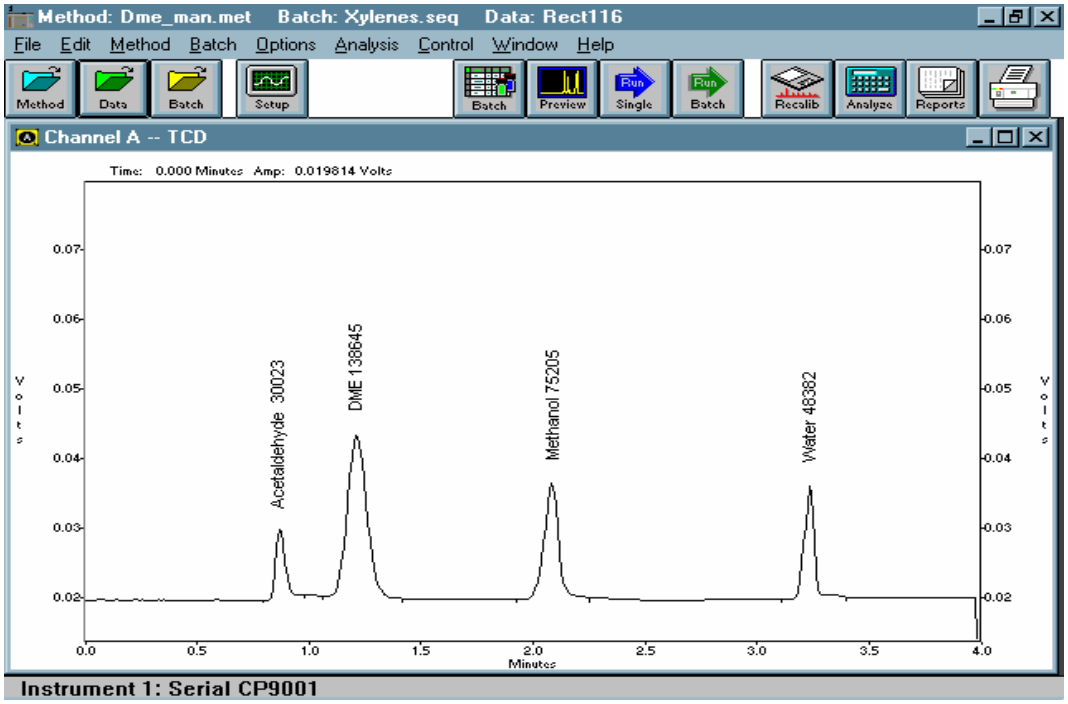

Figure A.21. Reaction Mixture Chromatogram at 30 mins.

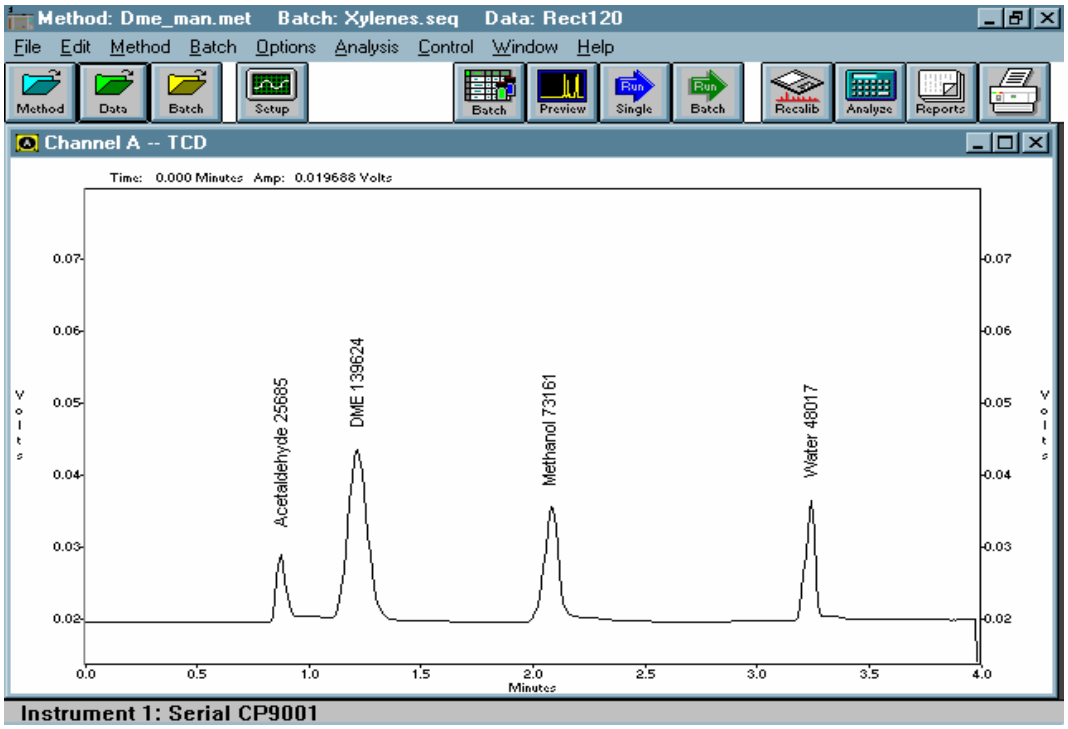

Figure A.22. Reaction Mixture Chromatogram at 60 mins.

Appendix B: Safety Data

1. Acetaldehyde

1.1 General

Synonyms: ethanal, ethyl aldehyde, acetic aldehyde

Molecular formula: CH_3CHO (C_2H_4O)

CAS No: 75-07-0

1.2 Physical data

Appearance: colourless liquid

Melting point: -123 ºC

Boiling point: 20.1 ºC

Specific gravity: 0.78

Vapor pressure: 755 mm Hg at 20 ºC

Vapor density: 1.52 (air = 1)

Flash point: -39 C

Explosion limits: 4% - 57%

Auto-ignition temperature: 185 ºC

Water solubility: miscible in all proportions

1.3 Hazards Identification

1.3.1. Major Health Hazards

1.3.1.1. Target Organs

Respiratory System, Liver, Kidney, Blood, Lungs, Skin.

1.3.1.2 Inhalation

Inhalations of acetaldehyde causes **irritation of Mucous Membranes**, **Central Nervous System depression**, **sever irritation of Respiratory System**, and **unconsciousness**.

1.3.1.3. Sink

Contact of acetaldehyde to skin causes irritation, prolonged contact may cause dermatitis.

1.3.1.4. Eyes

Causes severe irritation or burning to eyes with acetaldehyde, acetaldehyde contact to eyes may also cause temporary Corneal damage.

1.3.1.5. Ingestion

Ingestion of acetaldehyde can cause Gastrointestinal irritation, Central Nervous System depression, severe burns to mouth, throat and stomach, respiratory failure, unconsciousness.

1.3.2. Signs and Symptoms of Overexposure

Inhalation: Irritation of Mucous Membranes, Headache, Vomiting, Dizziness, Drowsiness.

Skin Contact: Irritation.

Eye Contact: Severe irritation or Burning to eyes

Ingestion: Over ingestion causes Headache, Vomiting, Dizziness, Gastrointestional irritation, severe burns to Mouth, Throat and Stomach.

1.3.3. Physical Hazards

Highly flammable liquid and vapor. Vapor may cause flash fire. May polymerize. Containers may rupture or explode.

1.4. First Aid Measures

1.4.1. Ingestion

Contact local poison control center or physician immediately. Never make an unconscious person vomit or drink fluids. When vomiting occurs, keep head lower than hips to help prevent aspiration. If person is unconscious, turn head to side. Get medical attention immediately.

1.4.2. Inhalation

If inhaled, remove to fresh air or to uncontaminated area. If not breathing, give artificial respiration. If breathing is difficult, oxygen should be administrated by qualified personnel. Prompt actions are essential and get immediate medical attention.

1.4.3. Skin Contact

In case of contact to skin, immediately flush skin with plenty of water for at least 15 minutes while removing contaminated clothing and shoes. Wash clothing before re-use. Get medical attention if necessary.

1.4.4. Eye Contact

In case of eye contact, immediately flush with plenty of water for at least 15 minutes and then get immediate medical attention.

1.5 Stability

Stable. Substances to be avoided include strong oxidising agents, strong acids, reducing agents, alkalies, halogens, halogen oxides. **Highly flammable. Vapor/air mixtures explosive over a very wide concentration range. May form peroxides in storage.**

1.6 Toxicology

Harmful by inhalation, ingestion and through skin absorption. **Some experiments with animals suggest that this substance may be anticipated to be a carcinogen.**

1.7 Personal protection

Safety glasses. Effective ventilation.

• Keep away from sources of ignition.

• Take precautionary measures against static discharges.

• Wear suitable protective clothing.

• Wear suitable gloves.

1.8 WORKPLACE CONTROLS AND PRACTICES

Unless a less toxic chemical can be substituted for a hazardous substance, ENGINEERING CONTROLS are the most effective way of reducing exposure. The best protection is to enclose operations and/or provide local exhaust ventilation at the site of chemical release. Isolating operations can also reduce exposure. Using respirators or protective equipment is less effective than the controls mentioned above, but is sometimes necessary. In evaluating the controls present in your workplace, consider: (1) how hazardous the substance is, (2) how much of the substance is released into the workplace and (3) whether harmful skin or eye contact could occur. Special controls should be in place for highly toxic chemicals or when significant skin, eye, or breathing exposures are possible. In addition, the following controls are recommended:

• Where possible, automatically pump liquid Acetaldehyde from drums or other storage containers to process containers.

• Before entering a confined space where Acetaldehyde is present, check to make sure sufficient oxygen (19%) exists.

Good WORK PRACTICES can help to reduce hazardous exposures. The following work practices are recommended:

• Workers whose clothing has been contaminated by Acetaldehyde should change into clean clothing promptly.

• Contaminated work clothes should be laundered by individuals who have been informed of the hazards of exposure to Acetaldehyde.

• Eye wash fountains should be provided in the immediate work area for emergency use.

• If there is the possibility of skin exposure, emergency shower facilities should be provided.

• On skin contact with Acetaldehyde, immediately wash or shower to remove the chemical. At the end of the workshift, wash any areas of the body that may have contacted Acetaldehyde, whether or not known skin contact has occurred.

• Do not eat, smoke, or drink where Acetaldehyde is handled, processed, or stored, since the chemical can be swallowed. Wash hands carefully before eating or smoking.

PERSONAL PROTECTIVE EQUIPMENT WORKPLACE CONTROLS ARE BETTER THAN PERSONAL PROTECTIVE EQUIPMENT.

However, for some jobs (such as outside work, confined space entry, jobs done only once in a while, or jobs done while workplace controls are being installed), personal protective equipment may be appropriate.

The following recommendations are only guidelines and may not apply to every situation.

1.8.1. Clothing

• Avoid skin contact with Acetaldehyde. Wear protective gloves and clothing. Safety equipment suppliers/manufacturers can provide recommendations on the most protective glove/clothing material for your operation.

• All protective clothing (suits, gloves, footwear, headgear) should be clean, available each day, and put on before work.

• ACGIH recommends Butyl Rubber as a good to excellent protective material.

1.8.2. Eye Protection

• Wear splash-proof chemical goggles and face shield when working with liquid, unless full

face piece respiratory protection is worn.

• Wear gas-proof goggles, unless full face piece respiratory protection is worn.

1.8.3. Respiratory Protection

• IMPROPER USE OF RESPIRATORS IS DANGEROUS. Such equipment should only be used if the employer has a written program that takes into account workplace conditions, requirements for worker training, respirator fit testing and medical exams, as described in OSHA 1910.134.

• Where the potential exists for exposures over 100 ppm, use a MSHA/NIOSH approved full facepiece respirator with an organic vapor cartridge/canister. Increased protection is obtained from full facepiece powered-air purifying respirators.

• If while wearing a filter, cartridge or canister respirator, you can smell, taste, or otherwise detect Acetaldehyde, or in the case of a full facepiece respirator you experience eye irritation, leave the area immediately. Check to make sure the respirator-to-face seal is still good. If it is, replace the filter, cartridge, or canister. If the seal is no longer good, you may need a new respirator.

• Be sure to consider all potential exposures in your workplace. You may need a combination of filters, prefilters, cartridges, or canisters to protect against different forms of a chemical (such as vapor and mist) or against a mixture of chemicals.

• Where the potential for high exposures exists, use a MSHA/NIOSH approved supplied-air respirator with a full facepiece operated in the positive pressure mode or with a full facepiece, hood, or helmet in the continuous flow mode, or use a MSHA/NIOSH approved self-contained breathing apparatus with a full facepiece operated in pressure demand or other positive pressure mode.

• Exposure to 10,000 ppm is immediately dangerous to life and health. If the possibility of exposures above 10,000 ppm exists, use a MSHA/NIOSH approved self-containedbreathing apparatus with a full facepiece operated in continuous flow or other positive pressure mode.

1.9 HANDLING AND STORAGE

• Prior to working with Acetaldehyde you should be trained on its proper handling and storage.

• Acetaldehyde is not compatible with STRONG OXIDIZERS, ACIDS, BASES, ALCOHOLS, AMMONIA, AMINES, PHENOLS, KETONES, HYDROGEN CYANIDE, HYDROGEN SULFIDE, ACID ANHYDRIDES, and HALOGENS.

• Store in tightly closed airtight containers in a cool, dark, well-ventilated area.

• Nitrogen or another inactive gas should be used as an "inert blanket" over liquid Acetaldehyde in storage containers.

• Sources of ignition, such as smoking and open flames, are prohibited where Acetaldehyde is handled, used, or stored.

• Metal containers involving the transfer of 5 gallons or more of Acetaldehyde should be grounded and bonded. Drums must be equipped with self-closing valves, pressure vacuum bungs, and flame arresters.

• Use only non-sparking tools and equipment, especially when opening and closing containers of Acetaldehyde.

1.9.1 Hazard rating

FLAMMABILITY: 4=severe

REACTIVITY: 2=moderate

EXPLOSIVE GAS OR LIQUID POISONOUS GASES ARE PRODUCED IN FIRE

1.10. Fire Hazards

• Acetaldehyde is a FLAMMABLE and EXPLOSIVE LIQUID or GAS.

• Use dry chemical, CO2, or alcohol foam extinguishers.

• Use water spray to keep fire-exposed containers cool.

• POISONOUS GASES ARE PRODUCED IN FIRE.

• The vapor is heavier than air and may travel a distance to cause a fire or explosion far from the source.

• If employees are expected to fight fires, they must be trained and equipped as stated in OSHA 1910.156.

1.11 Spills and Emergencies

If Acetaldehyde is spilled or leaked, take the following steps:

• Restrict persons not wearing protective equipment from area of spill or leak until clean-up is complete.

• Remove all ignition sources.

• Ventilate area of spill or leak.

• Absorb liquids in vermiculite, dry sand, earth, or a similar material and deposit in sealed containers.

If Acetaldehyde is leaked, take the following steps:

• Restrict persons not wearing protective equipment from area of leak until clean-up is complete.

• Remove all ignition sources.

• Ventilate area of leak to disperse the gas.

• Stop flow of gas. If source of leak is a cylinder and the leak cannot be stopped in place, remove the leaking cylinder to a safe place in the open air, and repair leak or allow cylinder to empty.

• Keep Acetaldehyde out of a confined space, such as a sewer, because of the possibility of an explosion, unless the sewer is designed to prevent the build-up of explosive concentrations.

• It may be necessary to contain and dispose of Acetaldehyde as a HAZARDOUS WASTE. Contact your Department of Environmental Protection (DEP) or your regional office of the federal Environmental Protection Agency (EPA) for specific recommendations.

FOR LARGE SPILLS AND FIRES immediately call your fire department.

1.12 Ecological Information

Acetaldehyde is a flammable liquid with a characteristic pungent odour. It is used to make paraldehyde, acetic acid, butanol, perfumes, flavours, aniline dyes, plastics, and synthetic rubber. It is also used in silvering mirrors and in hardening gelatine fibbers. It can enter the environment through manufacturing effluents or spills.

2. Acetal

2.1 General

Synonyms: 1,1-dimethoxyethane, acetaldehyde dimethyl acetal

Molecular formula: $C_4H_{10}O_2$

Structural: $CH_3CH(OCH_3)_2$

CAS No: 534-15-6

2.2 Physical data

Physical State: Liquid

Appearance: Clear, colorless

Molecular Weight: 90.12

Vapour pressure at 20 ^oC: 171 mm Hg

Density: 0.852 gm/cc

Melting point: -113 ^oC

Boiling point: 64.4 ^oC

Flash point: -17 ^oC

Autoignition: 202 ^oC

2.3. Stability

Stable under normal temperatures and pressures.

2.4. Potential Hazards

Flammable, volatile liquid (Polar/Water-Miscible) **May form peroxides in storage. Test for peroxides before use.** Vapors may form explosive mixtures with air, and may travel to source of ignition and flash back. Vapors may spread along ground and collect in low or confined areas (sewers, basements, tanks). Containers may explode when heated.

2.5. Health

2.5.1. Ingestion

May cause irritation of the digestive tract. May cause central nervous system depression, characterized by excitement, followed by headache, dizziness, drowsiness, and nausea. Advanced stages may cause collapse, unconsciousness, coma and possible death due to respiratory failure.

2.5.2. Inhalation

May cause respiratory tract irritation. May cause narcotic effects in high concentration.

2.5.3. Skin Contact

Causes skin irritation.

2.5.4. Eye Contact

Causes skin irritation or burns.

2.6. First Aid Measures

2.6.1. Ingestion

Contact local poison control center or physician immediately. Never make an unconscious person vomit or drink fluids. When vomiting occurs, keep head lower than hips to help prevent aspiration. If person is unconscious, turn head to side. Get medical attention immediately.

2.6.2. Inhalation

If inhaled, remove to fresh air or to uncontaminated area. If not breathing, give artificial respiration. If breathing is difficult, oxygen should be administrated by qualified personnel. Prompt actions are essential and get immediate medical attention.

2.6.3. Skin Contact

In case of contact to skin, immediately flush skin with plenty of water for at least 15 minutes while removing contaminated clothing and shoes. Wash clothing before re-use. Get medical attention if necessary.

2.6.4. Eye Contact

In case of eye contact, immediately flush with plenty of water for at least 15 minutes and then get immediate medical attention.

2.7. Protective Clothing

Eyes: Wear appropriate protective eyeglasses or chemical safety goggles.

Skin: Wear appropriate protective gloves to prevent skin exposure.

Clothing: Wear appropriate protective clothing to minimize contact with skin.

2.8. Spill or Leak

Eliminate all ignition sources (no smoking, flares, sparks or flames in immediate area). All equipment used when handling the product must be grounded. Do not touch or walk through spilled material. Stop leak if you can do it without risk. Prevent entry into waterways, sewers, basements or confined areas. A vapour suppressing foam may be used to reduce vapours. Absorb or cover with dry earth, sand or other non-combustible material and transfer to containers. Use clean non-sparking tools to collect absorbed materials.

3. Methanol

3.1 General

Synonyms: methyl alcohol, wood alcohol, Columbian spirit, carbinol

Molecular formula: CH_3OH

CAS No: 67-56-1

3.2 Physical data

Appearance: colourless liquid

Melting point: -98 ^oC

Boiling point: 64.6 ^oC

Specific gravity: 0.789

Vapour pressure: 127 mm Hg at 25 ^oC

Flash point: 11 ^oC

Autoignition temperature: 455 ^oC

Water solubility: miscible in all proportions

3.3 Stability

Stable at room temperature in closed containers under normal storage and handling conditions.

3.4 Toxicology

Causes skin and eye irritation. Ingestion can cause nausea, vomitting and inebriation; chronic use can cause serious liver damage.

3.5. Health

3.5.1. Ingestion

Cannot be made non-poisonous. May cause irritation of the digestive tract. Poison by ingestion. May cause respiratory failure. May cause vascular collapse and damage. May cause kidney failure. Ingestion can cause blurred vision, narrowing of the visual field, or blindness.

3.5.2. Inhalation

May cause respiratory tract irritation. May cause adverse central nervous system effects including headache, convulsions, and possible death. May cause visual impairment and possible permanent blindness. May cause effects similar to those described for ingestion. Toxic if inhaled.

3.5.3. Skin Contact

May cause skin irritation. May be harmful if absorbed through the skin.

3.6. First Aid Measures

3.6.1. Ingestion

If victim is conscious and alert, give 2-4 cupfuls of milk or water. Get medical aid immediately. Induce vomiting by giving one teaspoon of Syrup of Ipecac. Get medical attention immediately.

3.6.2. Inhalation

Get medical aid immediately. Remove from exposure to fresh air immediately. If not breathing, give artificial respiration. If breathing is difficult, give oxygen.

3.6.3. Skin Contact

Get medical aid. Flush skin with plenty of soap and water for at least 15 minutes while removing contaminated clothing and shoes.

3.7. Protective Clothing

Eyes: Wear appropriate protective eyeglasses or chemical safety goggles.

Skin: Wear appropriate protective gloves to prevent skin exposure.

Clothing: Wear appropriate protective clothing to minimize contact with skin.

Appendix C: Thermodynamic Properties

1. Properties Estimation

The correlations presented in this section are from (Reid *et al*, 1987).

1.1 Estimation of critical properties

Critical temperature, pressure and volume could be calculated with Joback modification of Lydersen's method, using the following relations:

$$T_c = T_b\left[0.584 + 0.965\sum\Delta_T - \left(\sum\Delta_T\right)^2\right]^{-1} \quad \text{(C.1)}$$

$$P_c = \left(0.113 + 0.00329n_A - \sum\Delta_P\right)^{-2} \quad \text{(C.2)}$$

$$V_c = 17.5 + \sum\Delta_V \quad \text{(C.3)}$$

The acentric factor ω could be estimated from the value of critical compressibility factor, Z_c, accordingly to:

$$Z_c = \frac{P_c V_c}{RT_c} = 0.291 - 0.080\omega \quad \text{(C.4)}$$

1.2 Estimation of liquid heat capacity

The liquid heat capacity for acetal was calculated with group contributions for Missenar method, at several temperatures. The values are presented in Table C.1. Plots of all components at different temperatures are represented in the Figure C.1.

Table C.1. Heat Capacity of acetal

T (K)	248	273	298	323	348	373
C_p (J/mol.K)	194.2	202.4	209.1	216.4	225.0	234.9

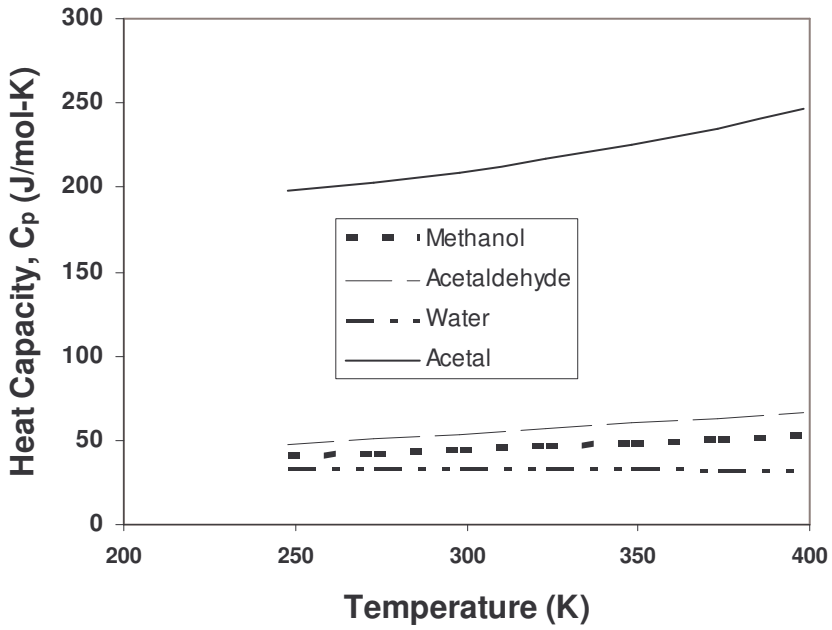

Figure C.1 Heat capacity versus temperature plot

1.3 Estimation of molar volume

The molar volumes for all components were estimated with Gunn-Yamada method:

$$V(T) = \frac{f(T)}{f(T^R)} V^R \quad \text{(C.5)}$$

Where

$$f(T) = H_1(1 - \omega H_2) \quad \text{(C.6)}$$

$$H_1 = 0.33593 + 0.33953T_r + 1.51941T_r^2 - 2.02512T_r^3 + 1.11422T_r^4 \quad \text{(C.7)}$$

$$H_2 = 0.29607 - 0.09045T_r - 0.0482T_r^2 \quad \text{(C.8)}$$

$$T_r = \frac{T}{T_c} or \frac{T^R}{T_c} \quad \text{(C.9)}$$

V^R is the molar volume at the reference temperature T^R (cm^3/mol), ω is the acentric factor and T_c is the critical temperature (K). Gunn-Yamada method can be used just in case the liquid molar volume is known at some temperature (reference temperature). The reference molar volumes are presented in Table C.2.

Table C.2. Molar volumes at the reference temperature used for all calculations.

Component	Acetaldehyde	Acetal	Methanol	Water
Molar volume – V (cm3/mol)	56.21	105.80	40.52	17.96
Reference temperature - T^R (K)	293.0	293.0	293.0	293.0

1.4 Estimation of viscosity

The viscosity of pure components could be calculated by the Przezdziecki and Sridhar method by using the Hildebrand-modified Batschinski equation:

$$\mu = \frac{V_o}{E(V - V_o)} \tag{C.10}$$

Where μ is liquid viscosity (cP), V is liquid molar volume (cm^3/mol) and the parameter E and V_o are defined below:

$$E = -1.12 + \frac{V_c}{12.94 + 0.10M - 0.23P_c + 0.0424T_f - 11.58\left(T_f / T_c\right)} \tag{C.11}$$

and $$V_o = 0.0085\omega T_c - 2.02 + \frac{V_m}{0.342\left(T_f / T_c\right) + 0.894} \tag{C.12}$$

where T_c is critical temperature (K), P_c is critical pressure (bar), V_c is critical volume (cm^3/mol), M is molecular weight (g/mol), ω is acentric factor (dimensionless), T_f is freezing point (K) and V_m is liquid molar volume at T_f (cm^3/mol). Viscosities of all components are given in Table C.3.

Table C.3. Viscosities of Pure components at different temperatures (cP).

Component	**20 °C**	**30 °C**	**40 °C**	**50 °C**	**60 °C**
Acetaldehyde	0.223	0.199	0.178	0.160	0.144
Acetal	0.330	0.302	0.277	0.256	0.236
Methanol	0.554	0.490	0.438	0.395	0.359
Water	1.018	0.815	0.668	0.559	0.477

1.5 Estimation of molecular diffusivity

The diffusivities in multicomponent liquid mixture were estimated by the modified Wilke-Chang equation, proposed Perkins and Geankoplis:

$$D_{Am}^{o} = 7.4\times10^{-8}\frac{(\phi M)^{1/2}T}{\mu V_{ml,A}^{0.6}} \quad \text{(C.13)}$$

$$\phi M = \sum_{\substack{J=1 \\ J\neq A}}^{n} x_j \phi_j M_j \quad \text{(C.14)}$$

Where D_{Am}^{o} is the diffusion coefficient for dilute solute A into a mixture of n components (cm^2/s), T is the temperature (K), $V_{ml,A}$ is the molar volume of the solute A (cm^3/mol), x_j is the molar fraction for component j, ϕ_j is the association factor (dimensionless) for component j, that is equal to 2.6 for water, 1.9 for methanol and 1.0 for unassociated components. The mixture viscosity, μ (cP), was predicted by the generalized corresponding states method proposed by Teja and Rice (Teja and Rice, 1981).

References

Perry, R.H.; Green, D.W.; Maloney, J.O. *Perry's Chemical Engineers Handbook.* 7th Edition, McGraw-Hill: New York, 1997.

Reid, C. R.; Prausnitz, J. M.; Poling, B. E. *The Properties of Gases & Liquids*. 4th Edition, McGraw-Hill: New York, 1988.

Smith, J. M.; Van Ness, H. C. *Introduction to chemical engineering thermodynamics.* 4th Edition, McGraw-Hill: New York, 1987.

Teja, A.S.; Rice, P. Generalized Corresponding States Method for the Viscosities of Liquid Mixtures. *Ind. Eng. Chem. Fundam.* 20, 77-81, 1981.

Appendix D: Calibration of Recycling Pump and Recycling Flow-meter

The text presented in this Appendix was provided by Separex Group. It describes the methodology followed to calibrate the recycling pump and the recycling flow-meter of the Licosep 12-26 SMB pilot unit, using the manual screen option of the Licosep control software.

The purpose of the experiment described below is to calibrate the recycling pump and the recycling flow-meter. These experiments would better be performed every time when a new eluent or desorbent is used. The parameters a, b, c, and d of the following equations are sought:

$$V = a + bQ_t \tag{D.1}$$

for the recycling pump and

$$Q_f = c + dI \tag{D.2}$$

for the recycling flow-meter. Where V is the electric voltage applied to the recycling pump to get the flow-rate Q_t; Q_f is the flow-rate given by the flow-meter and is derived from the electric current I induced by the turbine flow-meter.

The SMB unit should be configured as described in the Figure D.1

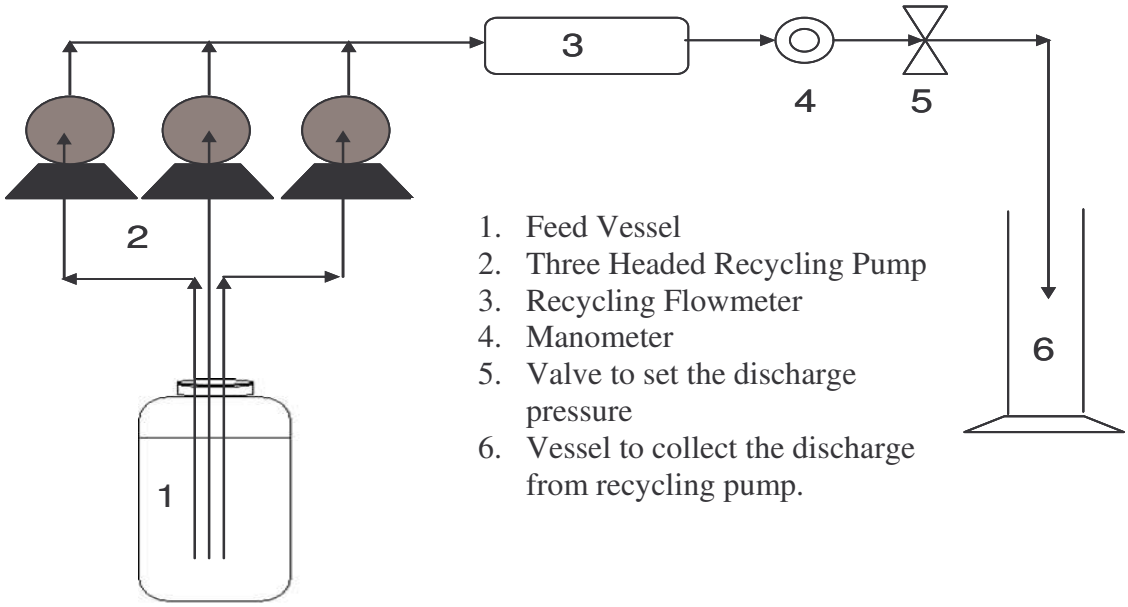

Figure D.1 Experimental configuration of the SMB System for the Calibration of the Recycling Pump and Recycling Flow-meter.

1. Disconnect the inlet of each recycling pump head and connect it to the eluent tank with a large pipe (1/4" diameter pipe is suitable). This operation is supposed to lead to a pressure drop as low as possible in the aspiration pipes and to avoid cavitations.
2. Connect a manometer to a valve in order to be able to adjust the recycling pump discharge pressure which must be chosen close to the SMB working pressure.

To perform an experiment simply means to run the recycling pump after setting its flow-rate to a value chosen in the range studied. When in the manual screen, choose pump: flow in the manual pump mode array and press F10. The steps to be followed are:

1. Choose the recycling pump flow-rate. Press Alt and F1 simultaneously and then press F10 to start the pump.
2. Wait a little bit until the pump is working in steady-state and click on the button ON. The mean value of the indication given by the flow-meter is calculated from

the time ON is pressed on to the time OFF is pressed on. In the mean time, evaluate the real flow-rate Q_m. Q_m is derived from the weight of a collection vessel measured before and after the experiment and from the duration of the collection.

3. At the end of the experiment, click the voltage which was applied to the recycling pump and the mean value of the indication given by the flow-meter.

The voltage applied to the recycling pump V can be read directly from the manual screen or, alternatively, can be estimated from the theoretical (expected) flow-rate of the pump Q_t and from the values a_{old} and b_{old} of the a and b parameters used by the software at the time of the experiment:

$$V = a_{old} + b_{old} Q_t \qquad \text{(D.3)}$$

The a_{old} and b_{old} values can be found in the manual screen or in the file C:\LICOSEP\PAR_LICO.INI. This file is made of five lines which are, successively, *a, b, c, d* and the system dead volume.

The intensity of the current induced by the flow-meter wheel I is calculated from the indication given by the flow-meter Q_f and from the values c_{old} and d_{old} of the c and d parameters used by the software at the time of experiment:

$$I = \frac{Q_f - c_{old}}{d_{old}} \qquad \text{(D:4)}$$

The flow-rate given by the flow-meter Q_f is the mean value calculated from the time button ON is pressed on to the time the button OFF is pressed on.

At this stage, a set (Q_m, V, I) of experiment data is available.

4. Repeat points 1 to 3 to get a new experimental point. To stop the pump, press Alt and F2 simultaneously.

When all the required experiments have been performed, the new values of a_{new}, b_{new}, c_{new}, and d_{new}, of the a, b, c, and d parameters are just derived from a linear regression involving respectively (Q_m, V) and (I, Q_m). The old values of the parameters should be replaced by the new ones in the manual screen and are automatically saved in the PAR_LICO.INI file after pressing F10 and leave the screen.

Appendix E: SMBR Experimental Profiles

Experiment Conditions Run 1	
Initial Condition : System saturated with methanol	
Switching time (t^*)	3.0 min
Configuration	3-3-3-3
Feed Composition (Molar fraction)	Mixture of 40 % Acetaldehyde 60 % Methanol
Desorbent flow-rate (Q_D)	25.0 mL/min
Feed flow-rate (Q_F)	3.0 mL/min
Raffinate flow-rate (Q_R)	8.0 mL/min
Extract flow-rate (Q_X)	20.0 mL/min
Section IV Recycling flow-rate (Q_4)	25.0 mL/min

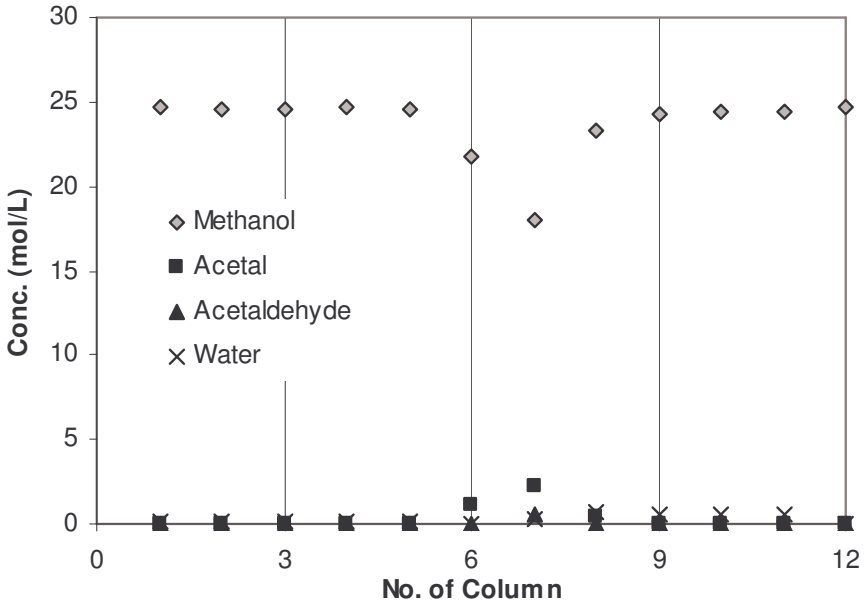

Figure E.1.1 SMBR profile Run 1, Cycle 1

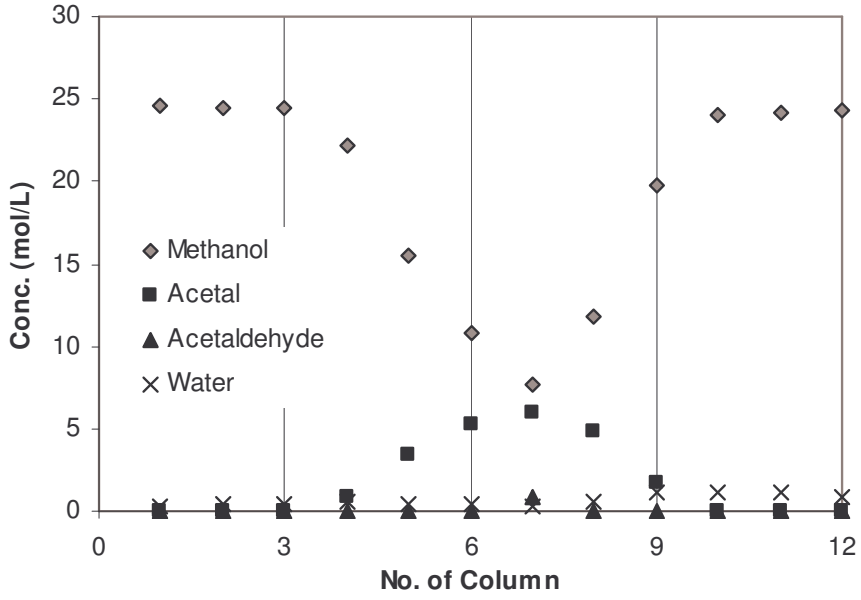

Figure E.1.2 SMBR profile Run 1, Cycle 3

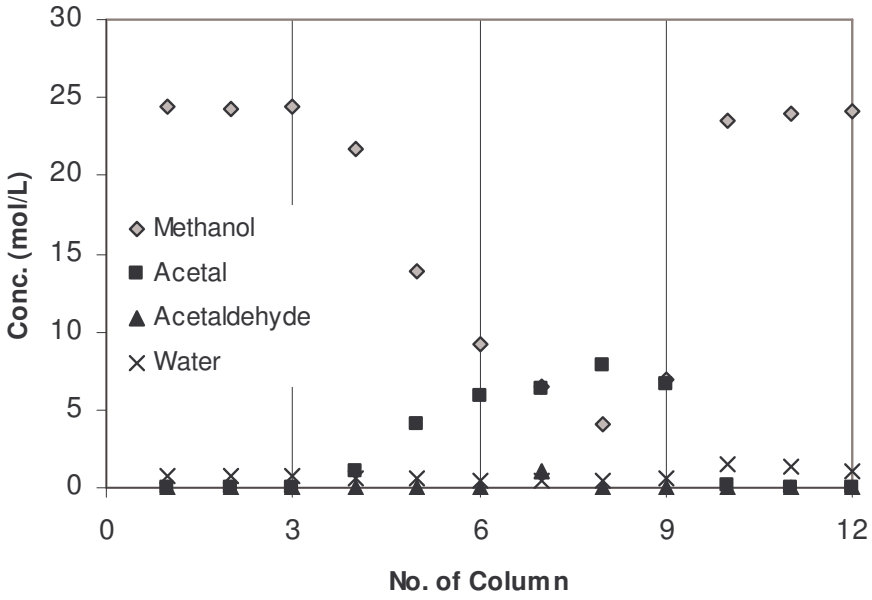

Figure E.1.3 SMBR profile Run 1, Cycle 5

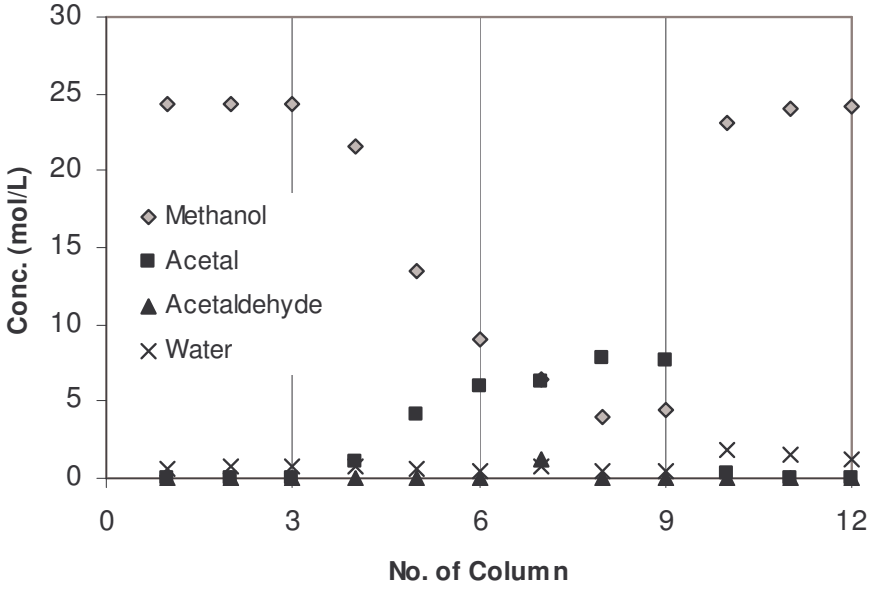

Figure E.1.4 SMBR profile Run 1, Cycle 6

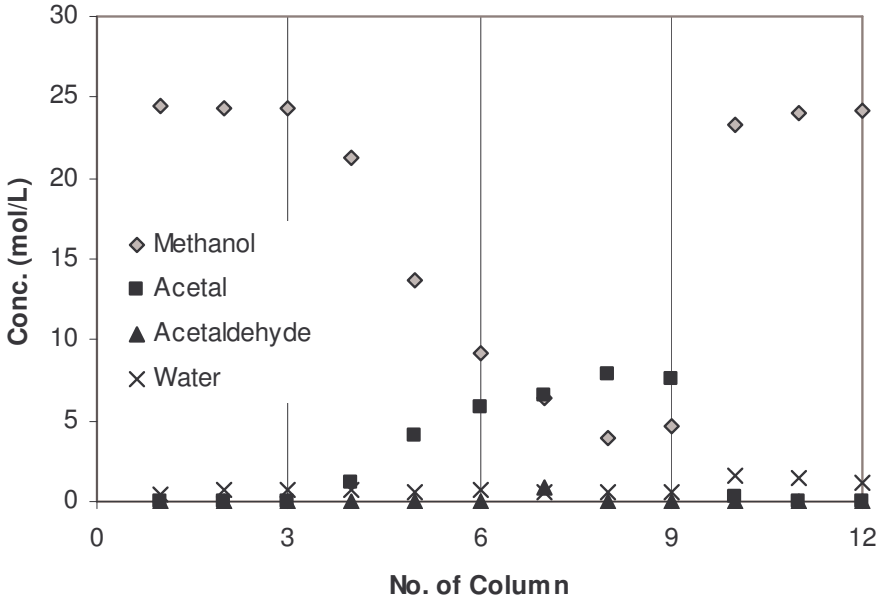

Figure E.1.5 SMBR profile Run 1, Cycle 7

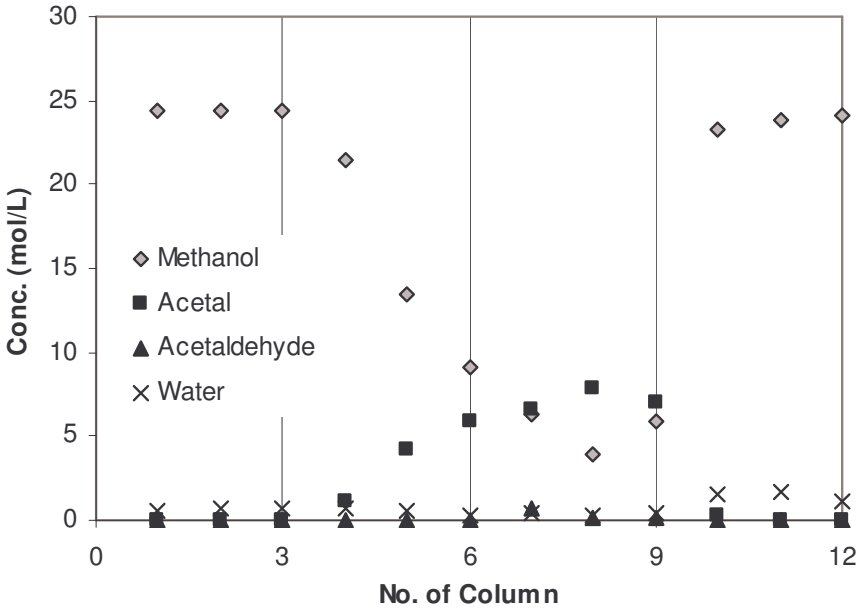

Figure E.1.6 SMBR profile Run 1, Cycle 8

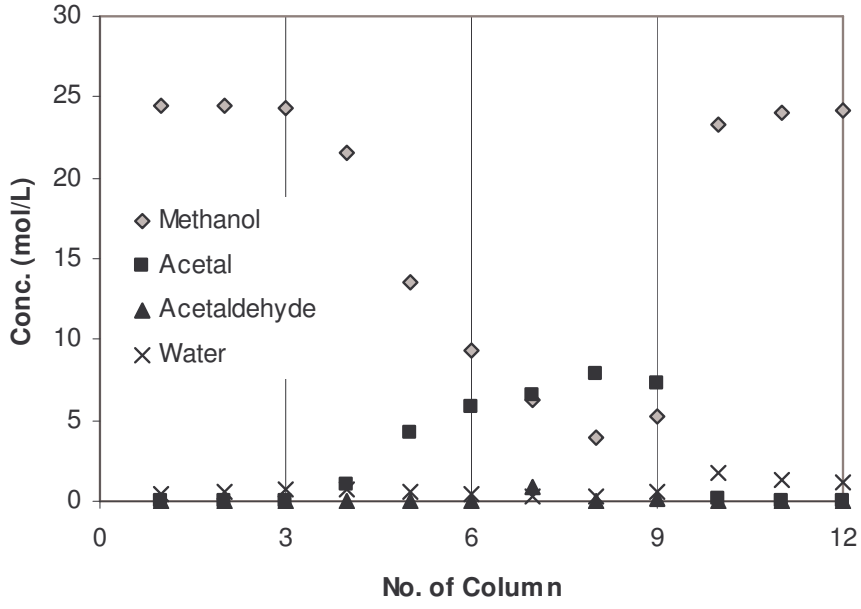

Figure E.1.7 SMBR profile Run 1, Cycle 9

Experiment Conditions Run 2	
Initial Condition : System saturated with methanol	
Switching time (t^*)	3.2 min
Configuration	3-3-3-3
Feed Composition (Molar fraction)	Mixture of 40 % Acetaldehyde 60 % Methanol
Desorbent flow-rate (Q_D)	25.0 mL/min
Feed flow-rate (Q_F)	3.0 mL/min
Raffinate flow-rate (Q_R)	8.0 mL/min
Extract flow-rate (Q_X)	20.0 mL/min
Section IV Recycling flow-rate (Q_4)	25.0 mL/min

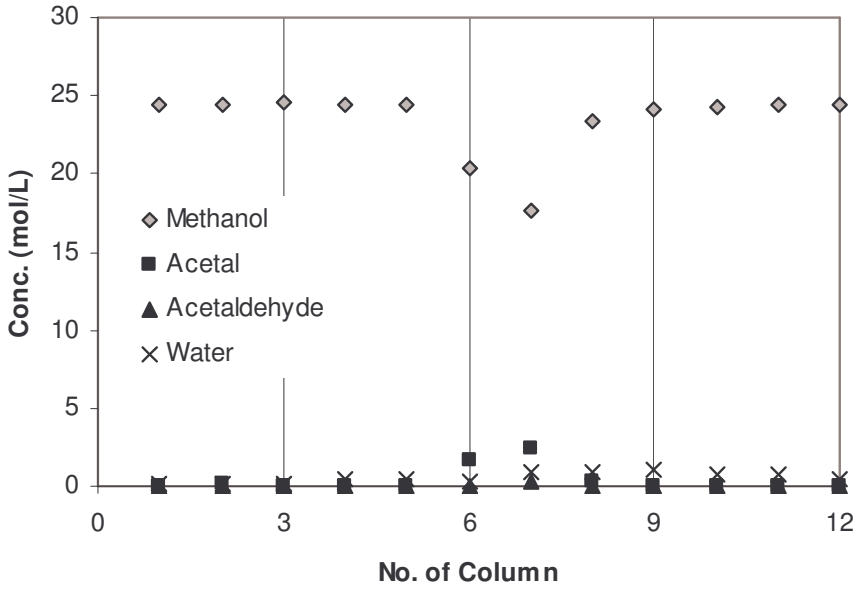

Figure E.2.1 SMBR profile Run 2, Cycle 1

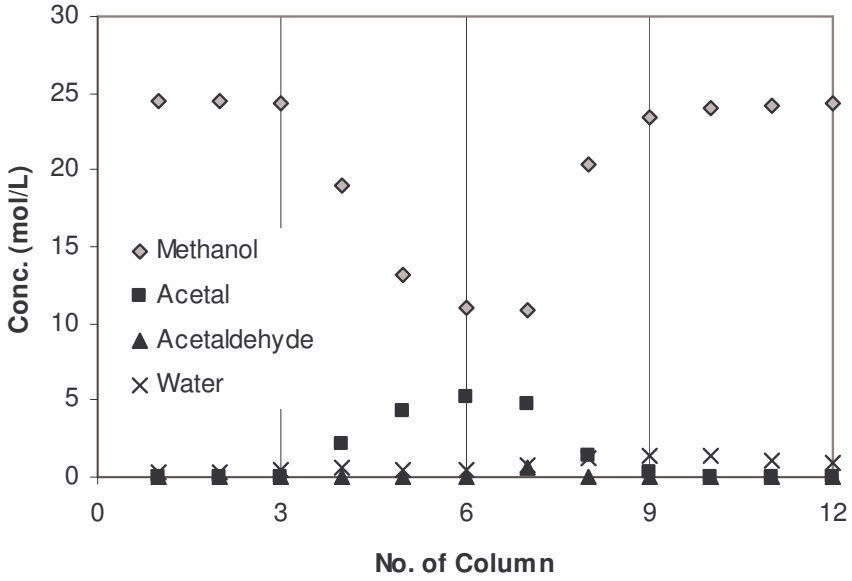

Figure E.2.2 SMBR profile Run 2, Cycle 3

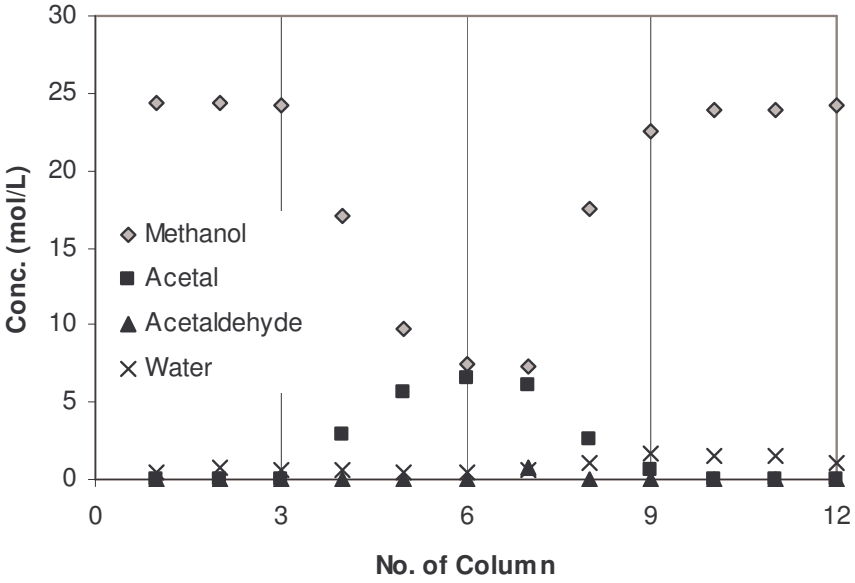

Figure E.2.3 SMBR profile Run 2, Cycle 5

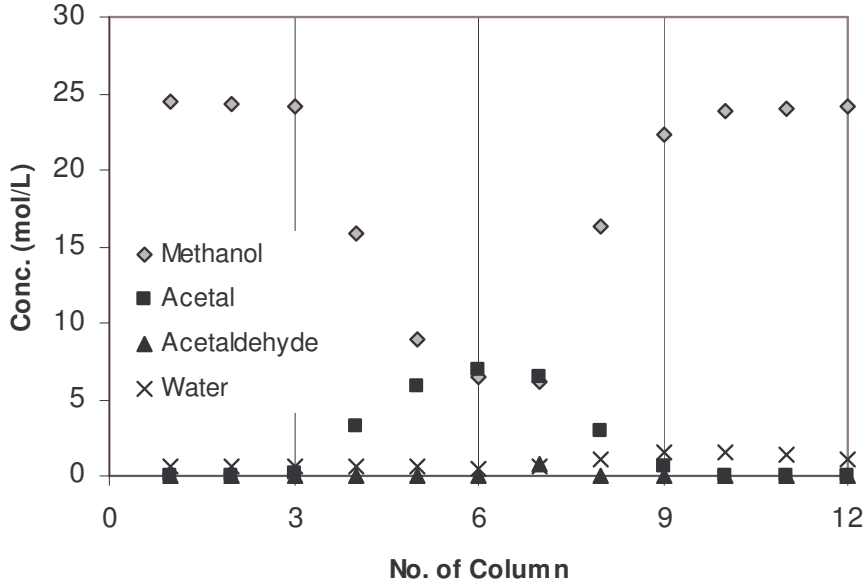

Figure E.2.4 SMBR profile Run 2, Cycle 6

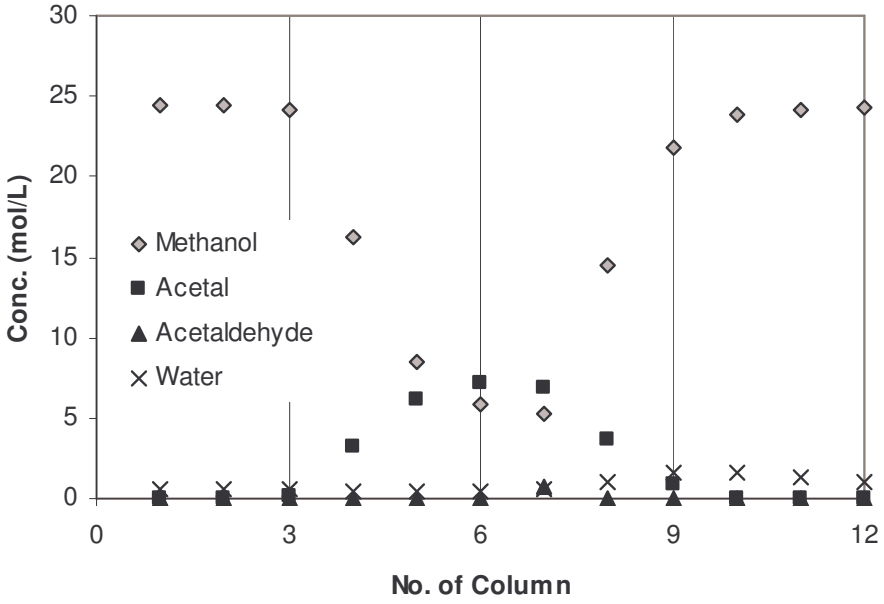

Figure E.2.5 SMBR profile Run 2, Cycle 7

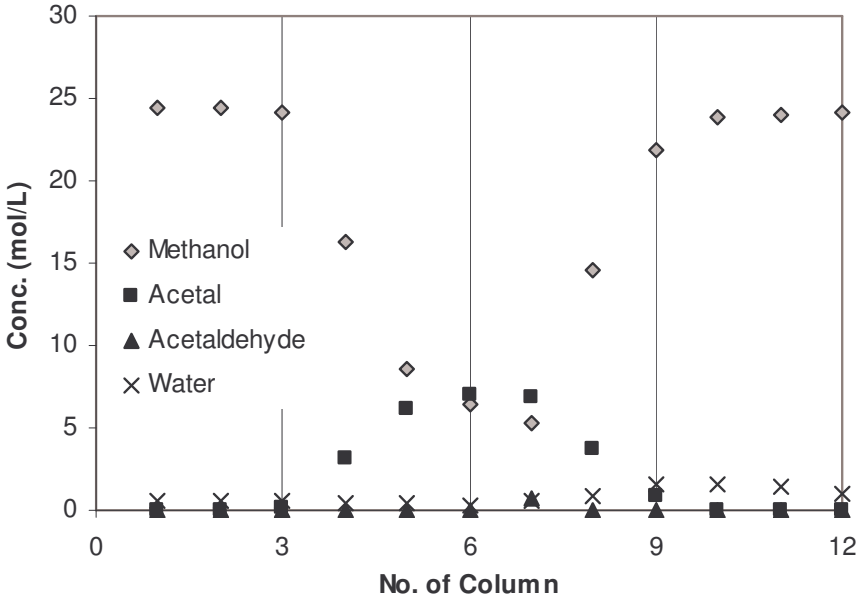

Figure E.2.6 SMBR profile Run 2, Cycle 8

Experiment Conditions Run 3	
Initial Condition : System saturated with concentrations of Run 2	
Switching time (t^*)	3.0 min
Configuration	3-5-2-2
Feed Composition (Molar fraction)	Mixture of 40 % Acetaldehyde 60 % Methanol
Desorbent flow-rate (Q_D)	25.0 mL/min
Feed flow-rate (Q_F)	5.0 mL/min
Raffinate flow-rate (Q_R)	10.0 mL/min
Extract flow-rate (Q_X)	20.0 mL/min
Section IV Recycling flow-rate (Q_4)	25.0 mL/min

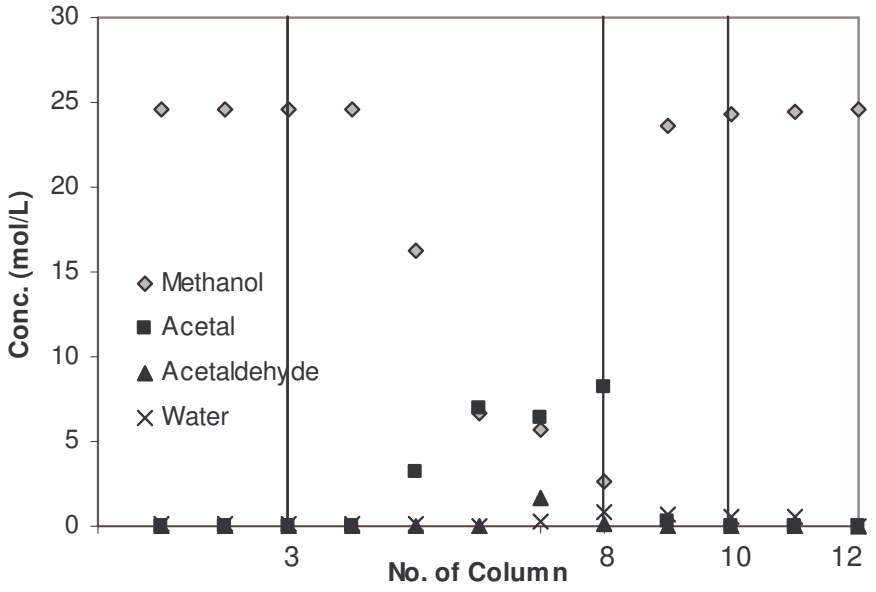

Figure E.3.1 SMBR profile Run 3, Cycle 1

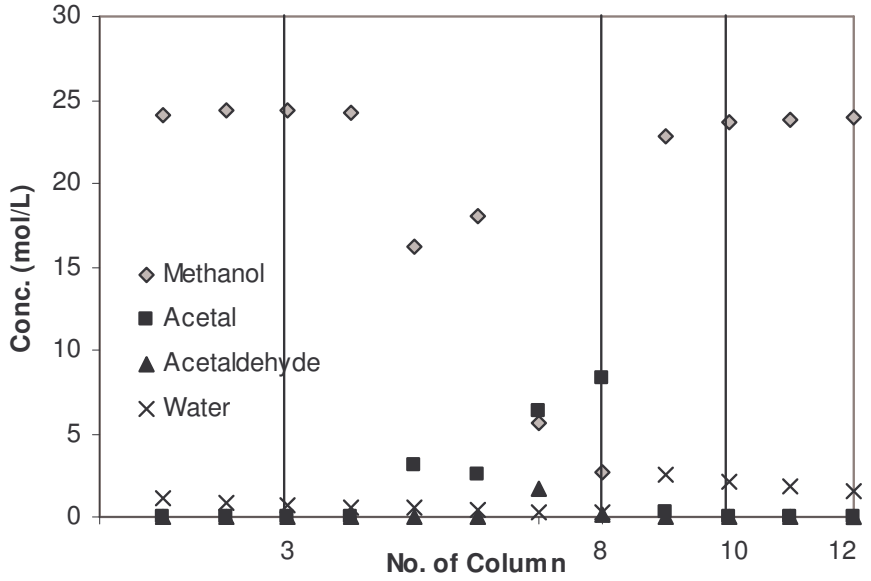

Figure E.3.2 SMBR profile Run 3, Cycle 3

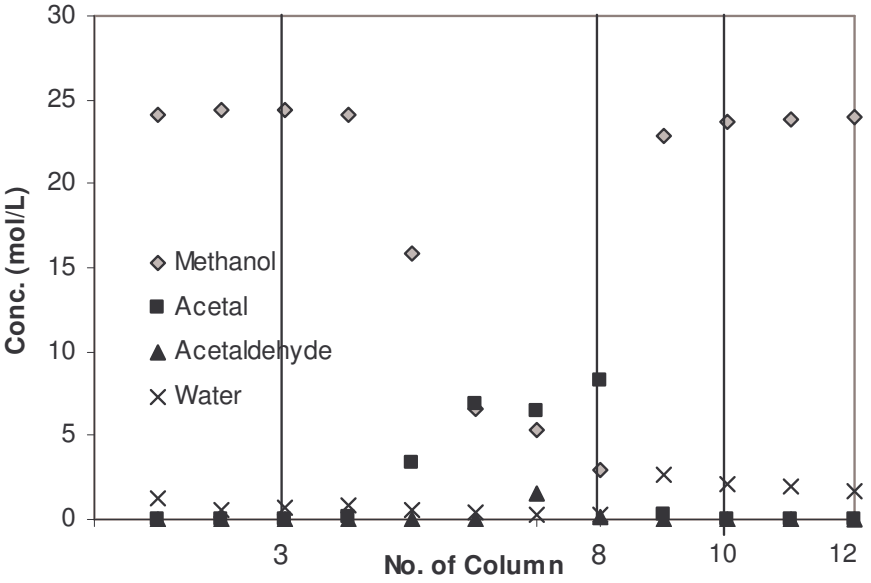

Figure E.3.3 SMBR profile Run 3, Cycle 5

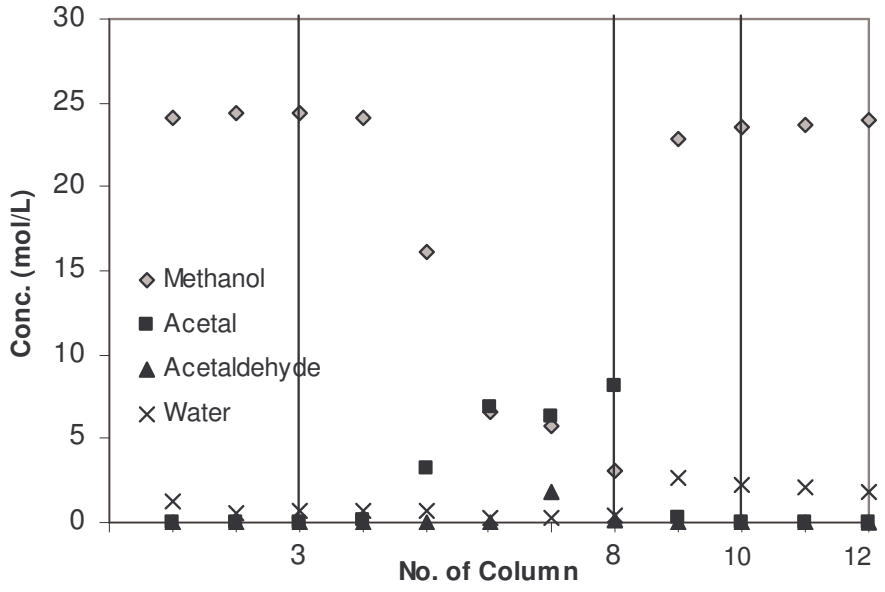

Figure E.3.4 SMBR profile Run 3, Cycle 6

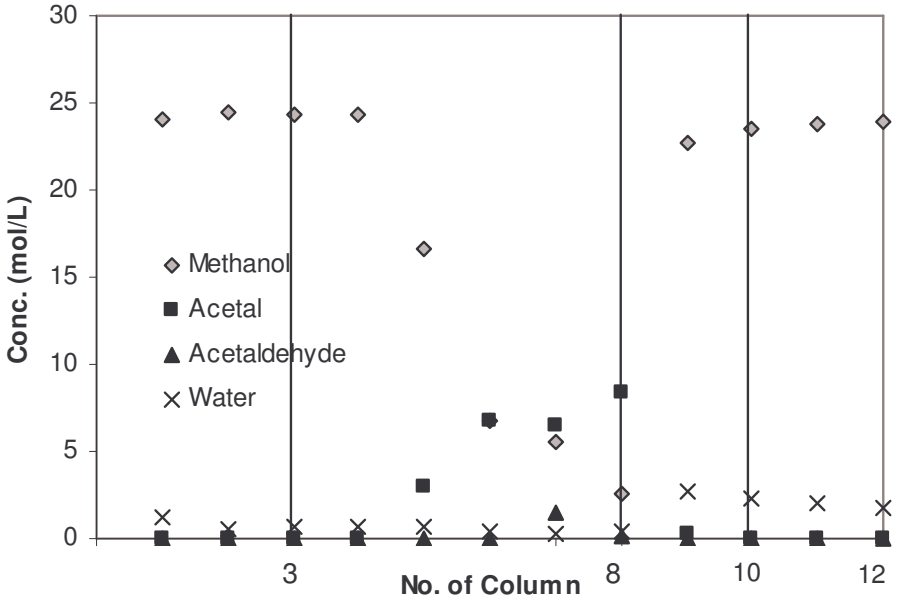

Figure E.3.5 SMBR profile Run 3, Cycle 7